TEXTURE, COMPOSITION AND PROVENANCE OF INNERSHELF SEDIMENTS BETWEEN NARAKKAL AND PURAKKAD, KERALA WITH SPECIAL REFERENCE TO THE FORMATION OF MUD BANKS

Thesis submitted to the
COCHIN UNIVERSITY OF SCIENCE AND TECHNOLOGY

for the degree of
DOCTOR OF PHILOSOPHY

in Marine Geology under the
FACULTY OF MARINE SCIENCES

K. K. RAMACHANDRAN

MARINE SCIENCE DIVISION
CENTRE FOR EARTH SCIENCE STUDIES
THIRUVANANTHAPURAM-695 031

April 1992

to my beloved parents

DECLARATION

I do hereby declare that this Thesis contains results of research carried out by me under the guidance of Dr. P. Seralathan, Reader, Marine Geology Division, School of Marine Sciences, Cochin University of Science and Technology and has not previously formed the basis of the award of any degree, diploma, associateship, fellowship or other similar title of recognition.

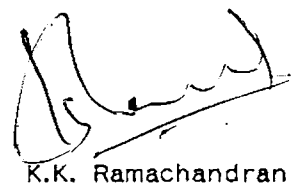

K.K. Ramachandran
Marine Science Division
Centre for Earth Science Studies
Thiruvananthapuram - 695 031

Thiruvananthapuram
April 10, 1992.

CERTIFICATE

This is to certify that this Thesis is an authentic record of research work carried out by Mr. K.K.Ramachandran under my supervision and guidance in the Centre for Earth Science Studies for Ph.D. Degree of the Cochin University of Science and Technology and no part of it has previously formed the basis for the award of any other degree in any University.

P. Seralathan

Dr. P. Seralathan
(Research Guide)
Marine Geology Division
School of Marine Sciences
Cochin University of Science & Technology
Kochi - 682 016

Kochi
April 10, 1992.

CONTENTS

PREFACE

Continental shelf, which is the interface between continents and oceans is one of the most dynamic, fragile and sensitive environments. This zone has great economic and strategic importance for food, transport, recreation, mineral wealth, etc. The innershelf region is more vulnerable to increasing developmental activities in the hinterland. Erection and construction of structures in the coastal zone and irrational approaches in exploiting the resources have brought severe imbalances in this environment. Therefore, knowledge of the nature of sediments and their response to various processes operating in the shelf is essential for a proper evaluation and management of this environment.

Considerable amount of work has been done on various aspects in the continental shelf of the southwest coast (Kerala) of India. However, the available data on sedimentological characteristics of the innershelf region are based on a wider sampling interval. With its wide variations in the sedimentation pattern, such a sampling would not yield a true picture of dynamic framework of the nearshore area. Innershelf processes of this coast are influenced by a strong seasonality in sedimentation and dispersal induced by alternating monsoon and non-monsoon. The reversal in current pattern, rough and fair weather wave conditions, copious rainfall restricted to monsoon months and the peculiar geomorphological settings impart spatial and temporal dynamism to the sedimentation pattern of Kerala coast. In addition, the most intriguing and unique aspect of this coast is the intermittent appearance of 'mud banks' in the nearshore zone during southwest monsoon. In this context, the present investigation is undertaken to provide a detailed account of sedimentation pattern, mineralogical and geochemical variabilities of the innershelf zone extending up to 30 m isobath between Narakkal and Purakkad region with an ultimate goal of identifying sedimentological processes leading to the formation, sustenance and cessation of mud banks.

The thesis is addressed in six chapters. First chapter introduces the work with objectives, location of study area, climatological, geomorphological and geological set-up and also surveying and sampling procedures.

Textural characteristics of the sediments are dealt in Chapter 2. Surficial variations of sand, silt and clay, and textural classification of sediments are described. Sedimentation characteristics of coarser sediments are interpreted in comparison with the present-day beach sediments from probability curves. A three-factor model derived from Q-mode factor analysis of the size data is used to differentiate spatial energy regimes of the innershelf. By considering progressive changes in the moment measures, transport pathways along different bathymetric contours are derived based on a statistical model. Study of quartz grains under Scanning Electron Microscope is used to substantiate the relict sedimentation.

Third chapter deals with mineralogy - heavy minerals and clay minerals. Variation in the concentration pattern of heavy minerals and their provenance are discussed. The inter-relationship among the heavy minerals is worked out using correlation matrix and also evaluated the factors responsible for their variability. Clay minerals are analysed usig X-ray diffraction technique. Spatial variation of clay minerals are discussed in the light of their source and dispersal pattern.

Geochemistry of the sediments is discussed in Chapter 4. Various major, minor and trace elements as well as organic matter are analysed in bulk sediments. Spatial distribution pattern of the elements are drawn. Size dependance of the different elements are discussed. Based on cluster analysis, elemental groupings are identified.

Fifth chapter deals with mud banks. Following an introduction to mud banks, previous literature on different hypotheses regarding nature, origin and other aspects of mud banks are examined. Suspended matter concentration and surficial sediment characteristics are studied. Sedimentological characteristics are discussed to understand the processes of formation and cessation of mud banks. Comparative evaluation of Alleppey and Quilandy mud bank sediments is carried out. The source of mud for mud bank and its relation to the innershelf sedimentation is also discussed.

Final chapter (Chapter 6) summarises the work and conclusions drawn from this investigation.

In connection with this study, the following research papers are published:

Ramachandran, K.K. and Mallik, T.K. 1985. Sedimentological aspects of Alleppey mud bank, west coast of India. Indian Jour. Mar. Sci., v. 14, pp. 133-135.

Mallik, T.K., Mukherji, K.K. and Ramachandran, K.K. 1988. Sedimentology of Kerala mud banks (Fluid mud ?). Mar. Geol., v. 80, pp. 99-118.

Ramachandran, K.K. 1989. Geochemical characteristics of mud bank environment - a case study from Quilandy, west coast of India. Jour. Geol. Soc. India, v. 33, pp. 55-63.

Ramachandran, K.K. and Samsuddin, M. 1991. Removal of sediments from the Alleppey nearshore region during the post mud bank formation. Proc. Indian, Acad. Sci., v. 100, pp. 195-203.

ACKNOWLEDGEMENT

I am deeply indebted to Dr. P.Seralathan, Reader, Marine Geology Division, School of Marine Sciences, Cochin University of Science and Technology (CUSAT), for his guidance, encouragement and friendship through the course of this investigation. I am also indebted to Prof.K.T.Damodaran, Head, Marine Geology Division, CUSAT, for encouragement.

I am grateful to Prof. C.G. Ramachandran Nair, Director, Centre for Earth Science Studies (CESS), and former Directors Dr. Harsh K. Gupta, Dr. M. Ramakrishna, Prof. N. Balakrishnan Nair and Shri. Subrato Sinha for extending necessary facilities and support. Dr. T.K. Mallik, former Head, Marine Science Division (MSD), CESS, guided me during the formulation stage of this work and Dr. M. Baba, Head, MSD, CESS, continued the support and encouragement.

The co-operation extended by Dr. M. Samsuddin and Dr. C.M. Harish, Scientists, CESS, through constructive criticism, lively discussions and encouragement during the various stages of this work is gratefully acknowledged. M/s. V. Vasudevan and G.K. Suchindan, Scientists, CESS are thanked for their help and suggestions. Thanks are also due to M/s. Terry Machado and T.N. Prakash for the help during the field work and to Drs. G.R. Ravindra Kumar and T. Radhakrishna, Scientists, CESS for sharing their knowledge on the hinterland Geology. My special thanks are due to Mr. Joseph Mathew, CESS for suggestions. The burden of my work was eased through the support rendered by all of my colleagues, especially Drs. N.P. Kurian, K.V. Thomas and T.S. Shahul Hameed of MSD, and Mr. Venkatesh Raghavan and late Mr. P.V. Panchanathan. M/s. R. Ravindran Nair, M. Ajith Kumar and R. Shivarajan are thanked for the arduous task of drafting the figures.

Dr. K.K. Mukherji, Concordia University, Montreal, Canada is thanked for valuable suggestions and encouragement. Sincere thanks are due to Prof. B.L.K. Somayajulu, Dr. J.N. Goswami and Dr. K. Dilli of Physical Research Laboratory, Ahmedabad for providing facilities to carry out the XRD and SEM studies. M/s. M. Balasubramaniam and P.P. Ouseph, Scientists, CESS, helped in the geochemical analysis.

The whole hearted support and timely help of my friends Dr. B.K. Purandara, M/s. D. Padmalal, Syriac Sebastian and Roy George deserve special mention.

My wife Usha and son Aaditya made my work enjoyable through their loving understanding.

LIST OF FIGURES

LIST OF TABLES

LIST OF PLATES

CHAPTER 1

INTRODUCTION

Sedimentary processes refer to a myriad of mechanisms, events and reactions, which include particulate material. It can occur to or result from sediment in the water column or in the sea bed and can affect quantity or composition of particles. Sediments that accumulate in a marine shelf reflect the general character of the material transported by rivers from adjacent land areas and are derived from shore line erosion. These sediments, along with the material produced *in situ* by organisms and contributed by anthropogenic activities, are carried by coastal currents and redistributed in the shelf. The continental shelf covers about one-sixth of the total land area. The study of shelf sediments is important owing to its proximity to land and easy accessibility to explore and utilise the ever increasing demand for mineral resources, and above all for a proper evaluation and management of the environment.

The sedimentological processes along the continental shelf bordering the north Indian Ocean are unique, primarily controlled by the monsoon regime. It is especially so along the southwest coast of India (Kerala), where the sediment supply through fluvial discharge is dominated by the precipitation received during the southwest monsoon (June - September). The coast experiences high wave activity during this period. Also, the coastal circulation reverses with the monsoon influencing sediment dispersal. Added to this, the peculiar geomorphologic setting of the coast regulates the rate and composition of the sediment supplied to the adjoining shelf. The 'mud bank' phenomenon, reported along the Kerala coast, could be a rare manifestation of this complex interplay of the causative processes and resultant sedimentation pattern.

Compared to the studies conducted on the continental shelves bordering the other major oceans, the Indian shelf is less explored. International co-operation in geoscientific endeavours started with the International Geophysical year (1957 - '59). The International Indian Ocean Expedition (IIOE) conducted during 1962 - '65 added impetus to this when a considerable amount of data on different branches of ocean sciences were generated. Remarkable studies were then initiated primarily on the western continental margin of India. After this, INS Darshak (1973 - '74) collected sediment samples in the northern half of the Arabian sea. On commissioning of R.V.Gaveshani, the first research vessel acquired by the National Institute of Oceanography, in 1976, systematic studies came of age in India. Studies on sedimentology, geo-chemistry and micropalaeontology of the shelf sediments were carried out. Significant contributions of these studies are reviewed in the following section.

The continental shelf bordering the west coast of India is remarkably straight which resulted from faulting during the Pliestocene (Krishnan, 1960). It is broader and flatter compared to world averages and the width of the shelf increases from 40 km off Trivandrum in the south to 320 km off the Gulf of Cambay in the north (Rama Raju, 1973). Topographic studies of the western continental shelf indicated small scale irregularities of the order of 1 - 8 m in height confined to the outer shelf (Nair, 1972, 1975). Siddiquie and Rajamanickam (1974) further classified the shelf based on surface roughness and observed that the shelf break occurs between 120 and 145 m depth.

Pliestocene sea level variations have affected shelf sedimentation and Nair (1974) inferred that this shelf can be considered as an example of a drowned coast due to subsequent transgressive episodes. Thus, the sediment

facies in the shelf embodies mixed distribution of both ancient and modern sediments inundated by reworking processes. Following Nair and Pylee (1968) and Nair (1971), surface sediment facies on the shelf have been further investigated by Nair *et al.* (1978) and Hashimi *et al.* (1978). Three distinct sedimentary facies have been identified, the first two facies consisting of sand and mud are of Recent origin, while the outershelf relict carbonate sand facies are of late Pleistocene (8,000 - 11,000 years) formed at the time of low stand of sea level. From the study of carbonate sediments and size of quartz grains, Nair and Hashimi (1980) inferred a warmer climate and low terrestrial run off during the Holocene (about 10,000 years ago). Further, feldspar content of the sediments have also been used to infer the climatic aridity over India 11,000 years ago (Hashimi and Nair, 1986). Therefore, these evidences indicate contrast in climate between the carbonate and clastics on the shelf suggesting rapid change from arid to humid climate. In common with other continental shelves of the world, the outer continental shelf sediments and rocks of western India, are of late Pliestocene (12000 - 9000 years).

Mineralogy of carbonate sediments and limestones of the shelf was studied by Nair and Hashimi (1981) and a comparative study of the carbonates on the eastern and western shelves around Cape Comorin were attempted by Hashimi *et al* (1981). Sedimentological and faunal evidences show that limestones on the outer continental shelf have been formed under shallow water conditions (Hashimi *et al.*, 1977; Nair *et al.*, 1979). The distribution of these sediment types over a large area of the western shelf shows that carbonate precipitation was quantitatively large in the past compared to the present (Nair and Hashimi, 1980). Nair *et al.* (1982) studied the relative proportions of clay minerals of the western shelf and has provided explanation for their distribution. The clay minerals of shelf and slope of Kerala were

also studied by Rao *et al.* (1983). These studies have stressed the importance of source rock influence on clay-mineral composition than physical transport mechanisms. Siddiquie and Rajamanickam (1979) reported the surficial mineral deposits of the shelf and indicated their spatial extent.

Geochemical and micropaleontological studies were also attempted on the sediment samples from the western shelf. Setty (1972, 1974) and Setty and Guptha (1972) identified foraminiferal assemblages in the sediments and reported the relict nature of the sediments on the outer shelf. Diversity in faunal species in the Arabian sea compared to the Bay of Bengal was observed by Rao (1972, 1973) and attributed it to the higher salinity of the Arabian sea waters. Nigam *et al.* (1979) and Setty and Nigam (1980) have delineated micro-environmental implications of benthic faunal assemblages. Nigam and Thiede (1983) encountered important species belonging to Miocene and Pliocene off the west coast. Geochemical investigations by Rao *et al.* (1972), Murty *et al.* (1973), Rao *et al.* (1974) and Murty *et al.* (1980) gave information on the major and trace elements of the surficial sediments and their partition pattern on the western shelf. Environment favourable for phosphatisation was indicated along the outer shelf/slope region by Rao *et al.* (1987). Paropkari (1990) carried out geochemical investigation of sediment samples from the Mangalore-Cochin shelf.

The series of investigation mentioned above have generated considerable amount of information on the sedimentation characteristics of the shelf. Excepting a few, many of the studies can be seen to be restricted up to Cochin in the south or mainly on the northwestern part of the Indian shelf; and the few reports on the sedimentological aspects of the southwestern part of the shelf are constrained with a sampling interval of 20 km apart in many

of the studies (Siddiquie *et al.*, 1987). However, information on the innershelf sediments is lacking. Considering the strong seasonality and influence of the peculiar geographical setting of the coast, it is imperative that the sediments of the innershelf is studied more closely with regard to its spatial configuration. The transient nature of the innershelf unfolded through the seasonal occurrence of 'mud banks' along this coast can not be studied in isolation. Further, the physical, chemical and mineralogical constituents of the sediments studied in detail could be a wealth of basic information for taking up future studies. Hence the present work envisages to decipher the sedimentology of the innershelf zone in detail, extending up to a water depth of 30 m isobath between Narakkal near Cochin to Purakkad near Alleppey. The study of this sector is all the more important owing to the persistent occurrence of Mud banks at specific locations, namely, Narakkal and Purakkad (Fig. 1.1). The investigation is also therefore intended to give new insights into the role of innershelf sediments in the formation of mud bank. For this purpose, Alleppey nearshore area is subjected to a season-wise study which would provide information on the spatial and temporal variation in the sedimentological characteristics. The mud bank location at Alleppey is backed by a barrier beach-backwater coastal setting. However, mud banks have been reported from other locations which are not influenced by such geomorphological set up. Hence, in order to evaluate the distinct characteristics of mud banks formed at locations with such diverse physical setting, Quilandy mud bank is also studied (Fig. 1.1). This has enabled comparative evaluation of the sedimentological aspects of the two mud banks.

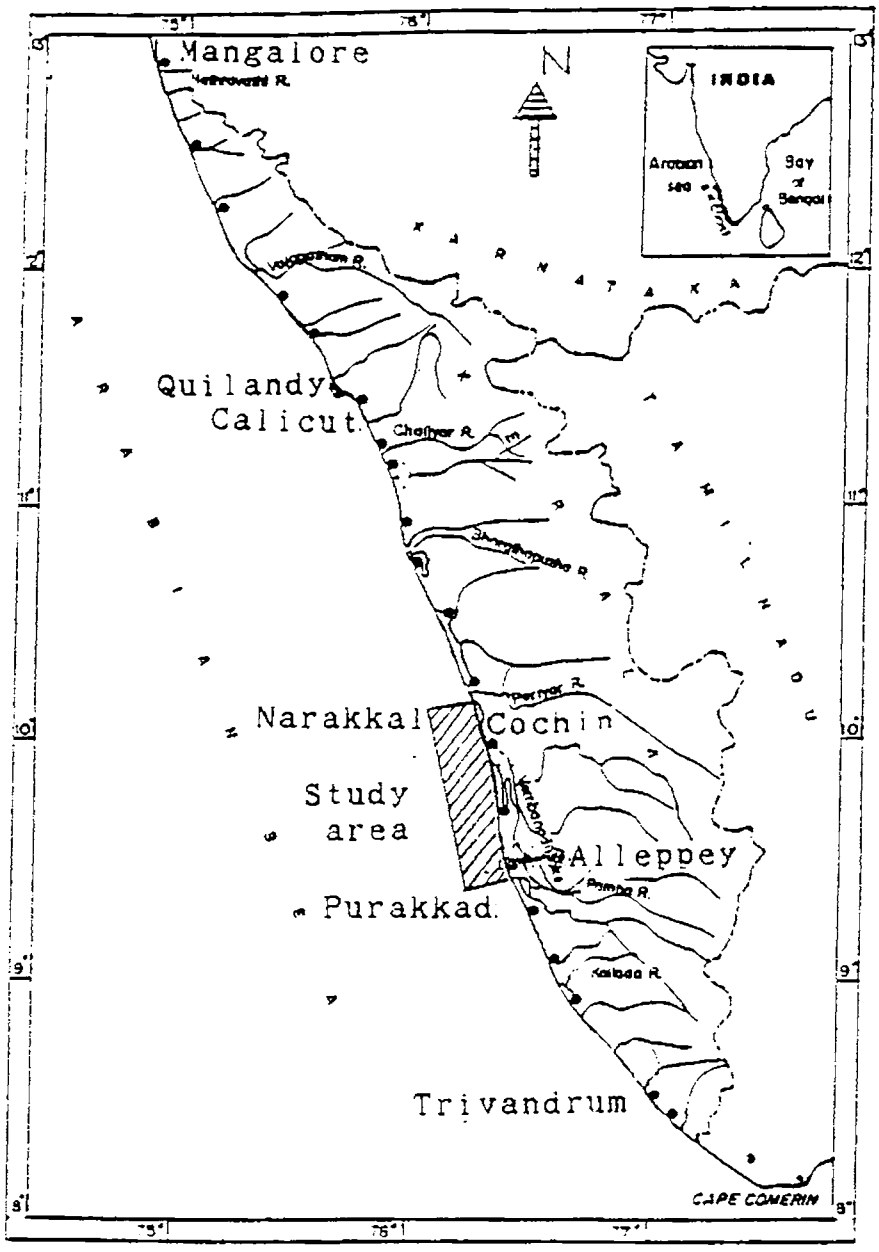

Fig. 1.1 Map showing locations of the study area

1.1 OBJECTIVES

The major objectives of this investigation are:

i. to study the granulometric composition and the spatial variations of the textural attributes of the sediments and to delineate the processes responsible for the depositional/dispersal pattern of the sediments,

ii. to analyse the mineralogical assemblages of the sediments and the reasons for their spatial differentiation; and to determine the provenance of the sediments,

iii. to understand the geochemical variability in terms of major, minor and trace element concentration of the sediments and to infer the processes of elemental incorporation,

iv. to observe the spatial and temporal changes in the sedimentological aspects of the mud bank region at Alleppey and to compare the Alleppey mud bank sediments with that of Quilandy mud bank so as to delineate their characteristics, and

v. to evaluate the role of the innershelf sediments in the process of mud bank formation.

1.2 GEOGRAPHICAL FEATURES

Kerala is a narrow strip of land on the southwestern part of the Peninsular India, with a width varying from 30 km in the north and south and to about 130 km in the central region. Though the area of the state is small compared to the other states in India, variation of physical features is very wide. Topography of the State covers altitudes ranging from below sea level

to about 3000 meters above sea level. The Western Ghats form almost a continuous mountain chain on the eastern border of the State, broken by the Palghat Gap, and a few other small passes. The Anamalai (2695 m) is the highest peak in peninsular India. Palghat Gap has a width of about 30 km and an elevation of around 300 m. This gap has got a significant role in determining the climate of the state. The northeast monsoon winds enter the state through this gap. The mountain ranges and the high intensity of rainfall during the monsoons gave birth to a number of perennial rivers which resulted in the formation of varied land forms.

Kerala has a coastline of 560 km. The Vembanad lake, the largest estuary in Kerala, with an area of 205 km^2, lies exactly on the landward side of the study area. The coastal plain between Cochin and Alleppey has a series of parallel sand ridges.

Based on the topography, the area is divided into three well defined natural divisions, viz, lowlands, midlands and highlands. The lowlands which are below 8 m elevation contains the coastal belt with its picturesque backwaters. This has extensive paddy fields and scattered areas with coconut, arecanut, etc., experiencing considerable population stress. The mid lands which ranges in elevation from 8 to 75 m, are intersected by a number of rivers. This zone shows diversity in landform and crops. The highlands are the hilly region on the western side of the Western Ghats covered with dense forests and small streams. This zone accounts for a large area with small population density and abundant in cash crop.

1.3 DRAINAGE

The State has 44 rivers, of which 41 debouch into the Arabian Sea. The hinterland of the study area is drained by as many as six rivers with numerous tributaries, all originating in the Western Ghats (Fig. 1.2). They are Chalakudy, Periyar, Muvattupuzha, Meenachil, Manimala and Pamba. Details of the river basins are given in Table 1.1. The Periyar is the second largest river in Kerala after Bharathapuzha, with a catchment area of 5284 km^2 and an annual yield of 11391 Mm^3.

The Chalakudy river joins the river Periyar near the coastal plain. A tributary of the Periyar joins the Vembanad Lake at its northern tip. The other four rivers join the Vembanad Lake at various points with Pamba at the extreme south. Many of the rivers are exploitable for irrigation and hydro-electric power generation. The major dams constructed across the above rivers are, Idukki, Pamba, Kakki, Mattupatti, Bhutatankettu, Sholai Ar, Poringal, Parambikulam and Tunakadavu. Many of the reservoirs experience considerable siltation thus checking the natural sedimentation through the rivers.

1.4 GEOLOGY

The rock types falling within this region can be classified into four major age groups as belonging to Archaean, Proterozoic, Cretaceous and Cenozoic (Table 1.2). A large part of the terrain has undergone poly-metamorphic and poly-deformation activities. Metasediments, granulites and gneisses constitute the major rock types in the hinterland. A brief description of the rock types are given below and are shown in Fig. 1.3.

TABLE 1.1

Drainage characteristics of the rivers.

River	Length (km)	Catchment area (km^2)	Annual yield (Mm^3)
Chalakudi	130	1704	3121
Periyar	244	5398	11607
Muvattupuzha	121	2004	3814
Minachil	78	1272	2349
Manimala	90	847	1829
Pamba	176	2235	4641

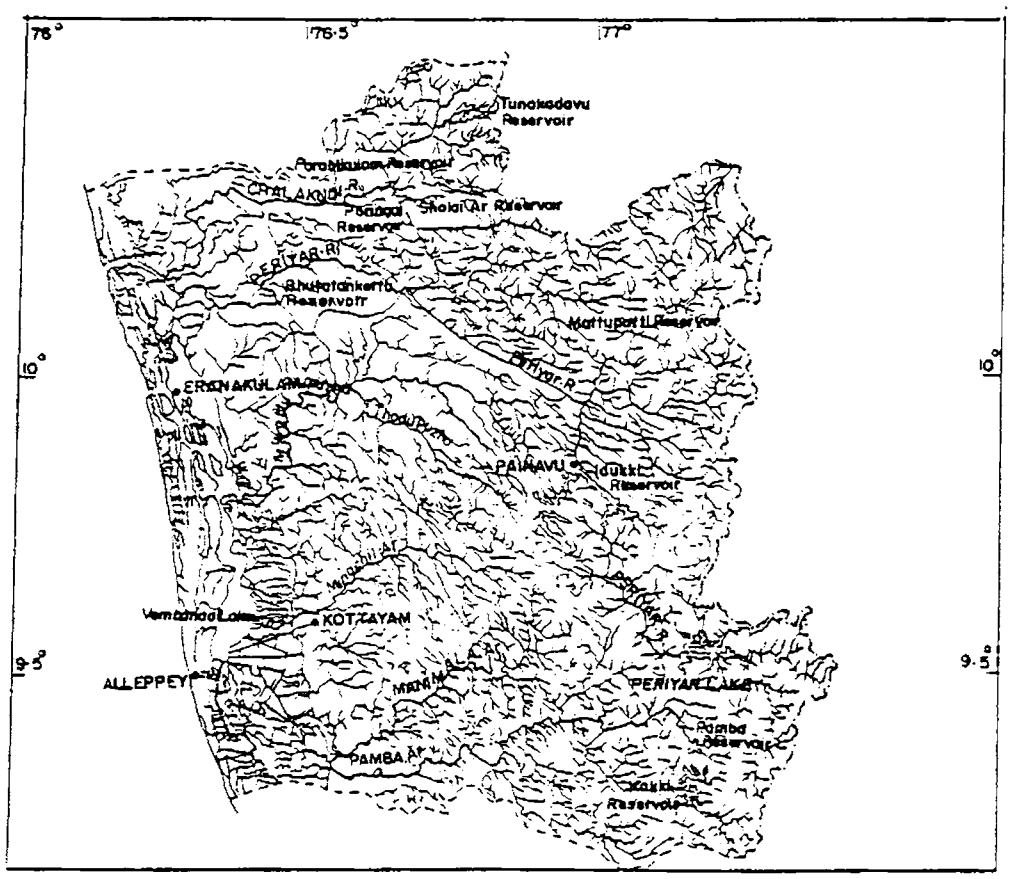

Fig. 1.2 Drainage map

(From: Resource Atlas of Kerala, CESS)

TABLE 1.2

GEOLOGICAL FORMATIONS	AGE
Beach sands and soils ; aeolian deoposits including white and red (teri) coastal sands; shell limestone and loose shelly sands	Recent to sub Recent
Laterite	
Warkalli beds; sandstones and clays, lignite.	Upper Miocene
Quilon beds;fossiliferous lime stones, sands and clays	Lower Miocene
Basic dykes	
Granite, pegmatite and quartz veins.	Late Proterozoic
Basic dykes	
Vengad Group: quartz mica schist, conglomerates	Proterozoic
Khondalite Group; meta sediments of garnet-biotite-sillimanite-cordierite-graphite gneiss, leptynite, calcsilicates,quartzites.	Late Archaean Early Proterozoic
Charnockites, migmatitic ortho-gneisses	
Wynad Group:(=Sargur Group) kyanite-sillimanite schist,calcareous bands, quartzite banded iron formations, hornblend-biotite gneisses.	Archaean

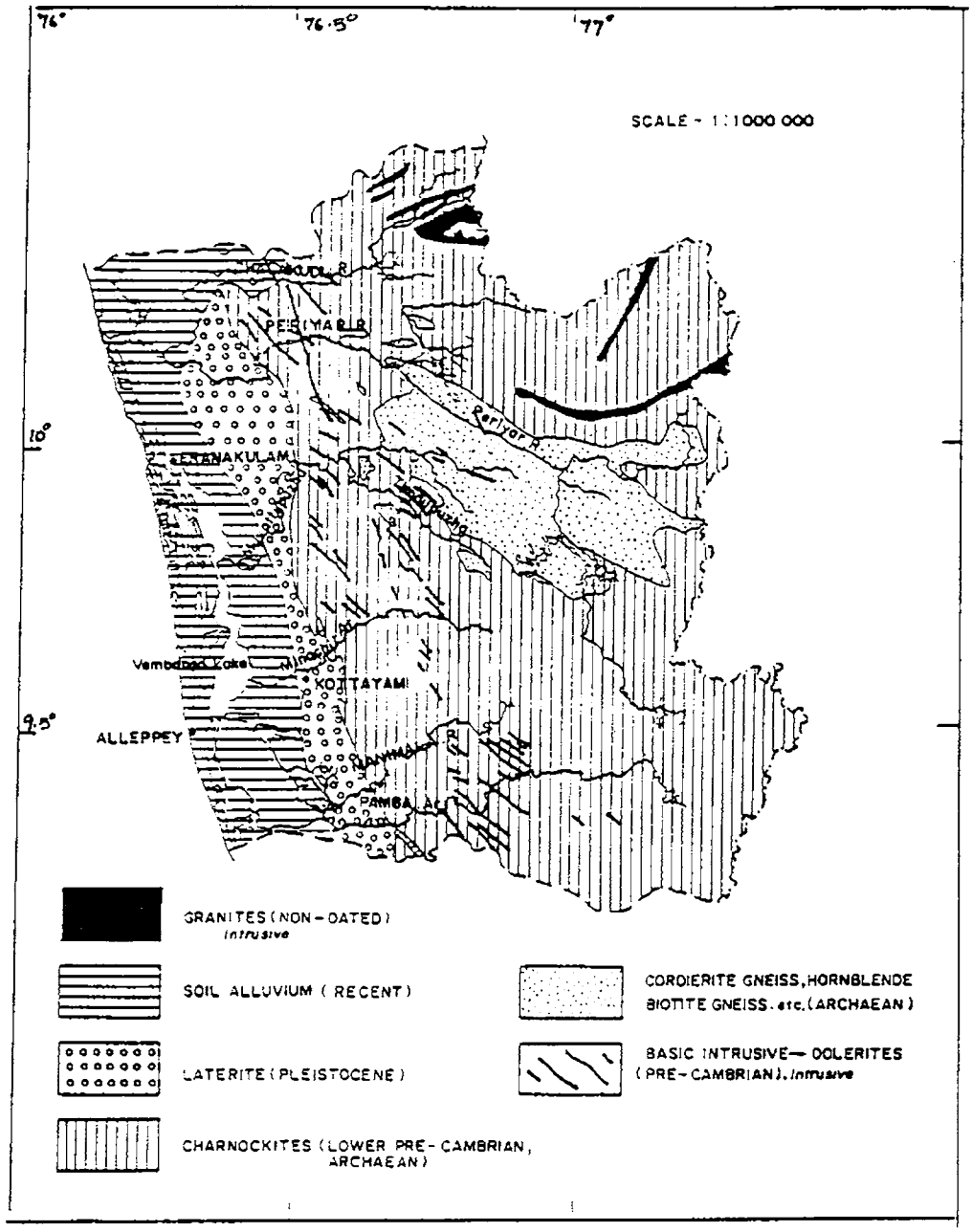

Fig. 1.3 Geological map

(From: Resource Atlas of Kerala, CESS)

Khondalite group: Major part of the Periyar and Thodupuzha river basins are occupied by Khondalite group of rocks. The group includes rocks like quartzite, calc-granulites, garnet-gneiss, and patchy charnockite. Age determinations carried out on khondalites occurring further south of the above river basins indicate a range of 2200 to 670 Ma (Santosh, 1987; Chacko *et al.*, 1988). Recent field and petrological studies indicate occurrence of incipient charnockites in the khondalite group of rocks (Ravindrakumar *et al.*, 1985). These prograde patches of charnockites are considered to be formed around 540 Ma (Srikantappa *et al.*, 1985).

Charnockites (*Massive type*): Major part of the hinterland geology are characterised by predominant occurrence of charnockites. Charnockites show wide variation in composition from acid to basic. These charnockites are massive in appearance, but on close examination good deformational banding/foliation can be recognised. They are essentially characterised by orthopyroxene, amphibole, feldspar and quartz minerals and significant by the absence of garnet. The incipient charnockites noted in the khondalite group are distinguishable from the massive charnockites by their post-deformation field characteristics and the presence of abundant garnets and absence of hornblende.

Granites, Pegmatites and Quartz veins: Several intrusives of acidic and alkaline composition are noted in the study area. These rock types are classified based on petrography as pink and grey granites. Syenites also occur as small patches in this area. Two major acid intrusives are noted in the region. The granite bodies are generally considered to be fault/lineament controlled and emplaced between 500 to 700 Ma ago (Santosh and Drury, 1988). Numerous pegmatites and quartz veins also traverse Precambrian rocks of the region.

Basic Dykes: Occurrence of basic dykes of post-archaean age within the granulite terrain of Kerala are well known. Several such basic dykes are noted in this area. In terms of their emplacement, direction and physical appearance, the dykes are grouped into two distinctive systems. The NNW - SSE dykes are leucogabbros exposed for over a strike length of 100 km with several intermittent offsets, the width of which is 30 - 50 m. The NW - SE trending dykes are dolerites. They vary around 3 - 5 m in width and spread around a 50 km wide zone. K-Ar isotope dating has yielded a coherent age estimate of 81±3 Ma for NNW - SSE dykes. NW - SE trending dolerites yielded 65 - 70 Ma of age (Radhakrishna *et al.*, 1989). It is surmised that basic dykes are the rift response of the late Cretaceous detachment of India from rest of the Gondwanaland.

Laterites: Laterites, which is a sub-aerial product of deep chemical weathering, covers nearly 60 % of the surface area of Kerala. Laterite cappings on the Precambrian crystalline rocks and Tertiary sediments are seen in the region. Chemically, laterite is characterised by higher Fe_2O_3, Al_2O_3 and low SiO_2. Subramaniam (1978) suggested a mid to late Tertiary age for laterites.

Recent to Sub-Recent Sediments: Sub-recent formations consisting of a great thickness of sand with shell fragments, sticky black clays, peat beds of both marine and fluvial environments occur in the low-lying areas between Kottayam and Ernakulam. These are separated from the Tertiary rocks by a polymict pebble bed. Recent formation includes fringes of parallel sand bars and sandy flats alternating with marshy lagoonal clays and beach sand deposits. Beach ridges are formed due to repeated regression and transgression of the sea and their orientation have been controlled by the change in direction of the waves (Mallik and Suchindan, 1984).

1.5 CLIMATE

Diversity of physical features results in the diversity of climate of the State. On the whole, the State has a pleasant climate with a cool winter and a warm summer. Cool climate exists in the highland region throughout the year while the rest of the state enjoys a temperate climate. Mean annual temperature varies between 18.5°C and 28.5°C in different zones of the state. Based on the patterns suggested by Indian Meteorological Department, the seasons in Kerala can be demarcated as follows:

a. Hot weather period (the pre-monsoon season): March - May
b. Southwest monsoon: June - September
c. Retreating southwest monsoon (northeast monsoon): October - November
d. Winter (cool weather season): December - February.

Rainfall: Kerala receives the highest annual rainfall among the states of India, which is three times the average annual rainfall for India. Average annual rainfall of Kerala is about 300 cm, of which 75 % occurs during the southwest monsoon (Ananthakrishnan *et al.*, 1979). It increases from 150 cm in the south to more than 350 cm in the north. In the hinterland of the study area, Pirmed (491 cm) and Kanjirappally (410 cm) recorded heaviest rainfall.

Wind: The direction and speed of wind are mainly controlled by the orographic features of the State. Notable change in wind direction and speed is observed between coastal and inland stations. In Cochin and Alleppey, which are coastal stations, the wind is mainly from west and north-west. Generally wind from north-east and east prevails in the morning (0830 hrs),

while in the afternoon (1730 hrs), it is from west and north-west. This is clearly attributable to the effects of land and sea breeze. Maximum wind speed of more than 20 km/hr was recorded for a good number of days. The wind speed is high during southwest monsoon, the direction being north-west. In general, the wind speed decreases from November to April.

1.6 WAVE CHARACTERISTICS

Waves is a very important dynamic factor in the nearshore areas. Nearshore wave measurements reported for Alleppey (Hameed, 1988) and deep water wave studies by Baba and Joseph (1988) off Cochin are presented here, which are representative for the study area.

Alleppey: The report classifies wave data into two groups; rough season (May - October) and fair season (November - April). The majority of waves arriving at this coast are confined to a small angular range of 230 - 265°N. Dominant direction of waves show consistency during the rough season (245 - 250°N). During fair season, one-fifth of the total occurrence is in the direction 235 - 240°N. 50 % of the waves during rough season is from 245 - 265°N and 44 % of fair season waves are from 230 - 245°N. The maximum significant wave height (H_s) during the rough and fair seasons are 3.0 m and 1.4 m respectively. Maximum height of the highest waves (H_{max}) during rough season is 3.8 m and that of fair season is 2.0 m. Rough season recorded 30, 50 and 75 % of H_s exceeding 1.3, 0.95 and 0.62 m respectively with corresponding values of 0.65, 0.52 and 0.42 m during the fair season. During rough season, 30, 50 and 75 % of H_{max} exceeded 1.9, 1.35 and 0.85 m respectively, the corresponding values during fair season were 0.9, 0.72 and 0.58 m. During the rough season, waves are of comparatively shorter period

than those during the other season. The most frequently occurring periods during the rough season are 8 and 9 s and that during the fair season are 9 to 11 s.

Cochin: Deep water wave climate of Cochin area is reported to be characterised by monsoonal high and non-monsoonal low wave activity. The direction of wave approach was found to be north-westerly (> 80 % frequency) during fair season. For the rough season only 47 % of the waves come from this direction and rest approach either from west or south-west. It is found that, during fair season, H_s exceed 0.5 m during 50 % of the time and for rough season H_s exceed the same height almost 100 % of the time. The most frequently occurring period for both the seasons are 7 and 8 s.

1.7 CURRENTS

The currents of west coast of India are of monsoonal origin (Rao and Molinari, 1991). The predominant current direction is south-south-easterly off the west coast of India from April through September. Progressive increase in velocity from 25 cm/s to 40 cm/s (in July and August) and consistency in direction is observed during this period. Maximum speed encountered on a few occasions is 100 cm/s. In October, the currents are highly variable followed by a reversal in current to northwesterly to northerly directions during November. Month of March is again marked by variability of current pattern, but the dominant direction is south-southeasterly. From October to March, the current speed remains around 25 cm/s.

1.8 STUDY AREA AND SAMPLING PROCEDURES

The study area lies between the latitudes 9°20' and 10°5'N and the longitudes 76°1' and 76°22'E. The coast line falls in the Ernakulam and Alleppey districts in the central part of Kerala (Fig. 1.4). The length of the coastal stretch covered is little more than 80 km with a maximum offshore extent of 20 km from the coast, with slight variation along the different profiles selected during the cruise. The study area is covered in Naval Hydrographic Chart No. 220 and 221. Detailed surveying and sampling of the study area between Narakkal and Purakkad was taken up during October 1984. A mechanised boat with winch and davit system was used for the surveying. Perpendicular to the 80 km coast, 17 parallel transects (A - Q) with approximately 5 km distance between the transects were selected for the cruise (Fig. 1.4). On each transects, 6 stations were fixed, except in the case of 3 transects, on which only 5 stations were occupied. A total of 100 stations were occupied in water depths ranging from 3 to 32 m. Each sampling site was located at the intersection of theodolite sightings of the boat undertaken by two shore-based surveyors. Locations beyond the theodolite sightings were fixed using a marine compass and by boat speed tracing, combined with depth cross checking. Water depth was measured at each sampling stations using a lead line and was cross checked with the hydrographic depth data. Peterson grab and a gravity corer were used for sediment sampling. PVC tubes threaded at both ends were used as the lower barrel which was replaced after each sampling. 100 grab samples and 17 core samples were collected from the area. Polythene bottles were used for sample storage. Bathymetric map for the area is prepared by superimposing the depth measured during the survey over the bathymetric chart (Fig. 1.5). The continental shelf break is approximately around 60 km from the coast along

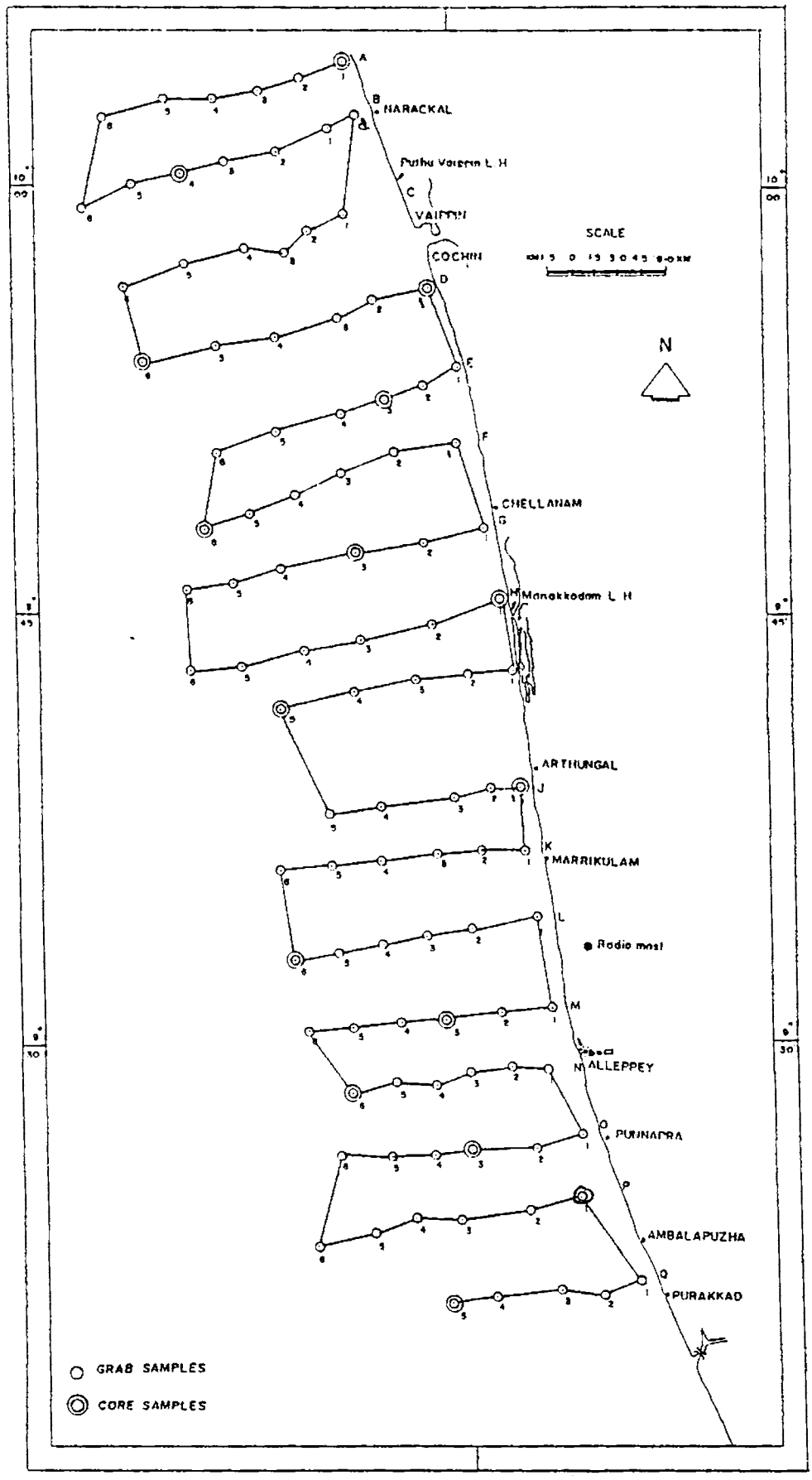

Fig. 1.4 Cruise track and sampling locations

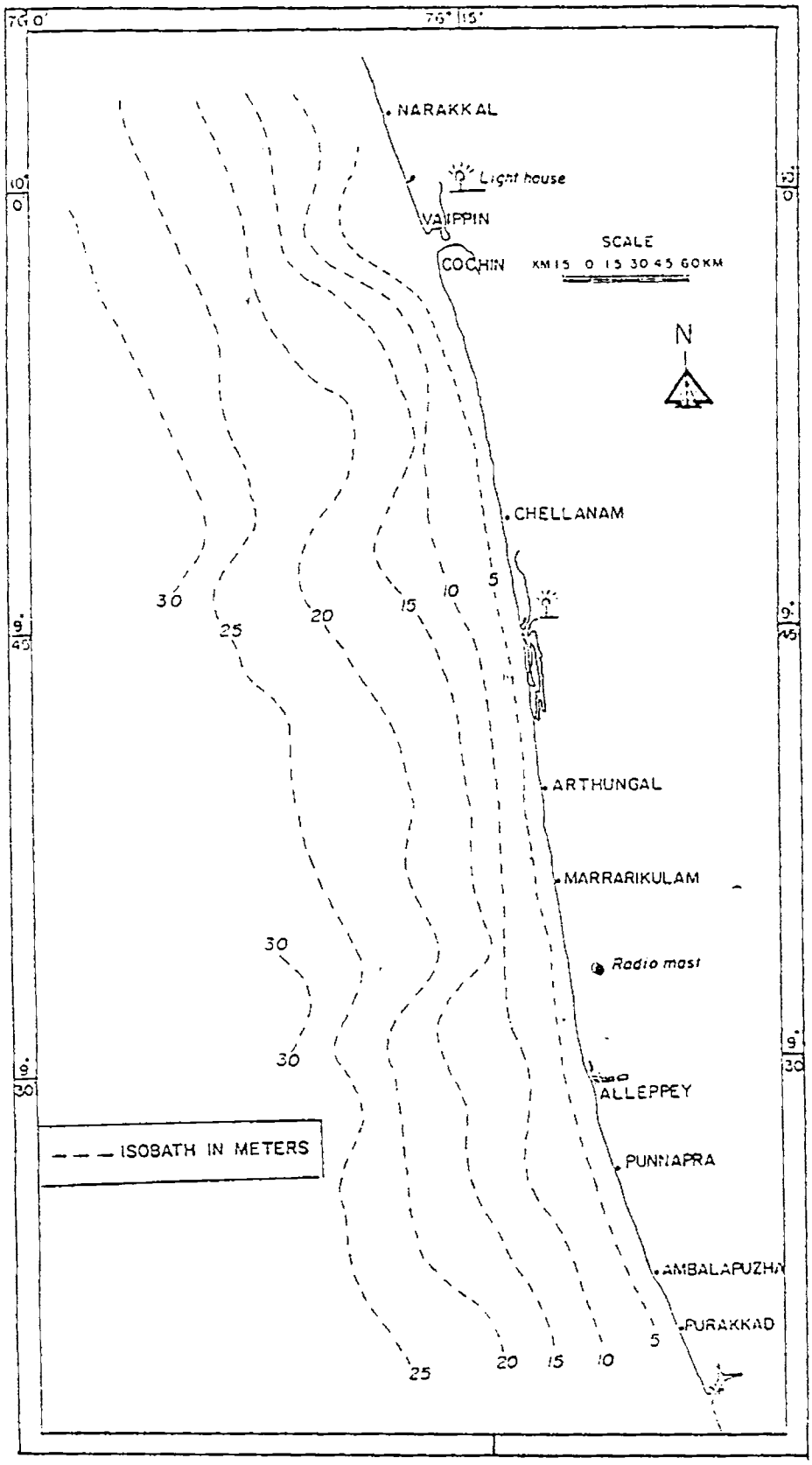

Fig. 1.5 Bathymetric map of the innershelf area

this sector. The innershelf and nearshore bathymetry show considerable variability parallel to the coast. The gradient of the innershelf shows slight increase from the northern part of the study area towards the southern part viz, from Cochin to Alleppey. The average slope of the shelf is 0°8.5'. The 100 fathom line kinks sharply seaward in line with the harbour entrance channel (Rama Raju, 1973). The depths of 10, 20 and 30 m are encountered at 4.8, 13.1 and 20.7 km distance from the shoreline off Cochin; and 3.5, 11.5 and 18.0 km off Alleppey. Though there is an initial increase in the gradient up to 10 m from the coast at Cochin and Alleppey (2.08 X 10^{-3} and 2.86 X 10^{-3} respectively), the gradient decreases further in the offshore direction. At 30 m isobath, the gradient becomes gentler with off Cochin and Alleppey recording 1.78 X 10^{-3} and 1.96 X 10^{-3} respectively.

CHAPTER 2

TEXTURE OF THE INNERSHELF SEDIMENTS

2.1 INTRODUCTION

During the past four to five decades the subject of sedimentology has made a steady progress. Scanning of the extensive literature illustrates the various attempts to use grain size as a tool to determine depositional characteristics in different sedimentary environments. Our understanding on the physical processes of deposition in various environments has reasonably improved, wherein interpretation of sedimentary deposit of unknown origin is made easier with its textural attributes.

The earliest task of the sedimentologists was to have a system by which the continuous distribution of particle size can be sub-divided into discrete class intervals or 'grades'. Udden (1914) proposed a grade scale to physically categorise the sediments into different size classes. Wentworth (1922) modified the Udden grade scale, which was widely applied in the grain size analysis in later years.

Statistical methods viz., graphic and moment measures were proposed to effect the interpretation of size frequency distribution. Trask (1930) introduced a measure of central tendency (median) and sorting coefficients based on quartile values of frequency distribution. Concept of log-normal distribution of grain size was proposed by Krumbein (1937, 1938). Krumbein (1938) also suggested logarithmic transformation of size from the metric system by expressing the grain size in 'phi' (ϕ) notation and which is having better comparability with Wentworth's grade scale.

Following Trask's (1930) method, several graphic measures were introduced. As a measure of dispersion, Griffiths (1951), proposed phi percentile deviation, which is more sensitive to fluctuations in the tails of distribution. Inman (1952) computed the mean, median and sorting measure by using different percentiles. He also recognised that the error of observation associated with each percentile values increases towards the tail of the distribution.

The most significant study in the development of the graphic measures was introduced by Folk and Ward (1957). They proposed formulae for calculation of inclusive graphic mean, standard deviation, skewness and kurtosis based on 7 (5, 16, 25, 50, 75, 84 and 95) percentiles derived from the cumulative probability curves. They also provided verbal scales for sorting, skewness and kurtosis for comparison of sediment types from different environments. McCammon (1962) suggested graphic percentile formulae for mean and sorting, by comparing the efficiencies of different measures existing then. Though the statistical efficiency of McCammon's method imparts an index of precision to the graphic measures, the method is being rarely applied as it is cumbersome due to the large number of percentile values involved in its computation. However, most of the sedimentologists still widely use the method of Folk and Ward (1957) for computing graphic measures because of its simplicity.

Friedman (1961, 1962, 1967) introduced moment measures by determining the moments of each size class. Successive higher moments are obtained by raising the distance term to progressively higher powers. Friedman (1967) argued that moment measures can represent the entire size-frequency spectrum and would be more effective than the graphic measures in

delineating environments. Unlike Folk and Ward (1957), the lack of descriptive terminologies (verbal scales) for comparing different parameters in this method makes it difficult to relate sedimentary deposits in terms of their textural attributes.

Utilising the grain-size distribution trends, Passega (1957) attempted to identify the hydrodynamic control of deposition in a variety of modern and ancient environments. Passega (1957) introduced the CM diagram, in which C is the one percentile of the grain-size distribution and M the median of a deposit, which can indicate mechanisms of sediment deposition in different environments.

Though there are several methods for computing the grain size measures, fruitful interpretation techniques using the parameters to delineate environments of deposition and transportational processes are not yet fully satisfactory. One of the major problems in the analysis of grain size distribution is that the same sedimentary processes could occur within a number of environments with similar consequent textural responses. Hence, Visher (1967) stressed the need for a genetic interpretation of sediment texture, with the basic assumption that, the distribution is multi-component in most sediments. Each size component is related to a fundamental population of grains or a mode of transport. Identifying individual log-normal size distribution of sub-population and relating it to different modes of sediment transport and deposition would provide insight into the genesis of the sediment unit. Visher (1969) identified three modes of transport, viz., surface creep or rolling, saltation and suspension.

Manifestations of dispersal pattern and trend of transportation of sediments based on size frequency distribution and textural parameters were attempted by many workers. Booth (1973) utilised the polynomial trend surface maps of moment measures to study the dispersal pattern of sediments. Establishing regional sediment-dispersal system from isopleth maps of moment measures, modal diameters, silt/mud and silt/clay ratios were attempted by Shideler (1973, 1978). Mazullo and Crisp (1985) worked out sediment trends from textural significance and grain shape aspects. Progressive trends by comparing grain-size moment statistics were found to have an effective bearing on transportation pattern of sediments (McLaren and Bowels, 1985).

The models and methods described above are only a few significant ones and not exhaustive. Based on some of these methods, interpretation of the textural data of the sediments collected from the innershelf zone is contemplated. Studies of modern sediment dispersal system in continental shelves became an active field of research throughout the world (Milliman *et al.*, 1982; Nittrouer and DeMaster, 1986; Park *et al.*, 1986; Hill and Nadeau, 1989). Effective assessment of the regional sediment transport phenomenon will sink the confusion and concern about the physical processes operating in the shelf. This is compounded by wide variety of purposes such as plankton productivity, contaminant transfer, substrate respiration and others apart from an environmental stand point. Keeping the above aspects in view, the objectives of the textural study are to:

i. document the textural composition of the surficial sediments,

ii. interpret the granulometric properties in terms of physical processes of sediment transport and deposition, and

iii. resolve the paradoxes of modern and relict sedimentation which would shed light on the admixtured sediment distribution pattern in the shelf.

2.2 METHODS

The innershelf sediments are composed of varying proportions of sand, silt and clay. Therefore, the textural analysis of samples were carried out by sieving and pipette method (Carver, 1971). Samples were subjected to preliminary treatment with dilute hydrochloric acid and hydrogen peroxide to remove shell fragments and organic matter, as they interfere in the settling of particles. Sieve analysis was undertaken for fractions above 4 ϕ size in a Rotap sieve shaker for 15 minutes at 1/2 ϕ interval. Pipette analysis was conducted for less than 4 ϕ fractions of sediments till 11 ϕ using sodium hexametaphosphate as a dispersing agent. For computation of size parameters, values were extrapolated linearly beyond 11 ϕ, by considering 14 ϕ as the finest range for particles (Folk and Ward, 1957).

Seventeen core samples collected from the area were also subjected to granulometric studies. Core liners (PVC pipe) were cut open using a indigenously fabricated core cutting machine (Mallik, 1986a), without causing disturbance to the sediment column inside. Sub-sampling was done approximately at 10 cm interval. Only sand, silt and clay content were studied for these cores (103 sub-samples).

The sand fraction separated from selected surficial samples were subjected to scanning electron microscopic (SEM) study. Sands below 1 mm diameter were chosen and were treated with dilute HCl and $SnCl_2$ to remove

carbonates and iron coatings. They were examined under a binocular microscope and about 15 quartz grains of varying size and shape were selected. Using a double sided adhesive tape, grains selected from each sample were mounted on sample stubs and were subsequently gold coated in a standard vacuum evaporator. Grains were scanned using a Cambridge Stereo Scan Microscope S4-10, in the emissive mode.

2.3 RESULTS

2.3.1 Sediment Size

Grain size components (sand, silt and clay) vary widely (Table 2.1). The sediments show various levels of mixing, thus exhibiting a heterogeneity in the percent constituents of different textural grades. The following section describes the variation in the distribution of three size grades.

Sand: Sand content in the study area shows a wide range from 0.18 to 99.38 %. Majority of the samples (67 %) contain < 20 % sand with a secondary mode of 16 % containing > 80 % sand. Frequency percent distribution of sand is depicted in the Fig. 2.1a. The spatial distribution shows some defined pattern (Fig. 2.2). A linear extensive stretch in the southwestern part shows high amount of sand. Similarly, the northwest portion also shows a higher concentration of sand, which may probably be the lateral extension of the southwestern patch. Pockets of high sand content are observed sporadically, like the one bordering the Manakkodam area. A sand depleted zone amidst the sand rich band in the southwest part is also observed.

TABLE 2.1

Sand-silt-clay Percentages of the Innershelf Samples

Sl.	Sample	Sand (%)	Silt (%)	Clay (%)	Texture Description
1	A1	0.67	34.66	64.67	Silty Clay
2	A2	19.21	57.61	23.18	Clayey Silt
3	A3	1.45	31.32	67.23	Silty Clay
4	A4	0.66	48.33	51.01	Silty Clay
5	A5	0.96	34.53	64.51	Silty Clay
6	A6	1.48	54.08	44.44	Clayey Silt
7	Ba	0.51	30.95	68.54	Silty Clay
8	B1	17.26	49.31	33.43	Clayey Silt
9	B2	0.90	41.29	57.81	Silty Clay
10	B3	0.85	55.40	43.75	Clayey Silt
11	B4	1.40	37.50	61.10	Silty Clay
12	B5	1.01	64.12	34.87	Clayey Silt
13	B6	99.38	0.16	0.46	Sand
14	C1	4.82	56.05	39.13	Clayey Silt
15	C2	1.33	46.53	52.14	Silty Clay
16	C3	0.78	59.57	39.65	Clayey Silt
17	C4	0.34	30.66	69.00	Silty Clay
18	C5	0.98	37.36	61.66	Silty Clay
19	C6	80.90	12.58	6.52	Sand
20	D1	7.98	44.94	47.08	Silty Clay
21	D2	0.96	35.34	63.70	Silty Clay
22	D3	47.19	21.06	31.75	Sand-silt-clay
23	D4	1.60	33.77	64.63	Silty Clay
24	D5	0.58	35.97	63.45	Silty Clay
25	D6	13.64	35.09	51.27	Silty Clay
26	E1	31.56	28.92	39.52	Sand-silt-clay
27	E2	7.17	56.02	36.81	Clayey Silt
28	E3	1.46	42.59	55.95	Silty Clay
29	E4	0.69	37.77	61.54	Silty Clay
30	E5	1.43	35.71	62.86	Silty Clay
31	E6	1.71	65.02	33.27	Clayey Silt
32	F1	58.04	14.12	27.84	Clayey Sand
33	F2	0.93	66.59	32.48	Clayey Silt
34	F3	3.78	38.19	58.03	Silty Clay
35	F4	0.60	42.22	57.18	Silty Clay
36	F5	1.66	42.52	55.82	Silty Clay
37	F6	0.42	52.36	47.22	Clayey Silt
38	G1	18.58	43.73	37.69	Clayey Silt
39	G2	6.89	78.27	14.84	Silt
40	G3	1.15	43.62	55.23	Silty Clay
41	G4	2.99	44.26	52.75	Silty Clay
42	G5	1.24	40.55	58.21	Silty Clay
43	G6	2.46	70.89	26.65	Clayey Silt
44	H1	57.90	24.40	17.70	Silty Sand
45	H2	25.20	42.59	32.21	Sand-silt-clay
46	H3	7.65	42.10	50.25	Silty Clay
47	H4	7.39	39.19	53.42	Silty Clay
48	H5	28.55	28.28	43.17	Sand-silt-clay
49	H6	91.63	5.18	3.19	Sand

Contd.....

Sl.	Sample	Sand (%)	Silt (%)	Clay (%)	Texture Description
50	I1	35.64	32.93	31.43	Sand-silt-clay
51	I2	1.00	37.97	61.03	Silty Clay
52	I3	4.61	35.55	59.84	Silty Clay
53	I4	17.73	39.84	42.43	Silty Clay
54	I5	13.13	33.36	53.51	Silty Clay
55	J1	3.43	43.76	52.81	Silty Clay
56	J2	0.46	39.54	60.00	Silty Clay
57	J3	2.93	40.79	56.28	Silty Clay
58	J4	37.28	26.29	36.43	Sand-silt-clay
59	J5	96.09	2.53	1.38	Sand
60	K1	0.63	31.09	68.28	Silty Clay
61	K2	0.33	37.20	62.47	Silty Clay
62	K3	4.25	47.29	48.46	Silty Clay
63	K4	28.50	29.96	41.54	Sand-silt-clay
64	K5	87.66	7.76	4.58	Sand
65	K6	75.51	14.85	9.64	Sand
66	L1	21.68	30.84	47.48	Sand-silt-clay
67	L2	65.11	15.44	19.45	Clayey Sand
68	L3	92.02	5.94	2.04	Sand
69	L4	92.04	5.87	2.11	Sand
70	L5	0.90	42.60	56.50	Silty Clay
71	L6	78.42	12.47	9.11	Sand
72	M1	0.18	34.32	65.50	Silty Clay
73	M2	0.18	36.69	63.13	Silty Clay
74	M3	5.94	45.97	48.09	Silty Clay
75	M4	13.88	32.49	53.63	Silty Clay
76	M5	93.83	4.02	2.15	Sand
77	M6	59.93	18.58	21.49	Clayey Sand
78	N1	1.39	37.25	61.36	Silty Clay
79	N2	18.50	39.92	41.52	Silty Clay
80	N3	93.19	4.12	2.69	Sand
81	N4	96.27	2.13	1.60	Sand
82	N5	92.26	5.40	2.30	Sand
83	N6	67.16	23.20	9.61	Silty Sand
84	O1	3.95	43.66	52.39	Silty Clay
85	O2	5.24	46.86	47.90	Silty Clay
86	O3	1.16	36.16	62.68	Silty Clay
87	O4	96.71	2.61	0.68	Sand
88	O5	98.79	1.21	0.00	Sand
89	O6	95.09	2.84	2.07	Sand
90	P1	1.24	35.64	63.12	Silty Clay
91	P2	7.84	45.38	46.78	Silty Clay
92	P3	94.75	3.46	1.79	Sand
93	P4	16.11	37.44	46.45	Silty Clay
94	P5	79.25	7.54	13.21	Sand
95	P6	96.01	2.42	1.57	Sand
96	Q1	23.91	31.45	44.64	Sand-silt-clay
97	Q2	6.15	43.36	50.49	Silty Clay
98	Q3	2.57	47.71	49.72	Silty Clay
99	Q4	4.75	49.07	46.18	Silty Clay
100	Q5	3.96	47.80	48.24	Silty Clay

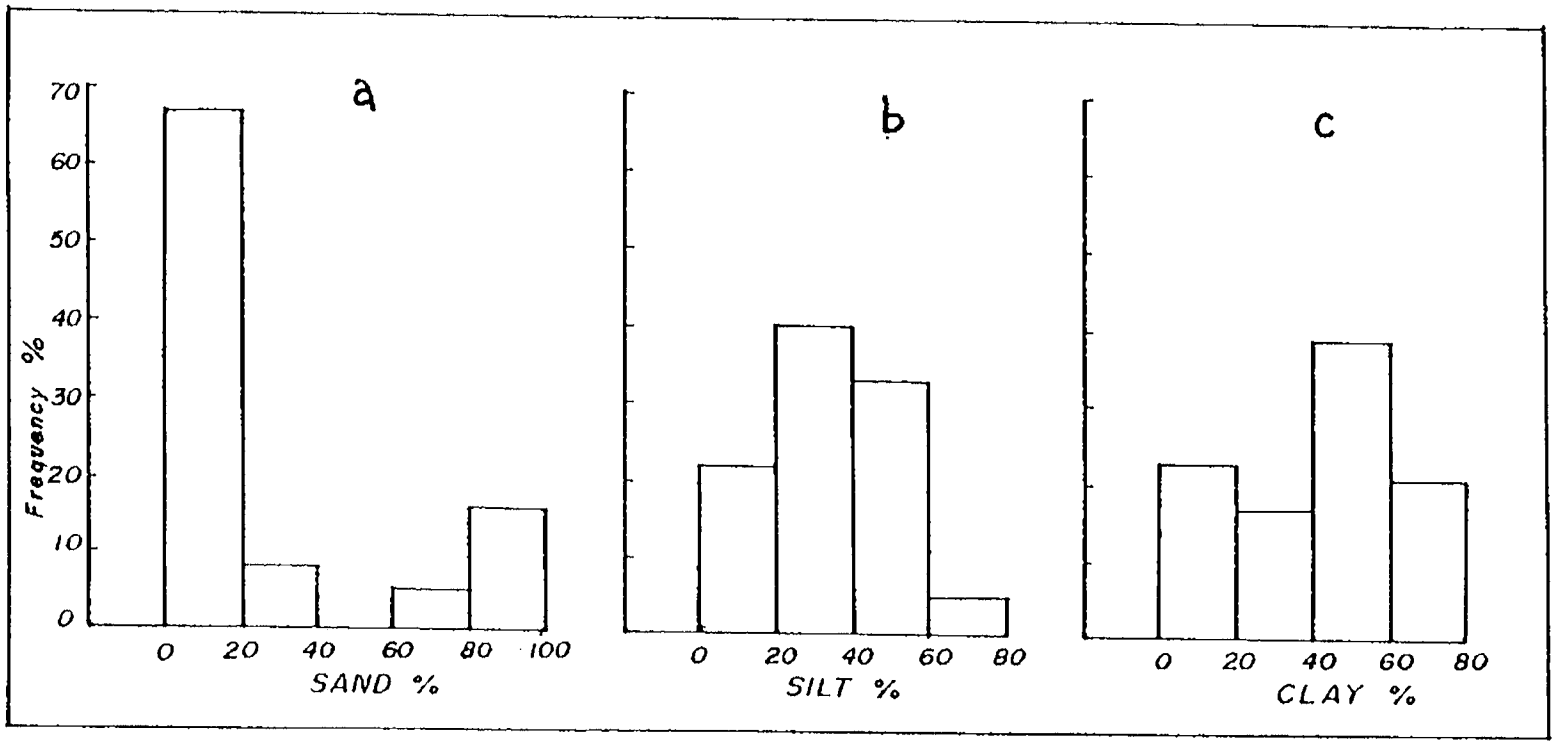

Fig. 2.1 Frequency distribution of (a) sand, (b) silt and (c) clay percentage among samples

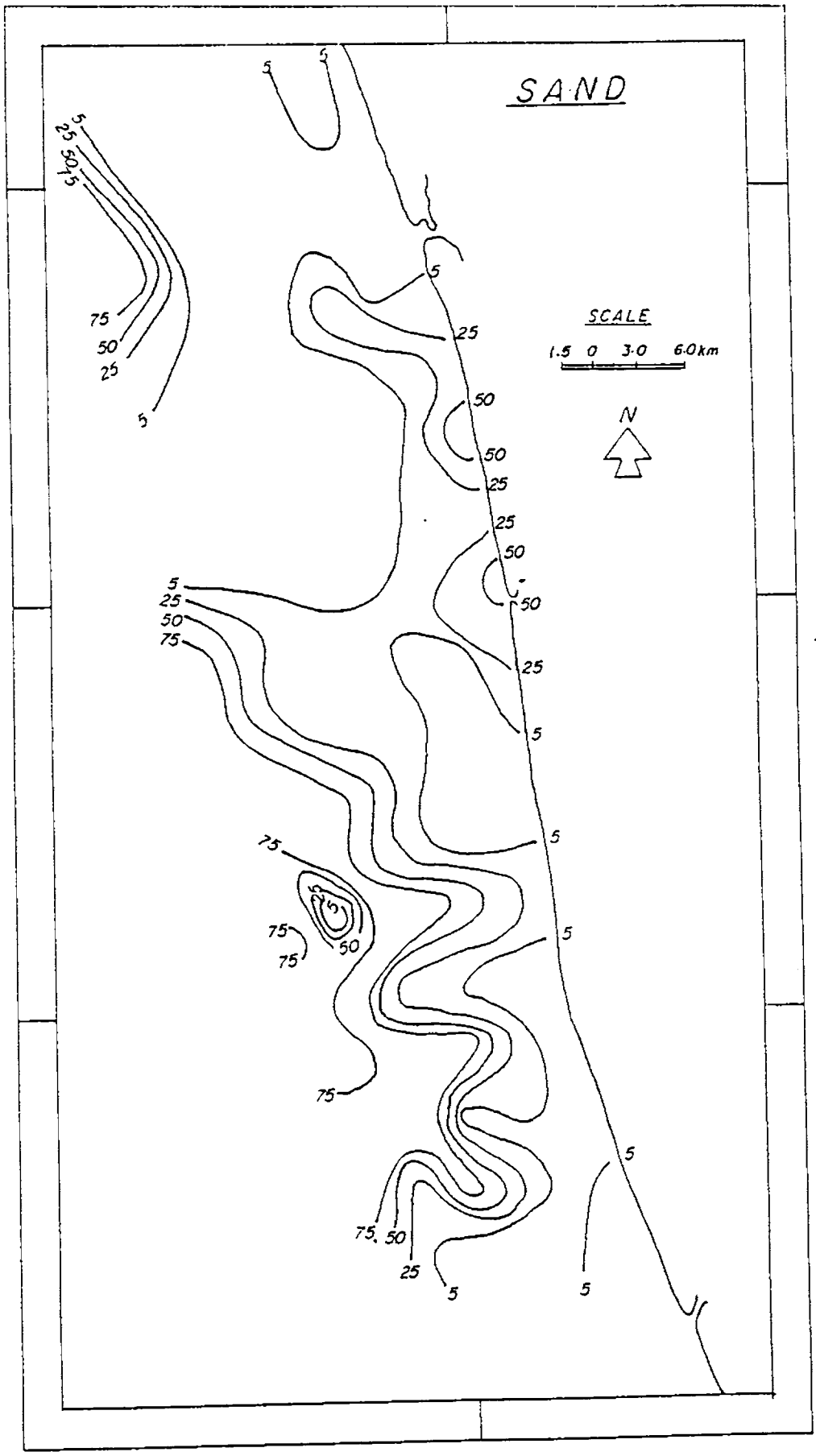

Fig. 2.2 Spatial distribution of sand percentage

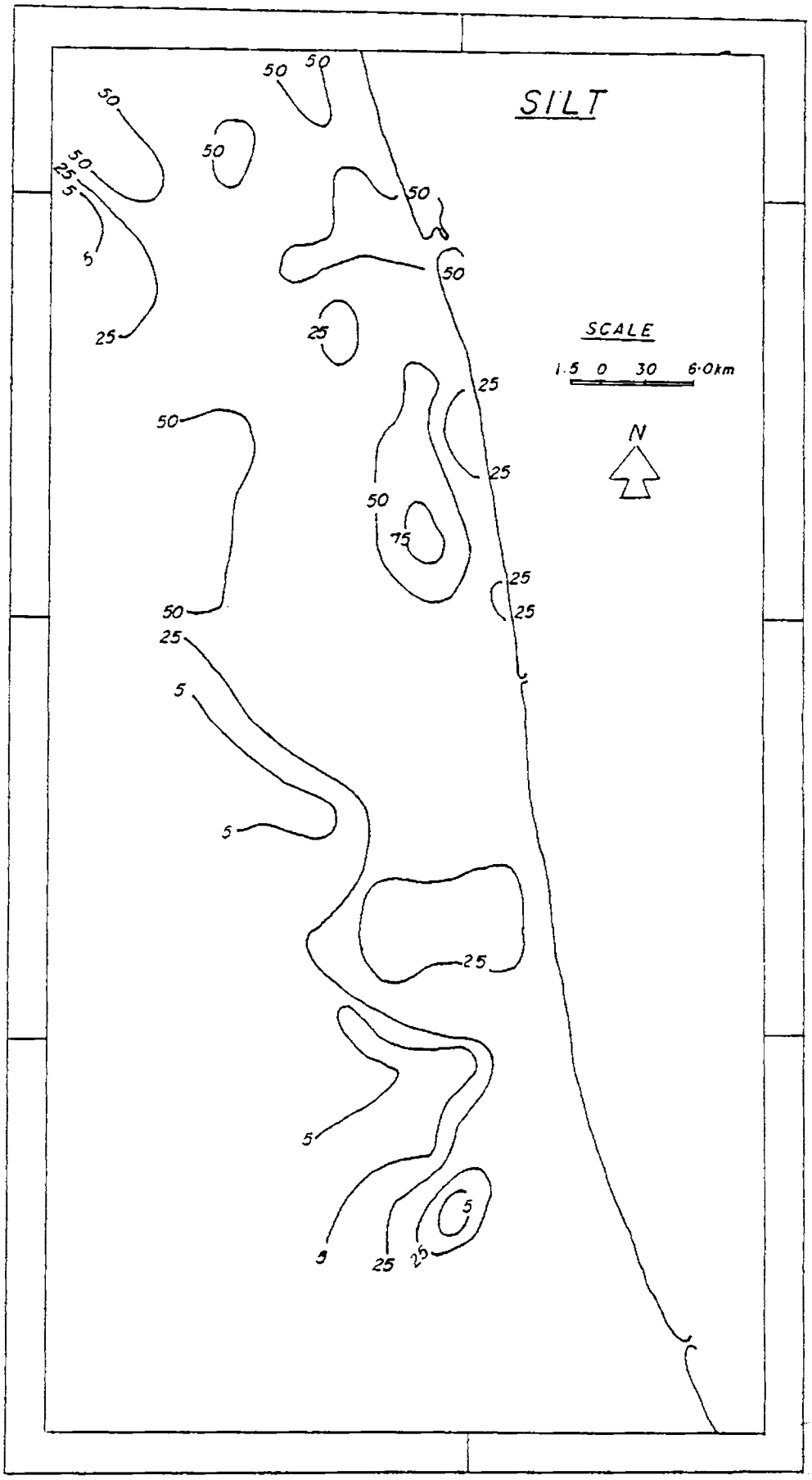

Fig. 2.3 Spatial distribution of silt percentage

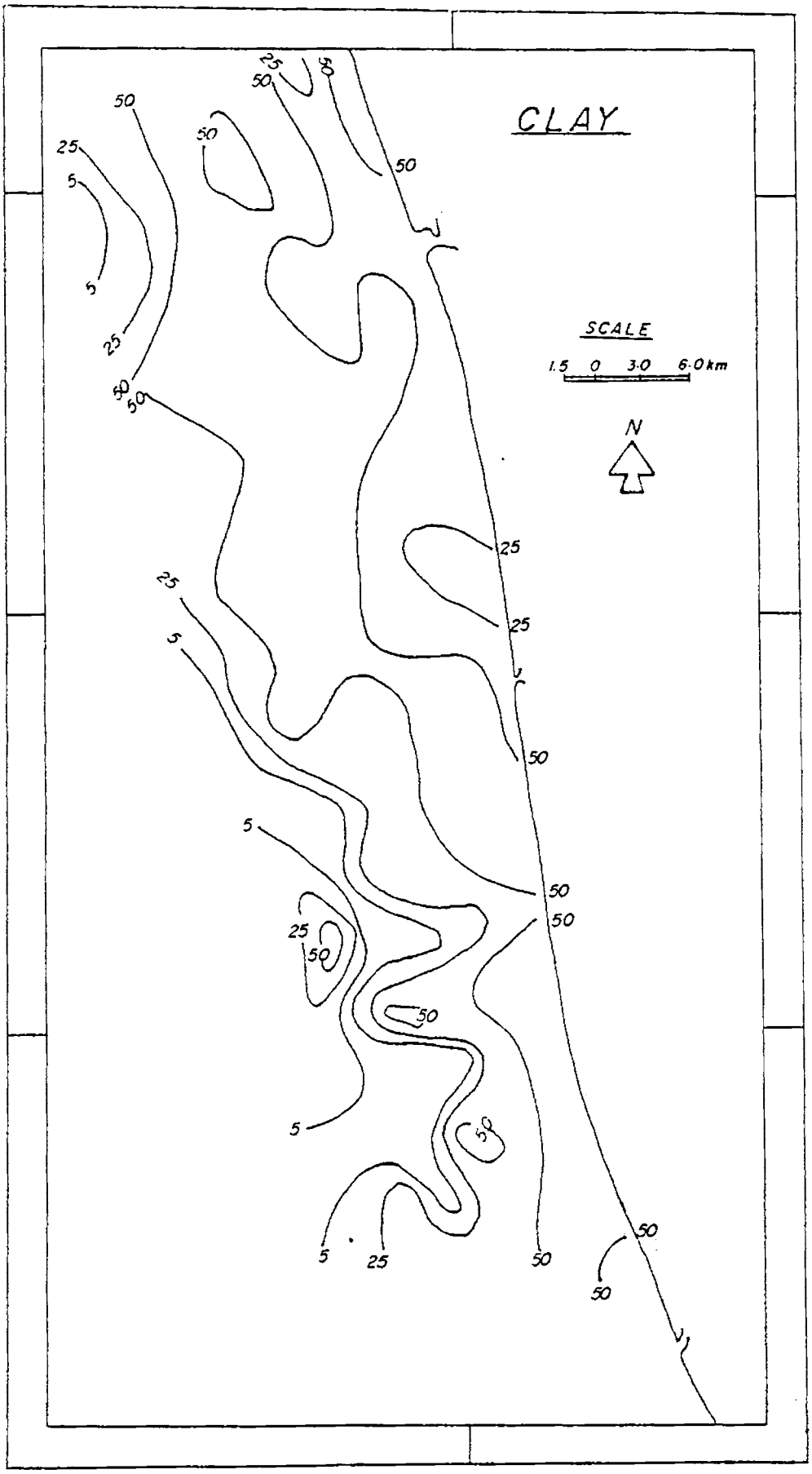

Fig. 2.4 Spatial distribution of clay percentage

Silt: Silt is present considerably in all the samples and it varies from 0.16 to 78.27 %. Percent variation of silt shows that about two fifth of the total samples contain 20 to 40 % silt (Fig. 2.1b). About one third of the samples show silt content between 40 and 60 %. Only 5 % of the samples show a silt exceedence of 60 % and about one fifth (22 %) are poor in silt content, that is, less than 20 % of silt. Patches of low and high concentration of silt are distributed sporadically all over the area (Fig. 2.3). However, the distribution of silt do exhibit some specific pattern of distribution in this area.

Clay: Clay content varies between 0 and 69 %. Clay-rich zones are more common than the other two size grades. Frequency distribution of clay shows bimodal distribution (Fig. 2.1c). A large number of samples (39 %) show higher content of clay (40 - 60 %) followed by 23 % of samples showing less than 20 % clay. Clay content with a range of 20 to 40 % is recorded only in 17 % samples. More than one fifth of the samples shows very high clay percentage (> 60 %). The aerial variation of clay shows a definite pattern with an inverse relationship to the distribution of sand (Fig. 2.4). Depletion of clay content starts at a lower depth in the southern side, compared to north. There is an elongated patch of clay rich zone, extending from south of Manakkodam to the northwest direction.

2.3.2 Sediment Distribution

The textural compositions according to the nomenclature proposed by Shepard (1954) are given in the Table 2.1 and the ternary diagram, in Fig. 2.5. The spreading of the sample points from the sand corner to the clay-silt line indicates different levels of sediment mixing. Table 2.1 shows

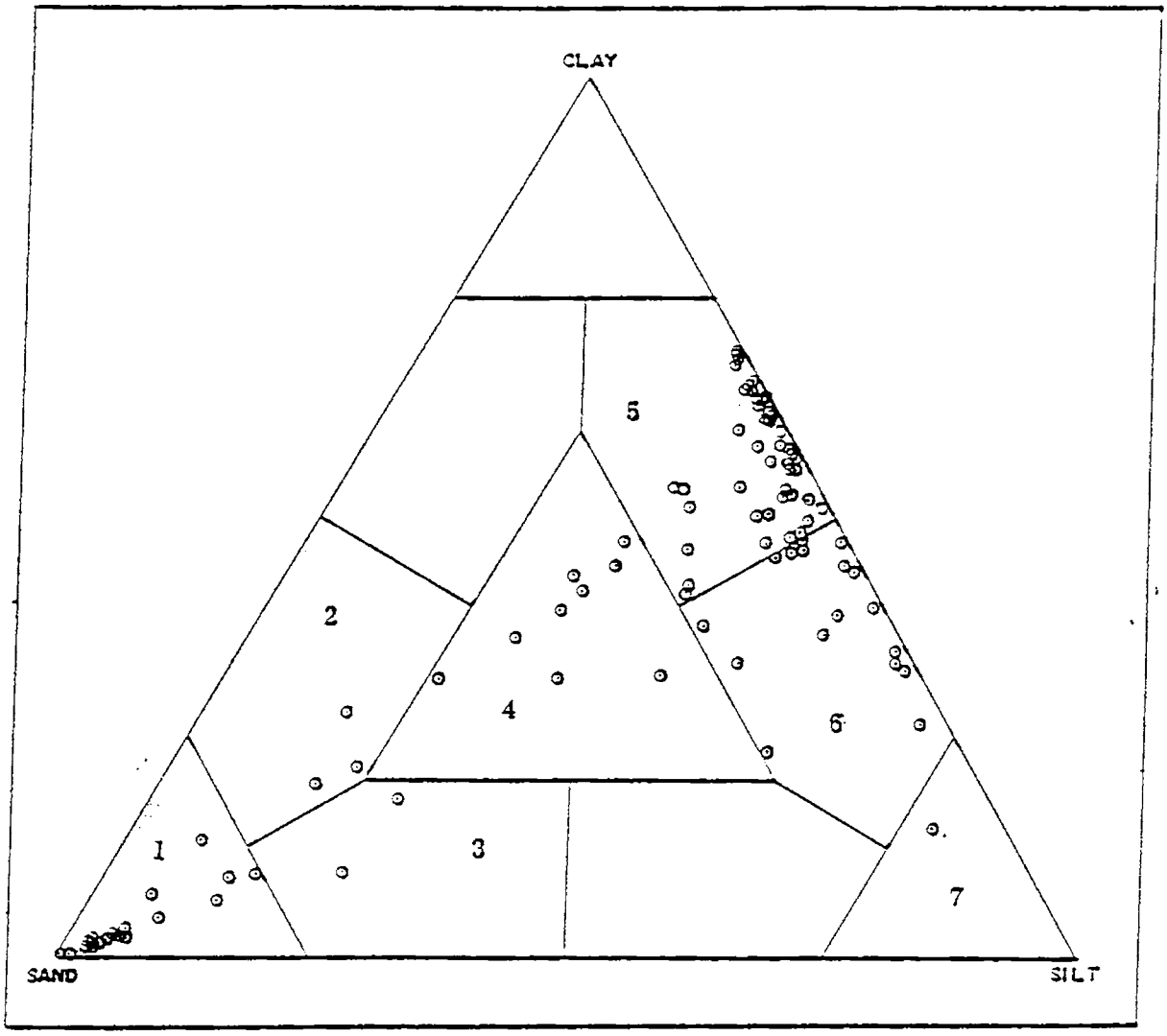

Fig. 2.5 Ternary plot of sand-silt-clay proportions

1 - Sand; 2 - Clayey sand; 3 - Silty sand;
4 - Sand-silt-clay; 5 - Silty clay
6 - Clayey silt; 7 - Silt.

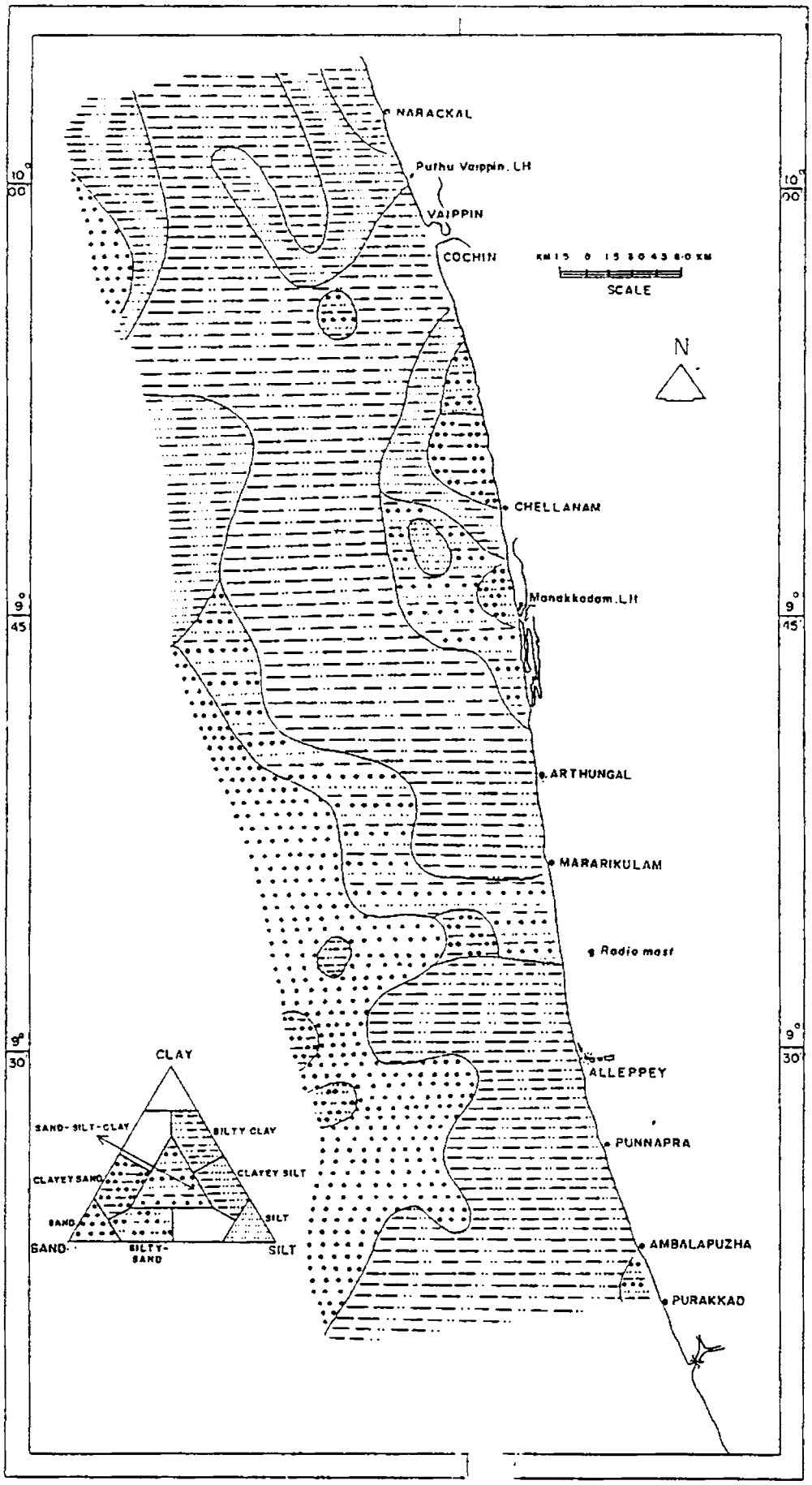

Fig. 2.6 Distribution of sediment types

that maximum number of samples fall within the silty clay zone (53/100). Sand is the next predominant class (19/100) followed by clayey silt (13/100). Sub-equal proportions of the three textural grades (sand-silt-clay) are found only in 9 samples. Clayey sand, silty sand and silt sediments are very few in number.

The distribution pattern of the sediment types (Fig. 2.6) shows the spatial dominance of silty clay sediments. A sand-rich zone occurs in the southwestern part of the area. In the northwestern part a small patch of sand is bordered by a clayey silt patch. Near Manakkodam area the silty sand zone is bordered by a sand-silt-clay horizon. The sand-rich zone in the southwestern part is followed by a sand-silt-clay and silty clay zone, indicating a progressive fining of the sediments shoreward. Sporadic occurrences of small patches of silt, clayey sand, sand-silt-clay and silty sand are also observed.

2.3.3 Size Parameters

To understand the environmental significance of the sediment deposit and spatial variation in the physical properties, grain size parameters were determined. Graphic parameters (Folk and Ward, 1957), namely, mean, standard deviation, skewness and kurtosis are used here to describe the textural significance (Table 2.2).

Mean size: The mean size values range between 1.29 and 9.63 ϕ. Such variations are attributed to the admixture of sand, silt and clay in different proportions. The histogram (Fig. 2.7a) reveals bimodality of the deposit in the phi ranges 8 to 10 and 2 to 4 respectively. The aerial variation of mean size

TABLE 2.2

Size Parameters of the Innershelf Sediment Samples (Graphic Measures)

Sl. No.	Sample No.	Mean	Standard Deviation	Skewness	Kurtosis
1	A1	8.80	3.24	-0.21	0.76
2	A2	6.47	3.35	0.65	1.22
3	A3	9.10	3.25	-0.09	0.76
4	A4	8.32	3.21	0.15	0.68
5	A5	8.95	3.18	0.00	0.70
6	A6	7.62	2.94	0.26	0.64
7	Ba	9.24	3.09	-0.09	0.83
8	B1	6.85	3.52	0.66	0.74
9	B2	8.98	3.20	-0.06	0.66
10	B3	7.83	3.04	0.34	0.66
11	B4	8.98	3.15	-0.06	0.66
12	B5	7.58	3.05	0.50	0.81
13	B6	1.54	0.65	0.23	1.32
14	C1	7.57	3.07	0.38	0.73
15	C2	8.50	3.26	0.15	0.67
16	C3	7.15	2.76	0.59	0.67
17	C4	9.35	2.78	-0.30	0.85
18	C5	9.08	3.02	-0.11	0.81
19	C6	3.13	1.71	0.69	3.82
20	D1	7.58	2.99	0.14	0.77
21	D2	9.07	2.80	-0.03	0.93
22	D3	5.55	4.24	0.37	0.75
23	D4	9.10	3.07	-0.16	0.79
24	D5	9.30	3.05	-0.17	0.72
25	D6	8.22	3.60	0.04	0.64
26	E1	6.83	3.57	0.31	0.66
27	E2	7.13	2.80	0.30	0.91
28	E3	8.45	3.10	0.02	0.82
29	E4	8.65	2.75	-0.03	0.86
30	E5	9.33	2.85	0.06	0.67
31	E6	7.34	2.86	0.42	0.69
32	F1	6.12	3.59	0.85	0.84
33	F2	7.81	3.21	0.50	0.93
34	F3	8.92	3.08	0.06	0.56
35	F4	8.93	2.97	0.22	0.76
36	F5	9.07	3.19	-0.04	0.60
37	F6	8.51	3.02	-0.05	0.78
38	G1	7.15	3.52	0.55	0.65
39	G2	5.92	1.84	0.54	4.97
40	G3	8.75	3.26	0.07	0.57
41	G4	7.78	2.52	-0.30	0.72
42	G5	7.93	2.28	-0.10	1.27
43	G6	7.20	1.94	0.24	1.76
44	H1	5.13	2.48	0.81	2.29
45	H2	6.90	3.52	0.42	0.72
46	H3	8.52	3.13	0.15	0.67
47	H4	8.53	2.92	0.03	1.00
48	H5	6.77	3.38	0.14	0.62
49	H6	2.26	1.11	0.22	2.31

Contd...

Sl. No.	Sample No.	Mean	Standard Deviation	Skewness	Kurtosis
50	I1	6.47	3.41	0.36	0.76
51	I2	9.23	2.31	0.41	1.26
52	I3	8.35	3.10	0.15	0.77
53	I4	7.47	3.44	0.10	0.81
54	I5	8.42	3.32	-0.02	0.90
55	J1	8.60	2.94	0.18	0.86
56	J2	9.15	2.69	0.12	0.78
57	J3	9.63	3.11	-0.20	0.61
58	J4	6.13	3.82	0.21	0.66
59	J5	2.16	0.52	0.17	1.14
60	K1	9.58	2.80	0.10	0.69
61	K2	9.37	2.70	0.04	0.75
62	K3	8.37	3.22	0.25	0.65
63	K4	7.10	4.33	0.14	0.58
64	K5	2.87	1.11	0.47	2.67
65	K6	2.78	2.68	0.30	1.45
66	L1	7.68	3.97	0.01	0.72
67	L2	4.75	3.86	0.69	1.06
68	L3	2.51	0.98	0.23	1.92
69	L4	1.94	1.00	0.48	2.18
70	L5	9.22	2.86	0.02	0.74
71	L6	3.22	2.17	0.56	2.87
72	M1	9.58	2.55	0.02	0.75
73	M2	9.35	2.79	0.04	0.69
74	M3	8.15	3.20	0.24	0.71
75	M4	8.97	3.56	-0.15	0.84
76	M5	2.08	0.91	0.08	1.80
77	M6	5.23	3.42	0.78	1.12
78	N1	9.25	2.69	-0.04	0.81
79	N2	7.52	3.77	0.91	0.71
80	N3	2.45	0.66	0.24	1.96
81	N4	1.71	0.63	0.18	1.19
82	N5	2.62	0.79	0.09	2.25
83	N6	3.53	2.99	0.53	1.16
84	O1	8.48	3.04	0.12	0.78
85	O2	8.47	3.12	0.24	0.71
86	O3	9.50	2.71	-0.04	0.69
87	O4	1.72	0.57	0.18	1.42
88	O5	2.06	0.60	0.22	0.82
89	O6	1.29	0.91	0.51	1.61
90	P1	9.63	2.78	-0.12	0.69
91	P2	8.15	3.37	0.26	0.65
92	P3	2.01	0.65	0.43	2.35
93	P4	7.98	3.72	0.06	0.64
94	P5	3.53	3.14	0.65	3.22
95	P6	2.21	0.56	0.23	1.29
96	Q1	7.40	3.48	0.05	0.68
97	Q2	8.33	3.30	0.52	0.66
98	Q3	8.53	3.17	0.21	0.65
99	Q4	8.32	3.18	0.27	0.69
100	Q5	8.50	3.16	0.24	0.64

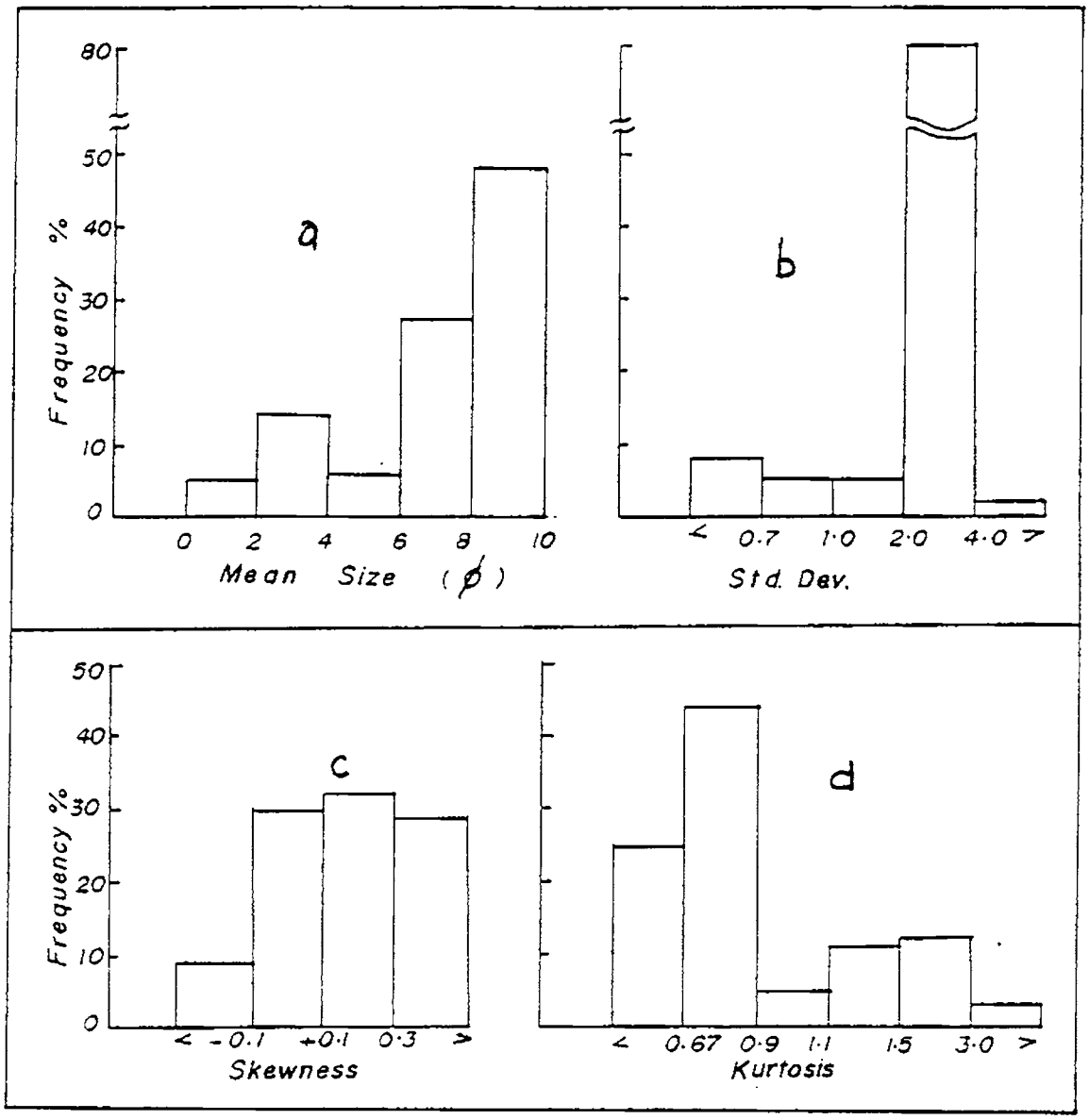

Fig. 2.7 Frequency distribution of size parameters among the samples

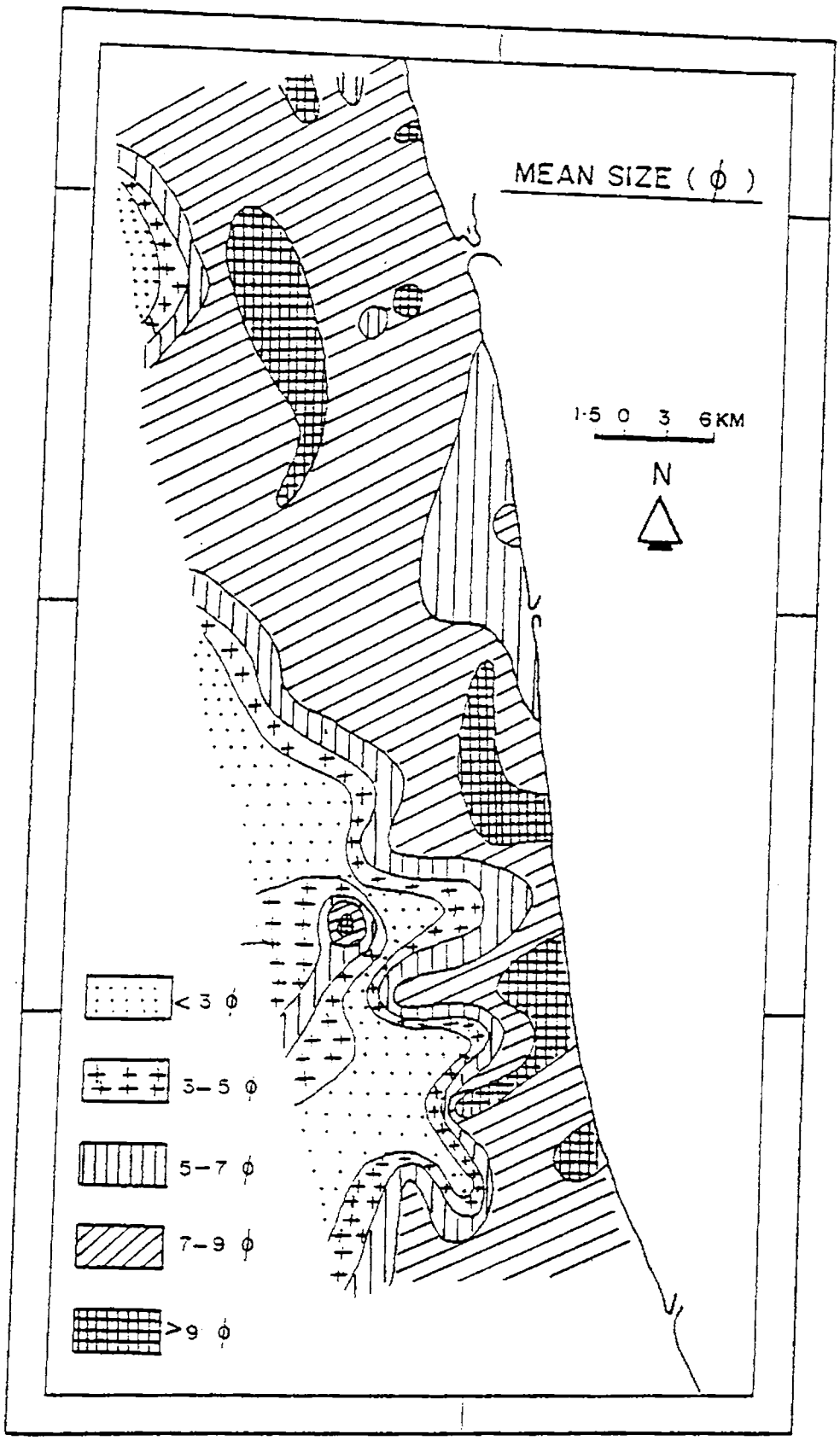

Fig. 2.8 Spatial distribution of mean size

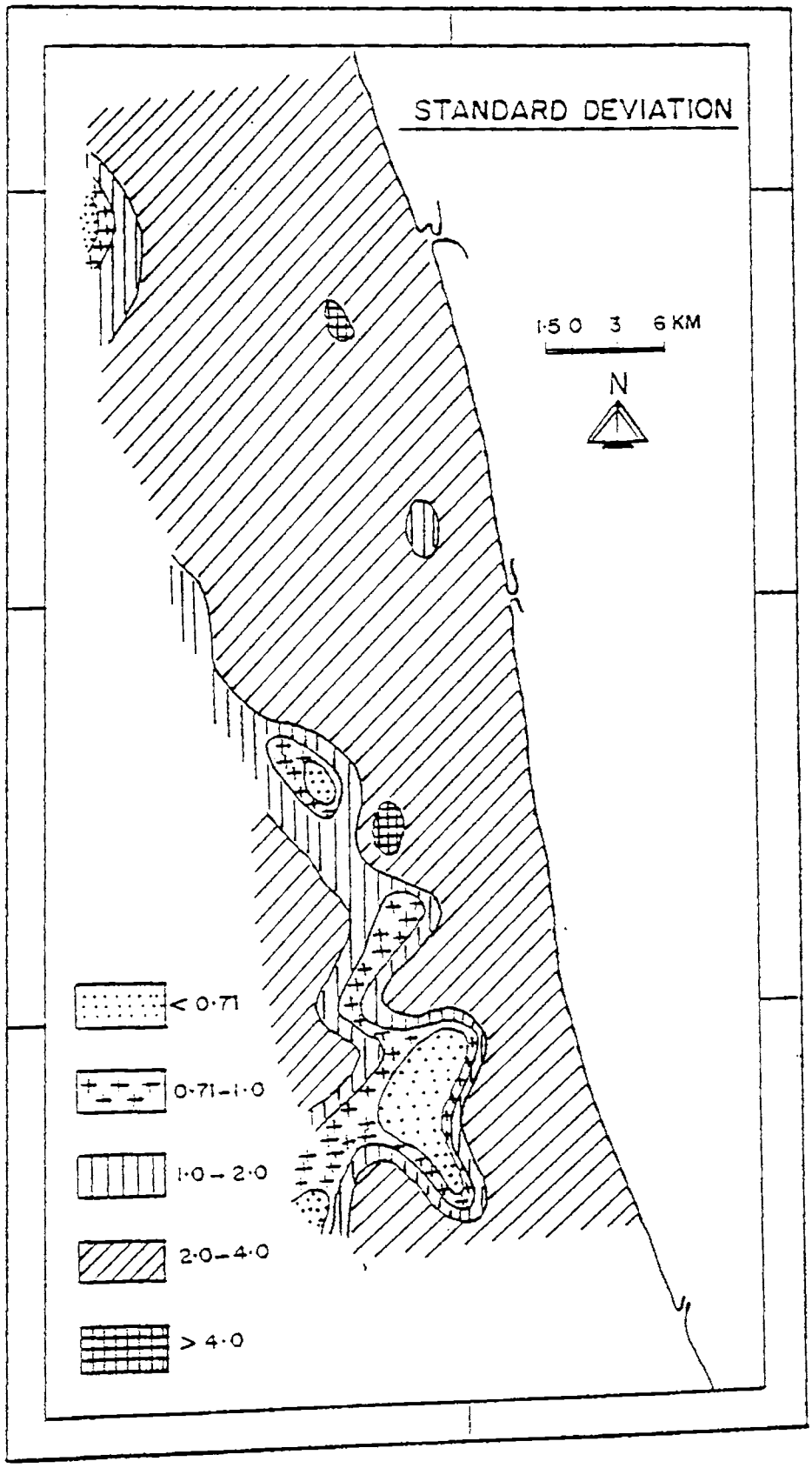

Fig. 2.9 Spatial distribution of standard deviation

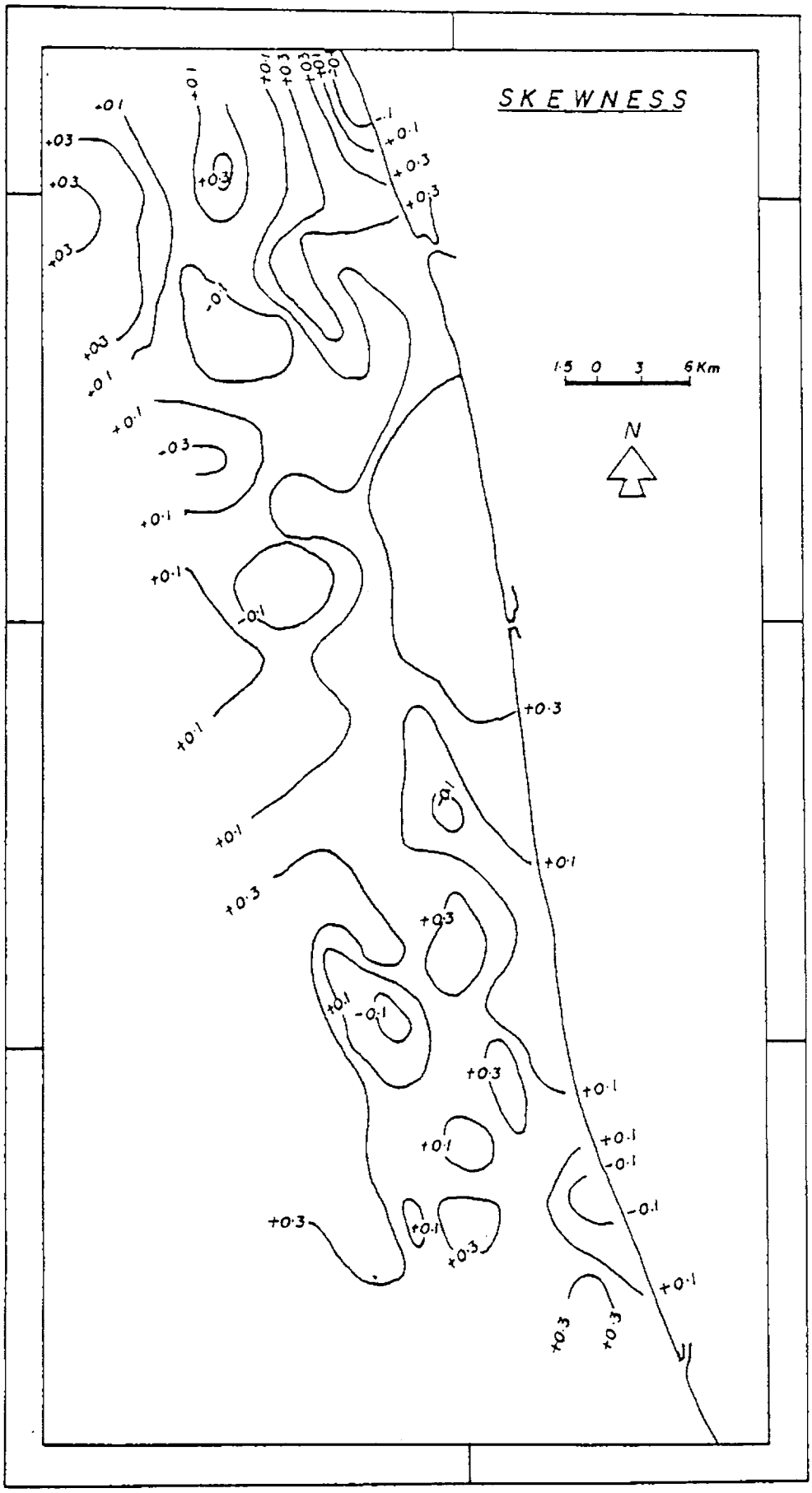

Fig. 2.10 Spatial distribution of skewness

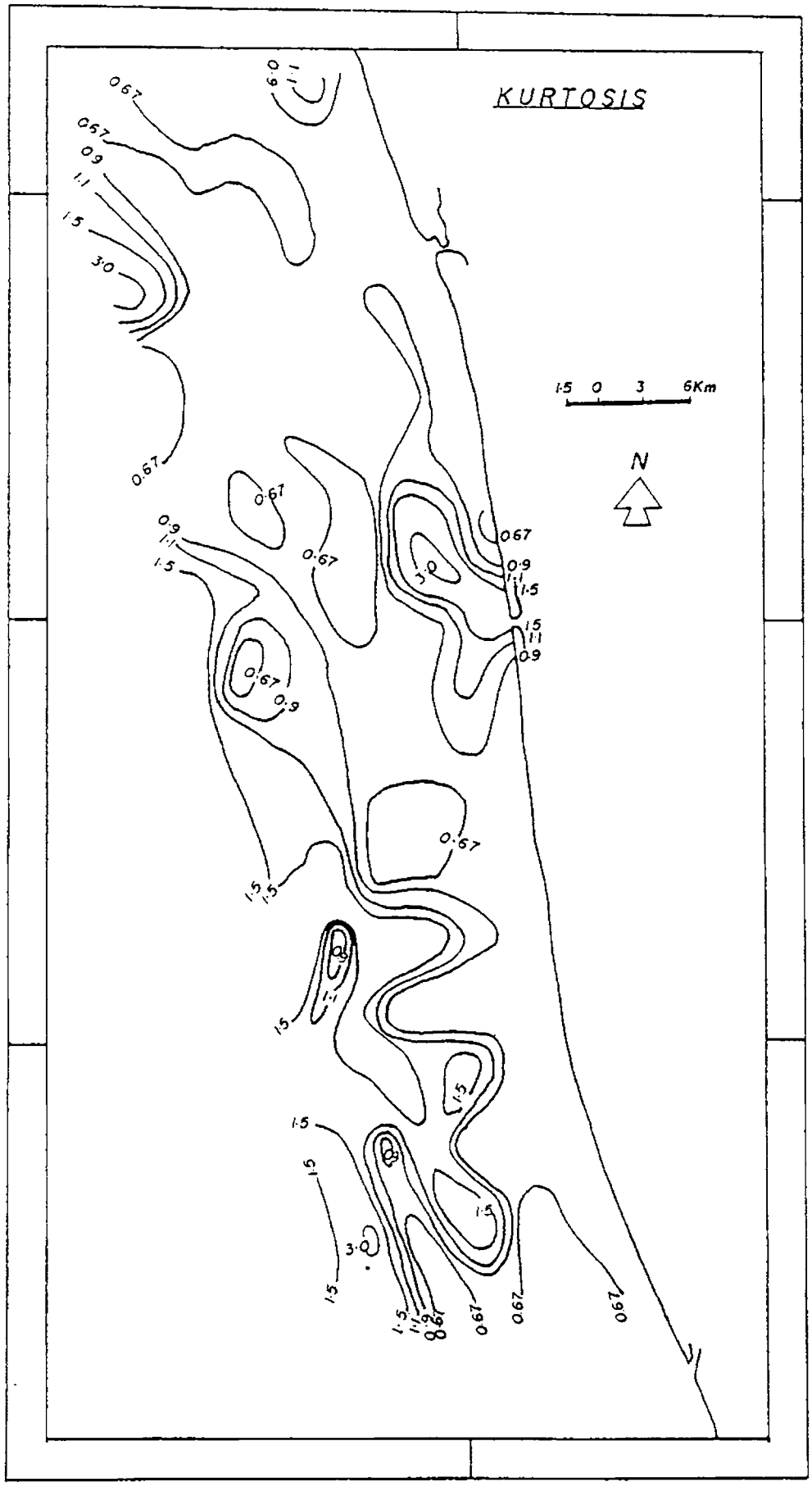

Fig. 2.11 Spatial distribution of kurtosis

(Fig. 2.8) shows that the mean sizes in the range of 7 and 9 ϕ are widely distributed. The southwest part of the innershelf is covered with coarser sediments of < 3 ϕ size. Transition zones from the finer phi values to coarser phi values demarcate mixed sediment size grades. In the northwestern portion a small patch contains sediments with smaller phi mean. Patches of high phi mean (> 9 ϕ), which represent clay-rich zones, are also seen.

Standard deviation: Sedimentologists use the standard deviation values as a measure of sorting of the sediments. In this study although the sorting ranges from moderately well sorted to extremely poorly sorted (0.52 to 4.33), maximum number of samples show standard deviation values between 2 and 4 (very poorly sorted; Fig. 2.7b). Samples of moderately, poorly and extremely poorly sorted are fewer in number. Sand-rich samples are moderately well sorted. With increasing amount of mud, sorting becomes poorer. The distribution pattern of the sorting coefficient shows that, the sediments in the southwestern and northwestern portions (sand-rich patches) are better sorted (Fig. 2.9). The two cross-hatched zones are covered with extremely poorly sorted sediments. The remaining area is covered with very poorly sorted sediments.

Skewness: The asymmetry of the central part of the distribution is assigned as skewness. Positive values of skewness indicate that the samples are having a tail of fines. Contrary to this, the negative values indicate a tail of coarser grains. In the study area, skewness values range from -0.30 to +0.91. Only 9 samples belong to negatively skewed category, whereas positively skewed and very positively skewed categories are equally distributed (Fig. 2.7c). Spatial variation of skewness values does not indicate any systematic pattern in the study area (Fig. 2.10). However, highly positively skewed

zones south of Cochin inlet surrounding Manakkodam and the northwestern area are striking.

Kurtosis: Kurtosis is considered as a sensitive and valuable measure of the normality of a distribution. A normal curve has a kurtosis value of 1.0. In the study area, kurtosis values range from a minimum of 0.56 to a maximum of 4.97. Frequency distribution of the kurtosis values shows that a maximum number of samples (25) are platykurtic in nature (Fig. 2.7d). Only a few samples are mesokurtic (5 samples) and extremely leptokurtic (3 samples). A good number of samples show leptokurtic (11 samples) and very leptokurtic (12 samples) values. Apparently, the kurtosis values indicate that majority of the samples contain a wide range of sediment size with subequal proportions of different size classes. Aerial variation of the kurtosis values is shown in Fig. 2.11. Spatial distribution of kurtosis approximately follows the pattern of mean size with sand-rich sediment zones in the southwestern and northwestern portions coinciding with zones of leptokurtic nature. Around Manakkodam area, the contours depicts a shoreward increase in the kurtosis values. The area is mostly covered with sediments which are platykurtic in nature. Patches of very platykurtic sediments are also observed in the innershelf zone.

2.3.4 Scatter Plots

Geological significance of scatter plots of the size parameters is widely known. It gives an insight into the niche of depositional regimes. In collusion with other environmental parameters, the interpretation of such plots do provide meaningful inferences on hydraulic processes. On the whole, a combined picture of the present day dynamics of transportation, mixing,

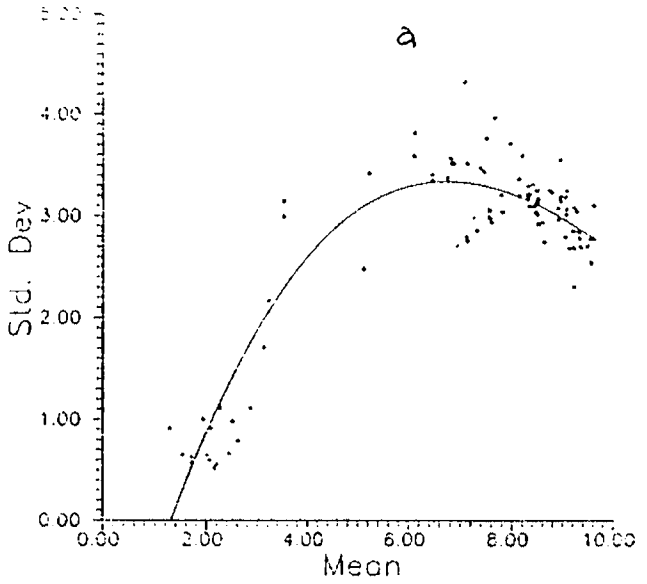

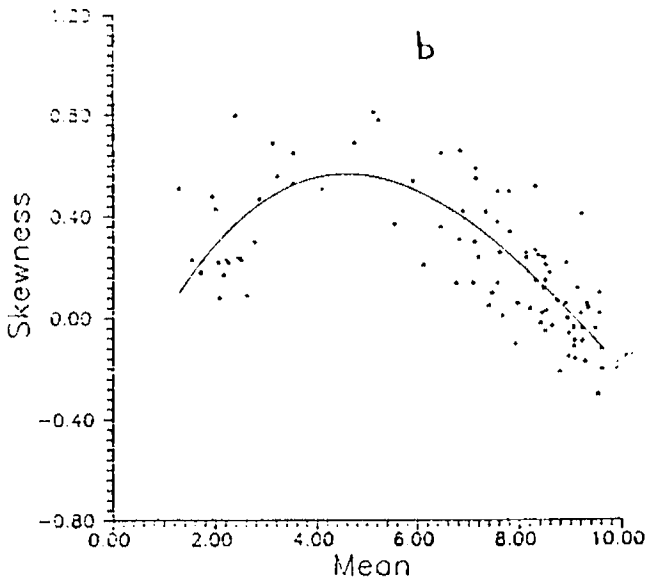

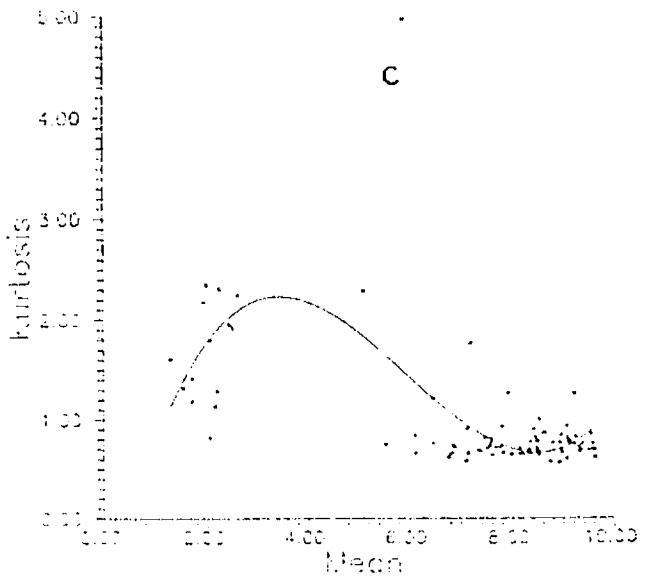

Fig. 2.12 Scatter plots:

(a) Mean size Vs Standard Deviation

(b) Mean size Vs Skewness

(c) Mean size Vs Kurtosis

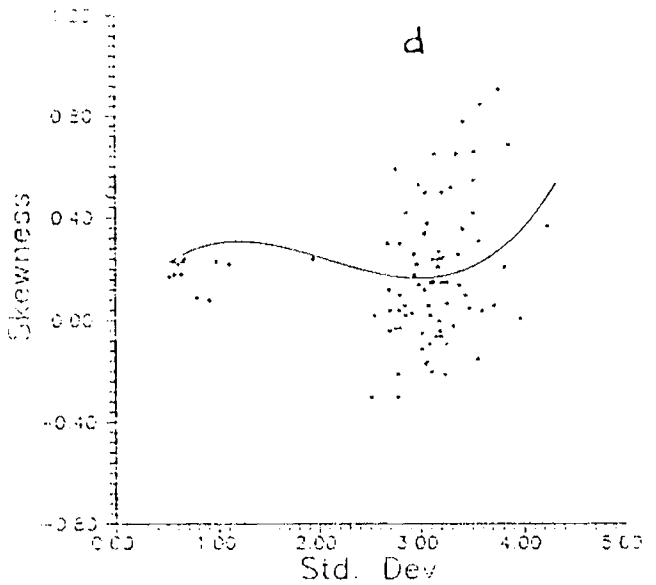

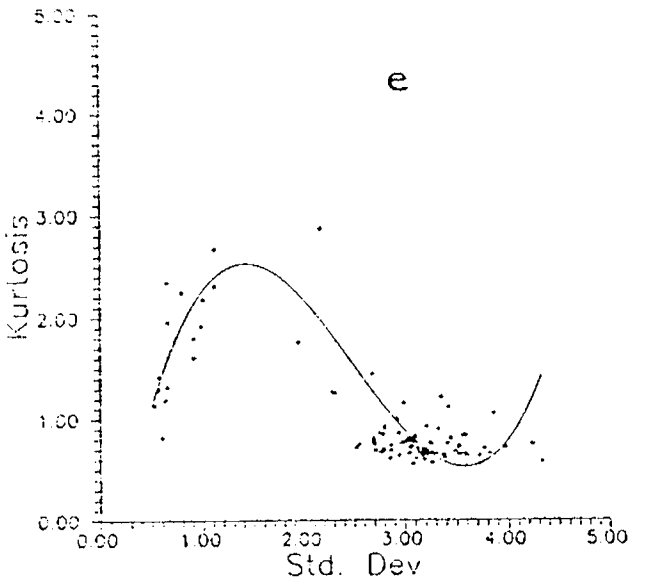

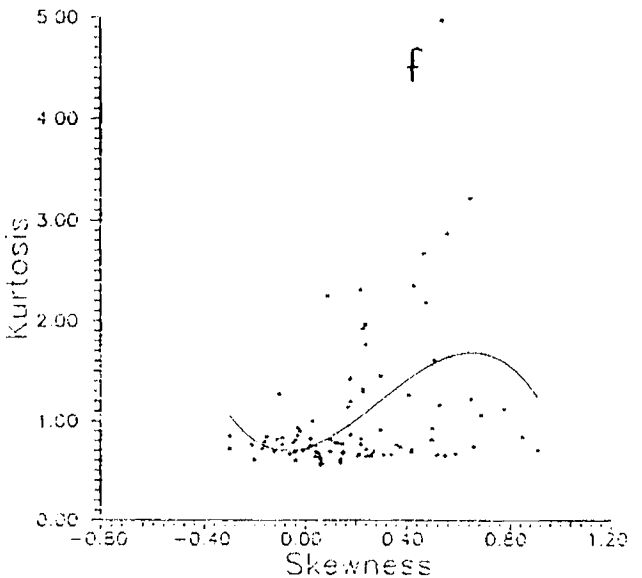

Fig. 2.12 (Contd...)

(d) Standard deviation Vs Skewness

(e) Standard deviation Vs Kurtosis

(f) Skewness Vs Kurtosis

fractionation, deposition and erosion of the sediments can be elucidated from the scatter plots of the graphic measures. The plotting was carried out employing a standard "Grapher" program in a personal computer and polynomial curve fitting was used to establish the trend line.

Mean size Vs Standard deviation: The trend of the scatter plot shows an inverted 'U' shape with an truncated right limb (Fig. 2.12a). According to Folk and Ward (1957), if the plot represents a wide range of grain sizes (gravel to clay), the scatter can form a broadened 'M' shaped curve. Inman (1949) and Griffiths (1951) pointed out that, sorting is rather a closely controlled 'V' shaped or sinusoidal function of mean size. In the study area, poorest sorting is observed for samples having a mean size of around 6 ϕ. Sorting improves towards coarser and finer ends. Samples which fall at the lower end of the left limb having a mean size of around 2 ϕ are moderately sorted. The clay-rich truncated right limb shows an improvement in sorting, i.e., from the extremely poorly sorted to poorly sorted category.

Mean size Vs Skewness: The diagram (Fig. 2.12b) shows an inverted 'U' shaped trend with a truncated left arm. The sediments are increasingly positively skewed in mean size ranging from 4 to 6 ϕ. Folk and Ward (1957) and Cronan (1972) pointed out that skewness is very closely a function of mean size and the trend is sinusoidal in nature. It is obvious that with addition of coarser materials to the fine, the sediments become symmetrically skewed. Whereas, with subsequent addition of finer sediments, the right arm crosses over the boundary of symmetry to negatively skewed side. Hence, the asymmetry of the curve in these samples are mainly controlled by sand and clay modes with a monotonous presence of silt. The plot tends to attain symmetry in the coarser mean size part, which could be due to the mixing of

a tail of fines (silt and clay). Whereas, the positively skewed portion of the curve represents samples which are predominant in sand modes with a tail of fines (mostly clay). The negatively skewed sediment population at the lower end of the right limb indicates an excess of clay mode with a tail of coarse (silt and sand).

Mean size Vs Kurtosis: The trend line is sinusoidal in nature (Fig. 2.12c). The complex nature of the trend of such plot was dealt by Folk and Ward (1957) and Cronan (1972). Highest kurtosis values (extremely leptokurtic to leptokurtic) are for sediments having mean size in the range of 3 to 4 ϕ. Around 9 ϕ mean size the kurtosis values are minimum (very platykurtic).

Standard deviation Vs Skewness: No definite pattern is observed in this plot (Fig. 2.12d). As standard deviation versus mean and mean versus skewness were showing definite relationships, theoretically, skewness should also yield some mathematical relationship with standard deviation. But the trends observed are complex. In similar situations, Folk and Ward (1957) and McKinney and Friedman (1970) have reasoned that it could be due to modal dominance and mixing of different modes of population. The scatter trend given by Folk and Ward (1957) was nearly a circular ring. Though the present set of samples show a wide variation in standard deviation and skewness values, the trend is much different. This could be mainly due to the application of polynomial curve fitting of third order used in this study. The plot indicates that better sorted samples show a very small fluctuation in the skewness values and they are mostly the sand dominant samples. But, towards the poorly sorted part, there is wide vertical scattering owing to the modal differences among the population towards fine and coarse skewness.

Standard deviation Vs Kurtosis: Fig. 2.12e gives the trend with a sinusoidal pattern. The inflexion points for higher and lower values of kurtosis are around the sorting values of 1.5 and 3.5 respectively. Almost a similar trend was observed by (Folk and Ward, 1957) from the study of the Brazos river bar . The trend indicates an improvement in sorting (standard deviation values from 3.5 to 1.5) with increase of kurtosis values, and thereon with the improvement of sorting the kurtosis values decrease. This could be due to the presence of a secondary mode along with the dominant mode which results in a moderately sorted sediment. Kurtosis minima is around the poorly sorted side, denoting subequal mixing of different modes.

Skewness Vs Kurtosis: These two parameters are the indicators of the non-normality of the size distribution. The polynomial trend is not giving a well developed sinusoidal pattern (Fig. 2.12f). The left side of the figure shows a decrease in the kurtosis values. The only significant limb indicates a linear increase in the kurtosis values with increase in the skewness to the positive side. Beyond the symmetrical skewness (towards positive side), wide scattering of values are observed.

2.3.5 Textural study of core samples

Percentages of sand, silt and clay fractions at different layers of the 17 core samples are given in Table 2.3 and are presented in Fig. 2.13. Some of the cores do not depict any noticeable vertical difference in the textural grades. The silt and clay contents vary substantially whereas the sand content do not show much fluctuation except in a few cores. Cores from mud-rich zone, in general, illustrate an increasing pattern of sand content with

TABLE 2.3

Size data of core sample analysis

Sl.	Sample	Sand (%)	Silt (%)	Clay (%)	Textural Description
1	A1 0	0.67	34.66	64.67	Silty clay
2	0-10	1.89	30.39	67.72	Silty clay
3	10-20	15.00	22.46	62.54	Silty clay
4	20-22	21.26	31.48	47.26	Sand-silt-clay
5	22-24	45.17	32.89	21.94	Sand-silt-clay
6	B4 0	1.40	37.50	61.10	Silty clay
7	0-10	8.67	27.28	64.05	Silty clay
8	10-20	6.19	23.35	70.46	Silty clay
9	20-30	6.63	32.51	60.85	Silty clay
10	30-40	3.89	28.79	67.32	Silty clay
11	40-50	4.15	30.50	65.35	Silty clay
12	50-55	1.52	47.62	50.86	Silty clay
13	D1 0	7.89	44.94	47.08	Silty clay
14	0-10	3.05	25.17	71.78	Silty clay
15	10-20	4.06	26.42	69.52	Silty clay
16	20-30	17.64	37.74	44.62	Silty clay
17	30-40	3.55	25.86	70.59	Silty clay
18	40-45	3.07	27.38	69.55	Silty clay
19	D6 0	13.64	35.09	51.27	Silty clay
20	0-10	16.15	27.86	55.99	Silty clay
21	10-20	9.26	21.34	69.40	Silty clay
22	20-30	7.73	21.52	70.75	Silty clay
23	30-40	9.17	38.53	52.30	Silty clay
24	40-50	9.16	11.92	78.92	Clay
25	50-60	7.72	31.07	61.12	Silt clay
26	60-62	6.23	34.94	58.83	Silt clay
27	E3 0	1.46	42.59	55.95	Silt clay
28	0-10	6.35	24.15	69.50	Silt clay
29	10-20	6.12	15.54	78.34	Clay
30	20-30	5.69	12.62	81.69	Clay
31	30-40	5.59	16.47	77.94	Clay
32	40-50	4.73	29.14	67.42	Silty clay
33	50-60	6.17	27.60	66.23	Silty clay
34	60-65	5.99	23.41	70.60	Silty clay
35	F6 0	0.42	52.36	47.22	Clayey silt
36	0-10	5.48	44.90	49.62	Silty clay
37	10-20	2.57	36.04	61.39	Silty clay
38	20-30	1.17	32.06	66.77	Silty clay
39	30-40	0.61	38.90	60.49	Silty clay
40	40-45	1.12	44.99	53.89	Silty clay
41	G3 0	1.15	43.62	55.23	Silty clay
42	0-10	6.69	28.66	64.65	Silty clay
43	10-20	3.21	23.81	72.98	Silty clay
44	20-30	5.68	16.32	78.00	Clay
45	30-33	4.35	32.13	63.52	Silty clay
46	H1 0	57.90	24.40	17.70	Silty sand
47	0-10	52.99	26.31	19.70	Silty sand
48	10-20	32.02	24.96	43.02	Sand-silt-clay
49	20-30	49.08	19.50	31.42	Clayey sand
50	30-37	66.81	15.50	17.69	Clayey sand

Sl.	Sample	Sand (%)	Silt (%)	Clay (%)	Textural Description
51	I5 0	13.13	33.36	53.51	Silty clay
52	0-10	8.28	35.41	56.31	Silty clay
53	10-20	5.84	28.89	65.27	Silty clay
54	20-30	1.85	33.83	64.32	Silty clay
55	30-40	0.93	21.95	77.12	Clay
56	40-48	0.40	30.92	68.68	Silty clay
57	J1 0	3.43	43.76	52.81	Silty clay
58	0-10	8.25	26.99	64.76	Silty clay
59	10-20	2.81	39.00	58.19	Silty clay
60	20-25	8.69	32.36	58.95	Silty clay
61	25-30	40.14	33.37	26.49	Sand-silt-clay
62	L1 0	21.68	30.84	47.48	Sand-silt-clay
63	0-10	3.82	37.83	58.35	Silty clay
64	10-20	3.86	30.70	65.44	Silty clay
65	20-30	6.52	44.96	48.52	Silty clay
66	30-32	2.79	64.87	32.34	Clayey silt
67	32-34	15.93	42.66	41.41	Clayey silt
68	34-36	23.59	31.52	44.89	Sand-silt-clay
69	36-45	11.59	34.82	53.59	Silty clay
70	L6 0	78.42	12.47	9.11	Sand
71	0-10	71.16	15.31	13.53	Silty sand
72	10-20	74.87	9.24	15.89	Clayey sand
73	20-30	79.12	9.90	10.89	Sand
74	30-35	79.43	8.41	12.16	Sand
75	M3 0	5.94	48.09	45.97	Clayey silt
76	0-10	4.75	27.35	67.90	Silty clay
77	10-20	3.39	30.90	65.91	Silty clay
78	20-30	3.10	34.01	62.89	Silt clay
79	30-40	3.44	30.95	65.61	Silt clay
80	N6 0	67.16	23.20	9.64	Silty sand
81	0-10	75.67	11.34	12.99	Sand
82	10-18	82.89	6.65	10.46	Sand
83	18-24	69.21	11.24	19.55	Clayey sand
84	24-30	31.69	22.63	45.67	Sandy clay
85	30-38	84.85	7.83	7.32	Sand
86	O3 0	1.16	36.16	62.68	Silty clay
87	0-10	7.94	35.44	57.62	Silty clay
88	10-20	3.89	23.28	72.84	silty clay
89	20-30	3.02	25.92	71.06	Silty clay
90	30-40	2.69	28.62	68.69	Silty clay
91	40-50	2.96	29.39	67.66	Silty clay
92	50-56	2.26	21.84	75.90	Clay
93	P1 0	1.24	35.64	63.12	Silty clay
94	0-10	3.90	36.26	59.84	Silty clay
95	10-20	3.56	36.66	59.78	Silty clay
96	20-30	5.48	35.73	58.79	Silty clay
97	30-40	5.04	33.70	61.26	Silty clay
98	40-50	4.93	28.98	66.09	Silty clay
99	50-53	1.94	32.28	65.47	Silty sand
100	Q5 0	3.96	47.80	48.24	Silty clay
101	0-10	12.98	39.51	47.51	Silty clay
102	10-20	17.33	22.74	59.93	Silty clay
103	20-25	55.73	7.18	37.09	Clayey sand

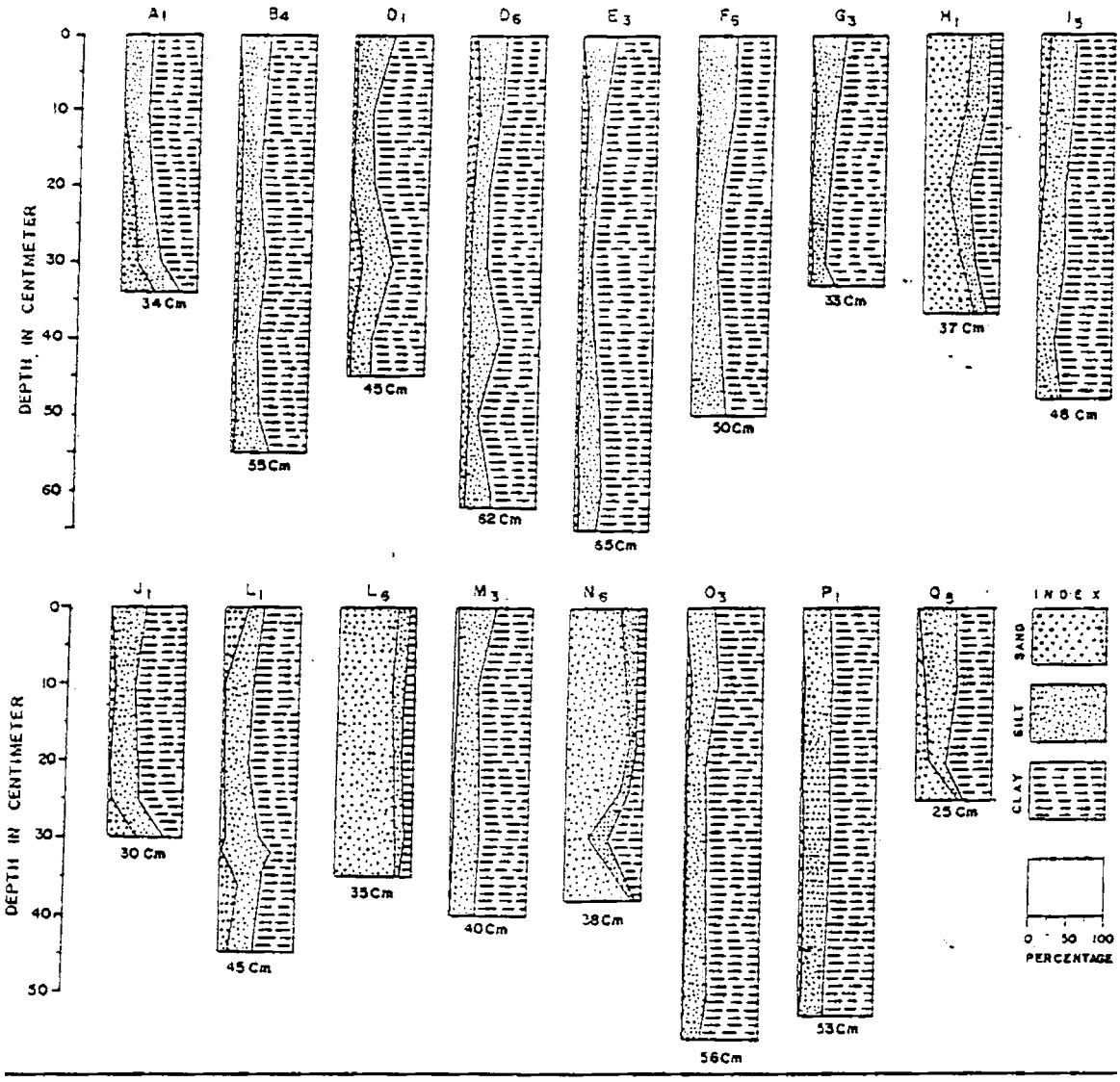

Fig. 2.13 Variation of texture in core samples

depth, though in many the variation is not very systematic. Samples A1, J1 and Q5 portray an abundance of sand towards bottom, but the increase is marginal in the cases of other mud-rich samples. I5 and L1 decipher a surficial enrichment of sand with a steady reduction with depth. Of the sand-rich cores, L6 does not show any vertical variation. But H1 and N6 display considerable change in the sand content with depth at 24 and 30 cm respectively. The sand content at these points drops down to 32 %.

2.4 DISCUSSION

The sediments on the innershelf show varied levels of mixing of the three textural grades viz, sand, silt and clay. Correlation coefficients show that sand variation have a negative bearing more on clay content ($r = -0.916$) and to a lesser extent on silt ($r = -0.867$). Presence of a sand rich zone in the seaward portion of southern side is very striking, where the sand percentage is as high as 98.79. Majority of the study area is covered with silty clays and a clear demarcation of sand zone in the offshore part of the southern half is significant. It was reported earlier by Kurian (1969) that, beyond the 18 m bathymetric contour there is a sand-rich zone that extend from Mangalore to Cochin up to a depth of 100 - 200 m. But south of Manakkodam, the sand enriched zone starts appearing at a shallower depth. Further south, along the Trivandrum coast, most strikingly, the clay/silt zone is almost missing and the sand-rich zone transcends right from the beach. Enrichment of silt at the Cochin channel mouth could be indicative of the flushing process during the semi-diurnal ebb and flood tides. Due to the tidal currents, the clay particles are set in motion in this zone, thereby resulting in the enrichment of silt sized materials.

Sand, silt and clay content show a significant correlation coefficient value of 0.319, -0.243 and -0.318 respectively (level of significance 0.01, 0.02 and 0.01 respectively) with depth. This indicate that the distribution of the size grades on the shelf has some bearing on the depth. This congruence in the distribution of size is very much evident from the spatial variations in texture (Fig. 2.6).

Distribution of sorting values (Fig. 2.9) indicate that sand rich sediments are moderately well sorted to moderately sorted. Sorting worsens with subsequent addition of mud. But the sinusoidal behaviour of sorting with mean size (Fig. 2.12a) shows that the sorting is worst for samples with mean size around 6 ϕ. In terms of sediment types, sand-silt-clay category shows the poorest sorting. This is a clear indication that, mixing of different proportions of the textural grades imparts a poorer sorting to the sediments. Marginal improvement in the sorting with increase of clay particles are also evident from the diagrams.

Skewness is observed as a function of mean size (Fig. 2.12b). All negatively skewed sediments contain very small percentage of sand. Positively skewed sediments show a predominance of coarser fractions. However, in the southwestern portion (dominant in sand), sediments show a decrease in their skewness value near to zero as it becomes unimodal. In general, the sequence of skewness variation indicates a similarity with the observation of Cronan (1972), who has studied the relationship of skewness with mean size in the Irish sea sediments. Nevertheless, introduction of silt component to sand as an end member changes the skewness value to the negative side.

The degree of polymodality of the sediments are explained in terms of the variations in kurtosis values. A wide variation is observed in the kurtosis values with very few samples falling within the mesokurtic category. The scatter diagram and aerial distribution pattern (Fig. 2.12c and 2.11) illustrate that predominance of sand content increases the kurtosis values. The diagram (Fig. 2.12c) is slightly different from that of Folk and Ward (1957) but has some similarities with Thomas *et al.* (1972). The reason for sand population becoming markedly more leptokurtic than the clay population could be that, the clay grades are spread over a large size range of 8 to 14 ϕ, whereas the sand grades are from 0 to 4 ϕ. Secondly, the maximum clay content of the sediments is 69 % and in majority of the samples silt forms a major component in the mud fraction, which imparts a lesser sorting for the fine grained sediments. These alternations are clearly indicated by the relationship of kurtosis with the sorting values (Fig. 2.12e). The higher kurtosis inflexion point is around the sorting value of 1.5 and thereafter, kurtosis value decreases with the worsening in sorting. The summation of the total asymmetry of the grain size distribution can be inferred from the variation of skewness with kurtosis. Markedly, leptokurtic samples are positively skewed. With continuous addition of clay population, skewness transcends into the negative side showing lower kurtosis. Cronan (1972) attributed the negative skewness to the episodes of erosion or non-deposition and positive skewness to deposition. However, the distribution of the negatively skewed sediments are restricted to small patches (Fig. 2.10); hence, it is difficult to conclude the reason for the negativity of the skewness. However, it could be due to the seaward increase of clay percentage along certain profiles as pointed out by Friedman (1967). The increase in the clay percentage in the inshore region can result from the sweeping oscillatory

motion at the breaker zone that separates the fine grained particles which are subsequently removed seaward.

The sediment distribution pattern is a result of the composite process of denudation, transport and deposition. Thus, it maintains the essential characteristics of the source material modified by the agents of transportation with its final texture and composition reflecting the overall conditions existing at the point of deposition. From the results discussed above, it is understood that, there are three types of sediments in the innershelf from their textural attributes. A sand rich zone in the seaward portion (outer innershelf) of the study area, especially more prominent in the southwestern portion. Secondly, a mud dominant zone covering major part of the study area. A third type is a mixed zone bordering the sand zone, which transcends into the mud zone with subequal proportions of the different size grades. The same set of hydrodynamic condition can not yield two extremely different sets of deposits from the same kind of material source. Hence, the following part of the discussion concentrates into the regional conditions controlling the sedimentation pattern, based on different sedimentological techniques in practice.

2.4.1 Nature of sedimentation

Mode of transportation and deposition in the basin is not adequately understood from the preceding section. Moreover, data on current pattern is inadequate to talk about the shelf transport regime. However, based on grain size attributes, different methods were proposed which are helpful to derive the dispersal history of the sediments in the basin. Of which, a few methods are tried here to characterise the depositional pattern in the innershelf.

CM Diagram. Sediments are brought into the basin of deposition in different ways and the finer fractions could be transported independently of the coarser particles. Passega (1957) demonstrated that, two parameters of the grain size distribution of individual samples are particularly significant in accounting for the transportational/depositional mechanisms; C, the one percentile and the M, the median diameter. Passega (1964) divided the general pattern of CM diagram into different segments by points N, O, P, Q, R and S, each representing a different pattern of transportation. The CM diagram of the innershelf sediments is given in Fig. 2.14. There are two distinct groups that are clustered in the right and left sides of the diagram. The sediments with coarser median falls in the segment 'PQ' (Passega *et al.*, 1967; Passega, 1977). This denotes that, the sediments are transported mostly in graded suspension and partly by rolling. Points which are nearer to the C = M line represent the sediments having the best sorting. A few sample points fall in the 'RS' segment represent the sediments transported in uniform suspension. Majority of the sample points are scattered in the left-hand side of the diagram and denote that they are transported in pelagic suspension for a long distance. This is generally an area of poor sorting where the pattern is away from the limit C = M. Thus the CM diagram gives two sets of sediments with different pattern of transportation. One set indicates bed composed of sand particles, deposited by rolling and graded suspension under conditions of maximum and minimum turbulence. Another set embodies large number of sample points illustrating a transportation pattern of pelagic suspension consisting of fine particles. The two types of sediments are very much in contrast with each other and could be deposited under different depositional regimes.

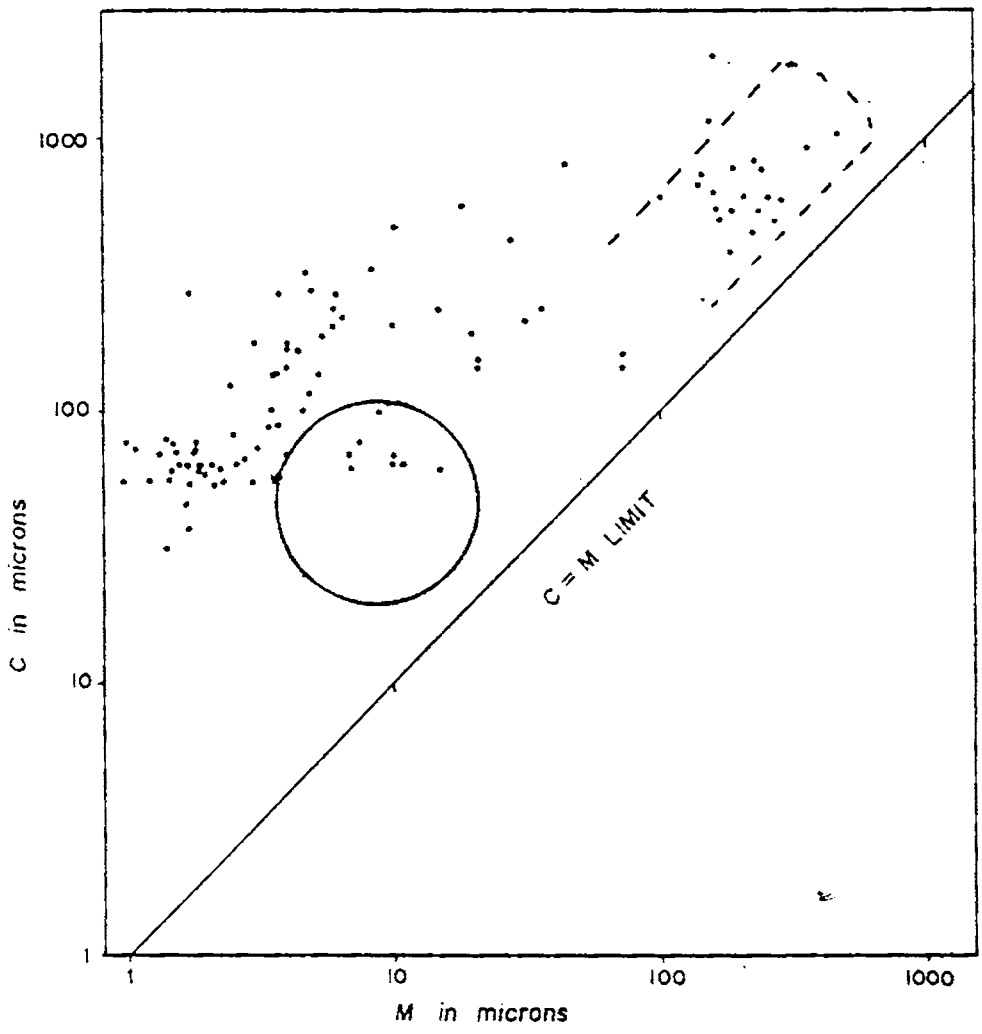

Fig. 2.14 CM pattern of the innershelf sediments

Sample points in the right-hand top corner falls in the pattern IV of Passega and Byramjee (1969) and represent a similar pattern with that of the beach sediments reported by Samsuddin (1986). Present day shelf processes can not account for such a deposit with the prevailing conditions *in situ*, as most of the sandy sediments are found in the outer innershelf. So it could be possible that the depositional mechanism of coarse sediments in the outer innershelf is a result of deposition in the past in an environment similar in nature to the present day beaches under similar hydrodynamic conditions (relict beach). The second set of samples, which mainly represents the pelagic suspension process is the result of the present day shelf processes. In the CM diagram, few sample points fall in the uniform suspension zone. Passega *et al.* (1967) while discussing the sediments transported by waves proposed that, with an increased wave induced turbulence in the nearshore the sediments are put into uniform suspension. Following a decrease in the turbulence, the sediments are settled down, where the nature of sand distribution is controlled by differential bottom turbulence.

Probability Curves: Certain features of grain-size distribution furnish important information enabling proper reconstruction of ancient environments (Visher, 1969; Middleton, 1976). According to Visher (1969), the probability curves of size distribution could be used as a tool to decipher environmental conditions of a sedimentary deposit. The shape and characteristics of the curves may be employed to infer the environment of deposition in conjunction with other information. The plots may also be used to infer the hydrodynamic conditions prevailing at the time of deposition.

From the preceding discussion (CM pattern), it is presumed that the offshore coarser deposit represents a relict beach environment. Three samples

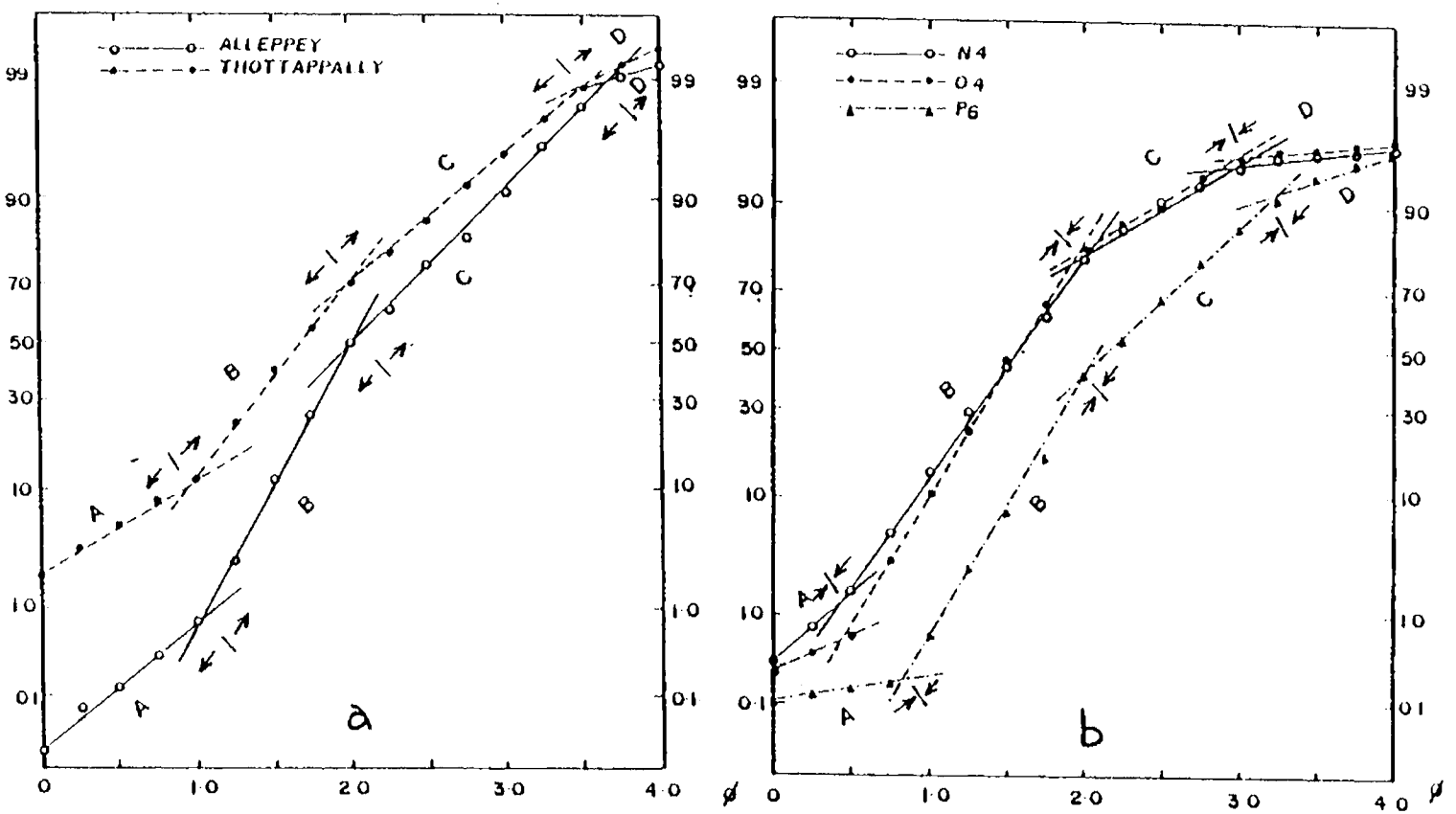

Fig. 2.15 Probability curves of (a) present-day beach and (b) relict sands in the innershelf

(N4, O4 and P6) containing > 95 % sand collected from the outer innershelf were selected to ascertain their mode of deposition. For comparing the validity of the findings, the present day beach samples from Alleppey and Thottappally were taken from the upper 10 cm of sediments at the mid-water line, as sampling at mid-water line are found to represent typical beach deposit (Samsuddin, 1986). As envisaged by Viard and Breyer (1979), these samples were sieved at 1/4 ϕ interval. The grain size cumulative curves (Fig. 2.15) are composed of 4 straight line segments, A, B, C and D representing four separated log-normal distributions. The line segments represents subjective best fit lines through groups of points. These four regions of the curve represent major sub-populations of grains moved by different transport mechanisms. In general the truncation points are around 1, 2 and 3 ϕ. In beach sediments, the segment-A represents the traction load, B and C the saltation population and D, the suspension load (Visher, 1969; Middleton, 1976). Suspension load was defined by Visher (1969) as the population which represents < 1 % of the sample. This is true in the case of the beach samples from Alleppey and Thottappally. The break between traction and saltation load is around 1 ϕ, indicating deposition of sediments by rolling and sliding. Among the two saltation population B and C, the coarser population (B) is better sorted than the finer population (C). In the beach foreshore, swash and backwash produce two differing transport condition, resulting in two saltation populations. The coarser saltation entity could be from the swash and the finer population which shows a lesser sorting presumably from a less competent backwash. Depending upon the competence of swash and backwash, sorting characteristics of this two population varies.

The probability curves of the outer innershelf samples also exhibit the 4-segmented nature (Fig. 2.15). However, the increased suspension load

(> 1 %) is presumably produced due to the mixing of present day fine sediments. Apart from this, it almost follows the pattern of beach plots except for minor variations in the inflexion points. The break between the traction and saltation load is at < 1 ϕ. The two saltation populations, which is typical of beach deposits, are also present in the innershelf sandy sediments. This indicates existence of the swash and backwash regimes (relict beach) at the time of its deposition.

Viard and Breyer (1979) have utilised grain size cumulative curves to classify environments of deposition. Similarly, in this study, grain size cumulative curves are interpreted assuming truncated and joined normal distributions. Table 2.4 gives a quantifiable difference in the amount of material and slope angle of each sub-population. Innershelf sand samples encompass higher proportions of suspended load, though the slope is very less compared to the beach curves (here, the percentage suspension load for the outer innershelf samples are the subtracted values of the traction and saltation load from 100). A comparative decrease in the amount of finer saltation population (segment-C) in the case of innershelf sands could be due to the reworking of the sediments by intermittent suspension at the wave base. Substantial increase in the coarser saltation population indicates absence of strong currents.

The above observations give further insight into the mode of deposition of the sand in the outer innershelf. From the evidences culminating from the analysis of CM diagram and probability plots, it is presumed that sand-rich zone of the outer innershelf is part of a foreshore depositional interface, lying detached from the mainland, thus clearly marking events of beach deposition in the geological past and subsequent transgression of the sea along the coastal tract.

TABLE 2.4

Characteristics of grain size distribution curves

Locality	Traction load %	Traction load Slope°	Saltation load %			Saltation load Slope°			Saltation load CT	Saltation load FT	Suspension load %	Suspension load Slope°
	A	A	B	C	T	B	C	X	0	0	D	D
Alleppey	1	39	49	49	98	61	45	53	1.02	3.67	1	18
Thottappally	11	31	60	28	88	52	40	46	0.98	3.50	1	27
N4	1	42	79	15	94	55	31	43	0.43	3.00	5	8
O4	1	24	80	15	95	59	31	45	0.45	3.00	4	7
P6	<1	10	60	32	92	59	43	51	0.83	3.22	7	19

Description of components: %, the amount of material within each line segment; A,B,C and D, corresponding numbers of the four segments of the fig(Fig. 2.15); T, total of the subpopulation; slope, the sorting of each component measured by slope angle in degrees; X, the average for the sub-population; CT, the coarse truncation point; FT, the fine truncation point. The slope values are obtained from plots on probability paper (433- Arithmetic probability chart of Chenna corporation of New Delhi) with 0.5 phi units on major horizontal subdivisions.

2.4.2 Q-mode factor analysis

Multivariate relationship of particle size versus the number of observations can be worked out using factor analysis. Subsequent to the introduction of factor analysis into geology by Imbrie and Purdy (1962), several workers used factor analysis as a prime method in confronting various problems in the field of geology (Imbrie, 1963; Imbrie and Van Andel, 1964; and Hope, 1968). Klovan (1966) and Solohub and Klovan (1970) applied Imbrie's Q-mode method to Bartaria Bay sediments effectively in differentiating depositional regimes.

Q-mode factor analysis deals with the inter-relationship between observation points. This gives a comprehensive comparison of the variables from sample to sample and provides a meaningful order of arrangements of different suite of samples formed under different processes. For the innershelf sediments, which cover a wide spectrum of grain size, Q-mode factor analysis was performed by applying varimax rotation procedure (Davis, 1971). The data matrix consists of 50 observations (due to memory constraint, alternate samples of the 100 samples were selected) with 15 variables (0 to 14 ϕ at 1 ϕ interval). The program was executed in a NEC personal computer.

The results reveal that the sedimentation process in the innershelf are controlled by a number of factors amongst which three factors are of particular importance. The eigen values for the three factors together account for 85.54 % of variance. Scores of the three factors for the 15 variables (size classes) are shown in Fig. 2.16. The first factor, which yields an uniform score for particles > 4 ϕ, and an eigen value of 59.36 %, is related to the dominance of fine fraction in the innershelf. The second factor

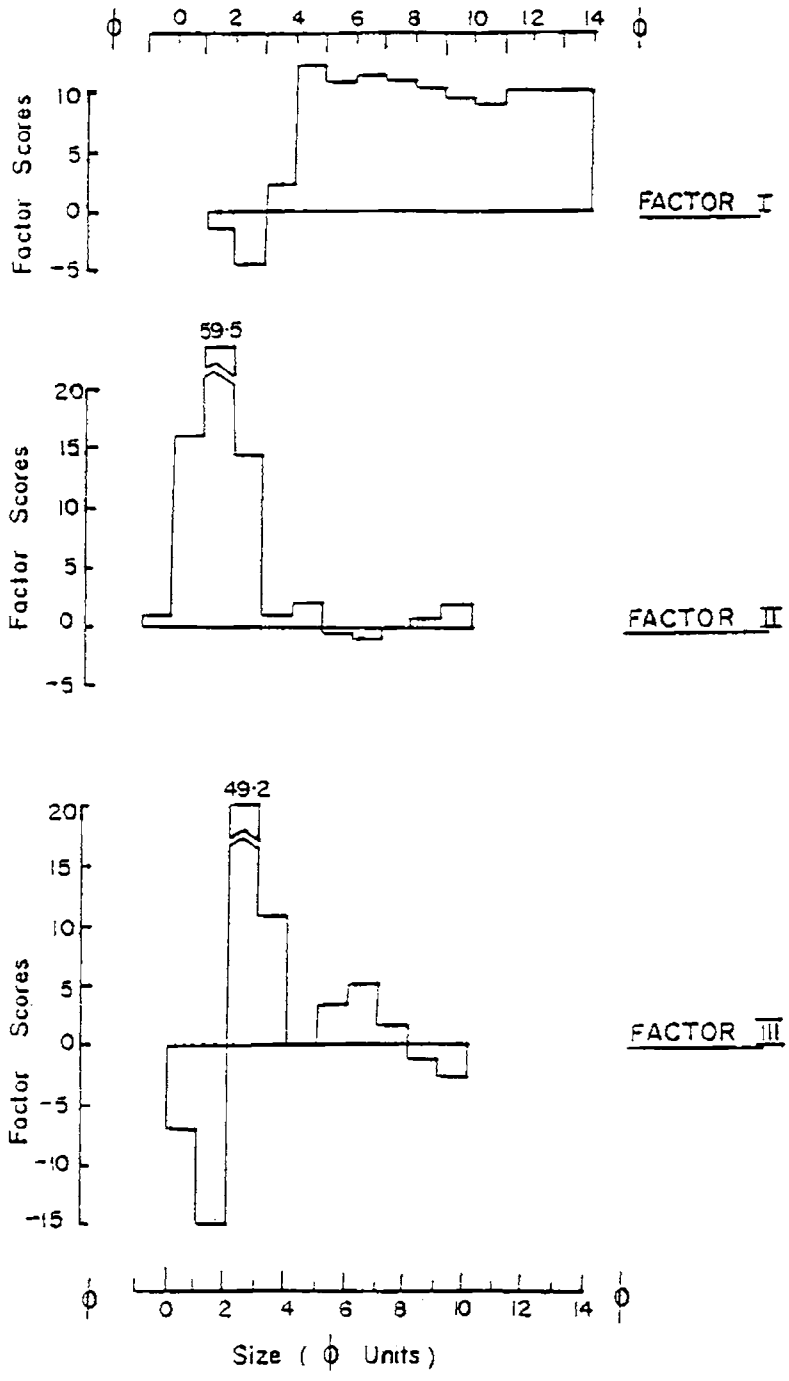

Fig. 2.16 Factor scores of the variables on the three factors

with an eigen value of 21.61 % is related to the coarser sediments with factor score modes falling between 0 and 3 ϕ classes. Though the third factor with high positive scores from 2 to 4 ϕ and negative scores from 0 to 2 ϕ is less significant (variance of 4.58 %), it is thought to be representing the process of homogenisation of texture.

Based on the concept of the composite end members used for the geological interpretation, the three factor model is analysed in terms of varying energy conditions of transportation and deposition of the sediment types (Imbrie and Van Andel, 1964). Even though this energy based tracing of the depositional pattern is found to have some inherent limitations, it has a merit of quantitative assessment of the processes.

Table 2.5 gives the communality and matrix of factor loadings for the 50 samples on the three factor axes. The communality of each sample represents the sum of squared loadings for the sample and reflect the degree to which that sample vector has been explained by the set of factor axes. A communality value of 1.0 indicates a perfect explanation for the factor loadings. The sample shows high value of communality and it ranges between 0.491 to 0.995. The range of values of communality and factor loadings with mean and standard deviation are given below.

TABLE 2.5

Communality and factor loadings

Sl.No.	Sample No.	Communality	Factor I	Factor II	Factor III
1	A1	.879	.936	.047	-.008
2	A3	.877	.936	.043	-.001
3	A5	.923	.960	.036	.006
4	Ba	.889	.942	.044	-.020
5	B2	.865	.929	.035	.010
6	B4	.926	.962	.036	.015
7	B6	.995	-.026	.993	.089
8	C2	.924	.957	.031	.086
9	C4	.773	.879	.025	.006
10	C6	.960	.050	.421	.883
11	D2	.805	.897	.027	.008
12	D4	.836	.914	.024	.020
13	D6	.856	.897	.074	.212
14	E2	.748	.860	.036	.081
15	E4	.785	.886	.024	.015
16	E6	.541	.731	.018	.080
17	F2	.641	.799	.035	.045
18	F4	.851	.920	.006	.065
19	F6	.690	.829	.048	-.019
20	G3	.910	.953	.032	.039
21	G4	.491	.699	.053	-.013
22	G6	.561	.741	-.012	.109
23	H2	.647	.732	.054	.329
24	H4	.798	.873	.024	.188
25	H6	.974	.003	.666	.728
26	I2	.822	.906	.016	.025
27	I4	.850	.844	.060	.365
28	J1	.910	.950	.011	.080
29	J3	.771	.874	.006	.085
30	J5	.954	-.035	.702	.678
31	K2	.898	.947	.018	.024
32	K4	.927	.753	.454	.392
33	K6	.708	.228	.733	.343
34	L2	.971	.272	.753	.575
35	L4	.966	.005	.950	.250
36	L6	.964	.076	.385	.900
37	M2	.871	.933	.017	.023
38	M4	.841	.849	.100	.332
39	M6	.977	.256	.254	.920
40	N2	.976	.861	.171	.454
41	N4	.988	-.015	.985	.131
42	N6	.961	.239	.648	.696
43	O2	.930	.956	.013	.126
44	O4	.965	-.016	.977	.103
45	O6	.759	.007	.871	-.017
46	P2	.924	.944	.061	.168
47	P4	.843	.852	.161	.302
48	P6	.960	-.039	.855	.476
49	Q2	.972	.981	.037	.091
50	Q4	.920	.950	.020	.129

	Communality	Factor I	Factor II	Factor III
Minimum:	0.491	-0.039	-0.012	-0.020
Maximum:	0.995	0.981	0.993	0.920
Average:	0.855	0.657	0.242	0.212
Std. dev.:	0.122	0.379	0.337	0.265

Interpretative procedures require standardisation of factor loadings by which the sum total can be made to a constant. Normalisation of the factor components is attained by dividing the squared values of factor loadings by the corresponding communality (Klovan, 1966). The normalised factor components are plotted on a triangular diagram to place each sample in its proper place within the entire spectrum of grain size distribution (Fig. 2.17). The distribution of the sample points in the diagram segregates the sample suite into clusters around the three factors. A notable feature of the diagram is the absence of sample points along factors I-II. From the combination of the factor scores for each variable and the disposition of sample points in the ternary diagram, the following observation are made:

i. The clustering of points around factor I are those samples which are abundant in finer fractions. Sample number Q2 is having a maximum loading on this factor and it contains 93.85 % of mud.

ii. Factor II denotes sediments which are abundant in coarse fractions. This is typically represented by the sample number B6 with a maximum factor loading of 0.993, which contains maximum percentage of sand (99.38 %).

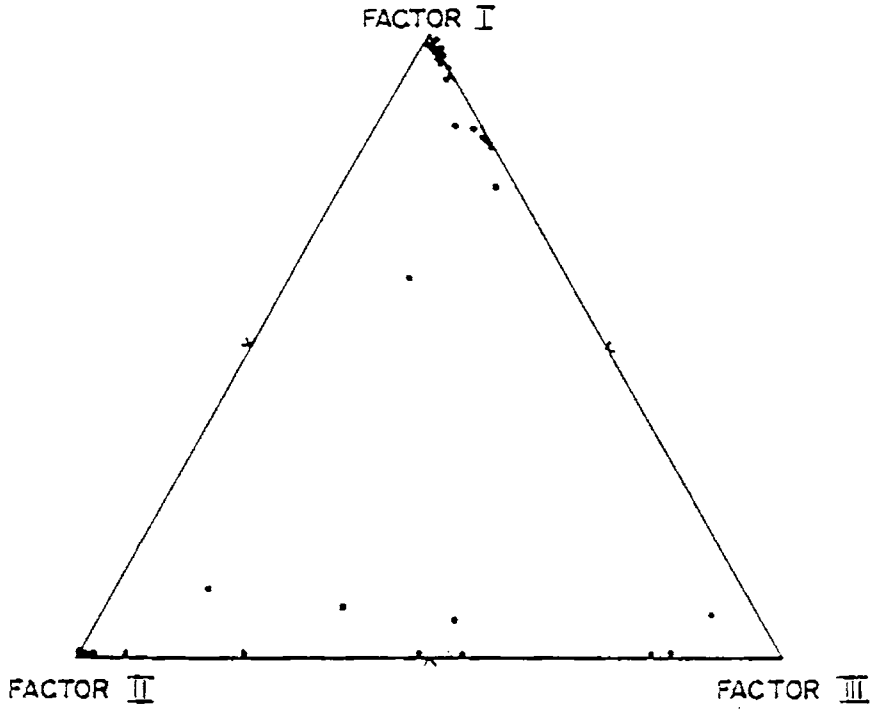

Fig. 2.17 Ternary diagram of the three normalised factor loadings

iii. Factor III, though not a very significant one, denotes sediment mixing, as it shows a combination of negative and positive scores over the variables. The resultant textural class is a typical mixed facies with sub-equal proportions of sand and mud. The sample M6, which yields a maximum loading on this factor contains sand : mud ratio of 59.93 : 40.07.

The spread of sample points on I-III and II-III factor sides of the ternary diagram enumerates the sort of mixing that take place in the environment. The absence of sample points on I-II side is an indication that facies change is a gradational one and not an abrupt change in the textural transitions, owing to the reworking ability of the innershelf dynamics.

A combination of the above considerations lends credence to the idea that, each factor is an expression of different energy regimes for which the size spectrum forms an 'equilibrium subrange' *in situ*. Factor I implies a low energy regime where the transportation and deposition phase is controlled mostly by a pelagic suspension process. The second factor is inferred to be the result of a high energy regime which has been identified based on CM and probability curves as an environment similar to the present day beach regime. The third factor might be a transition phase representing the resultant flux of coastal circulation consisting of the re-suspension/deposition by onshore-offshore advection.

Documentation of the spatial variations of energy regimes are attempted in Fig. 2.18. The diagram exhibits a sympathetic variation with the nature of sedimentation described in the earlier part of the discussion. Seaward portion of the study area indicates a high energy zone transcending to a low energy

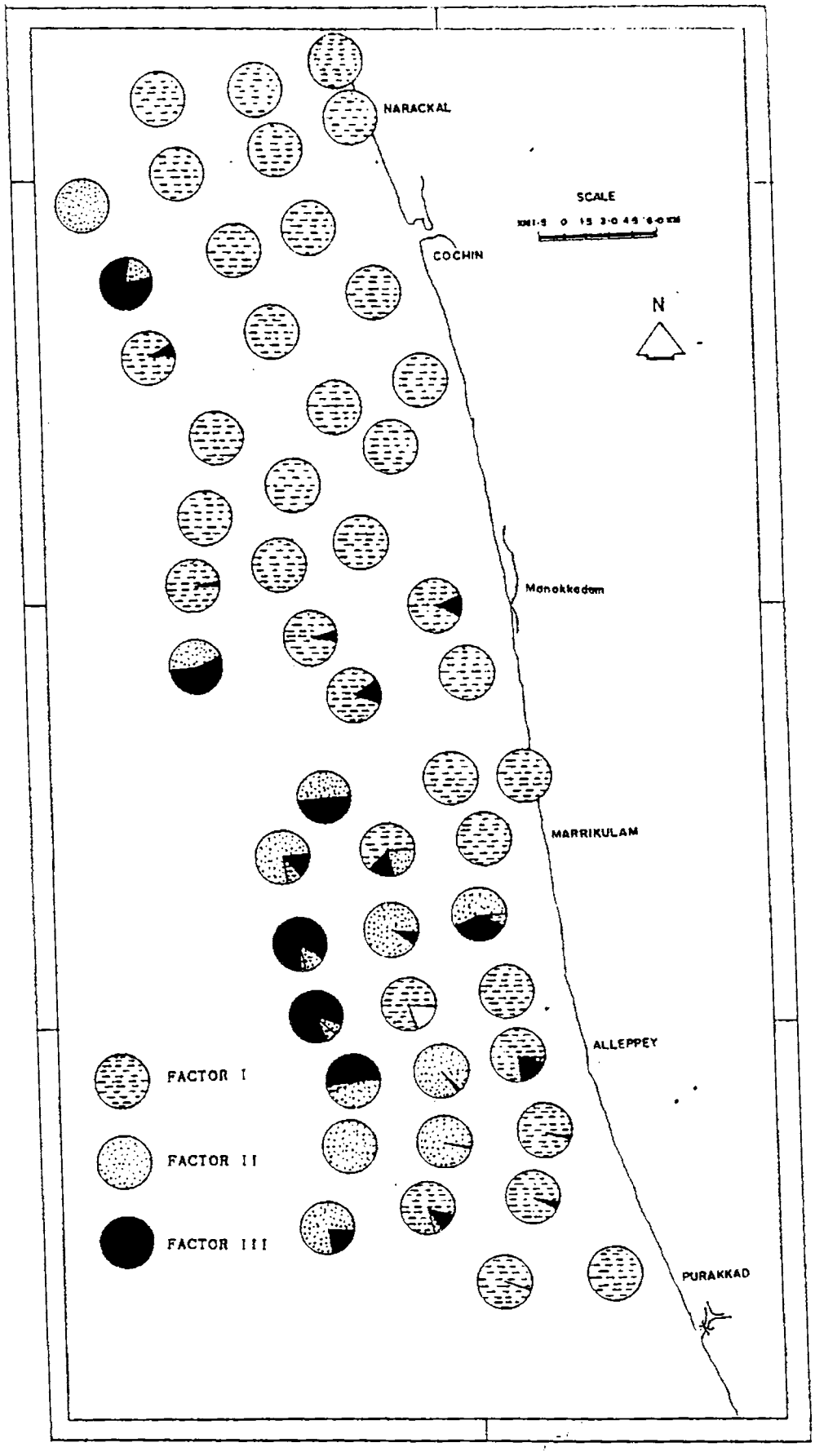

Fig. 2.18 Spatial variation of the three normalised factor loadings

one towards the coast. The transition zone with sand/mud admixture could be due to the strong onshore drift which carries the coarser sediments towards nearshore and re-deposition of the coarse sediments along with the fine-grained modern sediments. The diagram gives a composite picture of energy distribution in the innershelf of both past and present.

2.4.3 Sediment transport

Predictive knowledge of water motions on the continental margins is still a distant goal. Theoretical concepts and field observations using improved instrumentation eventually lead to recognize certain significant physical processes on the shelf, but interpretations may be made with caution. Added to this, the turbulent condition has posed serious problems in recording the different dynamic parameters in the innershelf, which has affected the progress of its documentation.

Field data on shelf water circulation and suspended matter distribution are meager or are of very uneven quality and density. The sediment distribution pattern on the shelf is mainly controlled by the circulation pattern, such as unidirectional currents and wave orbital motions (Komar, 1976). The mode of transportation of sediments varies widely depending on the particle composition, topography and hydraulics. The surficial layer of sediments respond sympathetically to the variation in the energy of incident waves, resultant wave-induced bottom currents and innershelf circulation pattern. Several techniques are in practice to deduce sediment movement in different environments. Radioactive and fluorescent tracer techniques (Ingle, 1966; Siddiquie and Srivasthava, 1970; Ray *et al.*, 1975; Machado and Baba, 1984), sediment trap method (Kraus, 1987) and current measurements are some

of the time consuming and expensive methods in practice to monitor sediment movements. Attempts have also been made to derive sediment dispersal from size, shape, chemistry and mineralogy. Mazullo and Crisp (1985), have utilised size and shape, Griffin *et al.* (1968) made derivation based on mineralogy, Shideler (1979) attempted silt/clay and sand/mud ratio to understand the process of transportation. Trace element data (Holmes, 1982) as well as isotope geochemical data (Solomons *et al.*, 1975) were also found useful to understand the direction of sediment transport. Complex functions of many intrinsically random variables such as, water movements and constituents of the sediments make accurate determination of the sediment movement but still an extremely difficult task. In the present study, the transport model suggested by McLaren and Bowles (1985) based on certain statistical considerations of the textural aspect of the sediments is contemplated. Derivation of transport direction from this method yield the probable direction of sediment movement occurring for the period of time actually resulted in the set of samples used in the analysis.

The model envisages a sequential change in the grain size parameters along the direction of transport. It is well known that depth plays an important role in the sediment movements especially in the innershelf zone. This fact is taken into consideration while processing the data set for working out sediment pathways along the bathymetric lines. The exercise is done by selecting samples approximately along 5, 10, 15, 20, 25 and 30 m isobaths. Along the 6 bathymetric profiles, 17, 14, 17, 17, 17 and 12 samples are taken respectively. Since moment measures were found to be more useful for delineating the sediment pathways (McLaren and Bowles, 1985), mean, standard deviation and skewness were computed based on the method described by Friedman (1967) using a FORTRAN program in a personal computer (Table 2.6).

TABLE 2.6

Size Parameters of the Innershelf Sediment Samples (Moment Measures)

Sl. No.	Sample No.	Mean	Standard Deviation	Skewness
1	A1	9.21	3.00	-0.19
2	A2	6.13	3.22	1.13
3	A3	9.35	3.04	-0.25
4	A4	8.48	2.99	0.09
5	A5	8.75	3.10	0.01
6	A6	7.84	3.01	0.29
7	Ba	9.37	2.87	-0.24
8	B1	6.98	3.48	0.60
9	B2	9.03	2.99	-0.05
10	B3	7.92	2.97	0.36
11	B4	8.97	3.00	-0.07
12	B5	7.30	3.11	0.75
13	B6	1.58	0.70	0.56
14	C1	7.55	2.99	0.51
15	C2	8.62	3.15	0.08
16	C3	7.38	2.90	0.58
17	C4	9.37	2.76	-0.29
18	C5	9.08	2.88	-0.16
19	C6	3.29	2.14	1.91
20	D1	7.74	2.97	0.17
21	D2	9.10	2.72	-0.19
22	D3	5.55	4.06	0.46
23	D4	9.15	2.91	-0.21
24	D5	9.23	2.95	-0.19
25	D6	8.23	3.56	-0.06
26	E1	6.92	3.60	0.35
27	E2	7.19	2.82	0.69
28	E3	8.57	2.89	0.05
29	E4	8.79	2.68	-0.06
30	E5	9.31	2.79	-0.06
31	E6	7.30	2.82	0.73
32	F1	5.90	3.61	1.02
33	F2	7.35	3.02	0.81
34	F3	8.85	2.94	0.02
35	F4	8.94	2.93	0.16
36	F5	9.04	3.19	-0.04
37	F6	8.39	2.89	0.13
38	G1	7.18	3.53	0.54
39	G2	6.37	2.47	1.78
40	G3	8.82	3.24	0.05
41	G4	7.75	2.70	0.14
42	G5	8.16	2.34	0.44
43	G6	7.40	2.09	1.06
44	H1	5.05	2.69	1.67
45	H2	5.87	3.42	0.57
46	H3	8.55	3.36	0.06
47	H4	8.38	2.83	0.00
48	H5	7.02	3.38	0.18
49	H6	2.63	1.70	2.62

Contd...

Sl. No.	Sample No.	Mean	Standard Deviation	Skewness
50	I1	6.45	3.36	0.58
51	I2	8.92	2.42	0.14
52	I3	8.31	2.98	0.18
53	I4	7.57	3.21	0.19
54	I5	8.36	3.18	-0.12
55	J1	8.59	2.80	0.15
56	J2	9.05	2.58	0.14
57	J3	9.47	3.20	-0.19
58	J4	6.24	3.80	0.39
59	J5	2.28	1.14	3.55
60	K1	9.83	2.77	-0.30
61	K2	9.33	2.66	0.02
62	K3	8.39	3.18	0.22
63	K4	7.27	4.17	0.10
64	K5	3.13	1.75	2.56
65	K6	3.25	3.09	1.54
66	L1	7.94	3.68	-0.07
67	L2	4.58	3.87	1.15
68	L3	2.65	1.56	2.92
69	L4	2.22	1.64	3.14
70	L5	9.06	2.76	0.07
71	L6	3.54	2.70	2.18
72	M1	9.48	2.50	0.02
73	M2	9.36	2.69	0.02
74	M3	8.09	3.14	0.25
75	M4	8.69	3.64	-0.27
76	M5	2.03	0.75	0.07
77	M6	5.12	3.60	1.04
78	N1	9.22	2.63	-0.06
79	N2	7.53	3.64	0.16
80	N3	2.71	1.37	3.32
81	N4	1.83	1.31	3.90
82	N5	2.80	1.46	2.92
83	N6	3.26	2.91	1.70
84	O1	8.49	2.91	0.13
85	O2	8.42	3.07	0.18
86	O3	9.34	2.65	-0.02
87	O4	1.82	1.05	3.62
88	O5	2.04	0.72	1.24
89	O6	1.47	1.60	3.42
90	P1	9.47	2.71	-0.14
91	P2	8.18	3.39	0.15
92	P3	2.16	1.34	3.73
93	P4	7.86	3.58	0.03
94	P5	3.49	3.30	1.70
95	P6	2.02	0.68	1.02
96	Q1	7.49	3.39	0.08
97	Q2	8.34	3.16	0.13
98	Q3	8.52	3.08	0.21
99	Q4	8.33	3.13	0.22
100	Q5	8.45	3.14	0.18

A comparison of the graphic measures with that of moment measures is shown in the Fig. 2.19. It is found that, almost a one to one correlation exists in the case of mean and standard deviation, but the skewness values vary considerably. The graphic skewness formulae restricts the skewness values between -1.0 and +1.0, but in moment skewness, for the present set of samples, the values goes up to +4.0. Hence, skewness values do not give any significant correlation.

As said earlier, the model is based on a sequential change in the grain-size distributions. But in nature, such a perfect sequentiality in the downcurrent direction is seldom observed. In order to obtain a probable direction of sediment transport, the model envisages a statistical approach involving examination of all possible pairs of size parameter combination in a sample suite. For a sequence consisting of 'n' number of samples, there are $(n^2-n)/2$ directionally oriented pairs suggesting a preferred transport in one direction and an equal number of pairs in the opposite direction. On comparing any two samples (D1 and D2) for their mean size, sorting and skewness, the following eight possible trends can exist. Compared to D1, D2 may be (1) finer (F), better sorted (B) and more negatively skewed (-ve); (2) coarser (C), more poorly sorted (P) and more positively skewed (+ve); (3) C,B and -ve; (4) F,P and -ve; (5) C,P and -ve; (6) F,B and +ve; (7) C,B and +ve; or (8) F,P and +ve.

While considering better sorting as the criterion for working out sediment pathways, two cases indicative of the transport direction are to be taken into account to avoid uncertainty associated with the variance (McLaren and Bowles, 1985). They are F,B and -ve (referred in the model as Case B) and C,B and +ve (referred as Case C), either of which have one-eighth

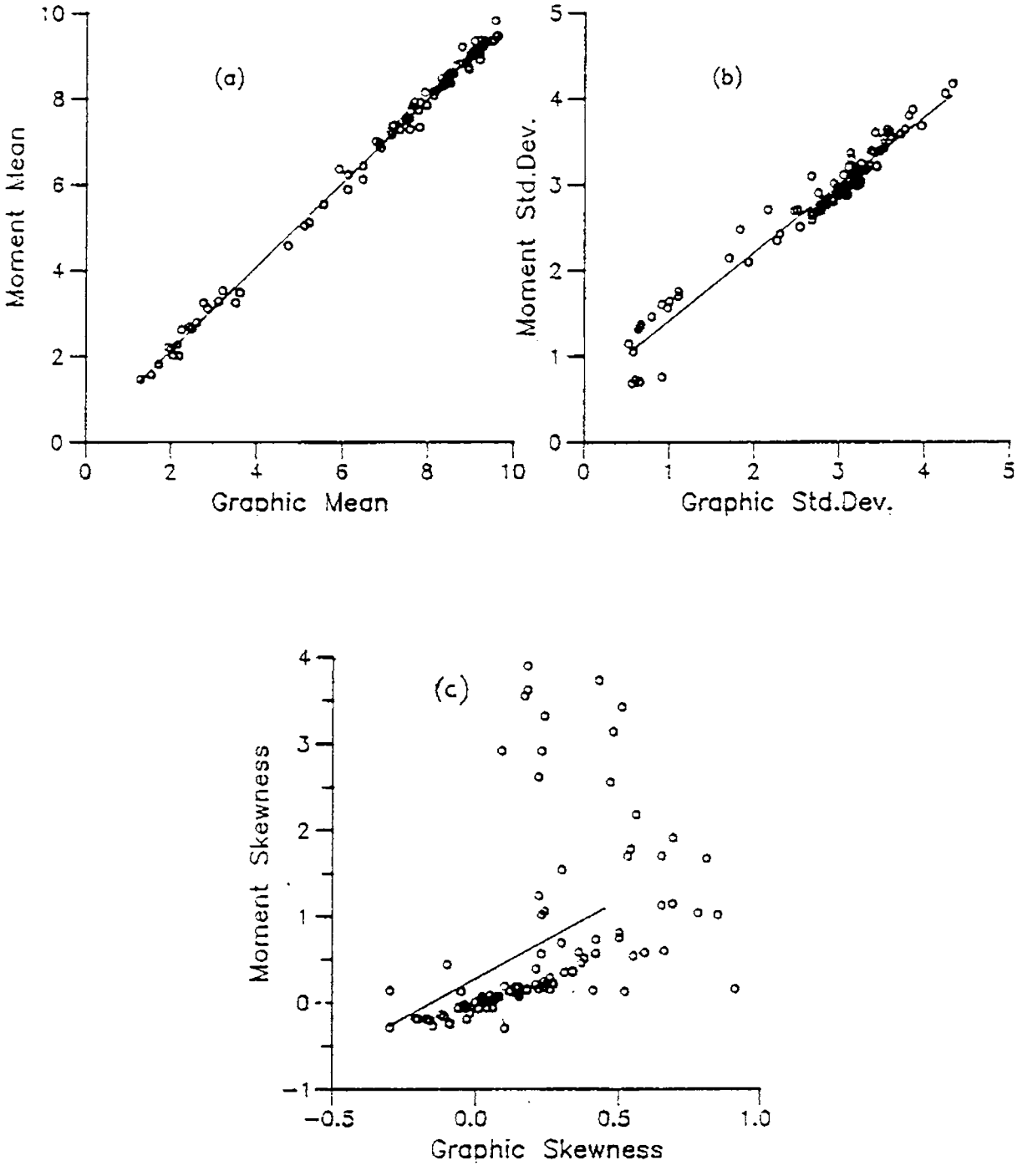

Fig. 2.19 Plots of graphic Vs moment measures

probability of occurrence at random (p = 0.125). In the first combination (Case B), fining of sediment with a progressive improvement in the sorting values and increase in negative skewness in the direction of transport indicates a low energy regime. The other combination (Case C) shows a coarsening tendency with an improved sorting and more positively skewed size distribution along the direction of transport and signifies a high energy regime.

Exceedence of random probability of 0.125 over the number of occurrence of a particular case are determined by the following two hypotheses:

H_o: when, $p < 0.125$, there is no preferred direction of transport.

H_1: when, $p > 0.125$, transport is occurring in a preferred direction.

In a one-tailed 'Z' score calculation (Spiegel, 1961), the hypothesis H1 is accepted only when Z is > 1.645 for 0.05 level of significance or > 2.33 for 0.01 level of significance, where,

$$Z = \frac{x - Np}{(Npq)^{1/2}} \quad \text{where,}$$

x = observed number of pairs representing a particular case in one of the two opposing direction,

N = $(n^2 - n)/2$, the total number of possible unidirectional pairs, where 'n' is the number of samples in the sequence,

p = the one-eighth probability of occurrence either Case B or C, i.e., = 0.125,

q = probability of not occurring transport in a particular direction = (1 - p) = 0.875.

For a proper evaluation of the transport direction, a minimum of 30 unidirectional pairs (N) are considered to be necessary. This requires a minimum of 8 or 9 samples in a sequence.

Sediment trends derived from the 'Z' score statistics, indicate a complexity both in direction as well as in energy regimes (Table 2.7). Notable variation in the number of possible pairs along each bathymetric contour can be related to the differences in the number of samples selected. At 5 m and 10 m contours, the 'Z' scores give a higher value for the Case B south trend. A north trend (Case B) score, though not high, is also significant (Fig. 2.20). As the depth increases the 'Z' score yields higher values with a south trend. This would probably indicate existence of high energy regime in the deeper areas beyond 15 m. However, low energy transport regime towards north is also significant both in 15 m and 20 m. But the northward Case B and C trend becomes insignificant further seaward at 25 m and 30 m contours. On careful examination, the 'Z' score statistics indicate seaward variation in the energy regimes and transport directions. The variations are summarised in the Fig. 2.21. Low energy (Case B) trend is significant up to a depth of 10 m. The 15 m bathymetric contour is marked as a transition zone, where, the low energy transport trend swing equally in both the directions. From the transition zone, the northward Case B trend intensifies again at the 20 m contour, beyond which it ceases to exist. Significant southward Case C trend exists from 15 m to 30 m. However at 30 m, even the Case C northward transport appears to be significant ('Z' score at 30 m is less because of the smaller number of samples considered for the calculation).

TABLE 2.7

Summary of number of pairs producing transport trends.

	5 METER		10 METER	
	NORTH TREND	SOUTH TREND	NORTH TREND	SOUTH TREND
CASE B	N = 136 X = 33 Z = 4.15"	N = 136 X = 54 Z = 9.59"	N = 91 X = 22 Z = 3.37"	N = 91 X = 29 Z = 5.59"
CASE C	N = 136 X = 14 Z =-0.78	N = 136 X = 19 Z = 0.52	N = 91 X = 8 Z = 2.42"	N = 91 X = 18 Z =-1.07
	15 METER		20 METER	
	NORTH TREND	SOUTH TREND	NORTH TREND	SOUTH TREND
CASE B	N = 136 X = 33 Z = 4.15"	N = 136 X = 29 Z = 3.11"	N = 136 X = 40 Z = 5.96"	N = 136 X = 14 Z =-0.78
CASE C	N = 136 X = 18 Z = 0.26	N = 136 X = 47 Z = 7.77"	N = 136 X = 17 Z = 0.00	N = 136 X = 45 Z = 7.25"
	25 METER		30 METER	
	NORTH TREND	SOUTH TREND	NORTH TREND	SOUTH TREND
CASE B	N = 136 X = 26 Z = 2.32'	N = 136 X = 13 Z =-1.04	N = 55 X = 7 Z = 0.05	N = 55 X = 1 Z =-2.40
CASE C	N = 136 X = 28 Z = 2.85"	N = 136 X = 57 Z = 10.36"	N = 55 X = 11 Z = 1.68'	N = 55 X = 20 Z = 5.36"

' Significant at 0.05 level
" Significant at 0.01 level

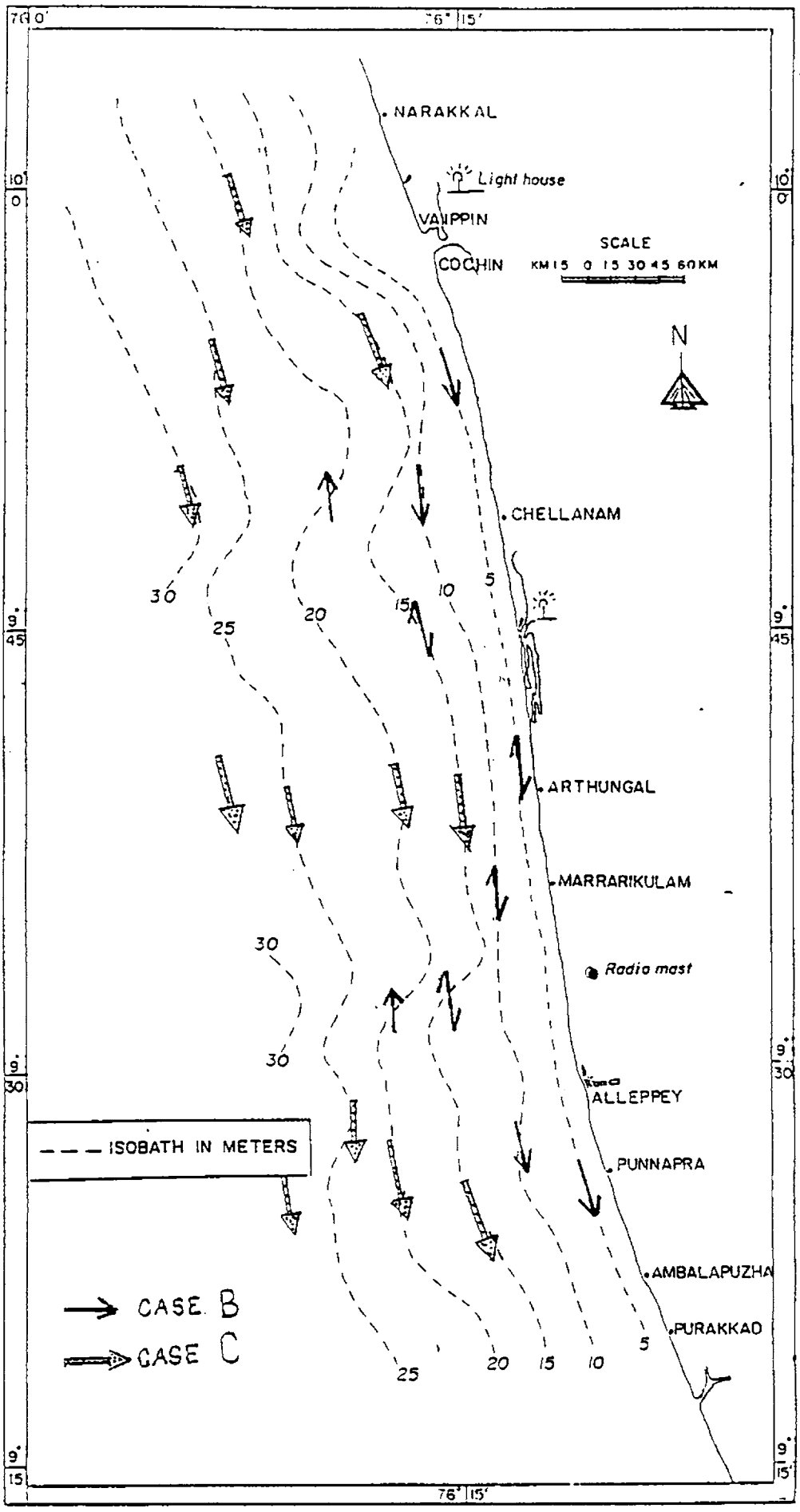

Fig. 2.20 Sediment pathways along different bathymetric contours

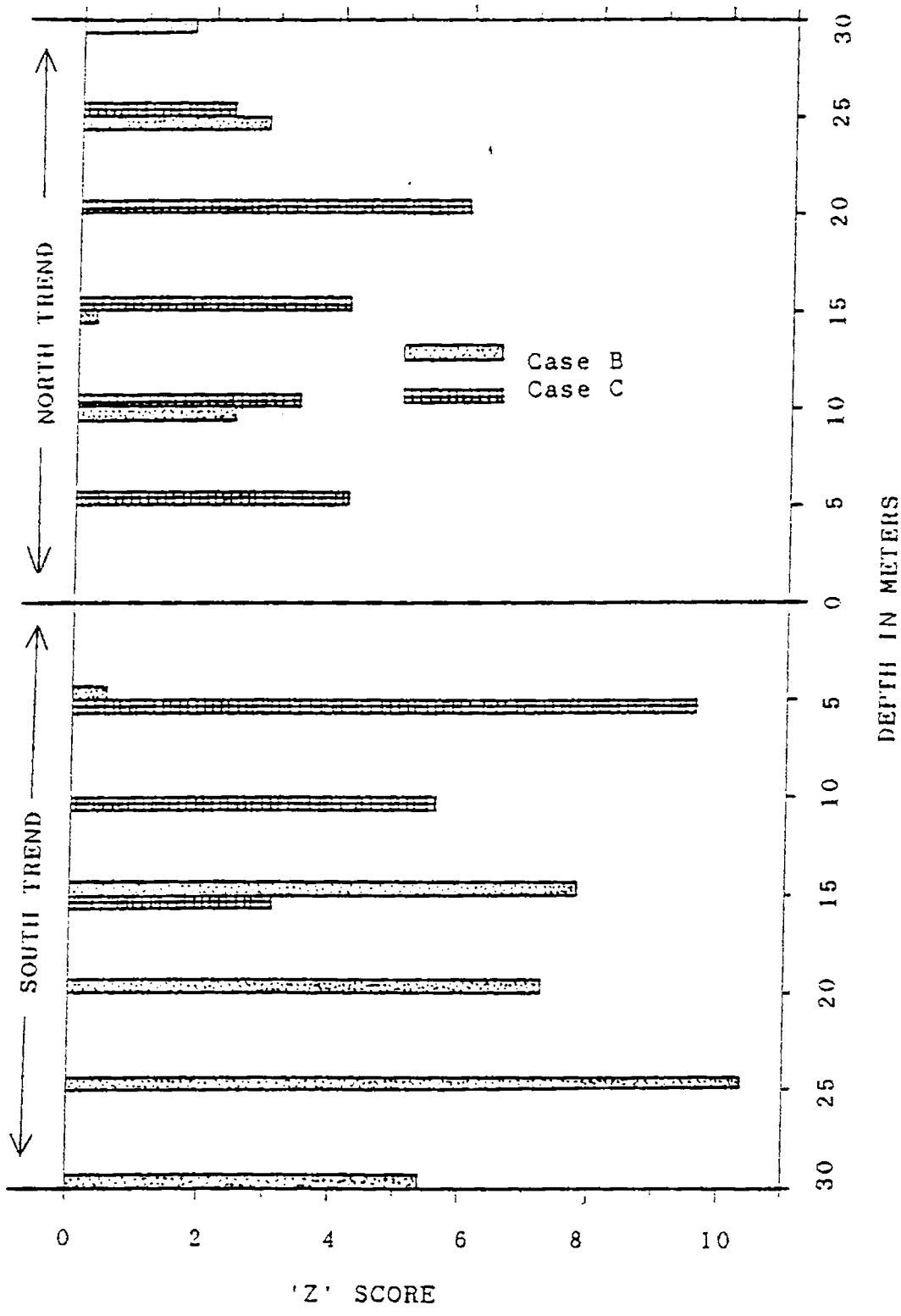

Fig. 2.21 'Z' score variations with depth

In general, the study shows (i) a significant southward transport of sediments along the shelf and (ii) the shallower areas are characterised by a low energy regime, whereas, deeper parts of the innershelf beyond 15 m contour are marked by a high energy regime. Earlier studies on longshore currents and refraction pattern along the coast shown that southerly currents are dominant during the monsoon, whereas during pre and post monsoon season the northerly currents are significant (Hameed, 1988). The southerly currents are estimated to be stronger compared to the northerly currents (Samsuddin and Suchindan, 1987). The coastal currents, which forms part of the ocean circulation pattern also show almost a similar trend. In this model, computation has been done using the samples collected during the post-monsoon season (October). Thus, the net sedimentation pattern encountered in the model is due to superposition of strong monsoonal conditions over the northerly drift of non-monsoons. So the net southward transport direction with a congruent low energy regime derived out of the model is fully justifiable.

However, high energy flow directions in the deeper levels may not be a true representation of the present day *in situ* processes. It has been pointed out in the preceding section that, the offshore part of the study area represents a coarser sediment facies, interpreted as a relict beach environment. The high energy 'Z' scores (Case C) could be the resultant response of coarse sand populations incorporated into the model, which otherwise does not characterise the present day conditions. In normal cases it is quiet unlikely to encounter such a high energy flow in the outer innershelf, when the turbulent nearshore area itself experiences a low-energy transport regime. There are no reports of such strong coastal currents which can enable deposition of a better sorted coarse sediment along the shelf. In

such cases, the model can not be applied with full confidence to explain present day transport patterns, when the sediment pathways are influenced by the relict coarse sediment deposit.

In the marine environment, cohesive sediments are transported predominantly as loosely bound aggregates (Berthois, 1961). An empirical approach, like the one presented here, can not be fully satisfactory to derive size based hydraulics, since the individual fine particles tend to loose their identity and move as aggregates (Krank, 1975). Kuel *et al.* (1988) found that, particles < 16 μ are transported as flocs and are not hydraulically sorted. Hence, cohesion of the fine particles may give a misleading picture of transportation. It was reported that even a current which can transport coarse silt and fine sand fractions as individual particles can not transport finer sediments due to their cohesion (Nair and Hashimi, 1987). This is one of the major limitations of the model, when it is utilised to deduce transport pathways for fine clastics. However, the model has been used successfully by Ramachandran and Samsuddin (1991) and Prithviraj and Prakash (1990) for deducing transport direction in fine grained sedimentary environments. The absence of data set on current pattern and circulation processes over the shelf forces the author to generalise the pattern of sediment transport in the southerly direction for the innershelf based on the model described.

2.4.4 Quartz grain surface texture and relict beach sedimentation

Scanning Electron Microscopic (SEM) techniques have been extensively used to study the surface textures of detrital minerals in particular to those of quartz grains to understand the mode of deposition in different regimes and their subsequent diagenetic changes. SEM studies of quartz grain

surface texture of the outer innershelf were undertaken to get more insight into the mode of deposition of these sediments from the analysis of the characteristic surface textures.

SEM study, well documents the effect of chemical and mechanical processes. The resulting surface features are regarded as important indicators of depositional characteristics of different environments (Krinsley and Donahue, 1968; Krinsley and Doornkamp, 1973; Bull, 1978; Georgiev and Stoffers, 1980; Bull *et al.*, 1980). With the introduction of SEM techniques, identification of sources, interpretation of genesis and diagenetic changes of various detrital sediments were made easier.

In general, surface features of mechanical processes dominate in the sand grains of the outer innershelf sand facies. Features resulting from precipitation and dissolution phenomena also can be observed. The grains from the sand dominant zone are generally sub-rounded to well rounded in appearance (Plate 1). While, the grains from mud-rich samples show some amount of angularity (Plate 2). The better rounded appearance of the grains from sand-zone would probably indicate pronounced mechanical action under the impact of rolling and abrasion of the grains.

Mechanical features like 'V' shaped pits (Plate 3) and conchoidal fractures (Plate 4) are common in the sand-zone grains. Though innershelf grains from mud-zone do show some 'V' pits, the intensity of such features are rather less. Quartz grains from the sand body exhibit larger number of regular 'V' pits with linear scratches, suggesting transport and deposition of the sediments under subaqueous and high energy collisions (Krinsley and Doornkamp, 1973). Often, the density and abundance of such features are

Plate 1

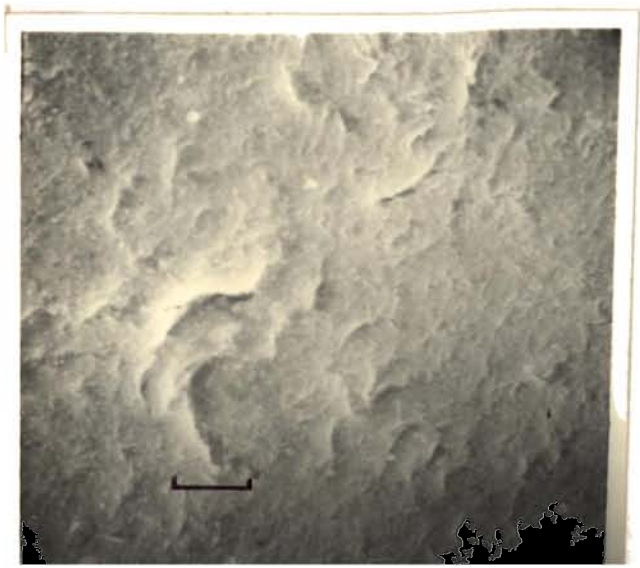

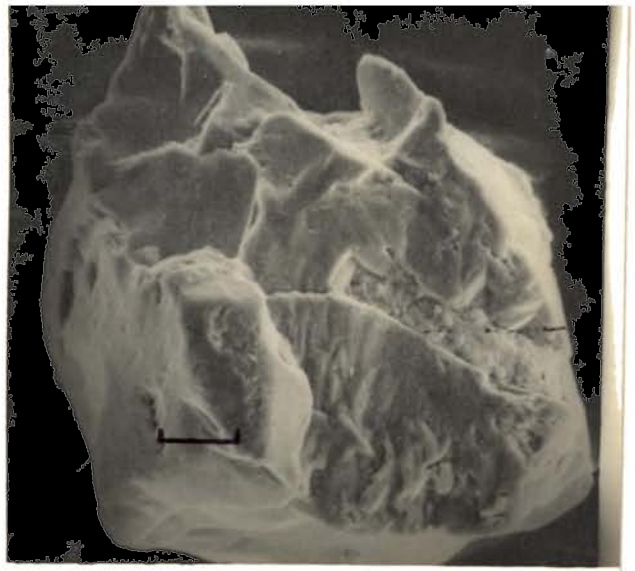

Plate 2

Plate 1. A whole grain from the sand dominant zone of the innershelf showing sub-rounded to well rounded appearance (Scale bar 20 μm)

Plate 2. A quartz grain from the mud rich zone of the innershelf showing characteristic angular edges (Scale bar 20 μm)

Plate 3. A quartz grain from the sand dominant zone showing V-shaped pits (Scale bar 5 μm)

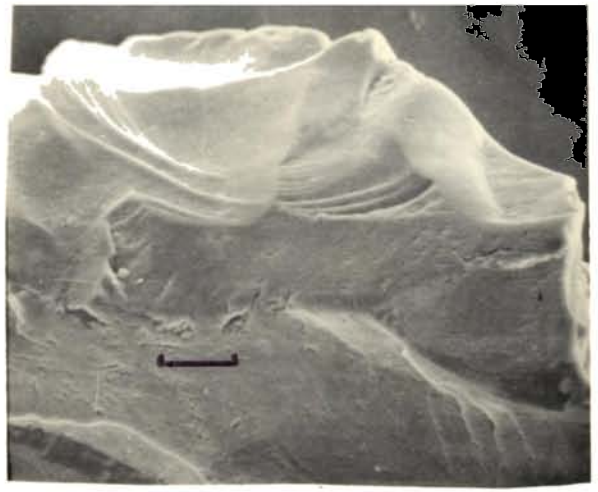

Plate 4

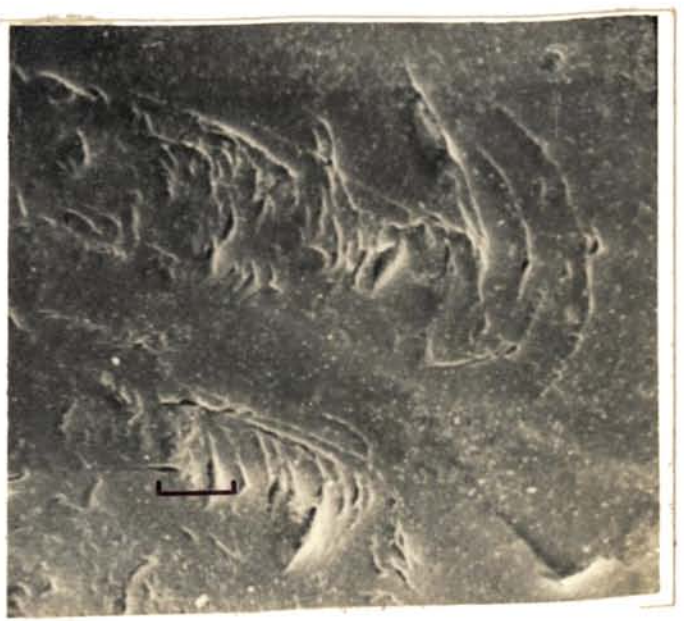

Plate 6

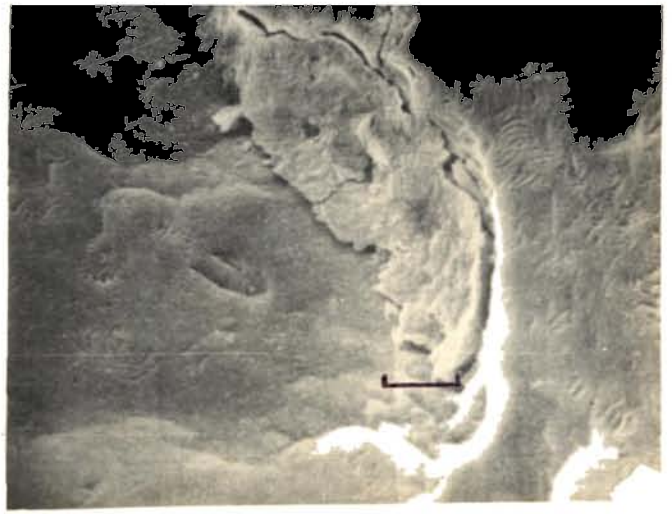

Plate 5

Plate 4. A quartz grain showing conchoidal fracture pattern and and chatter marks (Scale bar 20 μm)

Plate 5. Development of impact pits and chatter marks on the surface of quartz grain (Scale bar 10 μm)

Plate 6. Closer view of the chatter marked quartz grain developed under nearshore dynamics (Scale bar 5 μm)

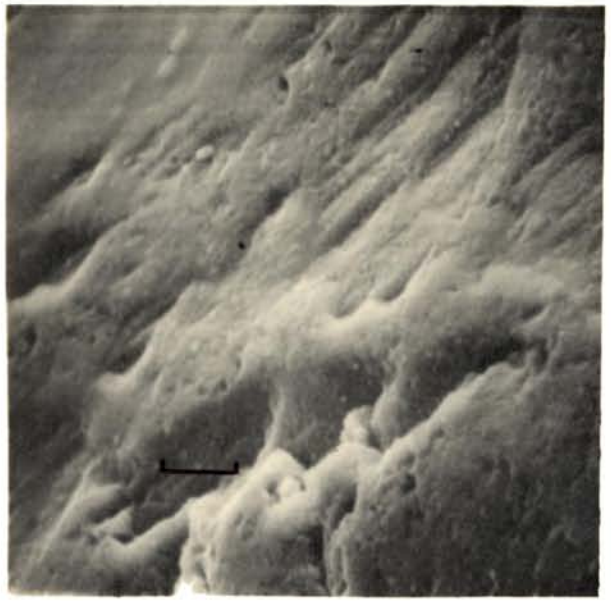

Plate 8

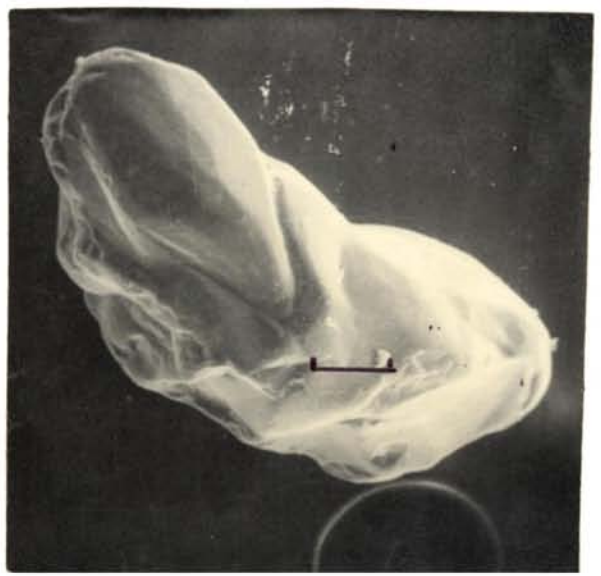

Plate 9

Plate 7. A quartz grain development of euhedral faces formed due to recrystallisation of silica
(Scale bar 50 µm)

Plate 8. V-shaped pits subsequently modified by surficial capping of sugary coatings of field by surficial capping of silica
(Scale bar 5 µm)

Plate 9. Formation of silica globules in the surfaces of quartz grain from the sand dominated zone
(Scale bar 10 µm)

related to the duration and intensity of subaqueous agitations (Krinsley and Donahue, 1968).

The chatter marks (Plate 5 and 6) are not common feature of the nearshore environments. These are considered as unique features developed due to glacial grinding (Folk, 1975; Bull, 1977; Gravenor *et al.*, 1977; Gravenor, 1982, 1985). Bull *et al.* (1980) identified chatter marked garnets from areas like Sierra Leon and Cape Comorin (India), which are unlikely to have been developed by glacial grinding. Karpovich (1971) also reported chatter marks from dune sands. However, many reports pointed out that, chatter marks are developed mainly on quartz grains from glacial environments or on garnets from the beaches (Gravenor, 1985). Samsuddin (1990) reported occurrences of chatter marks on the quartz grains from nearshore environment of Canannore coast and are considered to be developed from the mechanical abrasion of mineral grains. Similarly, chatter marks are found to be well preserved and abundant on the quartz grains from the study area. The development of chatter marks are related to the response of mechanical abrasion of the grains caused by the glancing blow across the face of a grain (Bull, 1978). Krinsley and Margolis (1971) also attributed that, such features are produced by a portion of one grain skipping across another.

In addition to the chatter marks, grains from the sand zone show evidences of super-imposition of chemical dissolution features such as euhedral silica precipitation (Plate 7) in the form of sugary coating (Plate 8) and silica globules (Plate 9), that tend to obscure the original surface textures. These globules are considered as deposited due to periodic evaporation of inter-granular water (Ribault, 1975). Upturned plates marked with secondary silica precipitation are also exhibited by the grains. Karpovich (1971) had related

the formation of silica globules and surface coatings of silica on quartz grains to crystal structure of the parent material. Preston (1977) opined that, they represent different stages of diagenetic history of the sediment.

It is therefore emphasized that, the innershelf sand bodies, being part of the relict sediments, are considered to be deposited during the lower stand of sea level in the geologic past. In general, quartz grains examined under SEM exhibits distinct history of superposition of surface textures. High concentration of 'V' pits and the silica globules on the surfaces of the grains from sand-zone could be considered as a product of subaqueous transport under high energy conditions. Higher degree of rounding exhibited by the grains also reaffirms this view. Such a process of mechanical action in the aqueous media can not take place at the present depth of its occurrence, as the wave orbital motions can not induce such strong movements. The process that might have developed the grain rounding and the mechanical pits most likely, could be due to the action of shallow waves. Grain to grain collision at the plunge point of waves and the subsequent rolling by swash and backwash would result in such surface features. The dissolution features, conchoidal fractures and the chattermarks may indicate its subsequent modification under the present day shelf processes.

From the combined analysis of granulometry and SEM studies, it is inferred that the sandy patches are of relict nature. They are the resultant responses of beach activity during the lower stand of sea level in the geological past. As the grains show re-crystallisation features, it would probably mean their subsequent exposure to sub-aerial weathering, where they are exposed to rain water, organic action and fairly rapid changes in the pH and temperature (Hey *et al.*, 1971). Occurrences of coarse sand deposits in

the deeper parts of the innershelf on the east coast of India were observed by Mohana Rao *et al.* (1989) and Srinivasa Rao *et al.* (1990). It was inferred to be the result of low stand of sea level at that depth. Similarly, Holocene low stand shore lines were identified at varying depth on many of the continental margins of the world (Franzier, 1974). Submerged terraces observed on the western continental shelf of India between Bombay and Karwar at depths varying from 92 to 55 m were inferred to be of Holocene age (Nair, 1974). Hashimi and Nair (1981) discussed the presence of relict calcareous sediments on the outer shelf. Subsequent studies have indicated change in climatic conditions (humid to arid) during Holocene (Hashimi and Nair, 1986). So it is quiet likely that, the coarse sediments on the innershelf could be the result of clastic sedimentation during the later part of Holocene due to transgression from the earlier carbonate facies. The very recent observation of Reddy and Rao (1992) amply supports this view, by noting mid-Holocene strand line deposits on the innershelf at 25 to 35 m depth off Cochin, though the alongshelf spatial extent of it was not depicted. Prithviraj and Prakash (1991) also identified such deposits in the outer innershelf off Kuzhipalli-Chawghat area (north of the study area). The present investigation depicts a shoreward bend of sand-rich zone off Alleppey. It is possible that, towards further south of this area (towards Quilon), these sand zone may merge with the modern sediments, where the nearshore is characterised by sand dominant modern clastic sedimentation.

2.4.5 Sedimentation details from core lithology

Core lithological study shows marginal variation in granulometric composition with depth. The maximum length of core collected was 65 cm and majority of the cores characterise uniform pattern of mud distribution. This

depicts that, the nature of sedimentation in the past essentially continued in a similar pattern as that of present for the period of time actually represented by the cores. It can be inferred from the pattern that, there is a blanket of mud of considerable thickness in the nearshore region. Certain core samples show higher sand content at the bottom indicating mixing of the modern sediments with relict sands. This also illustrates the deposition of modern terrigenous sedimentation over the relict sands of Holocene age marking a transgressive depositional facies.

The sand-rich sediment cores show a little vertical variation with varying percentages of mud mixed at various levels. Despite the minor textural variation, the sand zone keeps it identity presumably due to insufficient physical energy of waves and currents to rework and redistribute the sands with fine clastics. The fine sediments that are transported and deposited on the sand layer can get re-suspended with slight mechanical agitation as the sediments lack cohesion. Hence, in areas where the supply of fine sediments are lower than the amount of sediments that are re-suspended and transported, sands are exposed. Nair and Hashimi (1987) made an attempt to study the wave controlled depth of occurrence of cohesive (recent mud) and non-cohesive (relict calcareous sand) boundary on the western shelf of India. The depth of occurrence of the boundary is controlled by effective sediment movement by long period waves. But the depth of the sedimentary boundary in the northern half of the western shelf of India occurs at a deeper level (60 m) than on the southern half (20 - 40 m). So, apart from the effects of rate of re-suspension process over the rate of deposition of modern fine-clastics, the wave-dominated depth regulation of the sediment boundary layer (Nair and Hashimi, 1987), also plays an important role in maintaining the undisturbed relict sand sediments in the innershelf zone.

CHAPTER 3

MINERALOGY OF THE INNERSHELF SEDIMENTS

3.1 INTRODUCTION

The interest that attaches to the study of mineralogical assemblages in sediments is chiefly due to the effective use of them in identifying the source and dispersal characteristics of sediments. Minerals may be lost or modified by weathering in the source area, by transportation to the site of sedimentation, and by diagenesis. Because the mineralogy of the sediments is the inheritance from the source area as modified by sedimentary processes, it is one of the most practical studies that can be made to reconstruct the provenance, for the effects of transportation and chemical additions during sedimentation and diagenesis.

In the course of weathering, feldspars may be altered to kaolinite or intermediate product; pyroxenes and amphiboles are more likely to simply dissolve and be transported as dissolved ions. In contrast, some minerals such as quartz are slightly soluble, hence, in general they are transported unchanged in amount or character from source rocks. Thus, very largely, sediments represent a residuum from surficial chemical weathering processes. The effect of transportation results in attrition of minerals, whereby the softer minerals may be reduced in size relative to the harder minerals. Dissolution, precipitation or alteration during diagenesis may drastically alter the net composition of the minerals present. Over all compositional differences may also be brought about by mixing of sediments recycled from older sediments.

The interpretation of the mineralogy of sediments is dependant on a proper assignment of mineral species present to a meaningful genetic category. A single list of minerals present is virtually meaningless, instead several lists by categories, such as primary detrital, precipitated and post-depositional alteration products are required. So the problem of interpretation of mineral composition of sediments lies in separating out the effects of the sedimentary cycle of weathering, transport, deposition and diagenesis with a proper understanding of the basin of deposition.

This study examines the mineralogy of the innershelf sediments through heavy and clay mineral composition (Part A and Part B respectively).

3.2 PART A: HEAVY MINERALS

Assemblages of heavy minerals contained within sands have been used for many years to analyse the sources and transport paths of sediments. Heavy minerals range from tourmaline and zircon, which do not occur in large amounts in any source rocks but are resistant to mechanical and chemical attack, to the amphiboles and pyroxenes, which may be an abundant constituent of some source rocks but show little resistance to decay. To the extent that the heavy minerals survive the hazards of weathering, transport and diagenesis and to the degree that they occur in a restricted range of provenance type, they are most useful for source rock interpretation. The classical studies by Krumbein and Rasmussen (1941), Pettijohn (1941), Rasmussen (1941) and Rittenhouse (1943) in both modern and ancient sedimentary units have formed the excellent principal contributions in this regard. In an early application, Trask (1952) studied the movement of sand along the beaches of California, and demonstrated that the sand which fills the

harbour at Santa Barbara came from more than 160 km up the coast. Van Andel (1964) similarly studied the transport paths and depositional pattern of sands in the Gulf of California, relying on contrasting mineral assemblages to characterise the various river sources. The most recent studies on this topic by Morton (1984, 1985), Statteger (1986) and Mezzadri and Saccani (1989) have added a new dimension to provenance studies.

Rubey (1933) noted that the heavies are concentrated in the finer fractions than having the same mean grain size of the sediments in which they are found. Rittenhouse (1943) clearly established that heavy minerals have a strong tendency for sorting and concentration. The sorting process and dispersal pattern of sediments attempted recently based on heavy mineral assemblages are found to be successful (Komar and Wang, 1984; Clemens and Komar, 1988; Komar *et al.*, 1989).

Several studies have been reported on the heavy mineral distribution and concentration in river, beach and shelf from different parts of the world (Connah, 1961; Kulm *et al.*, 1968; Scheidegger *et al.*, 1971; Burns, 1979; Beiersdorf *et al.*, 1980; Meyer, 1983; Peterson *et al.*, 1985; Wickremeratne, 1986). In India, some amount of work have been carried out on the placer deposits and heavy minerals of the beach and shelf (Tipper, 1914; Mahadevan and Rao; 1950, Jacob, 1956; Roy, 1958; Mallik *et al.*, 1974; Siddiquie *et al.*, 1979). Recent work on the black sand placer deposits of Kerala by Mallik (1986b) and Mallik *et al.* (1987) are mainly restricted to the beaches and rivers in the southwest part of India. Prabhakar Rao *et al.* (1968) carried out studies on the heavy mineral concentration in the nearshore portions of the South Kerala. Purandara (1990) studied the heavy minerals of certain rivers of the South Kerala, Vembanad Lake and the nearshore areas around the Cochin inlet.

However, there are no significant attempt to study the mineralogical constituents of the innershelf zone of the study area. It is therefore imperative to study the heavy fraction of the innershelf sediments on a spatial consideration to:

i. evaluate the composition of the heavy minerals to characterise the sediment distribution,
ii. decipher the provenance of the sediments and
iii. identify the processes which control the mineralogical variations.

3.2.1 Methods

Representative sediment samples (26 nos.) were selected from the study area for heavy mineral analyses. Sand fractions were separated and sieved into different size fractions. The standard procedure now generally followed is to analyse the heavy minerals in specific sieve fractions of the distribution of size (Lewis, 1984). So the fractions in 63 - 125 and 125 - 250 μ were selected, the objective being to eliminate any potential grain-size control on the determined mineralogy. The heavies in these two fractions were separated using bromoform (specific gravity ≈2.89). The heavy mineral separates were mounted on slides using Canada Balsam. Around 300 heavy mineral grains were identified and counted under a petrographic microscope using standard micrographic techniques. Counting was carried out for all the 26 samples in 63 - 125 μ range. But for the 125 - 250 μ fraction, only 5 samples were counted for comparing the size-dependant differences in the mineralogy with their respective finer counter parts. The percentages of the minerals were prepared based on the petrographic count data.

3.2.2 Results

Total heavy mineral content in the sediments: The two fraction gravity separation results of heavy minerals show that, irrespective of the type of sediments and locations, the coarser fraction (125 - 250 μ) consists of lesser amount of heavies than the finer fraction (63 - 125 μ) (Table 3.A1). Invariably, all the samples contain heavies in coarser fraction, though in some of them it is in very subtle amount, with a range from 0.13 to 7.78 % with an average of 2.1 %. There is marked abundance in the amount of heavies in finer fraction, varying from a minimum of 0.55 to a maximum of 44.86 % with an average value of 13.03 %. Fig. 3.A1 depicts the sample-wise concentration of heavy minerals in both the fractions. The enrichment of heavies in the finer fraction is imminent, but the concentration difference of heavies between the two fractions in some samples are too small, while in some others, it is many fold.

Aerial distribution map (Fig. 3.A2) illustrates that, the vicinity of Cochin inlet is especially very poor in heavies in both the fractions. Even the entire nearshore area is having a low heavy mineral concentration, except a location near Manakkodam. The abundance of heavies in the seaward portions, especially in the southwestern part of the study area, reaches a maximum in both the fractions. But the enrichment in the finer fraction is very high compared to the coarser fraction.

Details of the percentage constituents of the heavy minerals in the finer fraction are given in Table 3.A2. The heavy mineral suite of the innershelf consists of opaques, garnet, sillimanite, zircon, monazite, rutile, hornblende, pyroxenes, kyanite, actinolite/tremolite, tourmaline, biotite and framboidal

TABLE 3.A1

Heavy mineral concentration in the sediments

Sl.	Sample	Heavy %	
		125 - 250 μ	63 - 125 μ
1	A1	0.54	0.78
2	B1	0.13	1.15
3	B3	2.93	3.91
4	B5	3.51	3.74
5	B6	3.64	20.12
6	C1	0.56	1.06
7	C6	0.26	7.39
8	D1	0.28	1.08
9	D6	0.29	0.55
10	E2	0.90	1.80
11	F4	1.09	1.47
12	H4	1.00	6.58
13	H6	2.74	20.29
14	I1	3.74	12.21
15	I5	0.57	1.77
16	J3	2.49	2.81
17	K4	5.19	6.18
18	K5	1.83	22.56
19	L3	1.28	13.84
20	M5	1.20	40.75
21	N3	2.06	44.58
22	N6	3.98	13.92
23	O2	0.84	1.13
24	O4	7.78	44.86
25	O6	7.22	38.54
26	P6	0.54	25.79

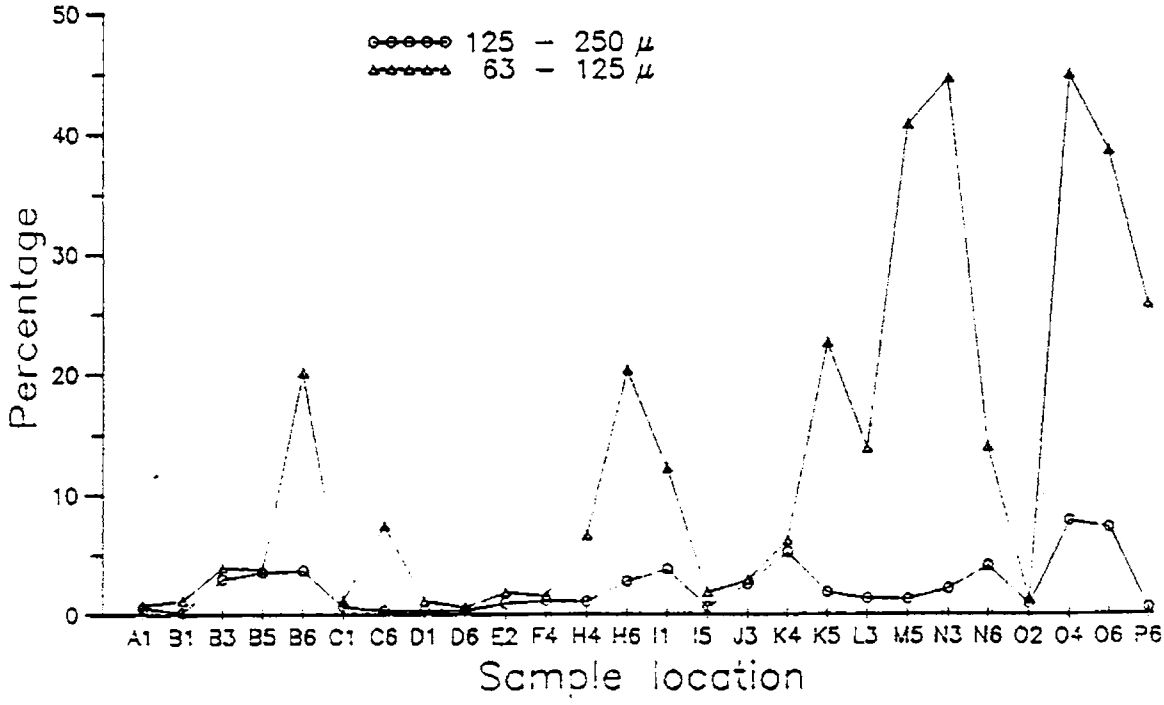

Fig. 3.A1 Locationwise distribution of total heavies in in finer and coarser fraction.

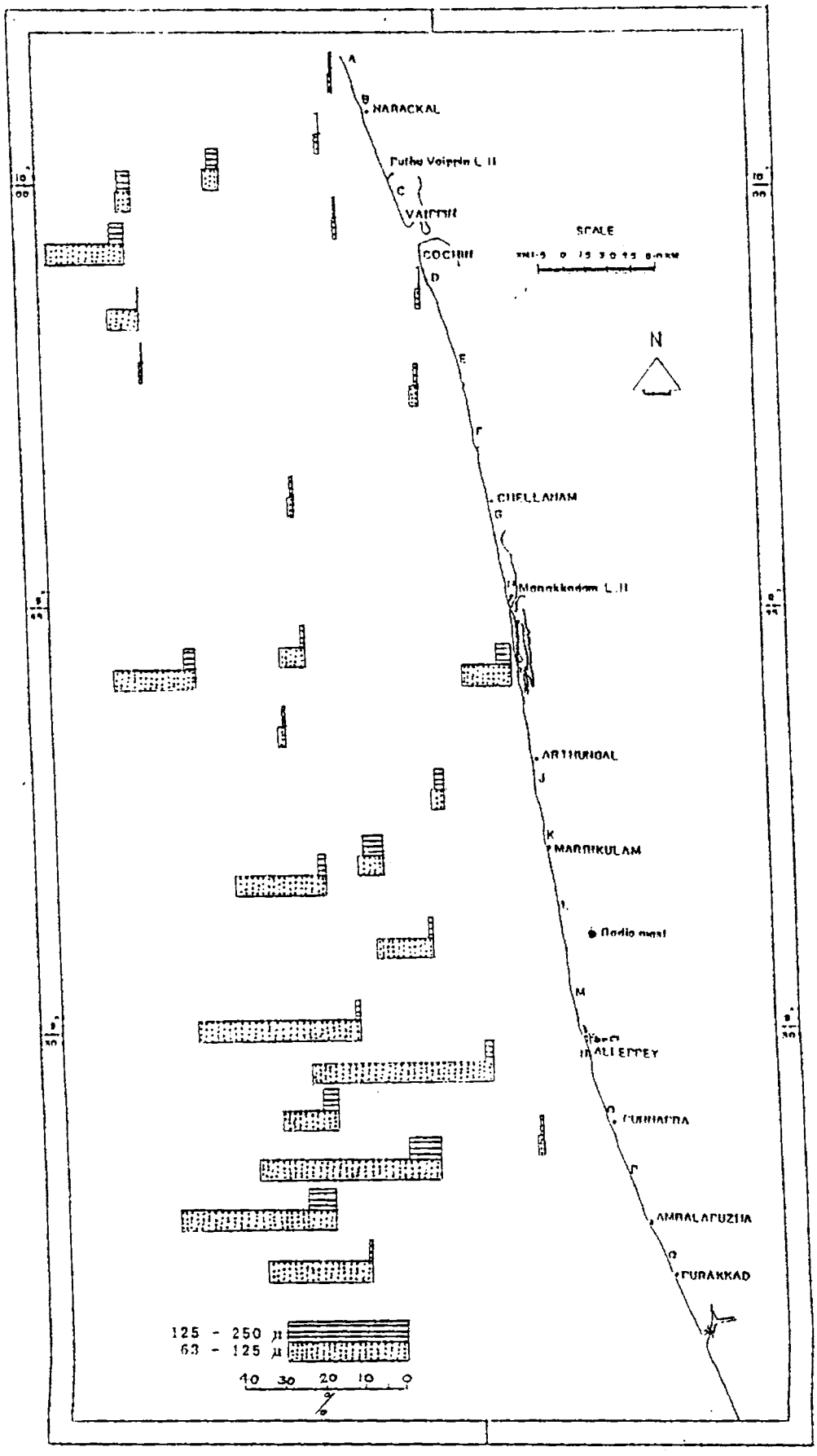

Fig. 3.A2 Spatial distribution of total heavies in finer and coarser fractions.

TABLE 3.A2

Heavy mineral distribution in the 63-125 micron fraction

	Op	Ga	Sil	Zi	Mo	Ru	Ho	O.Py	C.Py	Ky	Ac/Tr	Tu	Bi	F.P
A1	17.6	2.5	12.7	1.6	.8	1.6	45.9	7.0	2.0	.4	.8	-	4.9	2.0
B1	8.5	1.9	19.8	3.7	.4	-	40.3	4.1	1.9	1.1	1.5	-	14.2	2.6
B3	5.9	4.4	12.1	2.9	1.1	.7	49.1	12.8	1.5	-	.7	-	5.5	3.3
B5	25.8	1.5	15.9	3.4	1.1	.4	21.6	3.8	.8	.4	1.1	-	9.8	14.4
B6	51.9	.9	21.4	7.2	1.3	2.8	8.2	1.9	.9	1.6	-	.6	1.3	-
C1	11.1	3.4	14.1	3.4	1.1	1.5	37.4	10.3	5.0	3.1	-	1.1	6.9	1.5
C6	24.7	1.3	27.2	9.4	2.2	1.9	22.5	6.9	-	.9	-	1.3	1.9	-
D1	7.9	1.6	17.0	2.4	1.2	.8	34.8	7.9	1.6	1.2	1.2	-	5.5	6.3
D6	24.9	3.5	18.7	7.3	1.0	3.1	30.8	7.3	2.4	1.0	-	-	-	-
E2	14.7	4.4	12.8	4.7	1.6	.9	43.8	7.2	2.5	.3	-	-	2.2	5.0
F4	18.3	1.6	7.3	.8	.8	.4	28.0	6.5	3.3	1.2	-	-	11.8	19.9
H4	27.1	5.3	32.1	10.6	1.2	3.4	15.0	2.5	.3	.3	-	-	.9	1.2
H6	33.0	1.9	35.3	8.3	2.2	2.2	12.2	3.5	-	1.3	-	-	-	-
I1	17.5	3.1	25.2	6.8	.9	2.2	35.1	5.2	1.9	1.2	-	-	.6	.3
I5	33.4	2.7	20.9	9.4	.3	3.4	18.2	3.0	1.7	.7	-	-	2.4	3.7
J3	8.7	1.5	11.1	4.0	.3	.9	25.4	5.3	1.9	-	-	1.2	33.7	5.9
K4	31.1	2.6	43.5	10.1	1.2	1.7	7.8	1.7	-	.3	-	-	-	-
K5	36.2	1.5	37.1	8.5	2.1	2.4	6.7	3.0	-	1.5	.9	-	-	-
L3	39.1	2.6	28.5	11.5	1.6	2.2	9.3	3.2	.3	.6	.6	.3	-	-
M5	43.3	2.3	30.2	14.1	3.6	2.6	2.9	1.0	-	-	-	-	-	-
N3	33.8	2.1	39.1	19.1	1.8	4.1	-	-	-	-	-	-	-	-
N6	41.5	4.1	25.9	7.6	2.5	3.2	9.8	1.9	.9	1.6	.3	.6	-	-
O2	17.6	1.4	13.7	1.4	.7	2.1	24.1	5.4	2.5	2.5	.7	.4	9.0	18.3
O4	57.7	4.6	18.4	13.7	1.0	4.6	-	-	-	-	-	-	-	-
O6	42.0	3.4	26.2	12.3	5.2	3.1	4.9	1.9	-	-	.3	-	-	-
P6	20.4	4.1	43.0	27.0	1.5	4.1	-	-	-	-	-	-	-	-

Op=Opaques; Ga=Garnet; Sil=Sillimanite; Zi=Zircon; Mo=Monazite; Ru=Rutile;
Ho=Hornblende; O.Py=Ortho Pyroxene; C.Py=Clino Pyroxene; Ky=Kyanite;
Ac/Tr=Actinolite/Tremolite; Tu=Tuurmaline; Bi=Biotite; F.P.=Framboidal Pyrite

pyrite. Their range, mean and standard deviation values are shown in Fig. 3.A3. The characteristics of the minerals observed microscopically are described below.

The opaque minerals include mainly ilmenite and a little of leucoxene, spinel and rutile which are non-transparent. Opaque minerals exhibit various degrees of roundness under the microscope from elongated sub-rounded grains to spherical rounded grains (Plate 3.1). They are the most abundant minerals in the study area, the maximum percentage going up to 57.7. Many garnet grains are broken or angular irregular pieces and some grains contain inclusions. They are colourless, light pink to pink. Average percentage of occurrence of garnet is 2.7. Sillimanite is characterised by elongate prismatic grains (Plate 3.2). They are colourless and some of the grains are short. Zircon grains are euhedral and elongated with some of the grains showing rounded edges (Plate 3.3). Elliptical shaped grains are also encountered (Plate 3.4). Zoning is observed in many grains and some are characterised by inclusions. Zircon on the average gives 8.12 % of the heavy mineral suite. Well rounded and light yellow coloured grains are the very characteristic features observed optically in the case of monazites (Plate 3.5). Though the percentage is very low (average 1.49 %), the grains are so striking during the point-counting exercise. Many of the rutile grains are transparent and some are opaque. On careful examination, thin edges or central part of certain rutile grains show dark red or crimson colour (Plate 3.6). They are characterised by elongate grain morphology and smooth rounded surface. Except a lone sample, all the samples yielded, though fewer in number, rutile grains.

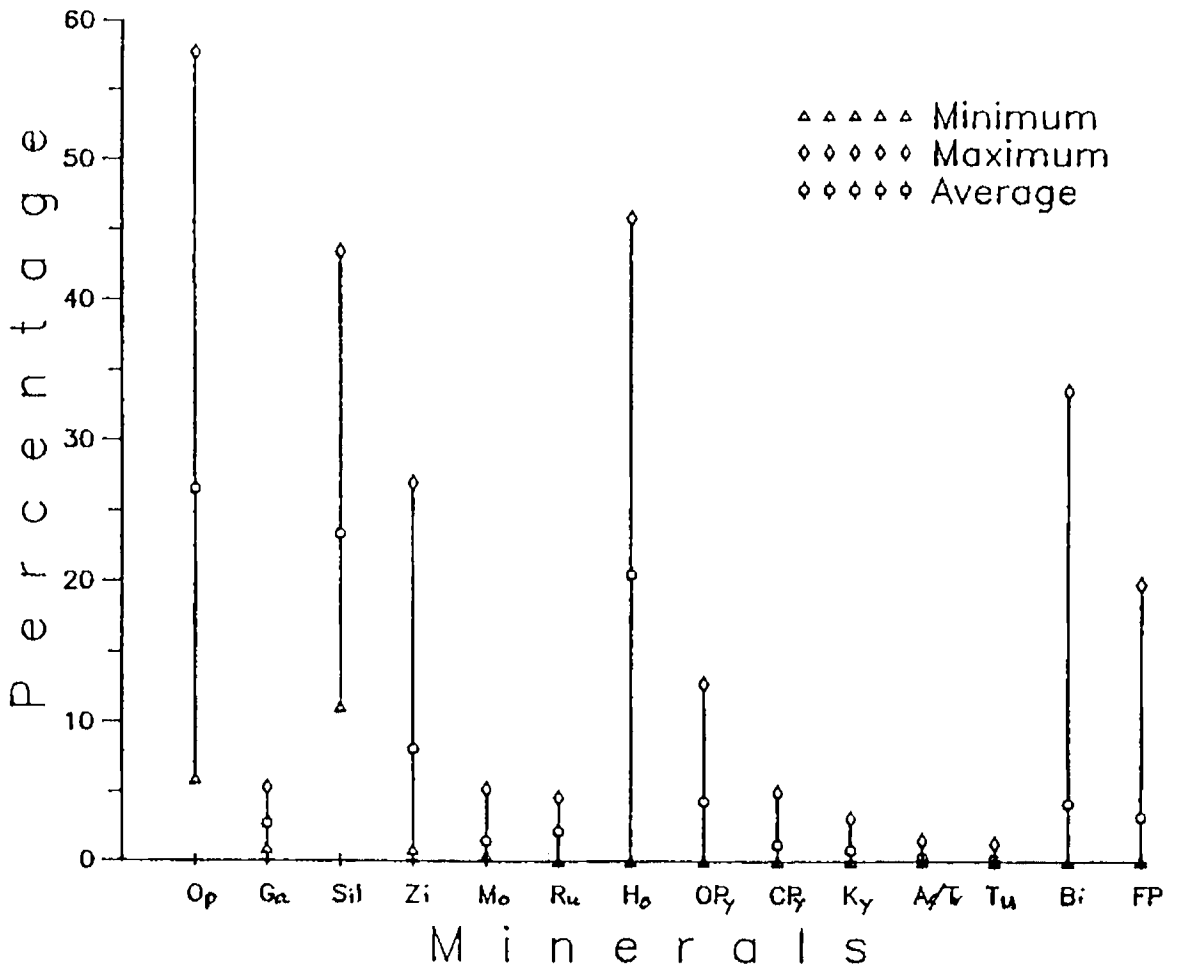

Fig. 3.A3 Plot of range and avarage concentration of heavy minerals in the finer fraction.

At least three varieties of hornblende are observed in petrographic identification with different colours and shades of pleochroism (Plate 3.7). Most frequently occurring ones are the one with pleochroism from light green to green. Many of the grains show pleochroism in shades of brown. A few grains are of intermediate variety. Some of them are toothed and some are altered. Except in three samples, the hornblende is present in adequate quantities in all. Percent variation of orthopyroxene shows that, it is present in almost all the samples, except in three. Hypersthene is the prevalent variety of orthopyroxene, with light coloured but showing characteristic pleochroism from brown to green. A few grains of enstatite are also encountered during the counting. The orthopyroxenes, which are mainly anhedral in morphology and some times toothed, are considerably altered. The percentage of clinopyroxene are relatively much lower than that of orthopyroxenes. It is found to be not present in some samples and ranges up to a maximum of 5 %. Diopside is the main clinopyroxene constituent and augite grains are encountered very rarely.

Kyanite, actinolite/tremolite and tourmaline are present in subtle amount. The average amount of kyanite, actinolite/tremolite and tourmaline are 0.84, 0.31 and 0.21 % respectively with corresponding maximum values of 3.1, 1.5 and 1.3 %. Many of the samples are completely devoid of these minerals. Kyanite occurs as elongate grains, whereas tourmaline shows characteristic pleochroism in brown and dark brown colour. Actinolite/tremolite grains are long and prismatic ones. Biotite is characterised by flaky, basal cleavage and brownish colour. Their concentration shows wide variation and some of the samples are devoid of biotite grains. But it gives a maxima of 33.7 % with an average amount of 4.25 %. Framboidal pyrites, being an authigenic mineral, are found as encrustation on or precipitations in the tests of micro organisms (Plate 3.8).

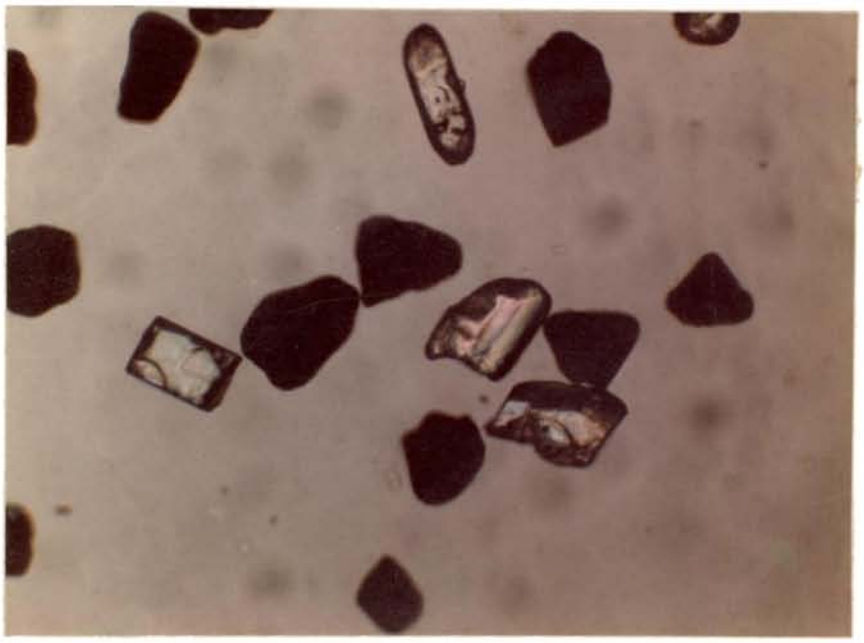

Plate 31. Opaques exhibiting various degree of rounding

Plate 32. Elongate prismatic grain of sillimanite

Plate 33. Elongated grain of zircon

Plate 34. Zircon grain showing elliptical shape

Plate 35. Well rounded yellow coloured grain of monazite

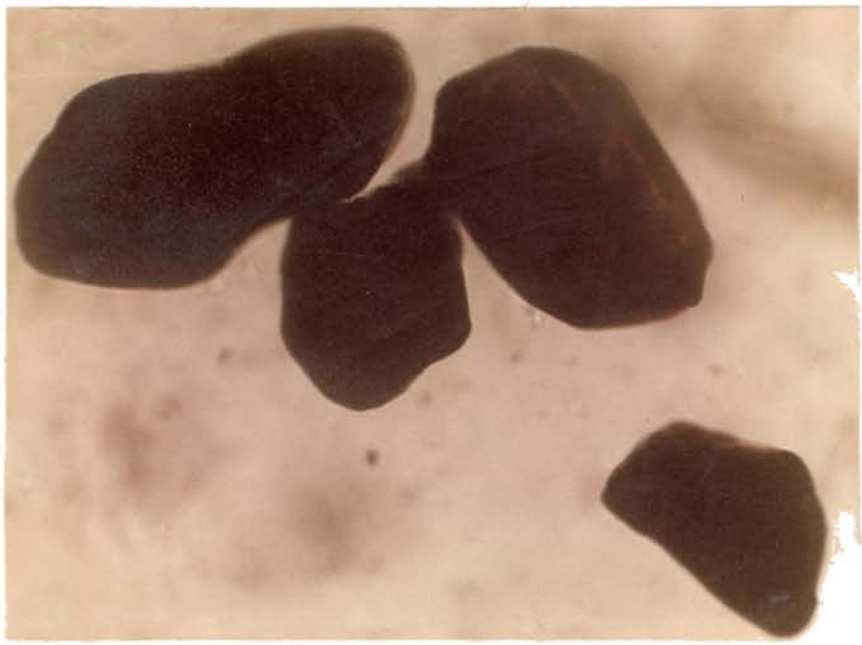

Plate 36. One of the transparent variety of rutile grain

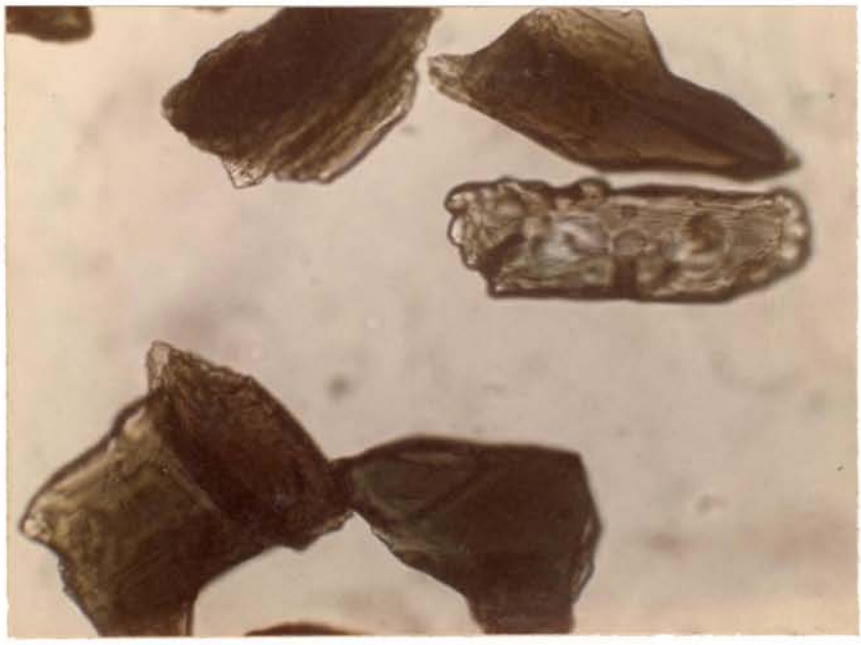

Plate3.7. Hornblende grains exhibiting different colours

Plate3.8. Framboidal pyrite found as infillings in fossil tests

Here it is found mostly in tests of globigerina as bundle of small oolitic precipitates. Though it is rare in some samples, the amount of framboidal pyrite goes up to 19.9 %, the average being 3.25 %. The pyrite bearing tests are not found to be broken.

Concentration of heavy minerals in the finer versus coarser fraction: For a comparative evaluation of the different minerals in the coarser and corresponding finer fraction, a plot is drawn (Fig. 3.A4). The samples (B3, B5, F4, M5 and O6) are so selected that, they represent different domains of heavy mineral assemblages. Considerable differences are observed in the proportions of the principal heavy minerals. However, it is apparent that the trend of variation remains the same for different minerals, except for the framboidal pyrites and biotite in the case of samples B5 and F4. In the case of opaques, except sample B3, all other samples show a relative enrichment in the finer fraction. The second most dominant mineral (sillimanite) is characterised by an enrichment in the coarser fraction than in the finer fraction. But a reverse trend is observed in the case of hornblende, with an abundance in the finer fraction. Even in samples which contain a low percentage of hornblende (M5 and O6), the pattern remains the same. Samples B5 and F4, exhibit an enrichment of biotite but a depletion of framboidal pyrite in the coarser fraction. The other minerals, which are present in small quantities do not display considerable variation in the two fractions. The reasons for attempting a detailed mineralogical study of the finer fractions alone are, (i) the low content of total heavies in the coarser fraction (ii) the striking similarity in the heavy mineral assemblages in the two fractions, though the size induced sorting of the heavy minerals persists.

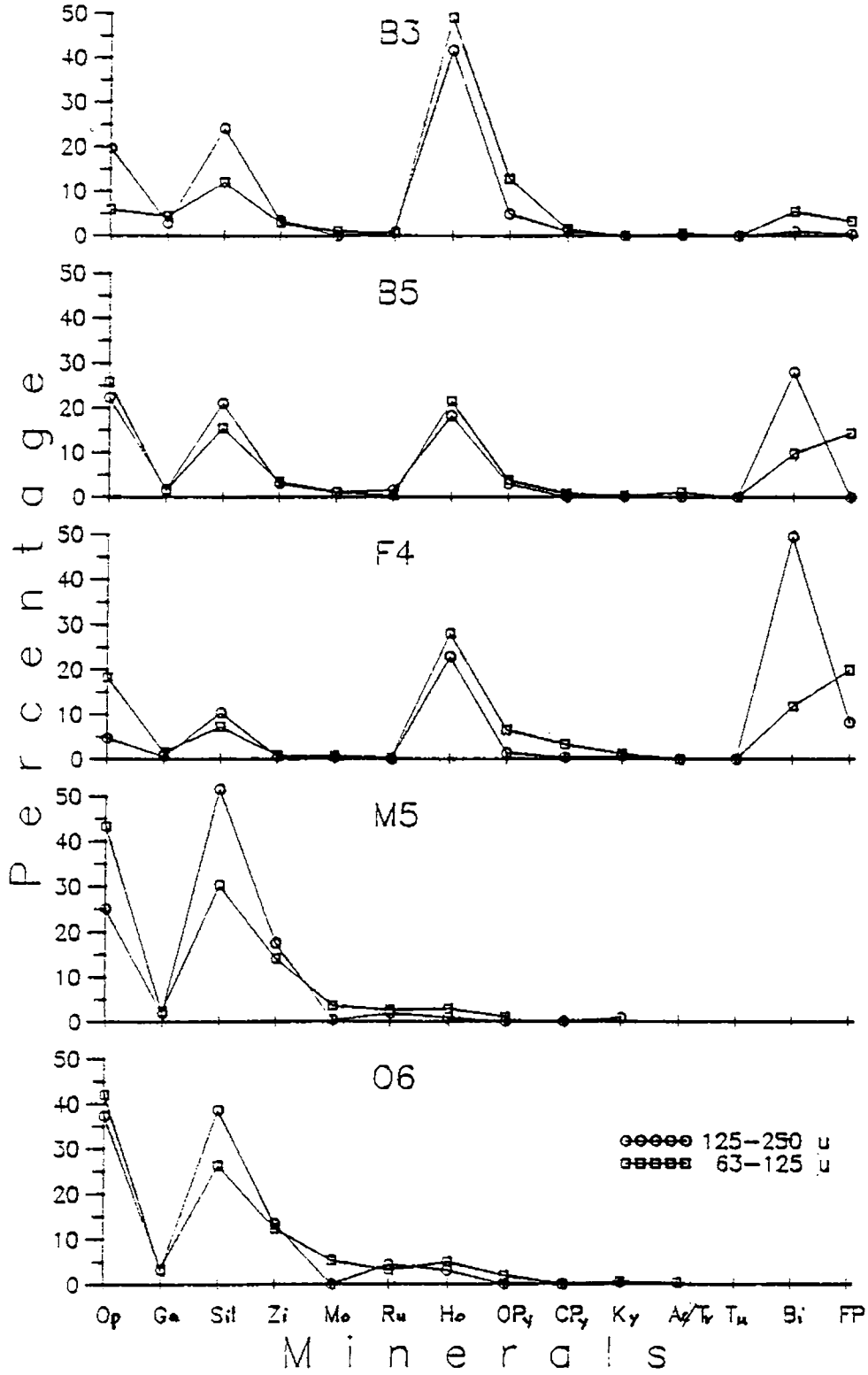

Fig. 3.A4 Comparative mineralogy of finer and coarser fractions

Aerial distribution of heavy minerals: Percentages of the 14 principal heavy mineral components in the finer fraction are plotted in order to decipher their spatial variation in the innershelf. The average abundance of the minerals in their decreasing order is opaques > sillimanite > hornblende > zircon > orthopyroxene > biotite > framboidal pyrite > garnet > rutile > monazite > clinopyroxene > kyanite > actinolite/tremolite > tourmaline.

The distribution pattern of the first four frequently occurring minerals are given in Fig. 3.A5. As observed in the case of total heavy mineral content, the nearshore region especially around the Cochin inlet depicts a low concentration of opaques but it increases offshore. The southwestern part is most conspicuous with the abundance of opaques. The distribution pattern of sillimanite follows that of opaques, except in a few locations, where they dominate over opaques or with lower concentration. Dearth of sillimanite in the nearshore especially around the Cochin inlet is notable.

Hornblende distribution clearly documents a different pattern of dispersal with higher proportions of the minerals in the sediments around the Cochin inlet and gradual depletion in the concentration towards the offshore and southern portions. The three samples, which are devoid of hornblende, fall in the southwestern part of the study area. The next dominant mineral, zircon, illustrates a distribution analogous to that of sillimanite with a depleted amount in the nearshore and Cochin inlet in general but a relative enrichment in other parts.

The next set of most dominant minerals are orthopyroxene, biotite, framboidal pyrite, garnet and rutile (Fig. 3.A6). Orthopyroxene follows the distribution pattern of hornblende as described above. Biotite shows subtle

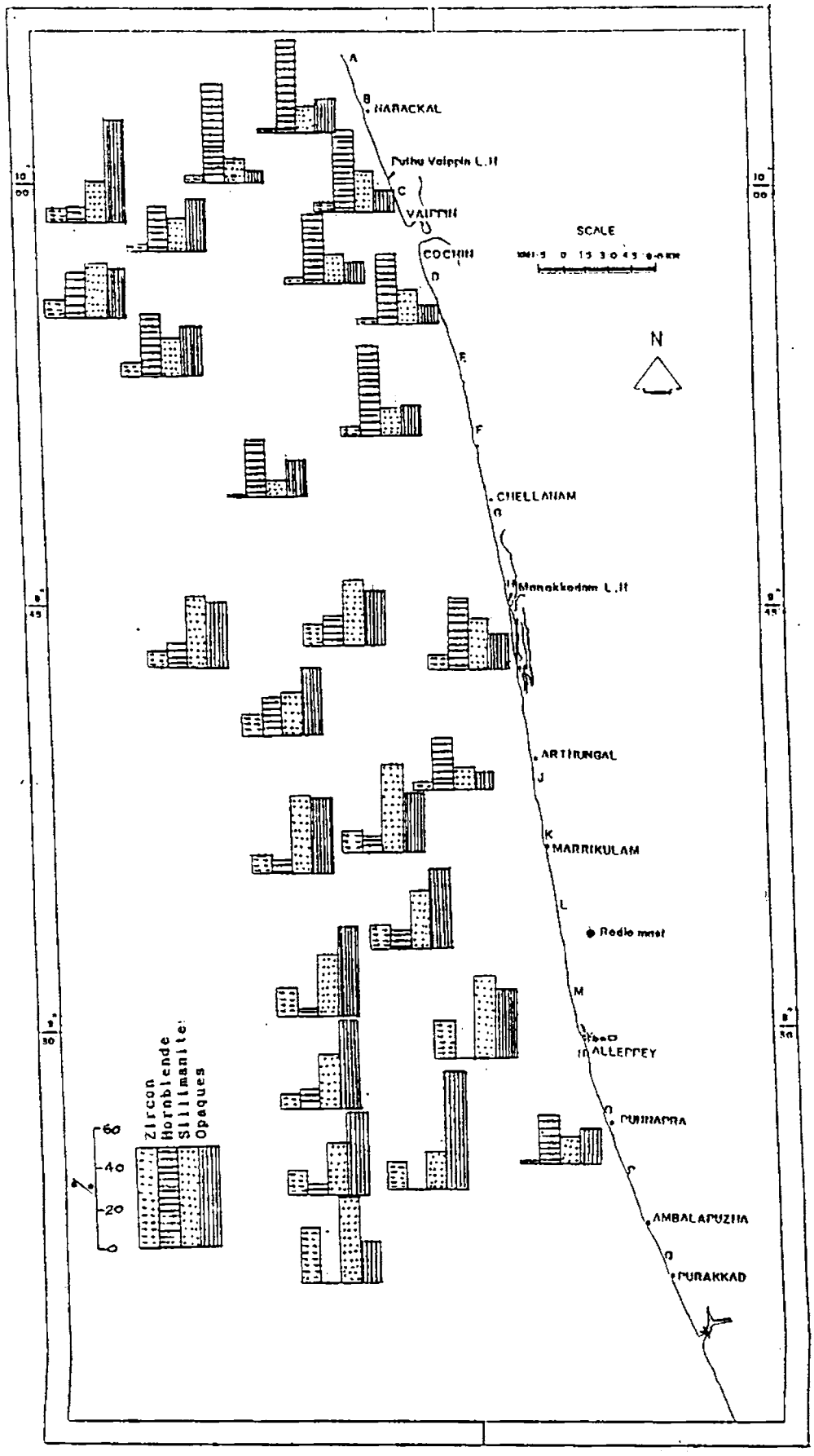

Fig. 3.A5 Distribution of opaques, sillimanite, hornblende an zircon

variation from the distribution pattern of orthopyroxene, with some sporadic high values especially off Arthungal and a few other locations. High concentration of biotite around the Cochin inlet is significant. But the samples in the southwestern part are characterised by either total absence or scant occurrence of biotite. Patchy and abrupt variation of framboidal pyrite distribution is evident from the figure. But to a major extent it follows the pattern of distribution of biotite. Monotonous presence of garnet with a low magnitude of variation is evident from the distribution pattern (Fig. 3.A6). It is present in all the samples but does not suggest a clear pattern of dispersal. Similarity in distribution is exhibited by rutile with opaques with an enrichment in the offshore and southwestern regions. The converse holds good in the sediments around Cochin inlet and nearshore portions.

The minerals available in low concentration are monazite, clinopyroxene, kyanite, actinolite/tremolite and tourmaline, and their distribution are depicted in Fig. 3.A7. Higher percentage of monazite are observed in the seaward portion, especially in the southwestern region, whereas clinopyroxene shows an opposite trend, with a highest percentage around Cochin inlet. No systematic pattern could be noticed for kyanite, actinolite/tremolite and tourmaline

3.2.3 Discussion

It is evident from the results presented above that, total heavy concentration show considerable differences in the finer and coarser fraction with certain spatial pattern of distribution. The granulometric variation discussed in the previous chapter depicts three types of sediment distribution patterns - clay-rich zone, sand-rich zone and a mixed unit. When the heavy

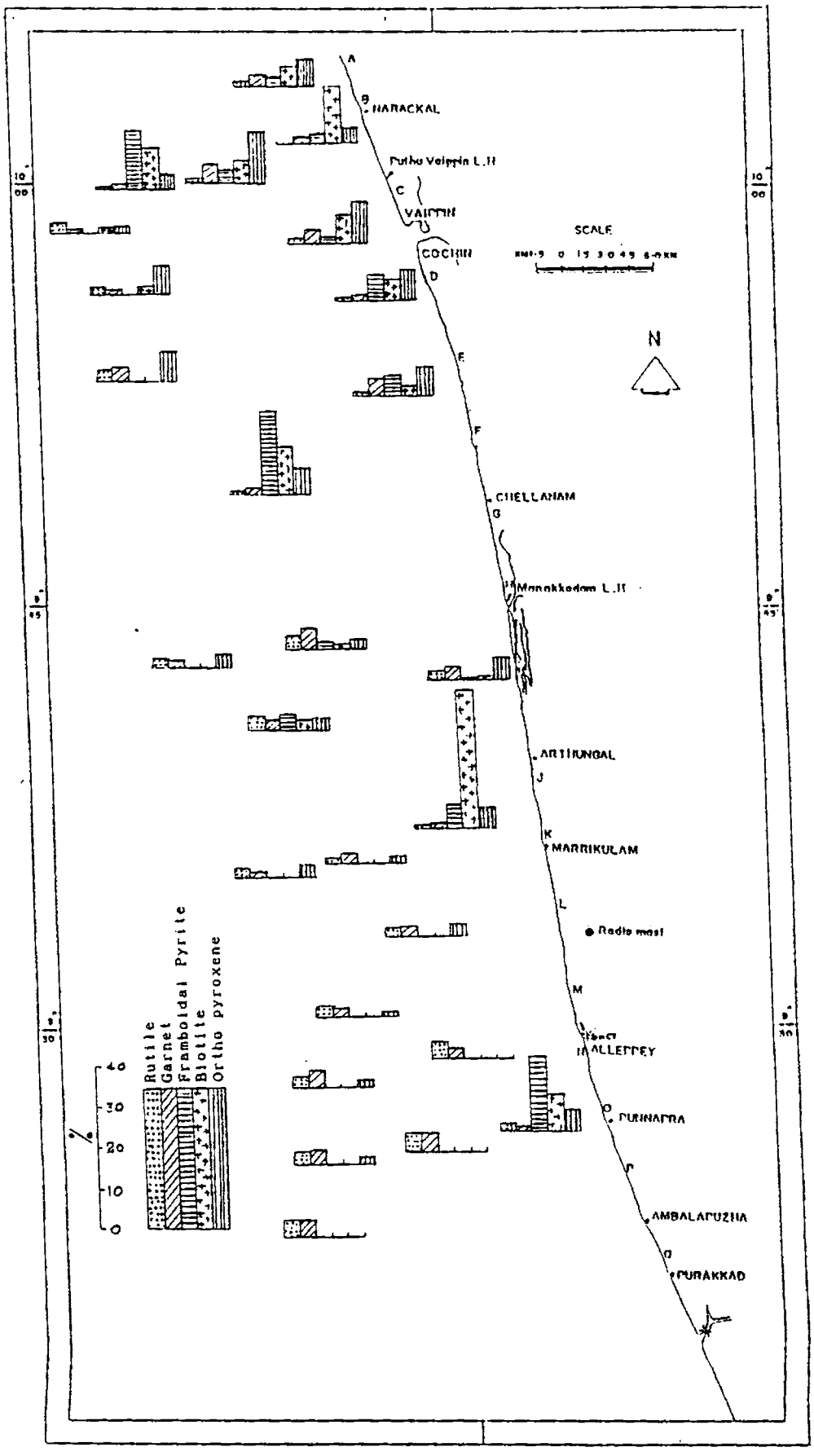

Fig. 3.A6 Distribution of orthopyroxene, biotite, framboida pyrite, garnet and rutile

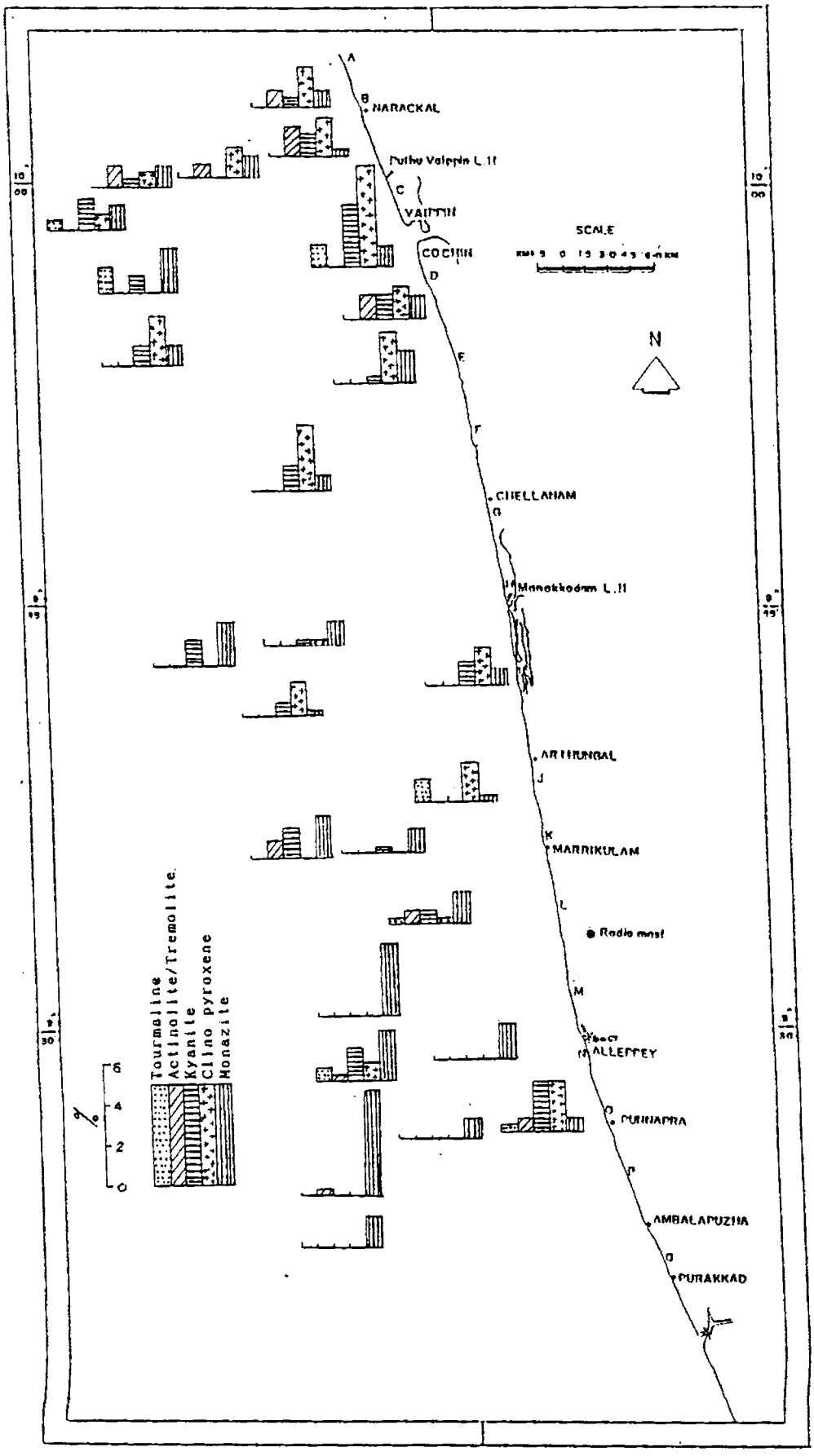

Fig. 3.A7 Distribution of monazite, clinopyroxene, kyanite, actinolite/tremolite and tourmaline

distribution is viewed in association with the textural pattern, a striking similarity is noticed. Hydraulically controlled sedimentation pattern, which results in the clay-rich sediment accumulation in the nearshore from a low energy transport regime, produces a consequent low concentration pattern of heavies. Similarly, the sand-rich zone, which has been identified as a paleo-beach deposit, evidently forms concentration zones of heavies. The mixed sediment unit behaves in an intermediate pattern. But the heavies in the finer fraction of the sand-rich zone far exceeds the corresponding concentration of heavies in coarser fraction. However, the difference of heavies between the two fractions in the clay-rich sediments are relatively very less. This documents the allochthonous sedimentation pattern of the present, since the clay-rich sediments are in equilibrium with the present-day sedimentation process *in situ*. The enriched concentration of heavies in the sand-rich sediments could possibly be due to hydraulically controlled wave-induced deposition, which carries the mean size equivalent fine heavy fraction of the sediments to the littoral zone thus resulting in the impoverishment of heavies in the coarser fraction of the paleo-beach deposit. This is a clear possibility owing to the observation of many previous workers, including that of Rittenhouse (1943).

The finer fraction depicts that, nearly 80 % of the variation in the heavy mineral assemblages are controlled by opaques, sillimanite, hornblende and zircon. Monazite, clinopyroxene, kyanite, actinolite/tremolite and tourmaline account for only around 4 % of the total composition. Except kyanite, actinolite/tremolite and tourmaline, all other minerals show specific pattern of distribution. Minerals such as biotite, framboidal pyrite, kyanite, actinolite/tremolite and tourmaline show high standard deviation around their mean value. This could be attributable to the abrupt changes and patchy

appearances of high concentration zones in the case of biotite and framboidal pyrite. But, for the other minerals, it may be due to their total absence in many of the samples in the seaward portion and also due to the percentage fluctuation from location to location.

It is rather difficult to infer the reasons for the variation in the mineralogical assemblages of the innershelf from the distribution pattern alone. It has been established from the previous work that, certain statistical processing of the heavy mineral data set can yield some meaningful order by which many of the uncertainties arising out of the visual interpretation of distribution/dispersal pattern of the heavy mineral assemblages can be avoided. The following section utilises some of them to delineate the factors controlling the heavy mineral variations.

Inter-relationship of heavy minerals: Combination of minerals with comparable source-sorting behaviour can be identified from mineral to mineral correlation computation. Correlation matrix of heavy minerals are given in Table 3.A3. The matrix shows significant positive and negative loadings between many minerals. It is very important to consider the loadings especially between the minerals which constitute major part of the heavy mineral suite. Significant positive loadings obtained for opaques on sillimanite, zircon, monazite and rutile are manifestation of their strong association. The strong antipathetic relation of opaques are apparent from the strong negative correlation with hornblende, orthopyroxene, clinopyroxene, biotite and framboidal pyrite. Garnet shows slight positive bearing on zircon and rutile, while it has negative relation with biotite and framboidal pyrite. Kyanite, actinolite/ tremolite and tourmaline do yield a few significant loadings on certain minerals. Positive coefficient of correlation of kyanite on clinopyroxene and

TABLE 3.A3

Correlation matrix of heavy minerals

	1	2	3	4	5	6	7	8	9	10	11	12	13	14
1	1.000	.046	.427	.485	.473	.693	-.810	-.739	-.616	-.131	-.332	-.120	-.550	-.385
2	.046	1.000	.073	.302	.093	.391	.029	.008	-.011	-.288	-.299	-.264	-.358	-.353
3	.427	.073	1.000	.775	.395	.547	-.711	-.661	-.737	-.224	-.234	-.212	-.558	-.586
4	.485	.302	.775	1.000	.383	.767	-.758	-.709	-.655	-.453	-.419	-.182	-.481	-.541
5	.473	.093	.395	.383	1.000	.298	-.472	-.321	-.489	-.098	-.143	-.067	-.448	-.354
6	.693	.391	.547	.767	.298	1.000	-.723	-.656	-.489	-.169	-.521	-.126	-.584	-.512
7	-.810	.029	-.711	-.758	-.472	-.723	1.000	.884	.732	.210	.356	.071	.386	.308
8	-.739	.008	-.661	-.709	-.321	-.656	.884	1.000	.696	.313	.231	.247	.307	.285
9	-.616	-.011	-.737	-.655	-.489	-.489	.732	.696	1.000	.560	.048	.253	.428	.459
10	-.131	-.288	-.224	-.453	-.098	-.169	.210	.313	.560	1.000	.128	.379	.004	.225
11	-.332	-.299	-.234	-.419	-.143	-.521	.356	.231	.048	.128	1.000	-.228	.217	.271
12	-.120	-.264	-.212	-.182	-.067	-.126	.071	.247	.253	.379	-.228	1.000	.424	-.031
13	-.550	-.358	-.558	-.481	-.448	-.584	.386	.307	.428	.004	.217	.424	1.000	.495
14	-.385	-.353	-.585	-.541	-.354	-.512	.308	.285	.459	.225	.271	-.031	.495	1.000

1=Opaque; 2=Garnet; 3=Sillimanite; 4=Zircon; 5=Monazite; 6=Rutile;7=Hornblende;
8=Ortho Pyroxene; 9=Clino Pyroxene; 10=Kyanite; 11=Actinolite/Temolite; 12=Troumaline;
13=Biotite; F.P.=Framboidal Pyrite.

Significant level of r values: >0.32 (0.1 level), >0.37 (0.05 level)
>0.47 (0.01 level)

tourmaline, and negative correlation with zircon are found to be significant. Antipathetic relation of actinolite/tremolite with rutile and positive loading of tourmaline on biotite are also notable. Biotite is correlated with framboidal pyrite, and in turn yield positive correlation with clinopyroxene.

Dendrogram, based on the correlation matrix, results in two significant group of mineral clusters (Fig. 3.A8). The group consisting of opaques, rutile, sillimanite, zircon and monazite are in turn connected with garnet, though at a lower level, forms one major cluster. The other group consists of two inter-related sub-groups. Hornblende, orthopyroxene, clinopyroxene and tourmaline forms one sub-group, which is connected with the other sub-group containing biotite and framboidal pyrite in turn connected with actinolite/tremolite.

The two groups obtained in the cluster analysis of the heavy minerals correspond to the two distinctive mechanisms resulted in their occurrence. It has been found from the distribution pattern that, the minerals belonging to the first group is mainly concentrated in the seaward and southwestern part of the area. As discussed previously (Chapter 2), these portions are sand-rich zones, owing their origin to a low stand of sea level in the past. The textural and mineralogical assemblages of these sediments subsequent to their submergence might not have been obliterated much by the present day hydraulic conditions of the innershelf. So, these sand-rich sediments, representing the textural hydrodynamic regime of a beach interface, contains altogether a different mineralogical assemblage independent of the heavy mineral suite of the clay-rich modern sediments.

The second cluster consisting of two sub-groups could be mostly the result of the modern sediment deposition. The dispersal pattern with a

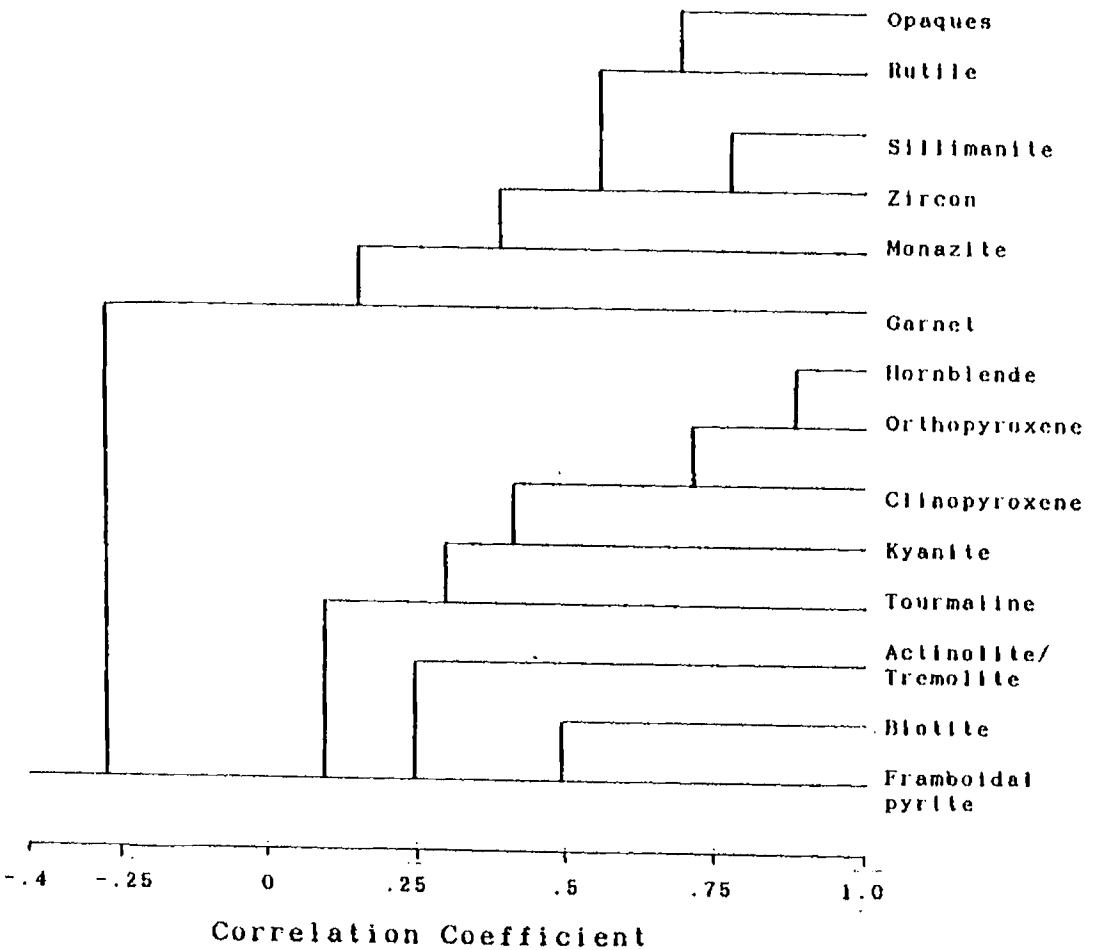

Fig. 3.A8 Dendrogram of heavy minerals

decreasing tendency of mineral concentration from the Cochin inlet to the offshore implicates direct input of a present day terrigenous source for many of the minerals. But at the same time, sub-grouping of the minerals in the dendrogram also indicate the importance of differing processes resulted in the sorting of the sediments. Biotite and framboidal pyrite form one sub-group, and both of them indicated sporadic concentration zones in the nearshore. Framboidal pyrite is a typical authigenic mineral and hence it does not give good correlation with many of the land-derived minerals in the other sub-group such as hornblende, orthopyroxene, clinopyroxene and tourmaline. Authigenic precipitation of this mineral requires certain conditions, like less turbulence and slightly reducing condition with the availability of sulphides in the sediments. In this context, the association of biotite with framboidal pyrite is very significant in the sense that, flaky micaceous minerals can be transported easily and can get deposited only in less agitated zones. So, the association of biotite and framboidal pyrite in the sediments could be the result of the physico-chemical condition *in situ*, with less agitated and slightly reducing environmental condition favourable for both biotite settling and pyritisation process. This is especially so, as the tests of the micro organisms containing the pyrite precipitate are found unbroken in microscopic examination, which indicates very clearly that, they are not transported ones.

The dispersal pattern of the lighter heavies (hornblende, orthopyroxene, clinopyroxene and tourmaline) are characterised by a depletion in its concentration towards offshore from Cochin inlet. This depicts that, these minerals are flushed from Vembanad Lake. It settles down depending on the flow pattern, indicating hydraulic sorting of the minerals (Komar and Wang, 1984; Clemens, 1987). But at the same time, influence of the offshore sand body in regulating the dispersal of the minerals belonging to the first cluster

group could be a possible inference for their converse trend, despite a very low input of these minerals through the Vembanad Lake. This consideration is all the more important as many of the minerals in this group are heavier heavy minerals (opaques, zircon, rutile, garnet and sillimanite) compared to the other (hornblende, orthopyroxene, clinopyroxene, tourmaline and biotite).

Assessments of source contributions (Provenance): An attempt is made here to evaluate the contribution of heavy minerals to the innershelf. Most often it refers to the source rocks from which the materials were derived (Pettijohn, 1975). Each type of source rock tends to yield a distinctive suite of minerals which therefore constitute a guide to the character of that rock. Though the nature of the source rock is most important in the assessment of provenance, the process of sedimentation is an interplay of many factors like, climate, topography, river characteristics, estuarine hydrodynamics (especially along this part) and so on. Precipitation details (chiefly monsoon controlled), river characteristics, geology and geomorphology of the hinterland area bordering this part are described in the introductory chapter. Six small rivers, with substantial drainage during monsoon season, cut across this area to join the Vembanad Lake, from which the sediments are flushed out into sea during tidal cycles. Table 3.A4 gives the representative heavy minerals present in major rock types in this region. Fig. 3.A9 is presented to evaluate the origin and concentration process of heavy minerals in the innershelf in collusion with heavy minerals in the rivers, beach and innershelf sand body. The data presented by Mallik *et al.* (1987) for the rivers and beach along this area are averaged and plotted, whereas the data for innershelf sand body is from the present investigation by taking average of samples which contains > 90 % sand. By utilizing these data set and involving the information on the other aspects of the terrain mentioned above, the discussion concentrates on

TABLE 3.A4

Representative heavy minerals present in major rock types in Central Kerala. (* present, ±may be present)

	C.G.	Lept.	Khond.	Char.	Gn.	Gnt.	Peg.	B.dy.
Opaques	*	*	*	*	*	*	*	*
Rutile	*		*			*		
Sillimanite			*					
Zircon	*	*	*	*	*	*	*	
Garnet	*	*	*	±	±	±	±	
Monazite		*	*	*	*			
Hornblende	*			±	±	±		
Orthopyroxene				*				
Clinopyroxene	*			±				*
Biotite		*	*	*	*	*	*	
Kyanite			*					
Tourmaline						*	*	

C.G:Calc-granulite; Lept:Leptynite; Khond:Khondalite; Char:Charnockite; Gn:Gneiss; Gnt:Granite; Peg:Pegmatite; B.dy:Basic dyke

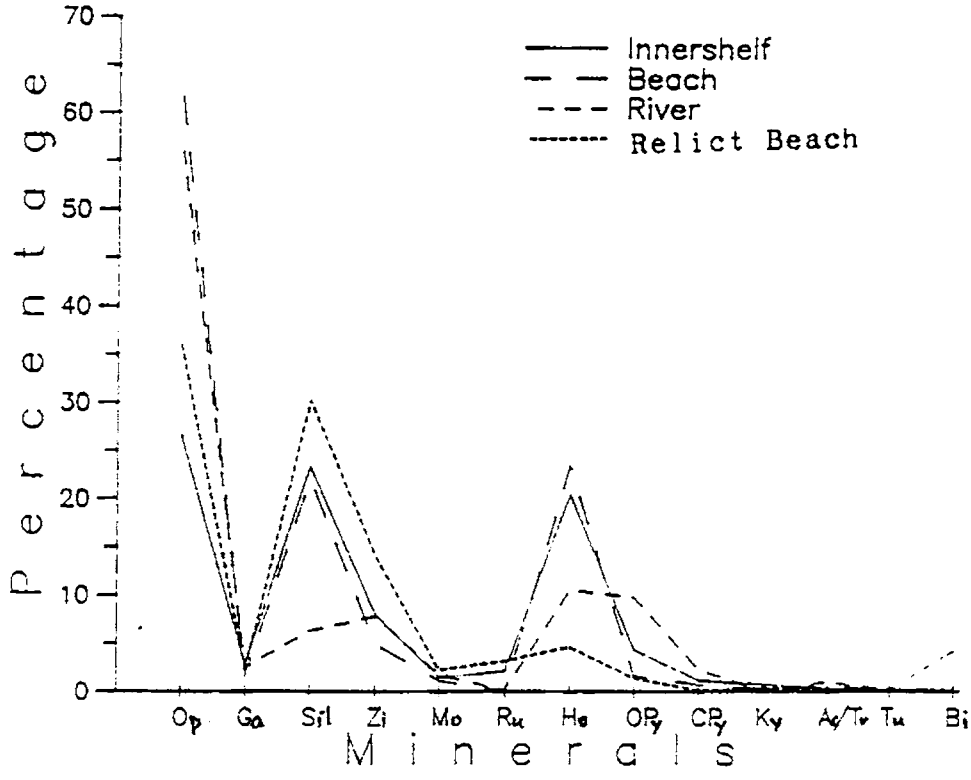

Fig. 3.A9 Comparative plot of heavy mineral variation

unravelling the probable source of these minerals in particular and sediments at large.

The classical method of identifying the provenance is to correlate the heavy mineral assemblages with the rock types available on the hinterland. Some minerals are diagnostic of a particular type of source rock (Pettijohn, 1975). In inter-related environments where the sediments are mainly derived from fluvial source, the process response of heavy mineral should be analysed by taking into consideration the intra-basinal hydraulic conditions during deposition and subsequent diagenetic changes. In the case of present day environments (river, beach and innershelf) where the effects of diagenetic changes are at minimum, the hydraulic sorting of minerals gain importance in accounting for dispersal and concentration of heavy minerals.

Perceptible differences in the heavy mineral concentration can be observed from the plot (Fig. 3A9) with beach and river showing a dominance of opaques, whereas the innershelf samples (average of the entire samples, including the relict sand samples) contains relatively lesser opaques. Innershelf sand make up an intermediate composition. Rivers which drain through the various rock types, by virtue of higher flow characteristics, transport more opaques, which are present in all rock types. While the abundance of hornblende over sillimanite in the river can be attributed to the occurrence of calc-granulites and charnockites in excess of khondalites in the spatial extent. This view is supplemented by the relative enrichment of hypersthene in the river, which is basically derived from charnockites. Due to the decreasing competency of the transporting agents, opaques are deposited on its way to the marine environment, thus supplying rich hornblende and sillimanite sediments to the shelf.

Petrographic identification has shown both rounded and euhedral (with rounded edges) grains of zircon which indicate their source to be controlled by both charnockite and khondalite group of rocks. Garnet concentration remains almost similar in river and innershelf, but marked by reduction in the beach. Broken pieces of garnet grains is an indication that, it has not been undergone much of transportation or it is not a product of reworking of relict sediments.

The minerals, which are available in traces, can also be useful in determining the source. Biotite shows a very low value in river but is not reported in the beach. But their increase in innershelf is a manifestation of the low energy regime. In the high energy fluvial transport, biotite keeps moving until it reaches a relatively turbulent-free zone. Except calc-granulites and basic dykes, all other rock types of this region contain biotite. Rare occurrence of augite grains might be related to the very faint contribution from basic dykes (dolerites). Presence of kyanite can only be attributed to the khondalites and tourmaline to the acid igneous rocks.

Thus, the mineralogy of river and innershelf sediments show that the minerals are mainly derived from charnockites followed by khondalite group of rocks (calc-granulites, leptinite and khondalites). But the quantitative contribution in terms of individual rocks is difficult to assess here, because of the admixtured sedimentation pattern. In the Vembanad Lake, the river-borne sediments undergo considerable change in their characteristics under estuarine conditions, thereafter flushing the sediments to the shelf. Since no precise study has been conducted till date to understand the relative contribution of different rivers in terms of variety of mineral species, it is also apparently difficult to attribute the sources precisely. The assemblages

contain many less stable (mainly ferro-magnesium) minerals. This could be attributed to the poor sediment maturity brought about by the higher yield of the run off under the high gradient geomorphological set up and a small period of heavy monsoonal precipitation.

Mineralogy of relict versus modern sediments: Sand-rich relict zone and modern innershelf mud zone have certain distinguishable mineralogical characteristics. Mud facies are evidently enriched in the lighter heavies such as hornblende, orthopyroxene, clinopyroxene, biotite etc., while, the sand facies are abundant in denser heavy minerals such as opaques, monazite, rutile and zircon (Fig. 3A9). It is stated above that, the sand-rich zone represents a high energy beach interface. Minerals deposited on the shelf of differing size, shape and density are transported onshore and deposited on the beach by simultaneous suspension and bottom drag by the longshore/ onshore currents. Entrainment of different kinds of minerals by internal turbulence results in deposition of some of them in the sub-bottom, while transporting the rest towards onshore. The lighter heavies such as hornblende are transported offshore by the retreating waves, ultimately resulting in relative concentration of opaques and other denser heavies in the beach. Along with this, lighter heavies which are larger in size and hydraulically equivalent to the fine grained denser heavies also get deposited (Komar and Wang, 1984). From the Fig. 3.A4 it is evident that invariably sillimanite is concentrated more in the coarser fraction than in the finer fraction. Sallenger (1979) attributed the abundance of ferro-magnesium minerals in the shelf to the differential settling and variable physical properties of heavy minerals.

Being tectonically a stable craton, there are no reports of upliftment or any other major tectonic events along this part of Indian Peninsula since late Pliestocene. So it is a reasonable assumption that, no major fluctuations have occurred in the heavy mineral province of this region since then. Hence the relict beach deposit should have a comparable mineralogy with the present day beach mineralogy along this coast. But Fig. 3.A9 depicts differences in the pattern of heavy mineral variation between the present beach and relict-beach deposit. Apparently there is a reduction in opaques, pyroxenes and amphiboles compensated by a relative increase in sillimanite, zircon and monazite in the relict beach. Pettijohn (1975) pointed out that the heavy minerals are extremely sensitive to diagenesis, with many mineral species suffering from the dissolution processes known as intrastratal solution. Dissolution may take place in a variety of diagenetic settings, but principally occurs either at the surface through circulation of meteoritic waters or in deep burial, under the influence of higher temperature saline fluids (Morton, 1984). In the case of the relict beach, it is quiet likely that the subaerial exposure of the sediments for a considerable length of time, might have resulted in the selective dissolution of the moderately and extremely susceptible heavy minerals leading to the depletion in the concentration of pyroxenes, amphiboles and opaques.

A similar pattern of dissolution phenomena was reported by Morton (1985). The enrichment of rutile and the depletion of opaques in the relict sand zone could be due to the alteration of ilmenite to leucoxene and finally to rutile. The observation of Mallik *et al.* (1987) on ilmenite inversion to rutile in the Chavara placer deposits supports the above view. The garnets of the relict beach sands are fresh and angular. Previous studies have shown that, garnet undergoes considerable change during intrastratal solution process

(Gravenor and Levitt, 1981; Morton, 1985; Samsuddin and Ramachandran, 1992). As the garnets in the relict sand did not show any alteration features, it is inferred that the garnets of the relict sands are from the re-distribution of the present day sedimentation. The depletion of unstable minerals have resulted in the relative enrichment of sillimanite, zircon, monazite and rutile. Thus, the heavy mineral studies of this area indicate that, the sands in the outer innershelf is of relict nature, were part of a littoral environment, got exposed for subaerial weathering for certain amount of time, and submerged subsequently during transgressive episodes.

3.3 PART B: CLAY MINERALOGY OF INNERSHELF SEDIMENTS

3.3.1 Introduction

The clay mineral compositions of the sediments are indicators of the geological conditions of sedimentation. It is the net product from the cumulative effect of source rock composition, climate, weathering, transportation, hydraulic regime and diagenetic process in the basin of deposition. Strong influence of climate on the genesis of clay minerals has been emphasised by Reiche (1962) and Keller (1970) and are largely supported by geological evidences. Clay minerals can be formed in a number of ways, some are stable weathering residues, some of them can be formed from hydrothermal alterations or reconstituted during reverse weathering processes. Geologists could reconstruct the palaeo-climates of wide latitudinally differing areas based on vertical variations of clay mineral assemblages in the sedimentary formations. Biscaye (1965) and Griffin *et al.* (1968) have used clay mineral composition and distribution to delineate the dispersal pattern of sediments in marine environments. According to Naidu (1985) utmost care

should be exercised in the palaeo-climate inferences based on clay minerals, owing to the surface processes of reworking. Much importance was also given for the transformation of clay minerals by the diagenetic processes (Boles and Franks, 1979; Velde, 1977; Churchman, 1980; Garrels, 1984; Velde and Nicot, 1985).

Previous studies on clay mineral distribution of the surficial sediments of the Indian Ocean are mainly by Griffin *et al.* (1968), Rateev *et al.* (1969), Goldberg and Griffin (1970), Kolla and Biscaye (1973), Kolla *et al.* (1976) and Rao and Nagendranath (1988). Goldberg and Griffin (1970) and Kolla *et al.* (1976) studied clay minerals, which include the western continental margin in the northern Indian Ocean, in a regional scale. Nair *et al.* (1982) studied the distribution and dispersal patterns of clay minerals on the western continental shelf of India. Rao *et al.* (1983) made a detailed note on the clay mineral distribution of the Kerala continental shelf and slope, with a limited number of sample set from the nearshore area. Nair (1976) and Nair and Murty (1968) reported clay mineral distribution of the mud banks of Kerala coast. In the present work, the author attempts to study the nature, distribution, dispersal and possible sources of clay minerals in the surficial sediments of the innershelf between Narakkal and Purakkad.

3.3.2 Methods

Twenty three samples representing different sediment composition, depths and aerial extent, were selected for clay mineral studies and are made free of salts. Calcium carbonate and organic matter were removed by treating with dilute hydrochloric acid and hydrogen peroxide respectively (Carver, 1971). The $< 2\ \mu$ fraction of the sediments were separated from the bulk

samples by gravity settling techniques. Oriented clay samples were prepared by pipetting the clay solution onto glass slides and allowing them to dry in the air. These samples were analysed on a Philips X-ray Diffractometer using Ni-filtered Cu Ká radiation operated at 20 mA and 40 KV from 2 to 30° 2θ at 1° 2θ/minute. These samples were treated with ethylene glycol and rescanned with the same instrumental settings. Samples were heated up to 500°C and was again scanned from, 2 to 15°. Major clay minerals were identified following the method of Biscaye (1965). Clay minerals were identified from the principal basal reflections of montmorillonite, illite and kaolinite at 17, 10 and 7 Å respectively. The proportions of each clay mineral were determined by measuring their individual area by a planimeter and also by comparing the data with that of visual counting of squares in the X-ray diffractograms. The principal peak areas of montmorillonite, kaolinite and illite were multiplied by the weighing factors 1, 2 and 4 respectively. The weighted peak area percentages of each clay mineral were calculated. Since the principal reflection of gibbsite (4.85 Å) interferes with the low angle peak of illite (4.46 Å), instead of measuring the principal peak area of gibbsite in diffractogram, only the height of the peak was measured above the base line.

3.3.3 Results

The X-ray diffraction data of clay minerals (< 2 μ) from the innershelf revealed varying amounts of montmorillonite and kaolinite with minor amounts of illite and gibbsite in the order of abundance. The sediment samples selected for the study constitute mainly silty clay, clayey silt and sand-silt-clay. Distribution of the percentage of sand, silt and clay in the samples selected are shown in Fig. 3.B1. Table 3.B1 shows the percentage wise list of the clay minerals in the samples.

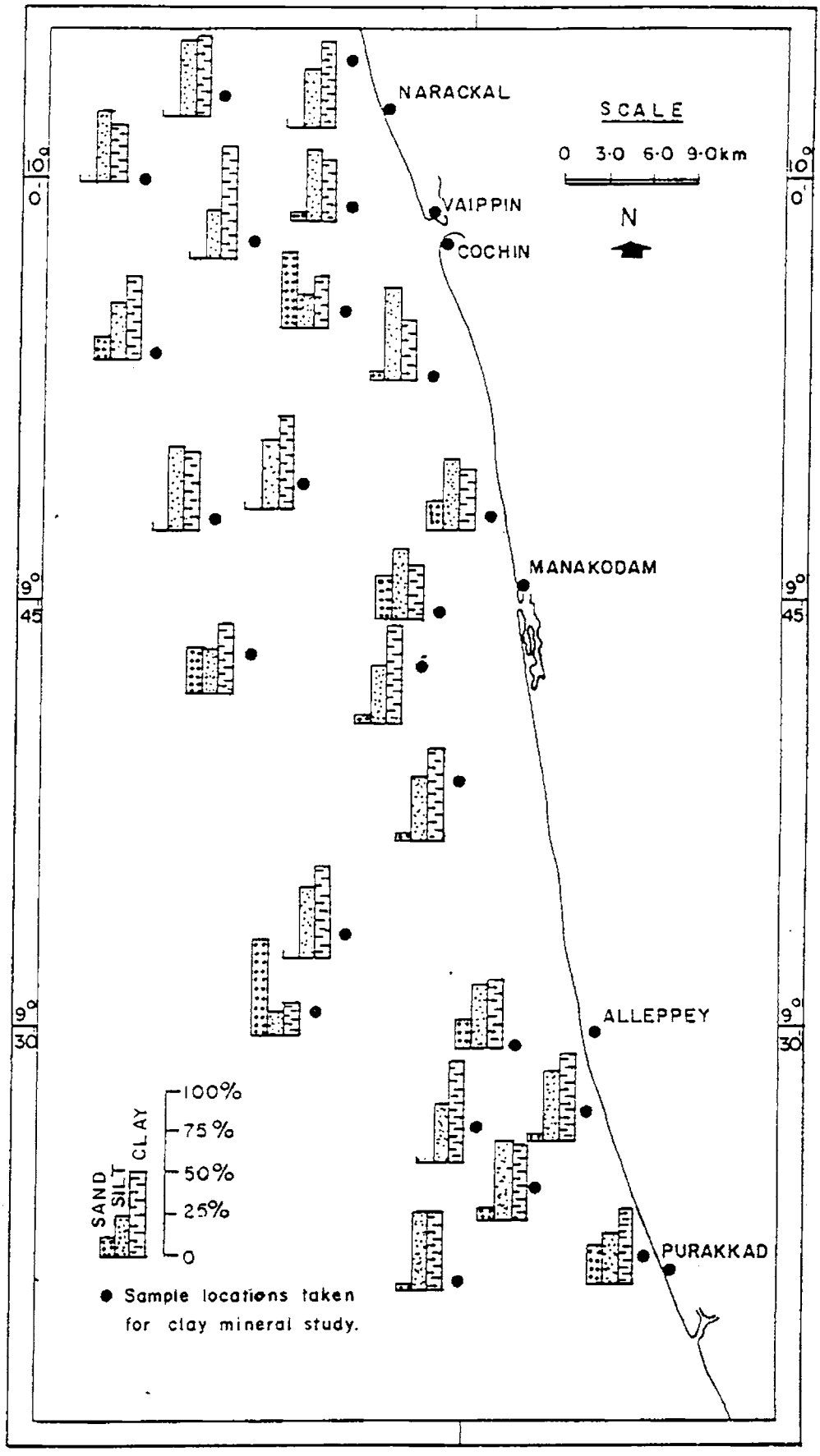

Fig. 3.B1 Distribution of sand-silt-clay in the samples selected for clay mineral analysis

TABLE 3.B1

Clay mineral assemblages in the innershelf sediments between Narakkal and Purakkad:

Sl.No.	Sample No.	Montmorillonite	Illite	Kaolinite	Gibbsite	M/K
1	A1	49.4	5.9	43.2	1.5	1.14
2	A4	54.2	6.1	37.9	1.8	1.43
3	B5	58.2	5.3	35.4	1.2	1.64
4	C1	48.3	5.3	44.6	1.8	1.08
5	C4	54.7	5.2	38.5	1.6	1.42
6	D3	53.6	4.4	40.9	1.1	1.31
7	D6	56.0	4.3	38.3	1.4	1.46
8	E2	54.6	6.9	37.5	1.2	1.46
9	F4	46.2	6.0	46.2	1.5	1.00
10	F6	53.0	5.4	40.3	1.3	1.32
11	G1	52.4	4.8	41.6	1.2	1.26
12	H2	45.5	6.8	46.0	1.7	0.99
13	H5	58.5	6.8	33.0	1.8	1.77
14	I3	49.8	7.8	41.2	1.2	1.21
15	J3	52.2	8.0	37.8	2.0	1.38
16	L5	54.4	8.2	35.8	1.6	1.52
17	M6	49.2	10.0	38.3	2.5	1.28
18	N2	60.0	7.4	32.6	T	1.83
19	O1	46.5	6.4	47.1	T	0.98
20	O3	55.8	7.8	35.0	1.4	1.59
21	P2	38.3	9.6	50.3	1.8	0.76
22	Q1	53.7	2.5	42.2	1.6	1.27
23	Q5	59.5	7.0	32.2	1.3	1.85

Montmorillonite: Montmorillonite is the major clay mineral in the sediments, the percentage ranges from 38.3 to 60.0 with an average value of 52.35. Frequency of occurrence of montmorillonite shows that, approximately half of the samples are distributed in the 52 - 56 % range (Fig. 3.B2a). Though the distribution pattern of montmorillonite is slightly complex (Fig. 3.B3), in general, there is an offshore increase in its distribution. Comparatively, low percentage of montmorillonite is observed in certain pockets of nearshore regions off Narakkal-Cochin belt, Manakkodam and south of Alleppey. A depth dependant picture is depicted by the distribution pattern of montmorillonite and the seaward portions of the innershelf contains > 50 % montmorillonite.

Kaolinite: Kaolinite is the next dominant clay mineral in the study area (average: 39.83 %). It registers higher values over montmorillonite in some samples, the highest and lowest percentage being 50.3 and 32.2 respectively). The area around Cochin inlet, Manakkodam and south of Alleppey show some local enrichment of Kaolinite (Fig. 3.B4). Depletion of kaolinite is noticed in the seaward direction. The histogram of frequency distribution of kaolinite does not indicate any modal range (Fig. 3.B2b).

Illite: Illite is present in small quantities. Percent range is from 2.5 to 10.0 with an average value of 6.43 %. More than half of the samples contain 5 - 7 % illite (Fig. 3.B2c). Aerial variation of illite indicates a general increase from north to south (Fig. 3.B5). Like the distribution pattern of montmorillonite, illite also shows a depleted concentration around Cochin inlet, Manakkodam and areas south of Alleppey.

Gibbsite: Gibbsite, the least abundant clay mineral in the study area, varies from traces to 2.5 with an average content of 1.41 %. Frequency distribution

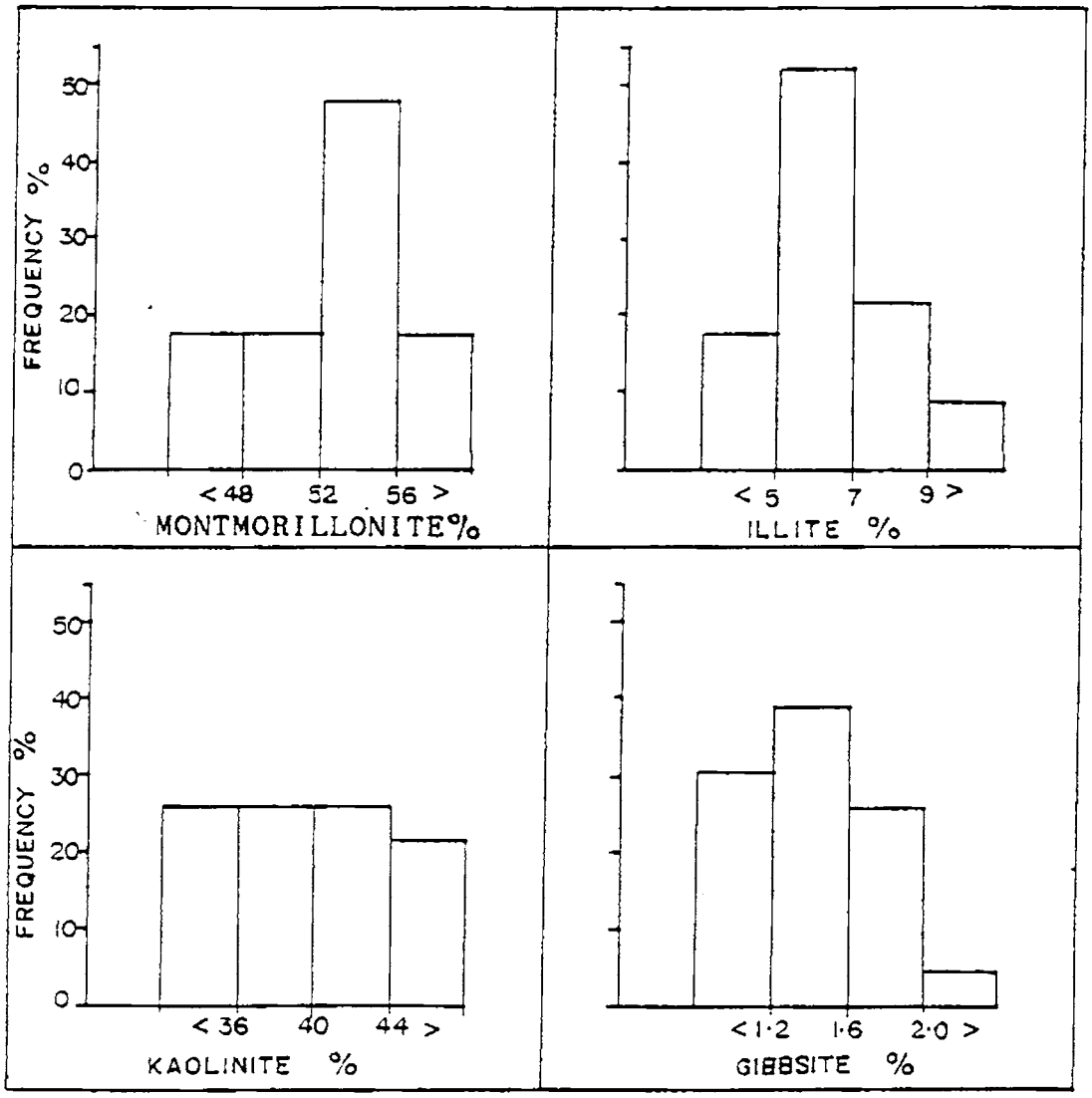

Fig. 3.B2 Frequency distribution of (a) montmorillonite, (b) kaolinite, (c) illite and (d) gibbsite

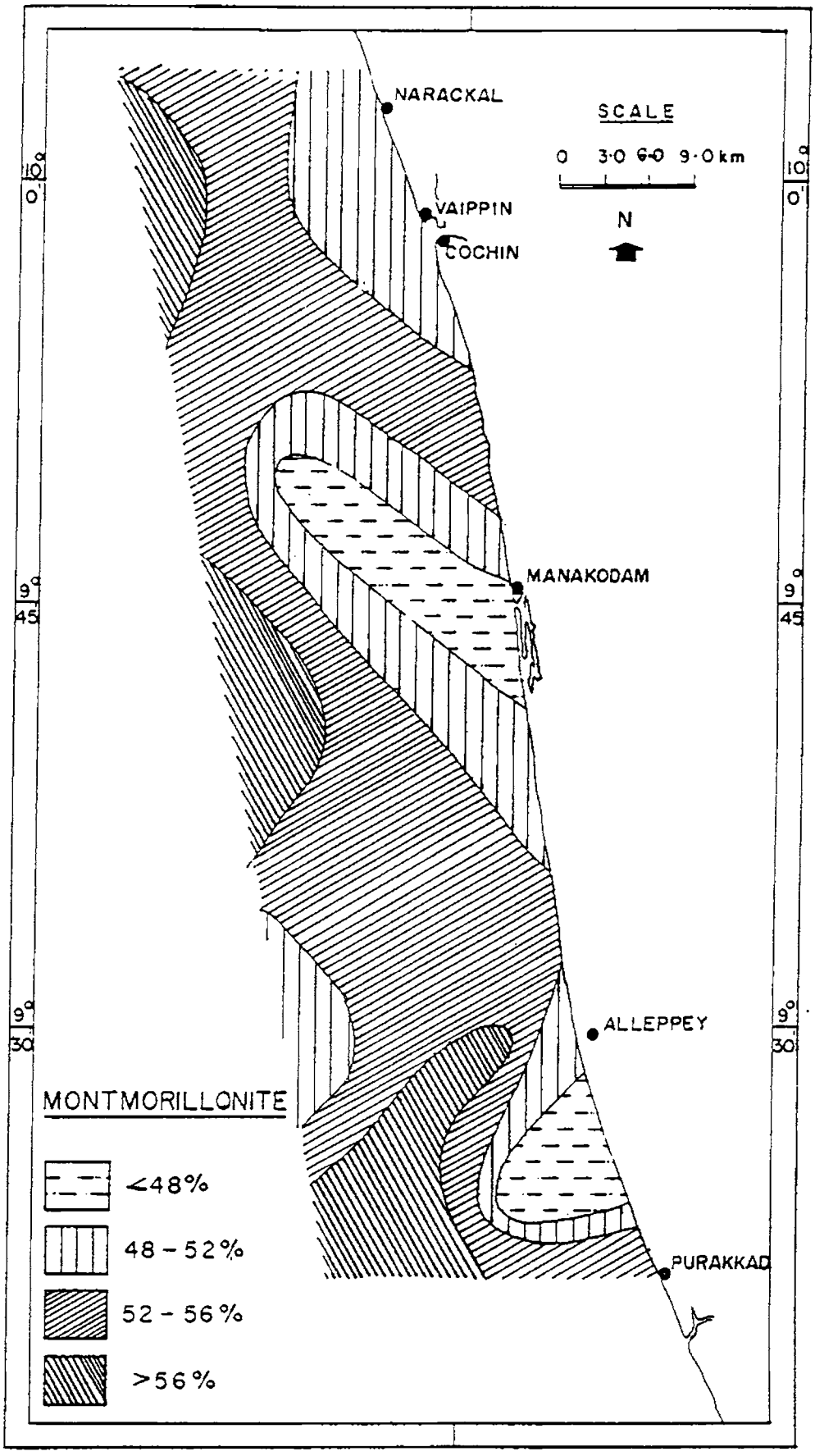

Fig. 3.B3 Distribution of montmorillonite

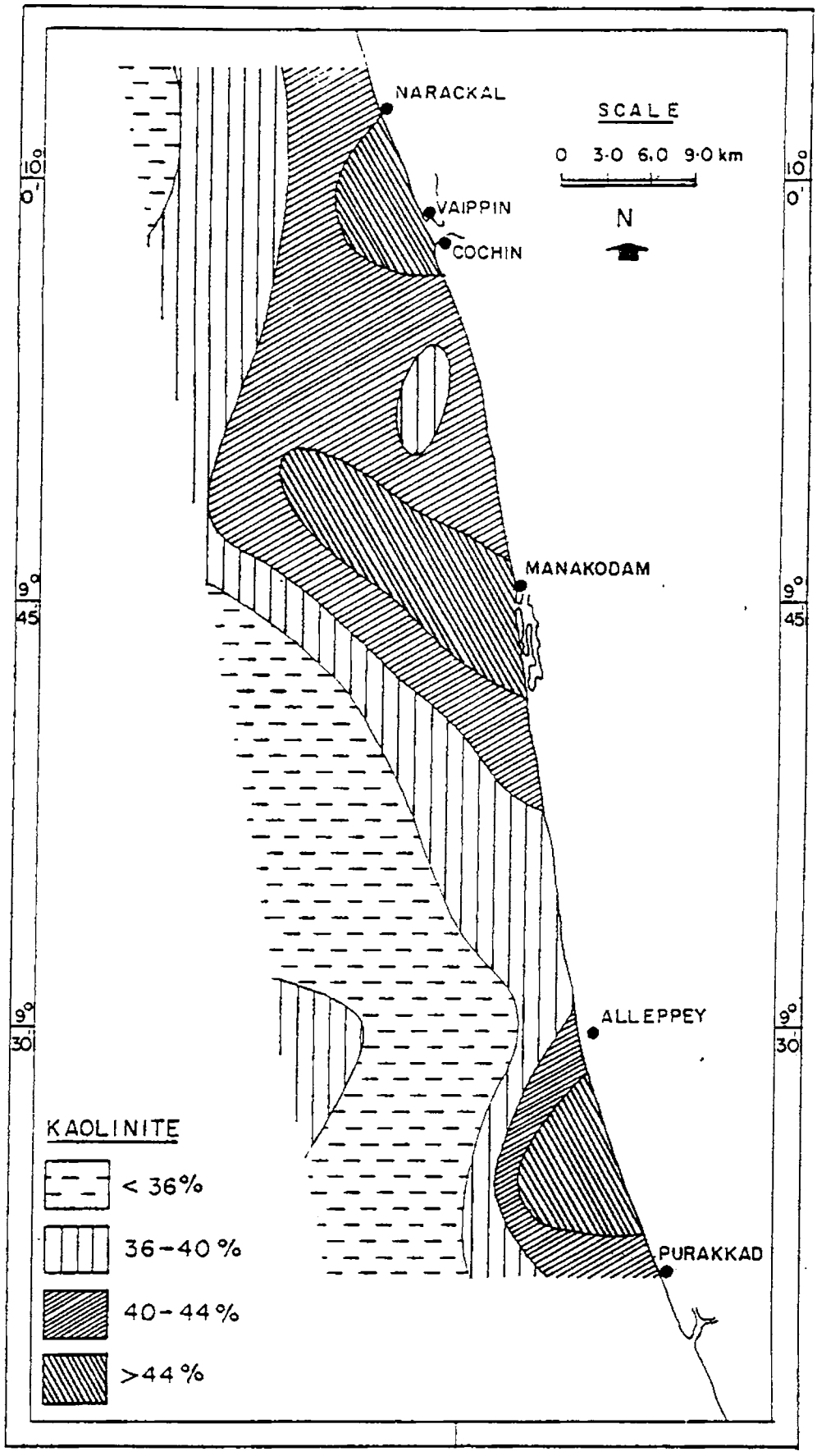

Fig. 3.B4 Distribution of kaolinite

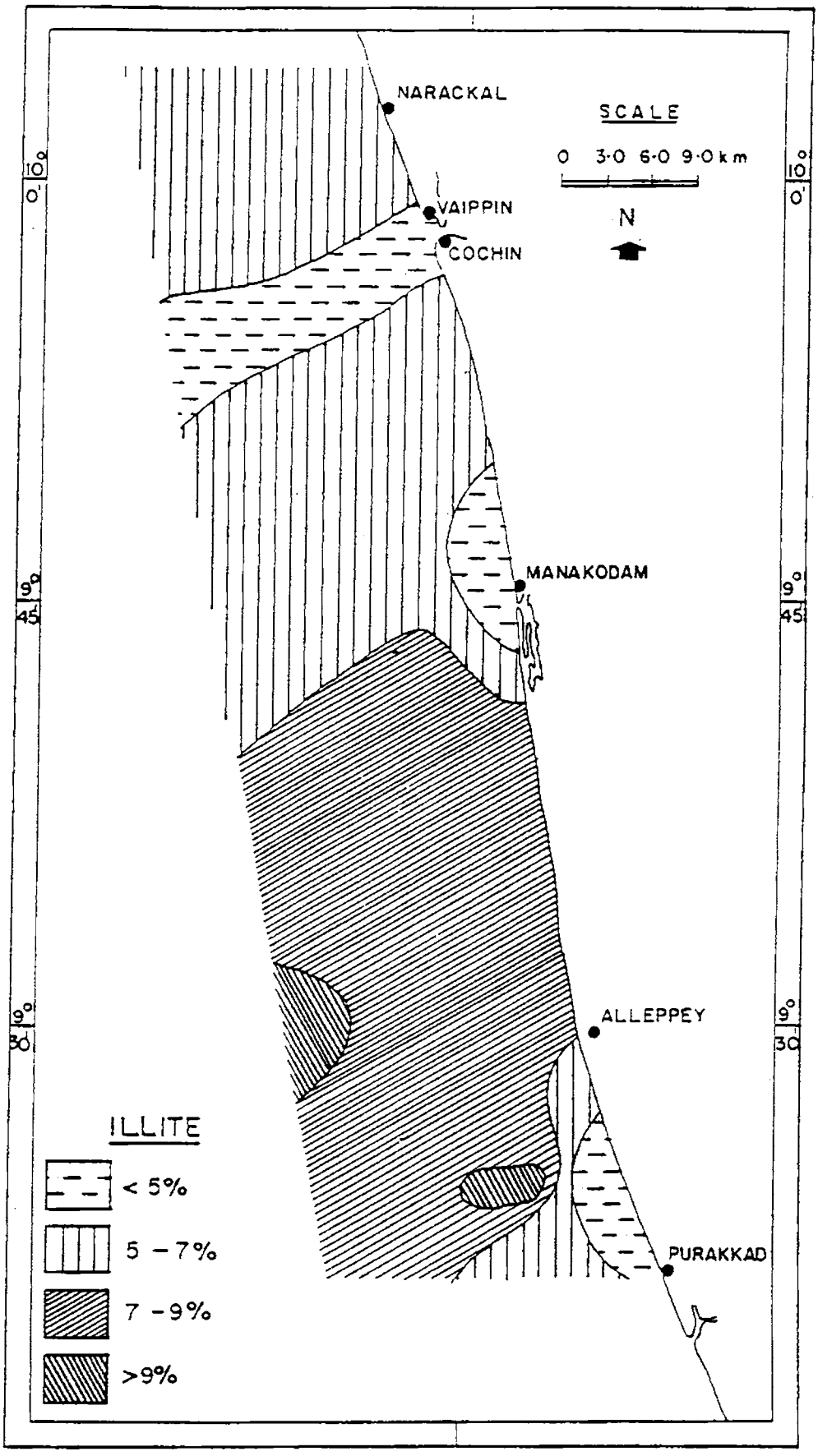

Fig. 3.B5 Distribution of illite

of gibbsite is given in Fig. 3.B2d. Distribution pattern of gibbsite does not show any pattern or zonation. However, the presence of gibbsite in the nearshore sediments is considered as an important clue to the source of the sediments.

3.3.4 Discussion

The results presented above illustrate the nature, assemblages and the distribution pattern of clay minerals in the sediments of the innershelf zone. The study shows that, montmorillonite is the most abundant clay mineral followed by kaolinite, illite and gibbsite. Kolla *et al.* (1981) reported > 50 % of montmorillonite along the southwest coast of India. Subsequently, Nair *et al.* (1982) observed a decrease in the montmorillonite content from Gulf of Cambay (87 %) towards the south till Quilon (60 %). Based on the M/K (montmorillonite/Kaolinite) ratio, the southern part of the shelf area from Bhatkal to Quilon was identified as montmorillonite-poor zone. Rao *et al.* (1983) pointed out that in the Kerala continental shelf and slope, even though montmorillonite is the most abundant mineral, its relative percentage is lower in the inner continental shelf compared to outer shelf as well as in slopes. Within 30 meter depth of the shelf, montmorillonite content is < 55 %. Paralleling the Indian Peninsula, a decreasing seaward gradient of montmorillonite was noticed by Goldberg and Griffin (1970). They considered the montmorillonite to have originated from the weathering of augite-rich basalts of the Deccan Traps, under the influence of the fluvial regime. Further they have argued that, though the eastern sedimentary domain of the Arabian Sea receives major contributions from the weathering of the Indian Peninsula as indicated by high montmorillonite levels, the basins' solid phases appear to be primarily wind borne from the north, perhaps the desert regions of the northern India

and West Pakistan. Rao *et al.* (1983) pointed out that the montmorillonite on the outershelf and slope in the Kerala region has a different origin from that of the innershelf. This interpretation was based on the comparison of 'd' spacing of montmorillonite in the innershelf and outershelf. In innershelf, the unglycolated samples have yielded a 'd' spacing value of 14.7 to 14.94 Å, whereas the outershelf samples show a spacing that vary from 15.5 to 16.36 Å. Further, a similarity was observed between the 'd' spacing values of the outershelf montmorillonite off Kerala and that of the sediments from the continental shelf between Bombay and Ratnagiri (average 'd' spacing value for ten samples is 15.92 Å: Rao *et al.*, 1983).

In the present study, the 'd' spacing values of montmorillonite varies between 13.23 and 14.73 Å with an average value of 14.32 Å. This is in near agreement with the values reported by Rao *et al.* (1983). Rao and Nagendranath (1988) identified two types of smectites from the central Indian Ocean, namely, one, an Al-rich montmorillonite with 17.3 Å peak on glycolated X-ray diffractogram and another, an Fe-rich montmorillonite with 18.4 Å reflections. Though differential thermal analysis (DTA) was not carried out for the present innershelf samples, based on the 'd' spacings (16.4 to 17 Å) of the glycolated samples, it is presumed that, the sediments are enriched in Al-rich montmorillonites. Crystallinity of the montmorillonites are calculated from the peak height ratio above the background (P) and the depth of the valley (V) on the low angle side of the peak (Biscaye, 1965). Crystallinity index (V/P) of the innershelf sediments ranges from 0.30 to 0.57 with an average value of 0.45. In the central Indian Ocean, compared to the calcareous sediment, the pelagic sediments show lower V/P value (Rao and Nagendranath, 1988). However, as the calcareous sediments are devoid of Fe-rich smectites, the higher value of V/P ratio is attributed to the Al-rich ones. The V/P ratio of the innershelf

sediments yields an average value similar to the calcareous sediments reported by them. Hence, it reiterates the above contention that, the innershelf montmorillonites are Al-rich.

Clay mineralogical data of the central Kerala rivers showed fluctuating values for the different rivers (Purandara, 1990). The average percentage of montmorillonite reported for Minachil river was the highest (30.22) and the minimum average value for Periyar (18.55). All the five rivers, viz., Pamba, Manimala, Minachil, Muvattupuzha and Periyar, debouch their sediment load into the Vembanad Lake. Consequent to this, there is a perceptible increase in the montmorillonite content in the Vembanad Lake, where the average value reported to be around 32.72 % (Purandara, 1990). The adjacent nearshore area (including some of the mud bank locations) recorded average montmorillonite content of 36.71 %. Such a distribution pattern depicts a gradient in the concentration of montmorillonite from terrestrial to marine environment through lacustrine system.

Reports on the granulometry of clay minerals have shown that montmorillonite is much smaller in size compared to kaolinite and illite. Because of this, compared to other clay minerals, montmorillonite remains in suspension for longer time resulting in differential settling pattern of the clay minerals (Whitehouse *et al.*, 1960). Flocculation of kaolinite and illite occur mainly at very low chlorinity, whereas, flocculation of montmorillonite increases gradually with increase in chlorinity. Preferential settling of montmorillonite over other clay minerals is attributed to its very stable double layer, thus resulting in size segregation (Gibbs, 1977). Thus, one of the main reasons for the increase of montmorillonite from terrestrial to marine environment can be attributed to both its size and preferential settling due to the differential flocculation.

Apart from this, transformation of clay minerals in changing physico-chemical conditions of the different environments can not be ruled out. Mackenzie and Garrels (1966) proposed that, the transformations need not necessarily be between existing clay minerals, it can be a transformation of either amorphous alumino-silicate minerals (formed during weathering) or degraded clays into new crystalline clay phases. The process occurring in the sea, in which cations, dissolved silica and bicarbonate are removed from sea water, are the reverse of the weathering processes on the continents (reverse weathering), ultimately leads to the formation of mixed-layer clays. But the equilibria reactions between the clay minerals remains a grey area. However, clay mineral transformations by cationic exchange to establish a equilibrium between the sediment phases and sea water is not a discredited idea.

Aerial variation of the montmorillonite (Fig. 3.B3) discerns a general tendency of enrichment towards offshore. In the nearshore regions around the Cochin inlet, Manakkodam and Purakkad, low values of montmorillonite are observed. Semi-diurnal ebb flows from Vembanad Lake brings sediments which are abundant in clay minerals undergoes flocculation at the higher salinity seawater front. Fine sized montmorillonites are carried offshore and the other clay minerals get deposited as floccules at the seawater/estuarine interface. So the general pattern of montmorillonite distribution with an increase in the offshore direction could be due to its seaward transportation. This may be true in the case of Cochin area, but the general pattern is observed for the entire innershelf region, though there are no discharge of sediments at other portions. So the montmorillonite distribution can also be attributed to the resuspension at the nearshore due to wave-induced turbulence and the subsequent transportation of fine-sized montmorillonite in the offshore direction. This observation is in consistency with the published results

elsewhere (Nelson, 1960; Parham, 1964) and along the west coast of India (Nair *et al.*, 1982; Rao *et al.*, 1983).

Lower values of montmorillonite observed around Cochin inlet (including Narakkal area) and Purakkad region are striking. These locations are known for the persistent occurrence of mud banks. Purandara (1990) reported that the materials that come into suspension during mud bank formation are enriched in montmorillonites. It is quiet possible that, following the cessation of mud bank, the montmorillonites are carried offshore resulting in the impoverishment of montmorillonites at such locations.

Kaolinite is considered as a 'low latitude' clay mineral (Griffin *et al.*, 1968), developed under tropical conditions. Previous studies along this shelf have indicated that maximum percentage of kaolinite encountered was 65 in mud bank sediments (Nair and Murty, 1968; Nair, 1976). Nair *et al.* (1982) reported a kaolinite maxima of 44 % in the shelf between Bhatkal and Quilon. Within 30 m depth, Rao *et al.* (1983) have obtained a percent variation of 40 to 50 for kaolinite. In the present study, kaolinite values range between 32.2 and 50.3 % with an average value of 39.83. These results are in good agreement with that of Rao *et al.* (1983).

The origin of kaolinite was mainly attributed to the extensive deposits of kaolin along this coast (Nair *et al.*, 1982). Scrutiny of the literature shows that, apart from the kaolin deposits along the coast, the lateritic soils also contribute a considerable amounts of kaolinite to the sediments. Purandara (1990) has estimated the average kaolinite content as 63.93 % for the five central Kerala rivers namely, Pamba, Manimala, Minachil, Muvattupuzha and Periyar. These rivers flow through Precambrian crystalline formations,

essentially made up of garnet-plagioclase-sillimanite graphite gneiss (Khondalites), cordierite gneiss, charnockites and the late granitic intrusions. In the coastal areas, the rivers flow mainly through laterites, Quilon and Warkalli formations and alluvium. The higher percentage of kaolinite observed in the river sediments could be released from the laterites (Narayanaswamy and Ghosh, 1987).

The average kaolinite percentage reported for the Vembanad Lake was 56.29 % (Purandara, 1990). When compared to the river, there is a significant reduction in the amount of kaolinite in the innershelf regions (average 49.59 %). This sort of reduction from the terrestrial to the marine environment may be due to preferential settling character of kaolinite, owing to its size and flocculation nature at a lower chlorinity value (Whitehouse *et al.*, 1960). The average value of kaolinite resulted from the present investigation is 39.83 %. Seaward decrease pattern of kaolinite (Fig. 3.B4) signifies an inverse relationship with that of the montmorillonite. Pockets of higher percentages of kaolinites are observed around Cochin inlet, Manakkodam area and Purakkad region. Griffin (1962), Hirst (1962), Nair *et al.* (1982) and Rao *et al.* (1983) have shown that, kaolinite increases 'shoreward' and yield lower quantity 'basinward'. Thus, the results of the present investigation is in consonance with the established fact of settling and dispersal of clay minerals.

Occurrence of illite in the innershelf sediment is < 10 %. Illite shows a decrease in the nearshore area, especially off Cochin inlet, Manakkodam and Purakkad. In general, the southern portion registered an abundance of illite over the northern portion. Though there are divergent views regarding the origin of illite, it is fairly established that weathering of K-rich minerals especially K-feldspars, gives rise to illite (Pettijohn, 1975). Purandara (1990)

has noted a steady increase in the illite content from terrestrial to marine environment. Rivers of Central Kerala show an average range between 2.20 to 7.31 %, and in Vembanad Lake the average values encountered was 7.99 %. Rao *et al.* (1983) noted an increase in the percentage of illite within the outershelf (3 - 5 % to > 7 %). They have also identified outcrops of aragonite cemented sandstone and limestone with substantial amount of illite in the upper continental slope, as the chief source of illite in the shelf, though the amount contributed by them is not known. The higher amount of illite on the upper continental slope is attribute to the low energy of the upper slop (Rao *et al.*, 1983). The average composition of illite in the innershelf of the study area is 6.43 %, with a range of 2.5 % to 10.0 %. In the areas which receive relatively fresh sediments from the land sources, the illite content is found to be less. Hence, it is presumed that, compared to kaolinite, illite being finer in size is winnowed away from the turbulent nearshore zone and deposited in relatively calm areas, thus favouring its deposition.

Gibbsite with its principal reflection at 18.5 Å 2θ, is the least abundant clay mineral in the innershelf with an average percentage of 1.41 %. Gibbsite is considered as a characteristic clay mineral along the shelf areas of the southwest coast of India (Nair *et al.*, 1982). It is a common product of laterites in humid tropical zones along with kaolinite and are essentially of continental origin (Grim, 1968). Gibbsite can result either directly from the parent rock or indirectly from desilicification of kaolinite. Occurrence of higher concentration of gibbsite in the river sediments from where it transcends to lower concentration towards the estuarine and marine zones were reported by Purandara (1990). So, it can be presumed that, the gibbsite present in the innershelf region is of terrestrial origin and the contribution from the desilicification of kaolinite is meager.

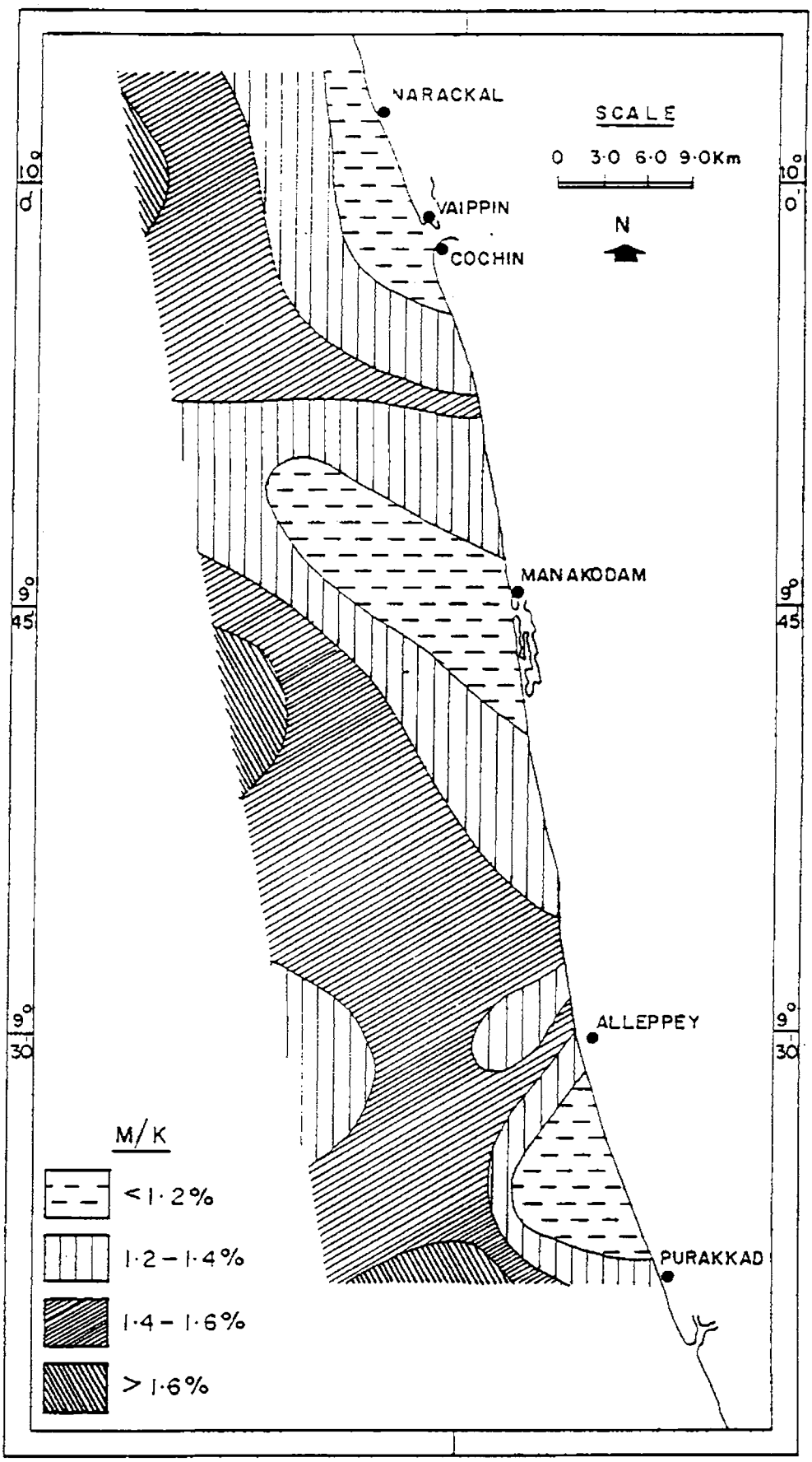

Fig. 3.B6 Distribution of M/K ratio

Montmorillonite/kaolinite (M/K) ratio for the area ranges between 0.76 to 1.85 (average 1.34). Aerial distribution of M/K ratio is shown in Fig. 3.B6. The general pattern depicts an increase in the ratio towards offshore. Thus it reflects the size dependant hydromechanics of transportation and salinity based differential flocculation mechanism of these clay minerals.

CHAPTER 4

GEOCHEMISTRY OF THE INNERSHELF SEDIMENTS

4.1 INTRODUCTION

Continental shelf region is marked by sedimentation from different sources and their characteristics vary widely in space and time resulting in diverse sediment chemistry, thus reflecting and recording conditions in the depositional environment. A good knowledge on the granulometry and mineralogy facilitates better understanding of geochemical variability of the sediments. Information on hydrography and geochemistry can be used in evaluating the processes in the incorporation of metal phases from different sources. This gives additional information on the quality of the environment. Though many elements are essential to the aquatic organisms in low concentration, they are toxic to them in high concentration (Mason, 1951). Carmody *et al.* (1973), Erlenkeuser *et al.* (1974), Helz *et al.* (1975) and others have shown that high trace element concentrations are found in estuaries and coastal sediments where high anthropogenic input occurs. With its dense population and varied developmental activities thereof, the Kerala innershelf zone is faced with a threat of environmental degradation. However, this may not cause any concern immediately, owing to the natural processes possessing the capacity to remove much of the man's input very rapidly near its source, thus eliminating any possibility of global or even a regional effect on biological productivity.

In the present work, organic matter, major, minor and trace elements are analysed in the bulk sediments. Partition geochemical studies are also attempted on a few samples. The objectives of the investigation is to provide information on the:

TABLE 4.1

Percentage of organic matter in the innershelf samples

Sl.	Sample	Concentration	Sl.	Sample	Concentration
1	A1	5.44	29	I1	3.76
2	A3	5.38	30	I3	3.54
3	A4	5.00	31	I5	3.62
4	A6	5.62	32	J1	4.52
5	B1	5.16	33	J3	4.63
6	B3	5.34	34	J4	3.71
7	B6	0.69	35	K2	4.82
8	C1	5.34	36	K4	4.26
9	C3	4.83	37	K6	1.03
10	C5	4.79	38	L1	4.51
11	D1	3.79	39	L3	0.82
12	D2	4.91	40	L6	1.03
13	D4	5.14	41	M1	4.28
14	D6	3.89	42	M3	3.83
15	E2	5.34	43	M5	0.78
16	E4	5.74	44	N1	4.84
17	E6	4.83	45	N3	0.76
18	F2	4.91	46	N6	2.67
19	F4	3.91	47	O1	4.89
20	F6	4.19	48	O3	5.16
21	G1	3.68	49	O5	0.26
22	G3	4.36	50	P1	3.86
23	G4	1.90	51	P2	4.12
24	G6	3.83	52	P4	4.23
25	H1	1.40	53	P6	0.17
26	H2	2.68	54	Q1	3.34
27	H4	3.97	55	Q3	4.75
28	H5	0.79	56	Q5	4.58

TABLE-4.2

Results of Chemical Analysis-Major Elements of Innershelf Sediments

Sl. No.	Sample No.	SiO_2%	Al_2O_3%	Fe_2O_3%	CaO%	MgO%	Na_2O%	K_2O%	P_2O_5%	TiO_2%
1.	A1	35.05	17.32	9.58	3.08	3.40	3.37	1.05	0.14	0.92
2.	A3	35.76	16.31	9.58	3.36	4.00	3.44	1.05	0.16	0.83
3.	A4	37.23	13.21	10.42	3.92	3.60	3.47	1.09	0.14	0.83
4.	A6	28.96	21.37	9.30	4.48	4.00	3.93	1.05	0.11	0.92
5.	B1	42.84	16.31	9.46	4.06	3.85	4.05	1.09	0.09	0.92
6.	B3	32.85	17.82	9.62	3.08	3.80	4.14	1.13	0.09	0.75
7.	B6	79.60	4.06	1.46	3.36	3.80	2.31	0.95	0.07	0.58
8.	C1	34.01	17.31	9.78	3.08	4.60	3.37	1.09	0.11	0.92
9.	C3	30.37	17.88	10.24	3.92	4.20	3.37	1.13	0.11	0.83
10.	C5	30.42	16.29	9.78	4.76	3.60	3.44	1.09	0.11	0.58
11.	D1	40.50	15.27	8.02	4.48	4.00	3.30	1.13	0.11	0.83
12.	D2	33.63	17.31	10.10	1.12	2.90	3.30	1.13	0.11	0.83
13.	D4	33.94	17.82	9.60	3.36	3.40	3.34	1.13	0.11	0.92
14.	D6	38.97	12.73	7.68	3.64	4.00	3.30	1.09	0.09	0.83
15.	E2	33.73	16.81	8.80	5.84	4.20	3.67	1.13	0.11	0.83
16.	E4	30.21	17.82	9.94	4.48	4.80	3.93	1.16	0.11	0.67
17.	E6	44.13	12.21	7.69	2.24	4.20	3.34	1.13	0.07	0.67
18.	F2	42.89	13.70	9.30	2.80	3.80	3.20	1.09	0.11	0.67

(Table 4.2 contd.)

Sl. No.	Sample No.	SiO_2%	Al_2O_3%	Fe_2O_3%	CaO%	MgO%	Na_2O%	K_2O%	P_2O_5%	TiO_2%
19.	F4	38.98	12.63	8.60	6.16	4.60	3.37	1.09	0.11	0.58
20.	F6	38.11	13.65	9.46	4.20	4.00	3.41	1.16	0.11	0.83
21.	G1	44.86	13.95	9.90	3.36	3.80	3.93	1.27	0.09	0.75
22.	G3	32.30	13.60	8.52	11.20	4.20	3.93	1.27	0.09	0.92
23.	G4	46.84	4.78	5.31	9.24	4.20	3.24	0.87	0.05	0.50
24.	G6	35.82	11.91	7.88	11.20	4.20	3.20	1.16	0.07	0.83
25.	H1	57.25	8.85	5.71	8.40	4.40	3.97	1.20	0.07	0.58
26.	H2	39.16	13.60	6.43	8.12	3.80	3.20	1.20	0.07	0.70
27.	H4	35.82	14.60	9.30	7.28	5.00	3.20	1.16	0.07	0.75
28.	H5	85.77	3.54	1.83	0.84	2.60	0.70	0.24	0.05	0.75
29.	I1	44.53	15.90	7.70	4.20	6.20	2.64	0.60	0.41	0.83
30.	I3	41.89	11.14	8.66	5.32	5.80	2.70	0.62	0.02	0.75
31.	I5	35.86	10.08	8.18	11.48	4.60	2.67	0.58	0.41	0.75
32.	J1	38.21	15.20	9.78	4.48	4.20	2.71	0.60	0.55	0.58
33.	J3	37.28	15.20	9.78	2.80	5.20	3.37	0.62	0.50	0.67
34.	J4	50.93	9.05	6.91	6.28	5.20	2.62	0.56	0.02	0.67
35.	K2	37.96	14.04	9.78	5.04	3.80	2.75	0.56	0.02	0.75
36.	K4	42.57	12.29	7.70	6.72	5.00	3.34	0.58	0.27	0.67
37.	K6	68.83	6.15	4.45	5.32	2.20	2.05	0.56	0.23	0.67
38.	L1	39.09	15.10	9.94	4.48	4.00	2.72	0.93	0.50	0.67
39.	L3	87.83	2.20	1.82	2.80	0.40	0.67	0.24	0.02	0.67

(Table 4.2 contd.)

Sl. No.	Sample No.	SiO_2%	Al_2O_3%	Fe_2O_3%	CaO%	MgO%	Na_2O%	K_2O%	P_2O_5%	TiO_2%
40.	L6	68.53	9.05	4.13	4.20	2.20	1.91	1.05	0.23	0.58
41.	M1	39.43	13.10	9.30	4.48	4.00	3.31	0.93	0.27	0.67
42.	M3	45.82	13.10	9.30	5.88	3.80	2.73	0.93	0.18	0.67
43.	M5	90.12	1.83	1.30	1.68	0.60	0.56	0.14	0.02	0.67
44.	N1	39.00	14.10	9.46	3.92	4.00	2.70	0.93	0.34	0.58
45.	N3	87.02	3.04	1.78	1.96	1.00	0.63	0.25	0.02	0.75
46.	N6	62.02	8.10	5.45	3.30	2.60	1.91	0.56	0.34	0.58
47.	O1	40.61	13.10	9.62	5.32	5.00	2.73	0.93	0.09	0.67
48.	O3	33.75	15.10	9.30	6.44	6.40	2.75	0.96	0.50	0.67
49.	O5	86.11	2.02	1.62	2.80	2.80	0.34	0.24	0.02	0.67
50.	P1	40.31	16.10	9.94	4.48	4.20	2.62	0.93	0.46	0.58
51.	P2	46.97	12.05	8.66	6.16	4.00	2.64	1.00	0.09	0.67
52.	P4	47.30	12.05	8.18	6.72	3.20	2.11	0.93	0.30	0.67
53.	P6	86.98	5.18	1.72	1.96	0.20	0.34	0.23	0.02	0.58
54.	Q1	52.79	7.01	8.04	5.60	3.40	2.02	0.93	0.41	0.67
55.	Q3	50.92	15.01	9.46	5.88	4.00	2.67	1.00	0.02	0.67
56.	Q5	43.69	12.10	9.14	5.60	4.20	2.67	1.00	0.18	0.67

TABLE 4.3

Range, average and standard deviation of major elements (in percentage)

	Minimum	Maximum	Average	Std.Dev.
SiO2	28.96	90.12	46.90	17.21
Al2O3	1.83	21.37	12.34	4.72
Fe2O3	1.30	10.42	7.76	2.73
CaO	0.84	11.48	4.83	2.34
MgO	0.20	6.40	3.81	1.23
Na2O	0.34	4.14	2.81	0.96
K2O	0.14	1.27	0.89	0.31
P2O5	0.02	0.55	0.16	0.15
TiO2	0.50	0.92	0.72	0.11

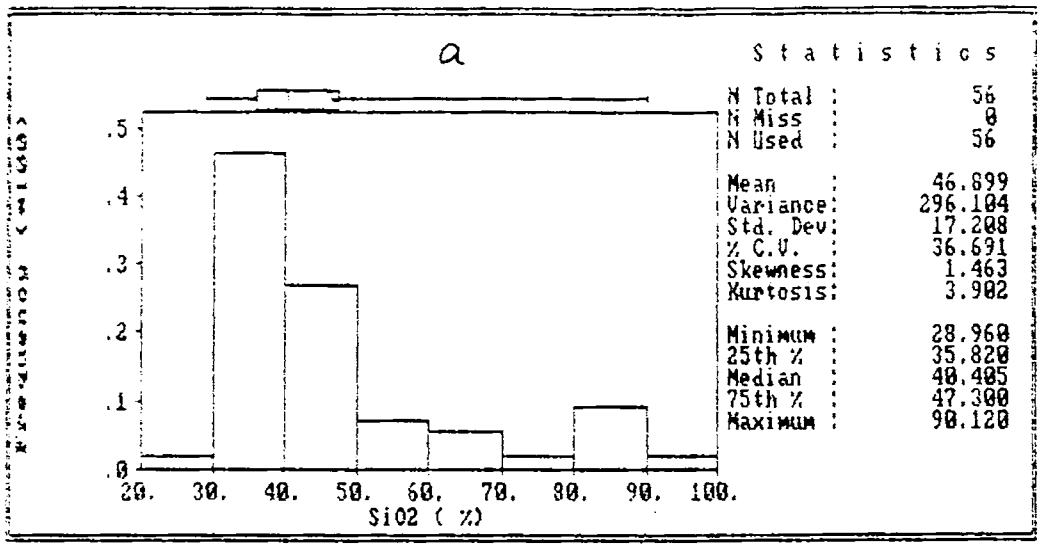

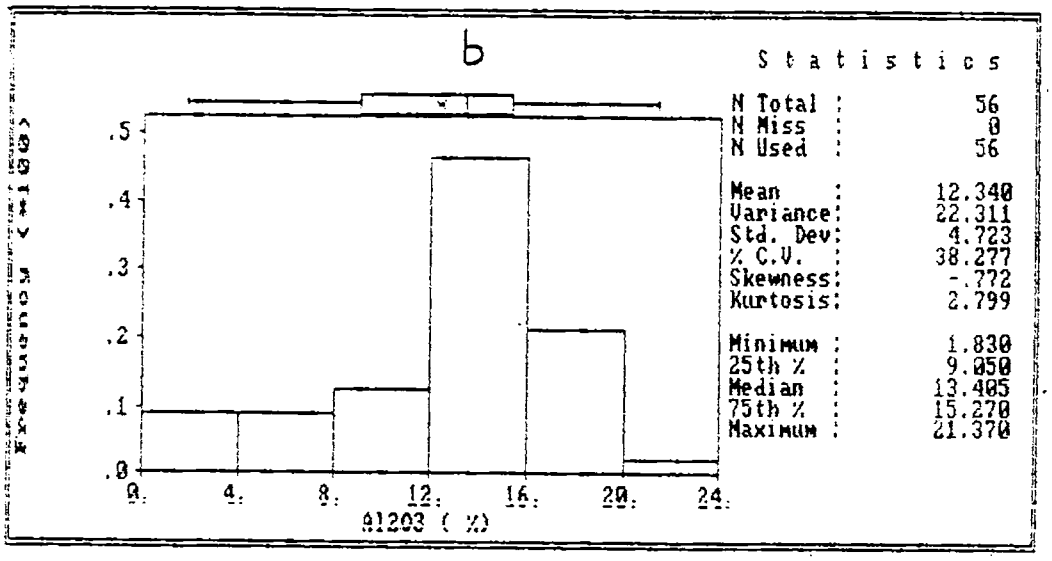

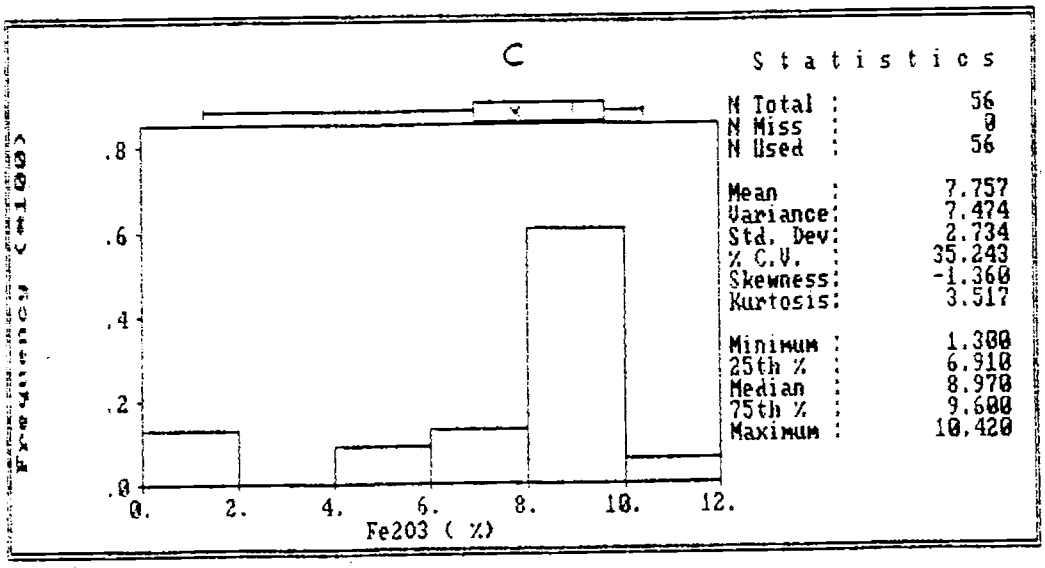

Fig. 4.1 Frequency distribution of major elements

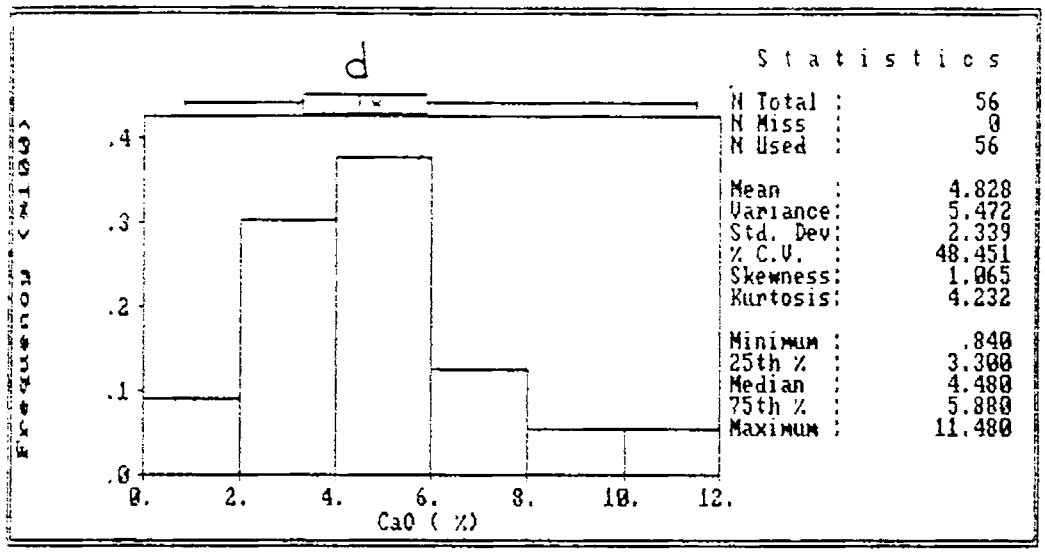
d
Frequency (*100)
.4
.3
.2
.1
.0
0.
2.
4.
6.
8.
10.
12.
CaO (%)
Statistics
N Total : 56
N Miss : 0
N Used : 56
Mean : 4.828
Variance: 5.472
Std. Dev: 2.339
% C.V. : 48.451
Skewness: 1.065
Kurtosis: 4.232
Minimum : .840
25th % : 3.300
Median : 4.480
75th % : 5.880
Maximum : 11.480

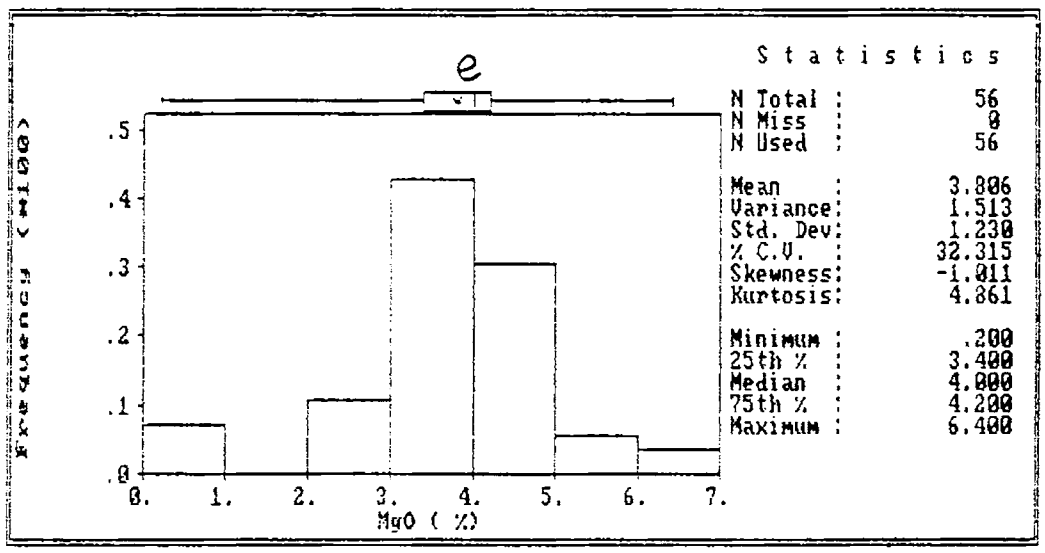
e
Frequency (*100)
.5
.4
.3
.2
.1
.0
0.
1.
2.
3.
4.
5.
6.
7.
MgO (%)
Statistics
N Total : 56
N Miss : 0
N Used : 56
Mean : 3.806
Variance: 1.513
Std. Dev: 1.230
% C.V. : 32.315
Skewness: -1.011
Kurtosis: 4.861
Minimum : .200
25th % : 3.400
Median : 4.000
75th % : 4.200
Maximum : 6.400

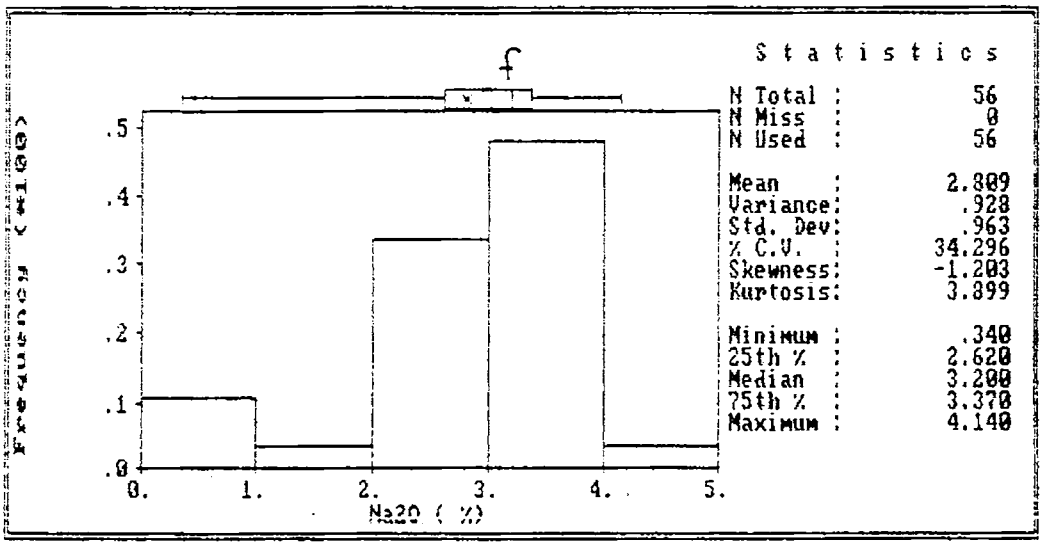
f
Frequency (*100)
.5
.4
.3
.2
.1
.0
0.
1.
2.
3.
4.
5.
Na2O (%)
Statistics
N Total : 56
N Miss : 0
N Used : 56
Mean : 2.809
Variance: .928
Std. Dev: .963
% C.V. : 34.296
Skewness: -1.203
Kurtosis: 3.899
Minimum : .340
25th % : 2.620
Median : 3.200
75th % : 3.370
Maximum : 4.140

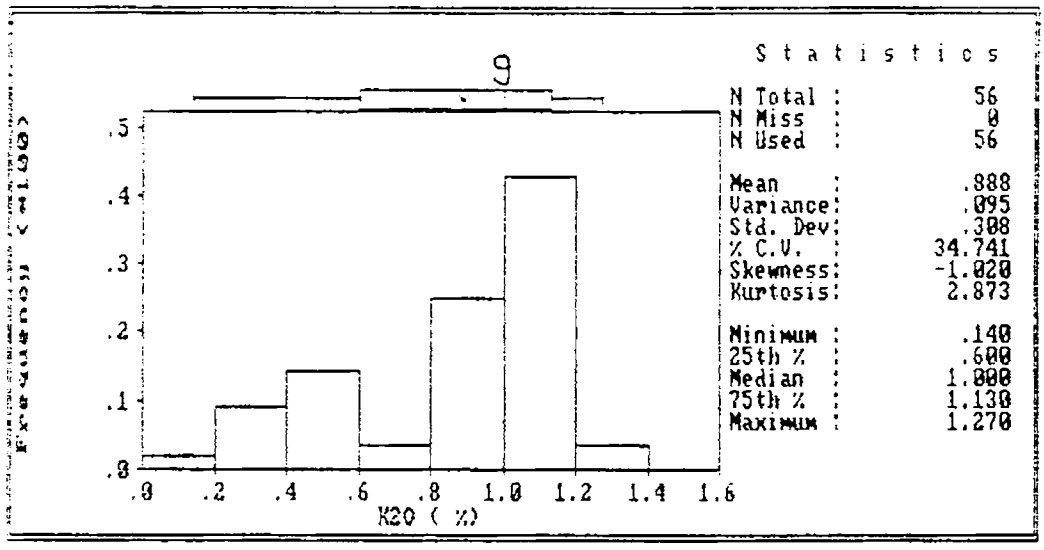
g
Statistics
N Total : 56
N Miss : 0
N Used : 56
Mean : .888
Variance : .095
Std. Dev : .308
% C.V. : 34.741
Skewness : -1.020
Kurtosis : 2.873
Minimum : .140
25th % : .600
Median : 1.000
75th % : 1.130
Maximum : 1.270
.5
.4
.3
.2
.1
.0
.0 .2 .4 .6 .8 1.0 1.2 1.4 1.6
K2O (%)

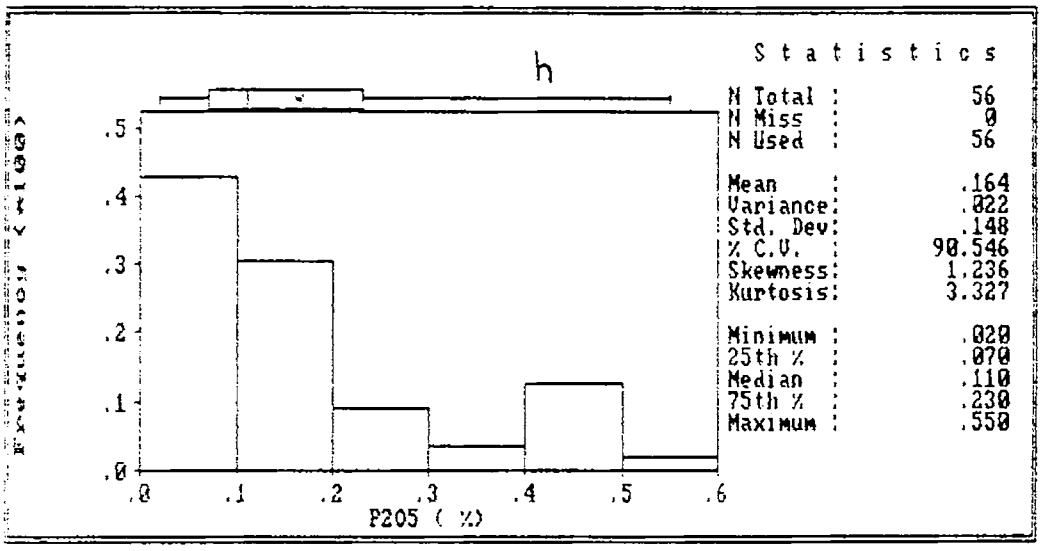
h
Statistics
N Total : 56
N Miss : 0
N Used : 56
Mean : .164
Variance : .022
Std. Dev : .148
% C.V. : 90.546
Skewness : 1.236
Kurtosis : 3.327
Minimum : .020
25th % : .070
Median : .110
75th % : .230
Maximum : .550
.5
.4
.3
.2
.1
.0
.0 .1 .2 .3 .4 .5 .6
P2O5 (%)

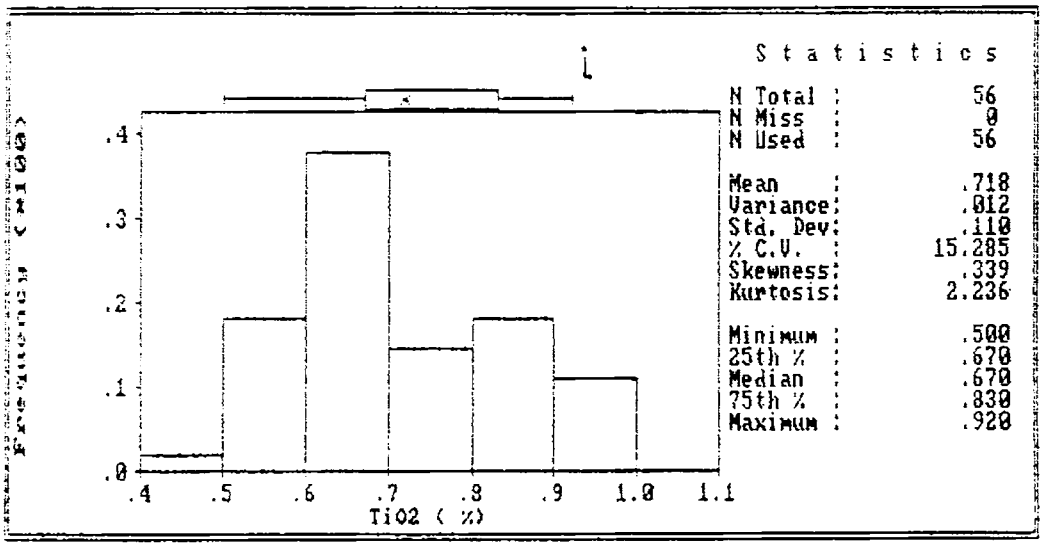
i
Statistics
N Total : 56
N Miss : 0
N Used : 56
Mean : .718
Variance : .012
Std. Dev : .110
% C.V. : 15.285
Skewness : .339
Kurtosis : 2.236
Minimum : .500
25th % : .670
Median : .670
75th % : .830
Maximum : .920
.4
.3
.2
.1
.0
.4 .5 .6 .7 .8 .9 1.0 1.1
TiO2 (%)

i. Concentration of the chemical elements in the sediments and their spatial variability,

ii. nature of geochemical association and

iii. possible origin and process of incorporation/removal.

4.2. METHODS OF ANALYSIS

Surficial sediments (56 nos.) were powdered and subjected to chemical analysis. The total organic matter was determined by wet oxidation method (El Wakeel and Riley, 1957). The samples were processed by the carbonate fusion method for the estimation of major elements (Vogel, 1978). Quantification of silica was carried out by hydrofluorisation. Estimation of Al_2O_3, CaO and MgO were carried out by EDTA; Fe_2O_3 by potassium dichromate; P_2O_5 and TiO_2 by the colorimetric method. Flame photometric method was used for the estimation of Na_2O and K_2O. Samples treated with HF and perchloric acid were taken for the analysis of Mn, Cu, Co, Cr, Ni, Cd, Pb, Zn, Ba, Sr, Rb, Be, Li, Mo and V by Atomic Absorption Spectrophotometer (AAS).

4.3 RESULTS

4.3.1 Organic matter and major elements

Concentration (Tables 4.1 and 4.2), average composition (Table 4.3), frequency distribution (Fig. 4.1a-i) and aerial distribution (Figs. 4.2 and 4.3a-i) of different elements are detailed in this section.

Organic matter constitutes 0.17 to 5.74 % of the sediment composition with an average amount of 3.75 %. Maximum number of samples fall in the > 4.5 % class followed by 3 to 4.5 % class interval, whereas 1.5 - 3 % class interval is having the least frequency. Spatial variation of organic matter shows an abundance in the vicinity of the Cochin inlet with sporadic highs near Mararikulam and Alleppey and also at the southernmost part of the study area. In general, organic matter content decreases towards the offshore, though in the southern portion the depletion starts at shallow depths. Nearshore portions of Manakkodam area also register a low content of organic matter.

SiO_2 ranges from 28.96 to 90.12 % (average: 46.90 %). Maximum number of samples show a composition range between 30 - 40 % followed by 40-50 % range. Around 9 % of the samples fall within 80 - 90 % range. The general distribution pattern shows a lower percentage in the northern part around the Cochin inlet. Certain offshore pockets mark high concentration zones. Nearshore portions between Arthungal and Alleppey show a depleted SiO_2 content (< 40 %).

Wide fluctuations in the amount of Al_2O_3 is noticed (varies between 1.83 and 21.37 %). Average distribution is 12.34 % with a maximum number of samples falling in the range 12 to 16 %. Contrary to the SiO_2 distribution pattern, Al_2O_3 shows high concentration in the northern part around Cochin inlet and also around Arthungal-Mararikulam area. Offshore portions are depleted in Al_2O_3.

The total iron content (Fe_2O_3) ranges between 1.3 to 10.42 % (average: 7.76 %). Around 60 % of the samples contain 8 - 10 % of Fe_2O_3, followed by

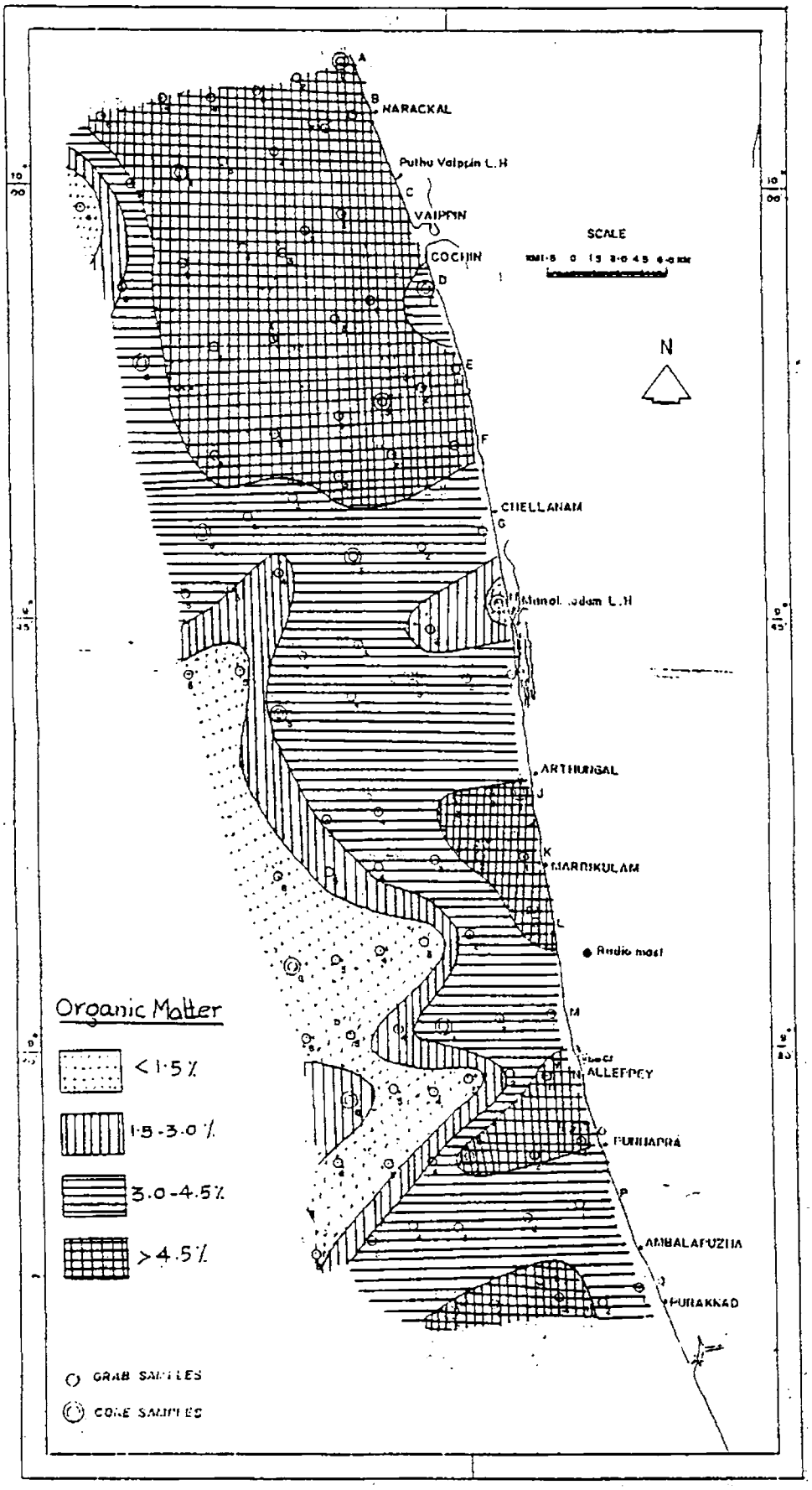

Fig. 4.2 Distribution of organic matter

6 - 8 % class range. One eighth of the samples yield a Fe_2O_3 percentage of < 2 %. Except for minor variations, the distribution pattern of Fe_2O_3 follows the same trend as that of Al_2O_3.

Percentage of CaO fluctuates between 0.84 and 11.48 (average concentration: 4.83 %). Frequency distribution shows that a large number of samples fall in the concentration range of 4 - 6 %. At certain locations in the central part of the study area, a high amount of CaO are noticed. Sporadic occurrence of low concentration (< 4 %) patches are also observed.

Average concentration of MgO is 3.81 % (ranging between 0.20 and 6.40 %). Maximum number of samples show the MgO content in the range of 3 - 5 %. Southwestern part of the study area shows the lowest concentration (< 2 % MgO). Mainly two patches of high concentration are observed, one in the central part and another near Punnapra.

With an average of 2.81 %, Na_2O concentration varies widely from 0.34 to 4.14 %. Majority of the samples contain 2 to 4 % of Na_2O. The southwest portion exhibits the lowest concentration. Northern half, in general, mark a high concentration (> 3 % Na_2O).

The average value of K_2O is 0.89 % with a range of 0.14 to 1.27 %. Large number of samples show a percentage range between 0.8 and 1.2 %. Like Na_2O, K_2O also registers a low percentage in the northwestern portion. Similarly, the northern part also contain high K_2O values. Nearshore portions of the southern part yield high values (> 0.8 %).

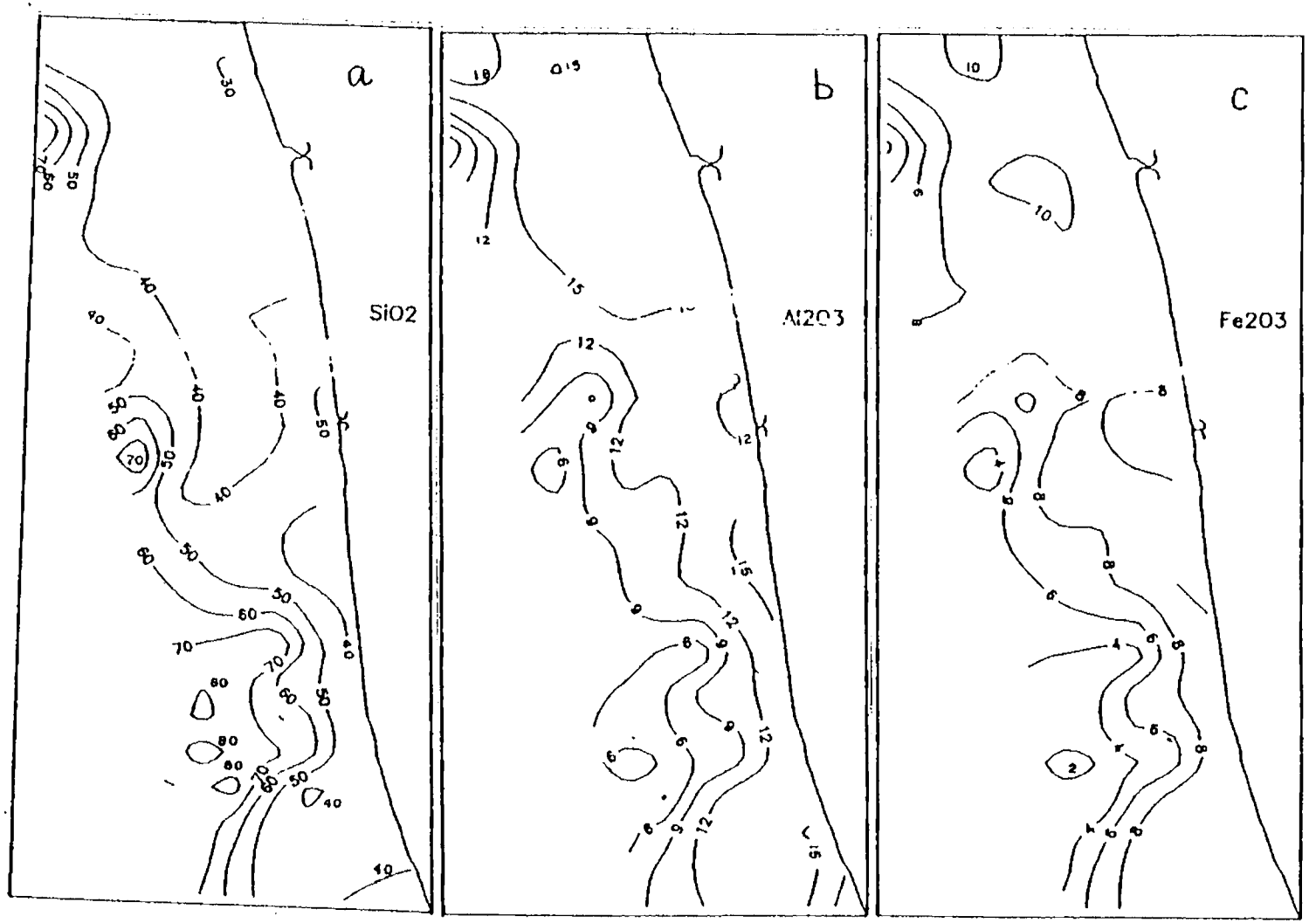

Fig. 4.3 Distribution of major elements

Fig. 4.3 Contd...

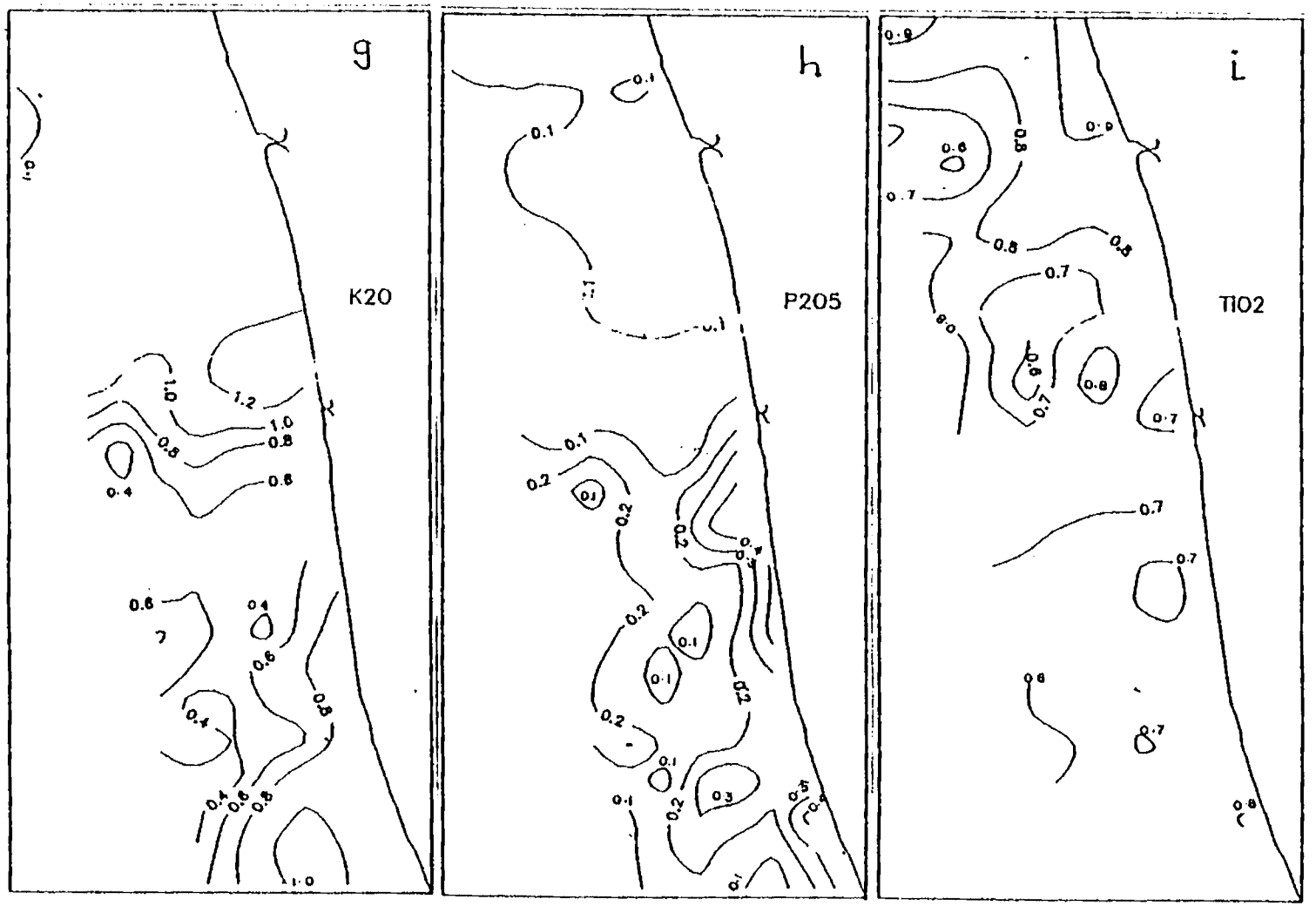

Fig. 4.3 Contd...

P_2O_5 ranges from 0.02 to 0.55 %. Average concentration is around 0.16 %. Three fourth of the samples show < 0.2 % concentration. Aerial distribution pattern of P_2O_5 is slightly complex with sporadic patches of high concentrations in the nearshore portions off Ambalapuzha and Arthungal - Mararikulam regions.

Percent variation of TiO_2 is between 0.50 and 0.92. Average concentration is around 0.72 %. More than one third of the samples contain TiO_2 percentage between 0.6 and 0.7. Except a few offshore locations, the northern part shows a higher concentration compared to the southern part. Sediments in certain nearshore locations around Ambalapuzha, Alleppey, Arthungal and Manakkodam are depleted in the TiO_2 concentration.

4.3.2 Minor and trace elements

Unlike the preceding section in which the distribution pattern of major elements are considered in isolation, here the variability of minor and trace elements are discussed together, since many of the trace elements show similar pattern of distribution.

Details of the elemental concentration, range, average and standard deviation of the different elements (Mn, Cu, Co, Cr, Ni, Cd, Pb, Zn, Ba, Sr, Rb, Be, Li, Mo and V) are given in Tables 4.4 and 4.5. Many elements, such as, Cu, Cr, Ba, Rb, Be, Mo and V show the minimum values as zero, as their presence is below the level of detection of AAS. None of the elements show a consistency in its concentration as indicated by the standard deviation values (Table 4.5). Depending on the decrease in average concentration, the elements can be read as Ba > Sr > Mn > Ni > Cr > Zn > Co > Li > Pb > V >

TABLE-4.4

Minor and Trace Element Concentration in the Innershelf Sediments (in ppm)

Sl. No.	Sample No.	Mn	Cu	Co	Cr	Ni	Cd	Pb	Zn	Ba	Sr	Rb	Be	Li	Mo	V
1.	A1	210	35.4	98.0	112.0	202	36.2	52	101.2	346	156	46.0	6.8	98.2	n.f	20
2.	A3	179	25.2	74.4	150.0	166	32.6	54	101.2	562	168	26.8	3.4	85.2	n.f	100
3.	A4	176	20.8	61.8	178.4	170	15.2	44	87.6	148	174	39.2	2.2	78.6	20.0	100
4.	A6	181	17.2	96.4	85.0	182	29.4	56	78.8	770	234	38.4	6.2	95.6	n.f	n.f
5.	B1	358	24.6	116.6	62.4	168	30.4	54	70.0	210	338	46.4	6.8	63.0	n.f	n.f
6.	B3	204	19.0	49.8	103.2	172	32.4	56	99.8	462	204	27.4	4.0	79.4	n.f	120
7.	B6	23	n.f	11.4	n.f	22	33.4	30	21.8	390	126	n.f	0.8	15.8	n.f	n.f
8.	C1	261	25.6	70.4	179.2	160	16.2	66	133.0	494	182	39.0	1.0	83.2	28.0	100
9.	C3	277	23.6	67.6	146.6	180	26.6	46	120.2	740	186	29.2	2.0	79.2	10.0	120
10.	C5	220	24.2	95.4	91.0	216	31.2	38	122.0	770	160	39.8	5.6	92.4	n.f	n.f
11.	D1	226	15.8	91.0	49.4	160	31.8	36	65.6	658	296	36.8	4.4	72.0	n.f	120
12.	D2	179	20.0	85.0	128.2	254	30.8	46	120.8	900	124	33.8	2.6	91.2	n.f	80
13.	D4	177	43.0	96.8	100.0	212	37.0	88	135.6	476	122	32.8	8.6	95.0	n.f	60
14.	D6	173	13.8	63.2	60.0	190	3.8	44	89.0	420	274	23.2	3.4	65.2	n.f	n.f
15.	E2	192	28.4	206.0	76.0	174	31.2	70	61.8	842	220	42.8	8.4	85.0	n.f	40
16.	E4'	183	16.8	63.2	162.2	202	33.8	80	90.8	370	148	29.4	4.2	85.4	n.f	n.f
17.	E6	156	12.8	65.6	44.2	164	35.0	62	123.8	90	508	28.4	4.0	58.2	n.f	80
18.	F2	179	18.2	92.6	43.0	162	30.6	52	66.8	502	420	26.2	6.4	67.8	n.f	60

(Table 4.4 contd.)

Sl. No.	Sample No.	Mn	Cu	Co	Cr	Ni	Cd	Pb	Zn	Ba	Sr	Rb	Be	Li	Mo	V
19.	F4	185	14.4	33.6	132.8	186	11.2	26	66.2	n.f	514	30.2	3.2	57.6	n.f	80
20.	F6	179	14.4	66.8	85.4	116	31.0	22	81.0	1012	326	22.4	2.0	39.6	n.f	n.f
21.	G1	251	13.2	56.8	64.8	102	33.2	68	93.8	606	372	22.8	2.0	52.2	n.f	20
22.	G3	234	17.0	45.8	76.2	150	32.4	46	95.4	382	204	20.0	2.8	63.4	n.f	60
23.	G4	46	5.4	74.4	n.f	284	18.4	62	56.0	736	1134	n.f	n.f	14.8	n.f	n.f
24.	G6	193	26.0	103.4	62.4	168	32.2	34	60.8	930	328	35.6	5.8	73.0	n.f	n.f
25.	H1	236	11.6	77.2	2.2	126	34.6	20	58.2	428	378	30.8	5.4	39.8	n.f	n.f
26.	H2	238	15.6	93.4	9.0	274	30.8	66	49.6	498	404	42.6	4.2	46.6	n.f	40
27.	H4	154	16.2	71.0	74.0	94	31.4	92	78.6	634	308	24.0	2.6	68.6	n.f	n.f
28.	H5	111	8.0	71.2	39.6	126	33.2	38	64.2	530	522	8.8	2.2	47.2	n.f	n.f
29.	I1	240	12.0	66.6	49.6	104	31.0	32	71.2	402	292	29.6	2.0	54.2	n.f	60
30.	I3	203	14.4	66.6	116.2	156	24.6	86	76.2	672	332	20.0	n.f	65.2	n.f	40
31.	I5	141	4.4	61.0	113.2	156	20.4	44	60.2	192	524	23.8	0.6	59.8	10.0	20
32.	J1	187	17.2	64.8	167.2	140	17.0	56	78.2	354	274	39.0	3.6	67.0	n.f	100
33.	J3	196	15.4	58.2	128.8	148	24.8	50	76.6	604	244	22.6	0.6	73.8	n.f	20
34.	J4	118	9.0	51.2	80.2	120	20.4	12	67.6	344	414	17.4	1.4	44.0	n.f	n.f
35.	K2	180	16.0	54.8	148.8	142	26.8	96	87.6	381	232	26.0	3.8	80.0	n.f	n.f
36.	K4	171	11.4	52.2	79.8	122	28.0	60	66.6	1052	270	42.2	0.2	52.8	20.0	80
37.	K6	156	8.0	44.8	n.f	86	31.6	38	71.6	336	246	19.0	3.8	31.0	n.f	40
38.	L1	185	15.2	62.2	135.6	136	30.2	62	84.0	1002	232	27.0	1.8	88.6	n.f	100

(Table 4.4 contd.)

Sl. No.	Sample No.	Mn	Cu	Co	Cr	Ni	Cd	Pb	Zn	Ba	Sr	Rb	Be	Li	Mo	V
39.	L3	50	1.2	21.8	n.f	152	24.8	50	23.8	828	98	0.2	0.2	14.4	n.f	n.f
40.	L6	175	5.6	36.2	30.2	60	20.8	58	48.6	834	316	18.8	0.4	25.4	n.f	20
41.	M1	200	21.6	57.4	185.8	180	12.0	2	91.4	194	246	38.8	n.f	83.4	n.f	20
42.	M3	239	16.6	77.0	113.2	128	27.2	62	82.0	668	274	n.f	3.0	67.8	20.0	100
43.	M5	29	n.f	10.6	n.f	8	27.0	28	39.0	402	50	n.f	n.f	16.0	n.f	n.f
44.	N1	181	18.6	65.8	192.0	174	14.0	76	82.0	180	208	38.2	1.4	89.2	n.f	120
45.	N3	58	1.4	58.2	12.6	26	20.0	34	70.2	86	50	1.0	n.f	15.6	n.f	20
46.	N6	117	8.8	42.8	33.2	86	26.4	34	45.2	858	160	3.2	1.0	39.8	12.0	60
47.	O1	208	19.2	70.6	177.2	144	8.8	46	87.2	510	294	41.8	2.6	78.4	n.f	40
48.	O3	183	18.2	67.2	187.8	146	10.8	48	74.4	242	210	43.2	2.4	82.0	n.f	80
49.	O5	51	n.f	24.0	6.2	36	20.2	26	49.4	314	80	10.4	0.4	16.4	n.f	140
50.	P1	173	26.8	39.0	104.4	182	31.0	76	114.4	434	222	33.0	2.8	85.4	n.f	n.f
51.	P2	244	32.2	41.4	59.2	180	33.0	68	89.6	246	316	19.6	5.2	59.2	n.f	20
52.	P4	201	15.0	49.4	65.8	112	31.8	66	115.2	304	282	26.2	2.0	64.6	n.f	40
53.	P6	35	n.f	42.0	n.f	74	31.2	30	62.8	466	68	n.f	2.0	15.0	n.f	20
54.	Q1	171	9.4	26.2	55.8	110	33.6	52	81.6	278	256	19.8	4.2	57.8	n.f	n.f
55.	Q3	231	12.0	76.6	75.6	160	33.8	56	80.0	460	270	24.2	6.0	69.2	n.f	n.f
56.	Q5	214	9.2	62.0	64.2	158	34.8	20	92.8	286	274	22.4	6.2	65.2	n.f	n.f

* n.f = not found

TABLE 4.5

Range, average and standard deviation of minor and trace elements (in ppm)

	Minimum	Maximum	Average	Std.Dev.
Mn	23.0	358.0	177.11	65.46
Cu	0.0	43.0	15.43	8.96
Co	10.6	206.0	64.40	30.38
Cr	0.0	192.0	83.93	57.50
Ni	8.0	284.0	146.57	55.75
Cd	8.8	37.0	27.36	7.35
Pb	2.0	96.0	50.29	20.12
Zn	21.8	135.6	79.69	24.89
Ba	0.0	1052.0	497.04	255.68
Sr	50.0	1134.0	272.57	163.88
Rb	0.0	46.4	25.54	13.43
Be	0.0	8.6	3.01	2.52
Li	14.4	98.2	61.67	24.28
Mo	0.0	28.0	2.14	6.14
V	0.0	140.0	41.79	43.20

TABLE 4.6

Correlation coefficients of major element Vs size

	Sand	Silt	Clay
SiO2	.908	-.784	-.811
Al2O3	-.753	.684	.644
Fe2O3	-.905	.764	.822
CaO	-.269	.277	.203
MgO	-.666	.558	.610
Na2O	-.753	.729	.607
K2O	-.642	.674	.474
P2O5	-.180	.021	.272
TiO2	-.331	.364	.232

Significant level of r values:

>0.22 (0.1 level), >0.26 (0.05 level)
>0.34 (0.01 levle), >0.42 (0.001 level)

Cd > Rb > Cu > Be > Mo. The first four elements (Ba, Sr, Mn and Ni) are present in more than 100 ppm level of average concentration and Be and Mo in less than 10 ppm average concentration. Cd gives a minimum deviation (27 % around the average) and the maximum deviation is shown by Mo (287 %). Similar is the case with V, which is present in 36 of the 56 samples yielding a coefficient of variance 103 %. Despite the presence of Be in all but 5 samples, sample to sample variation is higher, thus resulting in a higher standard deviation. Zn, Mn, Ni, Li and Pb show deviation less than 40 % around mean whereas Co, Ba, Rb and Cu show variance between 40 - 60 %. Sr and Cr yield a percentage deviation of little more than 60 % around the average.

The frequency percentage of histograms (Fig. 4.4a-o) shows the following patterns:

i. In majority of samples, Mn values vary between 150 and 250 ppm.

ii. Cu values show a modal class of 8 - 16 ppm.

iii. Sample frequency shows a maximum of 60 - 90 ppm for Co.

iv. Except for a small modality of 60 - 90 ppm class, Cr does not show a significant frequency concentration range.

v. In the case of Ni, a large number of samples yield a concentration range of 100 - 200 ppm.

vi. For Cd a highly significant modal class of 30 - 35 ppm makes other class intervals of subtle importance.

vii. Pb concentration among the samples give a typical normal frequency distribution with a gradual decrease of frequency around the modal class 45 - 60 ppm.

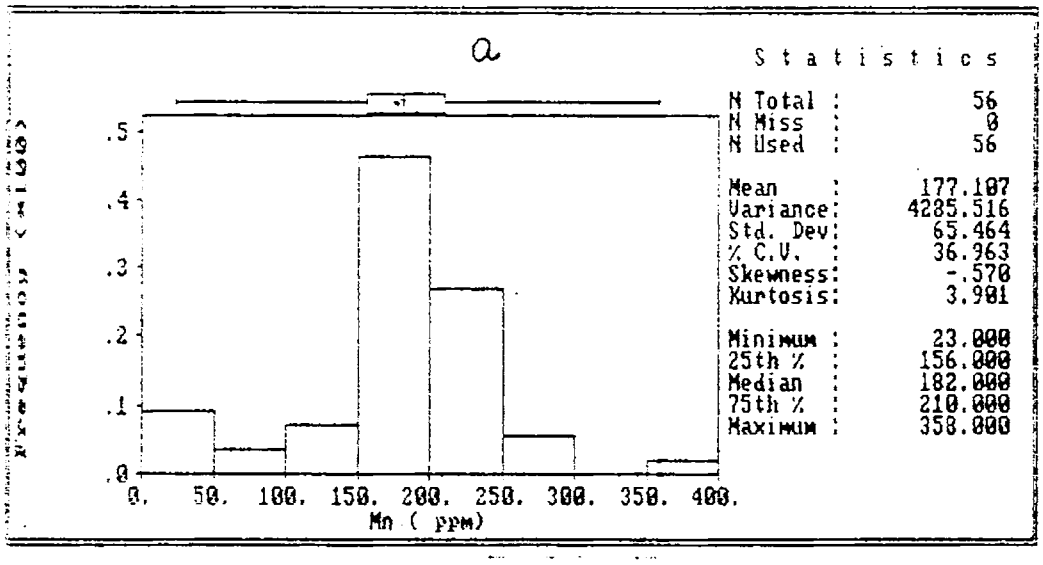

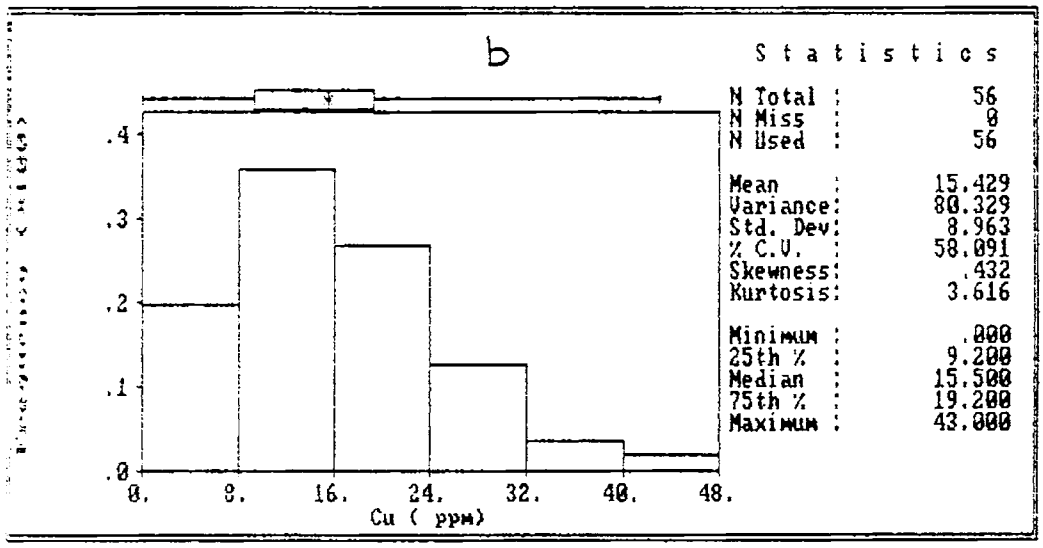

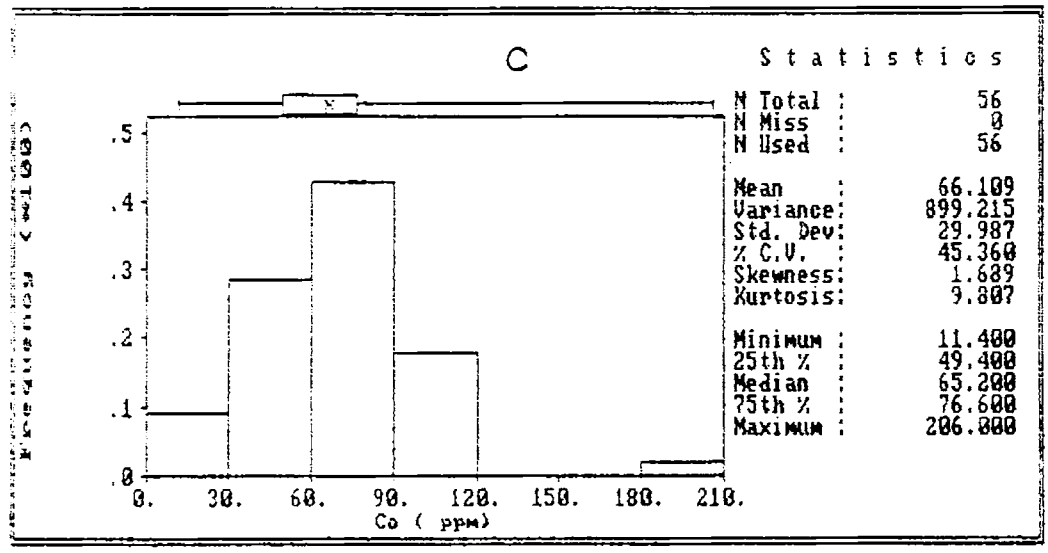

Fig. 4.4 Frequency distribution of minor and trace elements

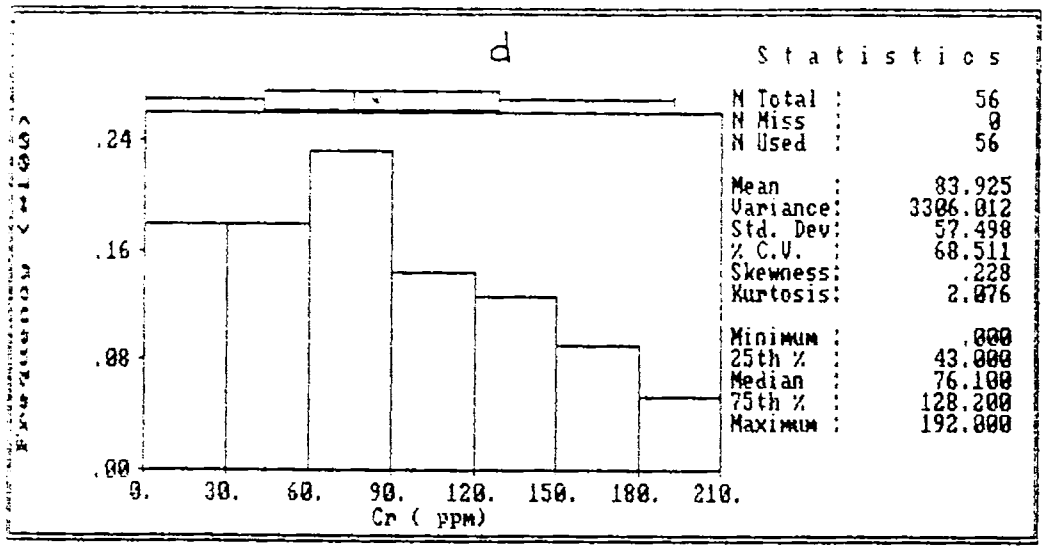
d
Statistics
N Total : 56
N Miss : 0
N Used : 56
Mean : 83.925
Variance: 3306.012
Std. Dev: 57.498
% C.V. : 68.511
Skewness: .228
Kurtosis: 2.876
Minimum : .000
25th % : 43.000
Median : 76.100
75th % : 128.200
Maximum : 192.000
.24
.16
.08
.00
0. 30. 60. 90. 120. 150. 180. 210.
Cr (ppm)

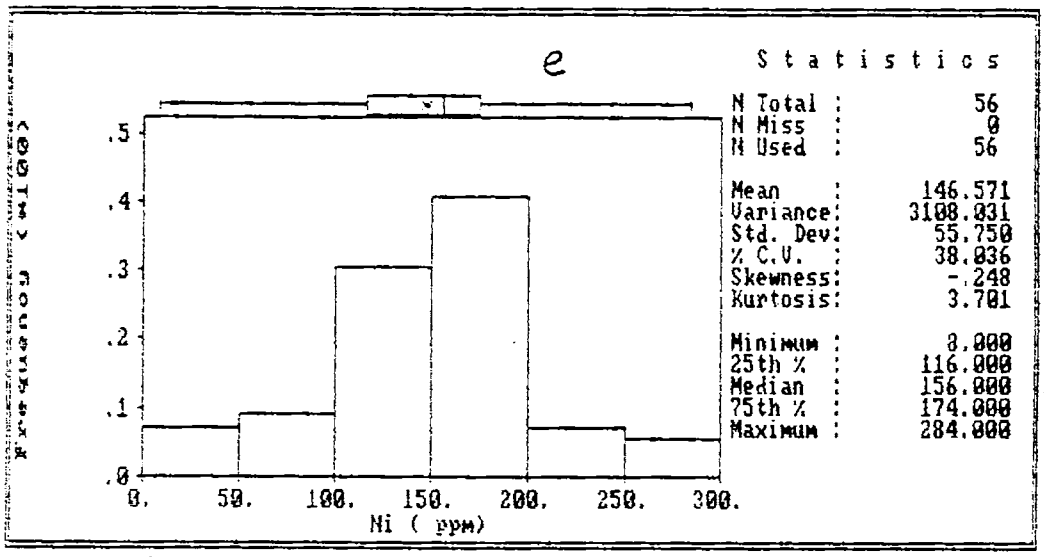
e
Statistics
N Total : 56
N Miss : 0
N Used : 56
Mean : 146.571
Variance: 3108.031
Std. Dev: 55.750
% C.V. : 38.036
Skewness: -.248
Kurtosis: 3.701
Minimum : 8.000
25th % : 116.000
Median : 156.000
75th % : 174.000
Maximum : 284.000
.5
.4
.3
.2
.1
.0
0. 50. 100. 150. 200. 250. 300.
Ni (ppm)

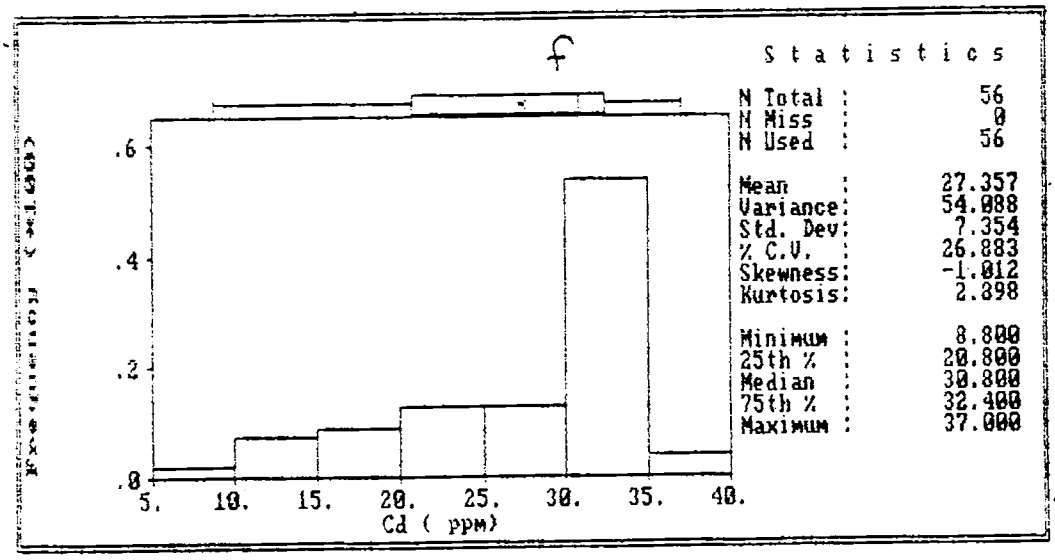
f
Statistics
N Total : 56
N Miss : 0
N Used : 56
Mean : 27.357
Variance: 54.088
Std. Dev: 7.354
% C.V. : 26.883
Skewness: -1.012
Kurtosis: 2.898
Minimum : 8.800
25th % : 20.800
Median : 30.800
75th % : 32.400
Maximum : 37.000
.6
.4
.2
.0
5. 10. 15. 20. 25. 30. 35. 40.
Cd (ppm)

Fig. 4.4 Contd..

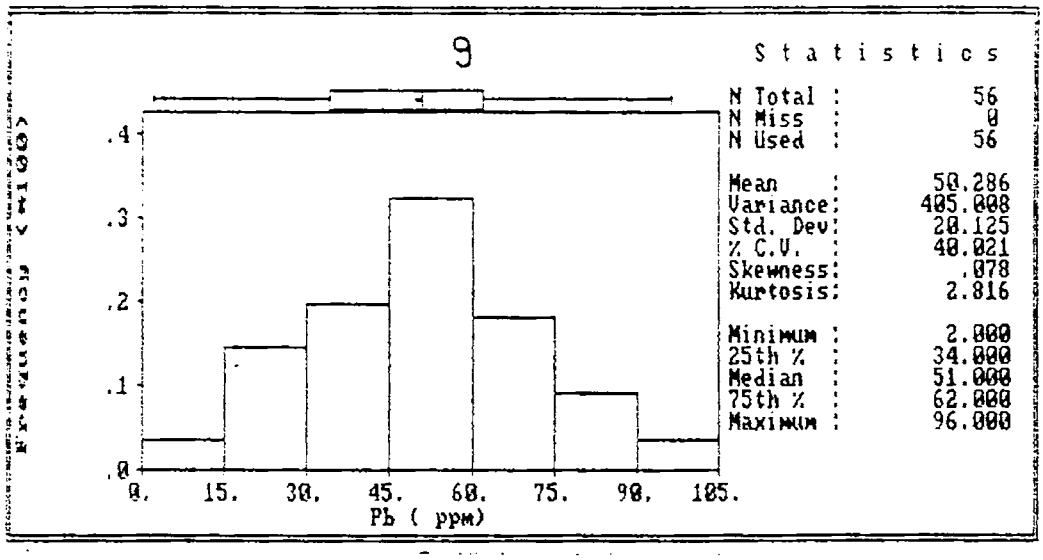
g
Statistics
N Total : 56
N Miss : 0
N Used : 56
Mean : 50.286
Variance: 405.008
Std. Dev: 20.125
% C.V. : 40.021
Skewness: .078
Kurtosis: 2.816
Minimum : 2.000
25th % : 34.000
Median : 51.000
75th % : 62.000
Maximum : 96.000
.4
.3
.2
.1
.0
0. 15. 30. 45. 60. 75. 90. 105.
Pb (ppm)

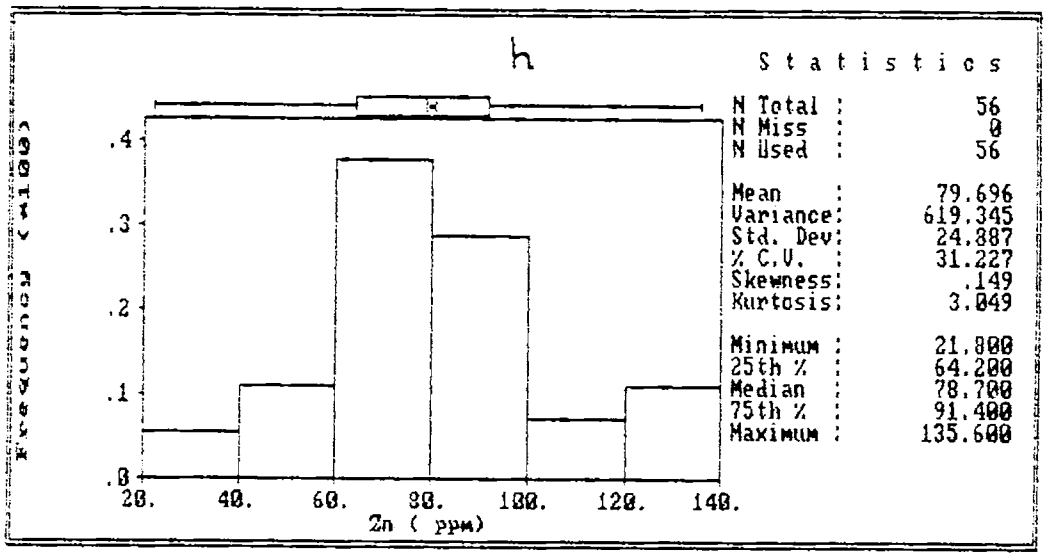
h
Statistics
N Total : 56
N Miss : 0
N Used : 56
Mean : 79.696
Variance: 619.345
Std. Dev: 24.887
% C.V. : 31.227
Skewness: .149
Kurtosis: 3.049
Minimum : 21.800
25th % : 64.200
Median : 78.700
75th % : 91.400
Maximum : 135.600
.4
.3
.2
.1
.0
20. 40. 60. 80. 100. 120. 140.
Zn (ppm)

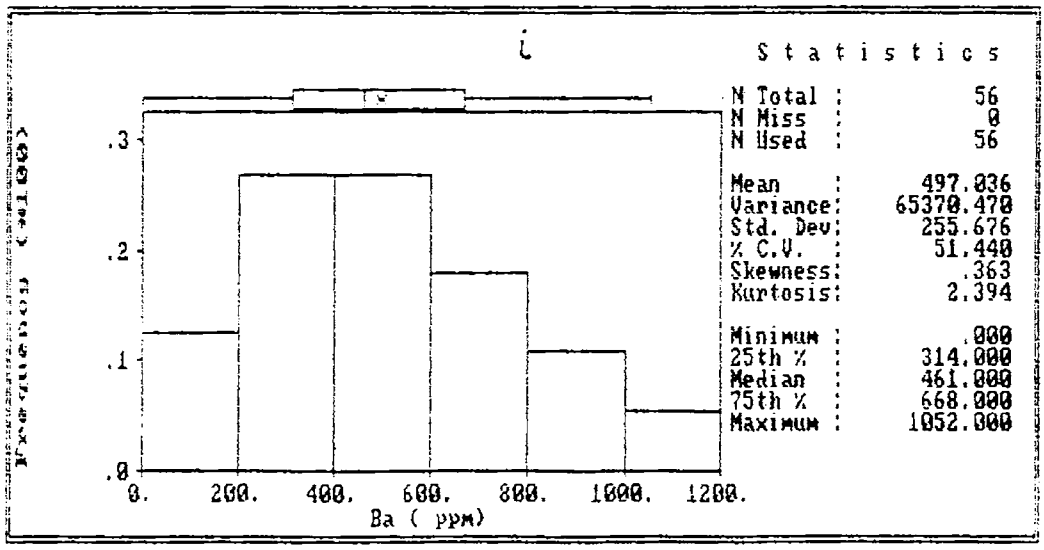
i
Statistics
N Total : 56
N Miss : 0
N Used : 56
Mean : 497.036
Variance: 65370.470
Std. Dev: 255.676
% C.V. : 51.440
Skewness: .363
Kurtosis: 2.394
Minimum : .000
25th % : 314.000
Median : 461.000
75th % : 668.000
Maximum : 1052.000
.3
.2
.1
.0
0. 200. 400. 600. 800. 1000. 1200.
Ba (ppm)

j

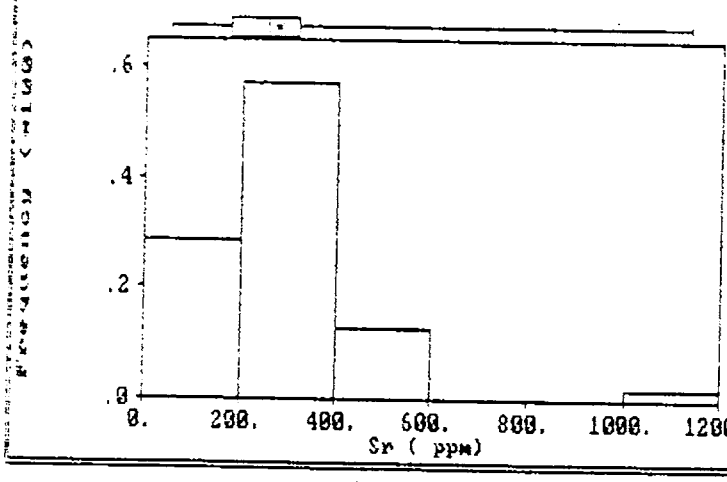

Statistics

N Total	56
N Miss	0
N Used	56
Mean	272.571
Variance	26856.100
Std. Dev	163.878
% C.V.	60.123
Skewness	2.688
Kurtosis	14.837
Minimum	50.000
25th %	174.000
Median	251.000
75th %	316.000
Maximum	1134.000

k

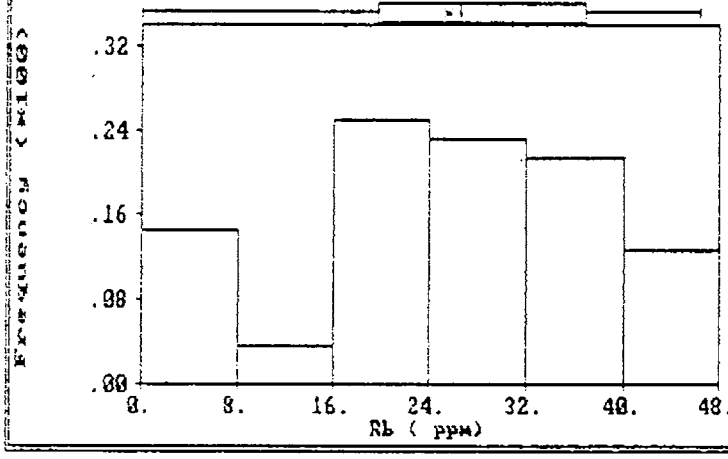

Statistics

N Total	56
N Miss	0
N Used	56
Mean	25.539
Variance	180.225
Std. Dev	13.425
% C.V.	52.565
Skewness	-.549
Kurtosis	2.475
Minimum	.000
25th %	19.600
Median	26.500
75th %	36.800
Maximum	46.400

l

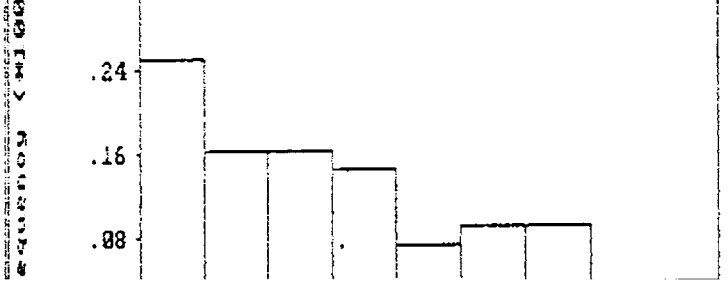

Statistics

N Total	56
N Miss	0
N Used	56
Mean	3.011
Variance	5.077
Std. Dev	2.253
% C.V.	74.840
Skewness	.570
Kurtosis	2.585
Minimum	.000
25th %	1.000
Median	2.600
75th %	4.200
Maximum	8.600

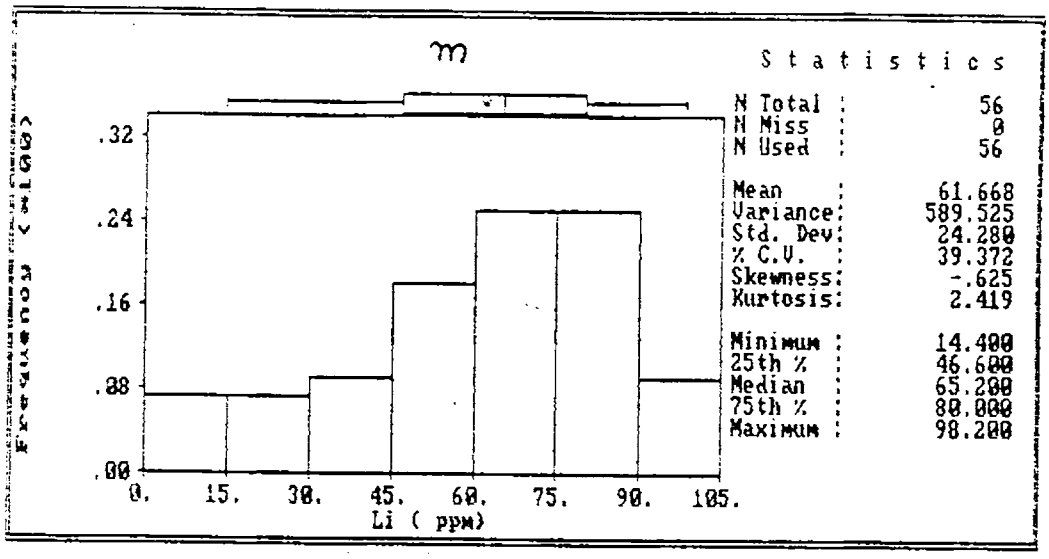
m
Statistics
N Total : 56
N Miss : 0
N Used : 56
Mean : 61.668
Variance: 589.525
Std. Dev: 24.280
% C.V. : 39.372
Skewness: -.625
Kurtosis: 2.419
Minimum : 14.400
25th % : 46.600
Median : 65.200
75th % : 80.000
Maximum : 98.200
Frequency (*100)
.32
.24
.16
.08
.00
0. 15. 30. 45. 60. 75. 90. 105.
Li (ppm)

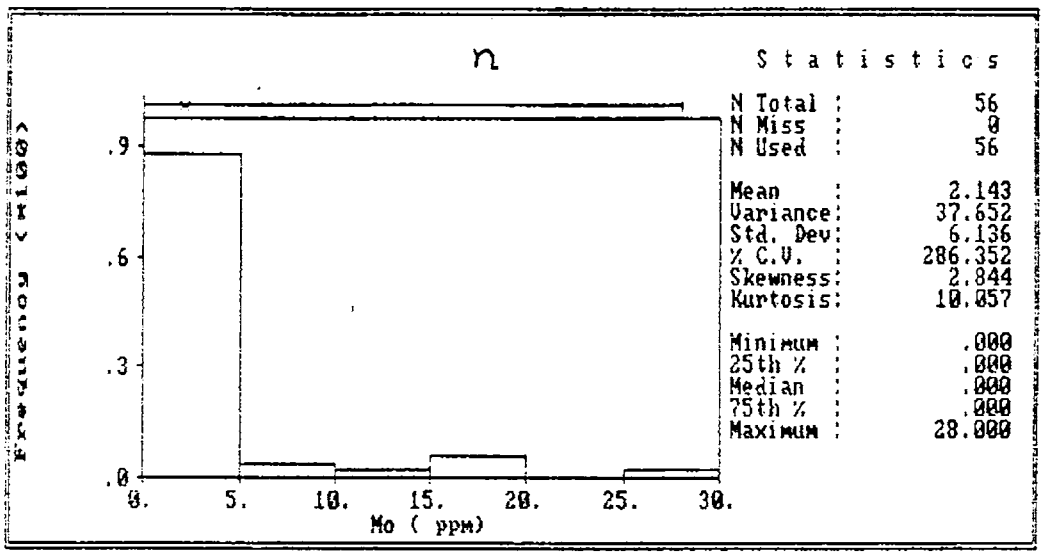
n
Statistics
N Total : 56
N Miss : 0
N Used : 56
Mean : 2.143
Variance: 37.652
Std. Dev: 6.136
% C.V. : 286.352
Skewness: 2.844
Kurtosis: 10.057
Minimum : .000
25th % : .000
Median : .000
75th % : .000
Maximum : 28.000
Frequency (*100)
.9
.6
.3
.0
0. 5. 10. 15. 20. 25. 30.
Mo (ppm)

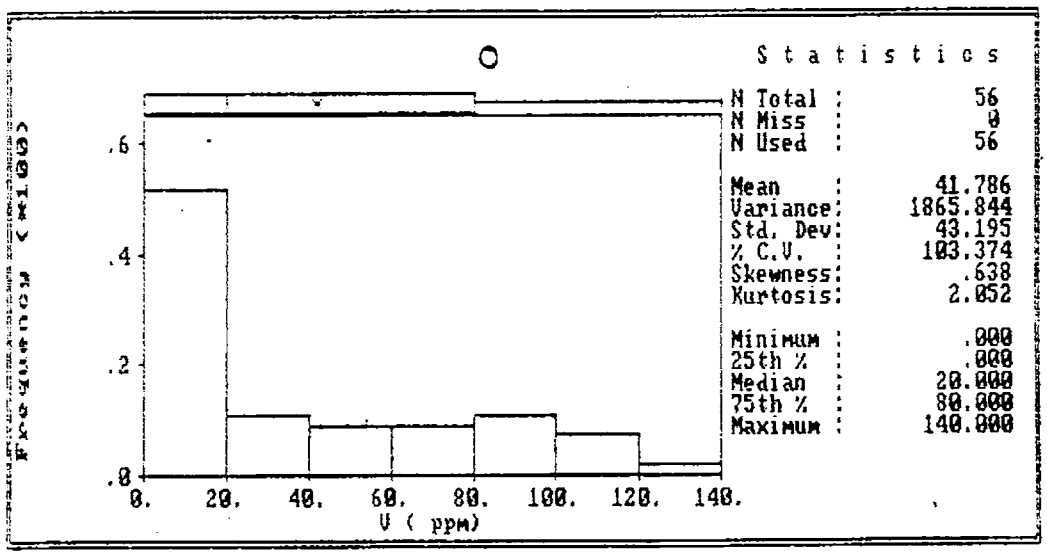
o
Statistics
N Total : 56
N Miss : 0
N Used : 56
Mean : 41.786
Variance: 1865.844
Std. Dev: 43.195
% C.V. : 103.374
Skewness: .638
Kurtosis: 2.052
Minimum : .000
25th % : .000
Median : 20.000
75th % : 80.000
Maximum : 140.000
Frequency (*100)
.6
.4
.2
.0
0. 20. 40. 60. 80. 100. 120. 140.
V (ppm)

viii. Enrichment of Zn between 60 - 100 ppm in a large number of samples is observed.

ix. Ba gives a wider modal class of 200 - 600 ppm representing > 55 % of the samples.

x. In majority of samples, Sr concentration is restricted between 0 - 400 ppm.

xi. Larger variation is observed for Rb without specific peaks in frequency distribution.

xii. Gradual depletion of frequency for Be concentration from the first class interval onwards is striking.

xiii. Maximum number of samples represents a Li range of 45 - 90 ppm.

xiv. Around 90 % of samples contain < 5 ppm of Mo.

xv. More than half of the samples contain > 20 ppm of V.

The spatial distribution patterns of the minor and trace elements are given in Fig. 4.5(a-o). In the nearshore portions, Mn shows an enrichment, which transcends to lower values in the offshore. An enrichment of Mn is discerned around Cochin inlet. Especially sand-dominant areas register a relative depletion in Mn concentration.

Except for a marginal variation here and there, the distribution pattern of Cu, Co, Cr, Ni, Zn, Rb and Li are similar to Mn distribution. Cu shows two highs, one off Cochin inlet and another one around Alleppey nearshore. Very high concentration of Co is observed near to the coast south of Cochin. Cr in turn shows semblance with Cu distribution with an enrichment around Cochin and Alleppey. In the case of Ni, the distribution is similar to Cu, but two zones of high concentration are located off Manakkodam. Zn follows the pathways of Cu, whereas Rb distribution correlates well with that of Mn and

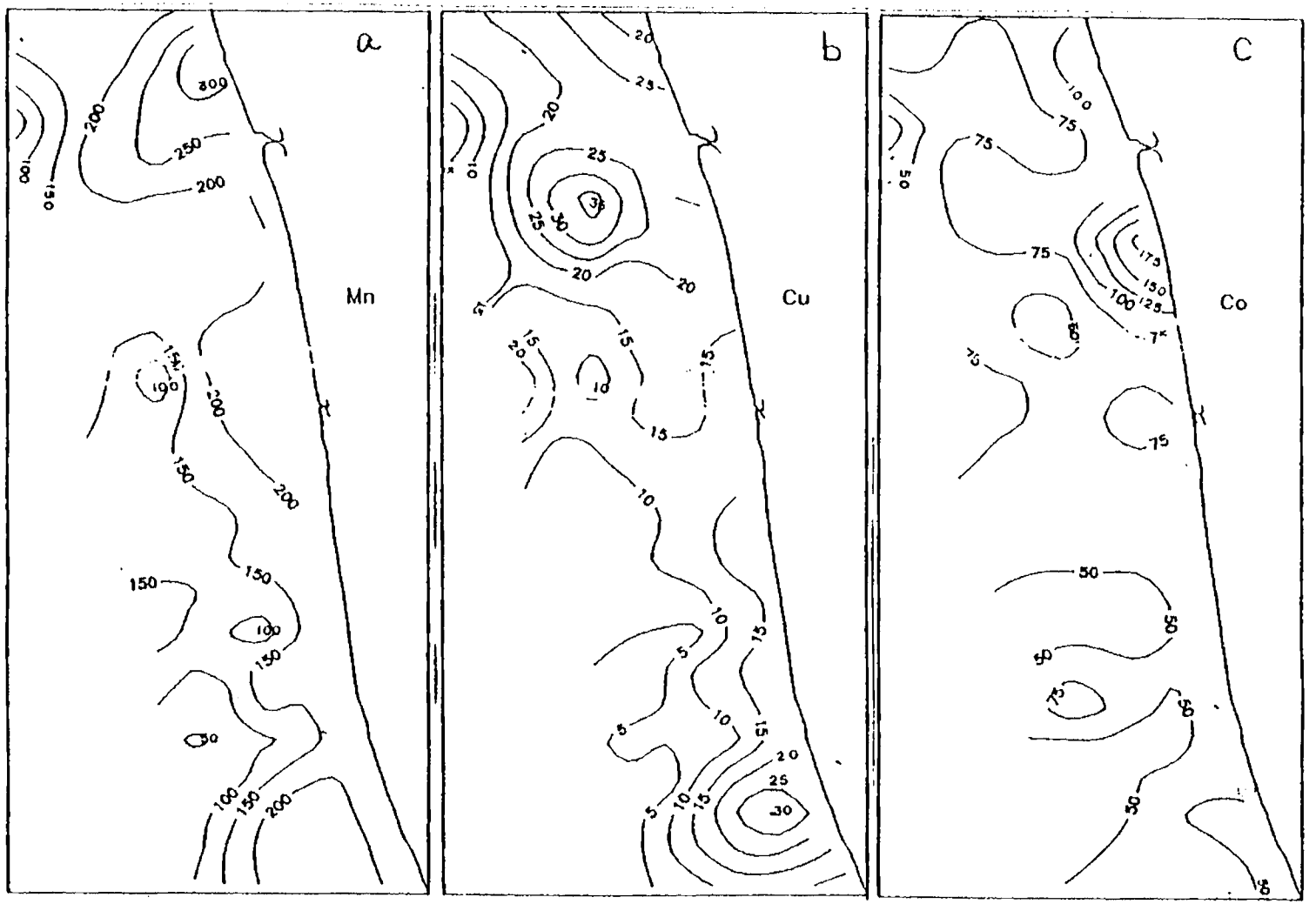

Fig. 4.5 Distribution of minor and trace elements

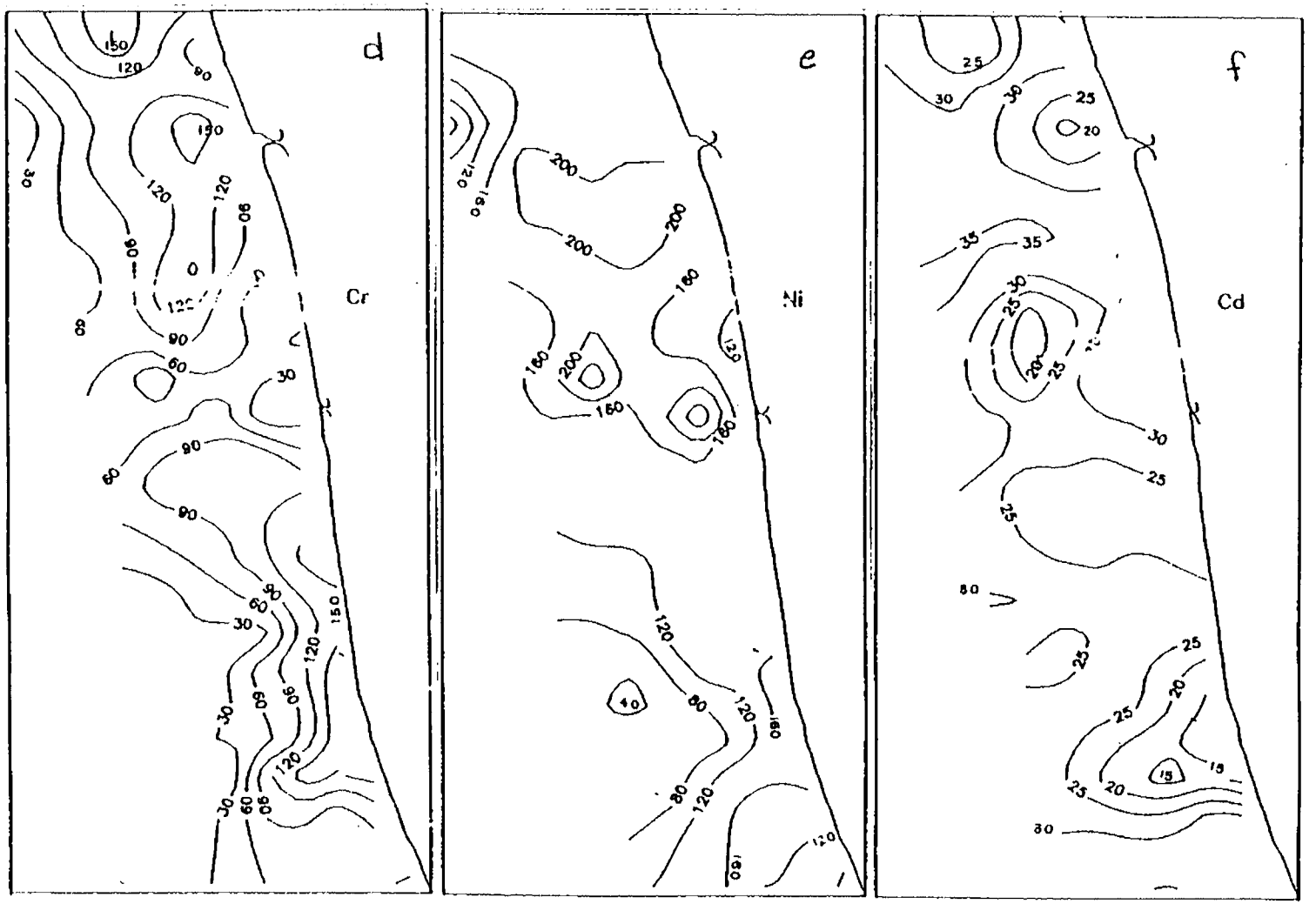

Fig. 4.5 Contd...

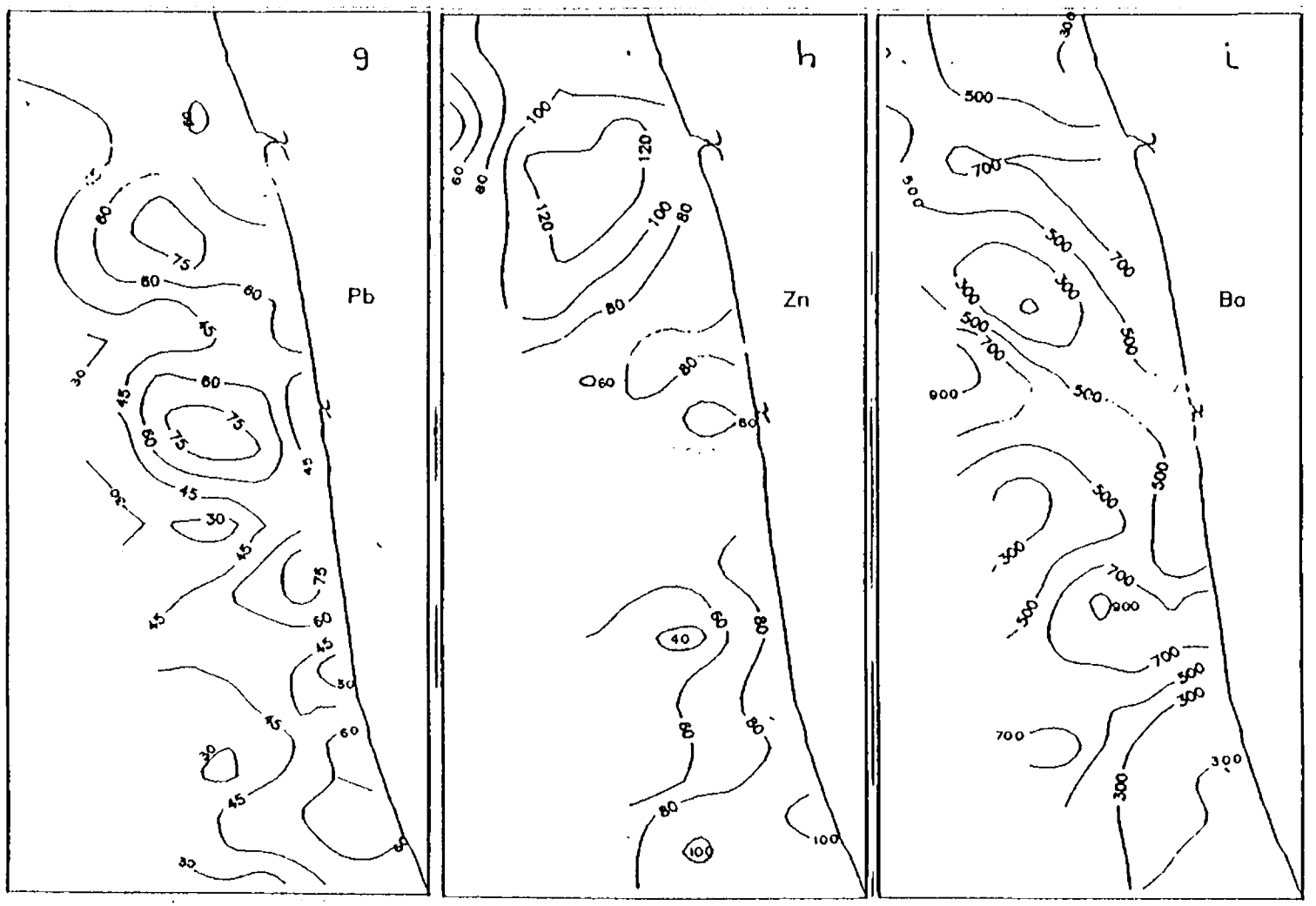

Fig. 4.5 Contd...

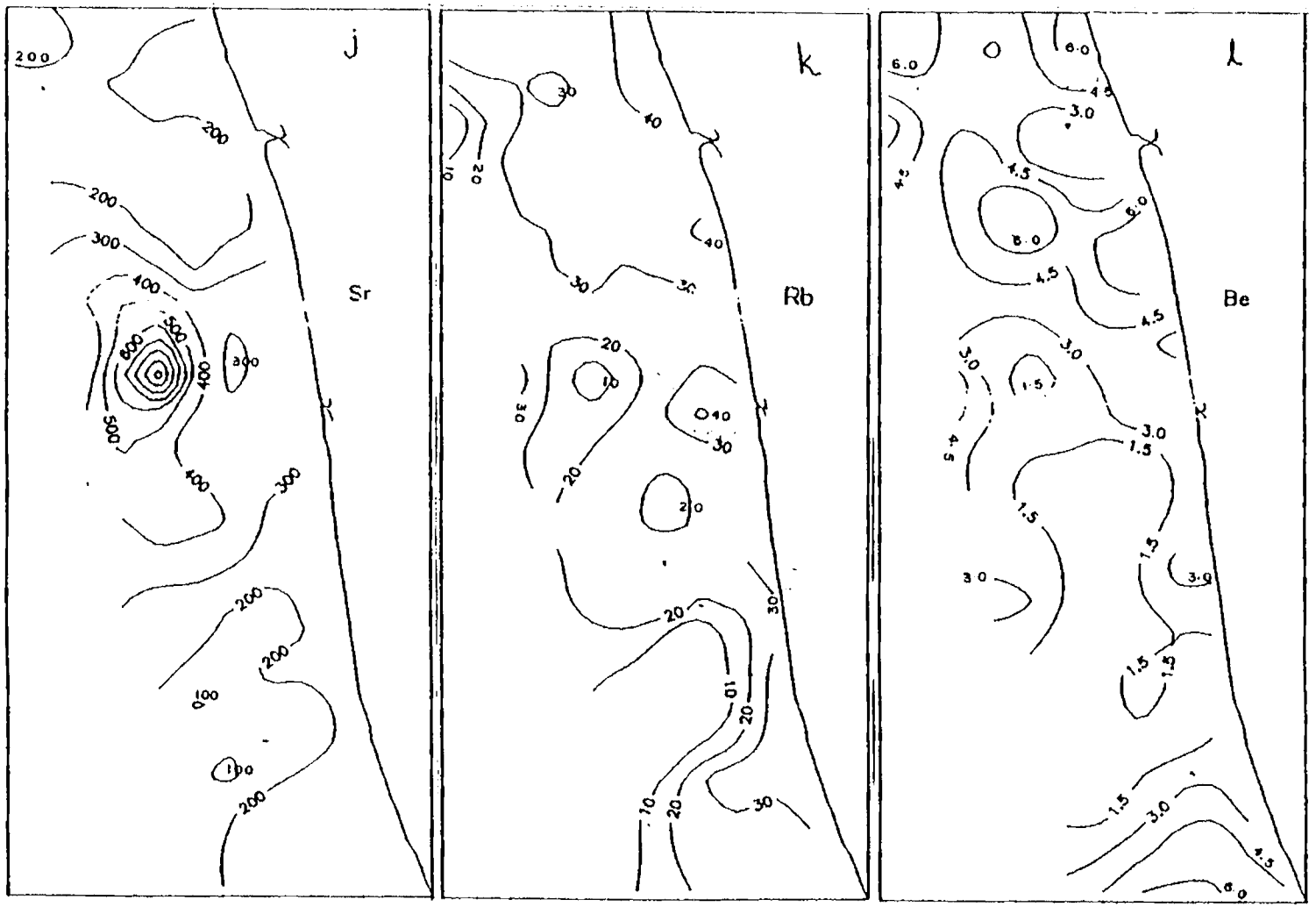

Fig. 4.5 Contd..

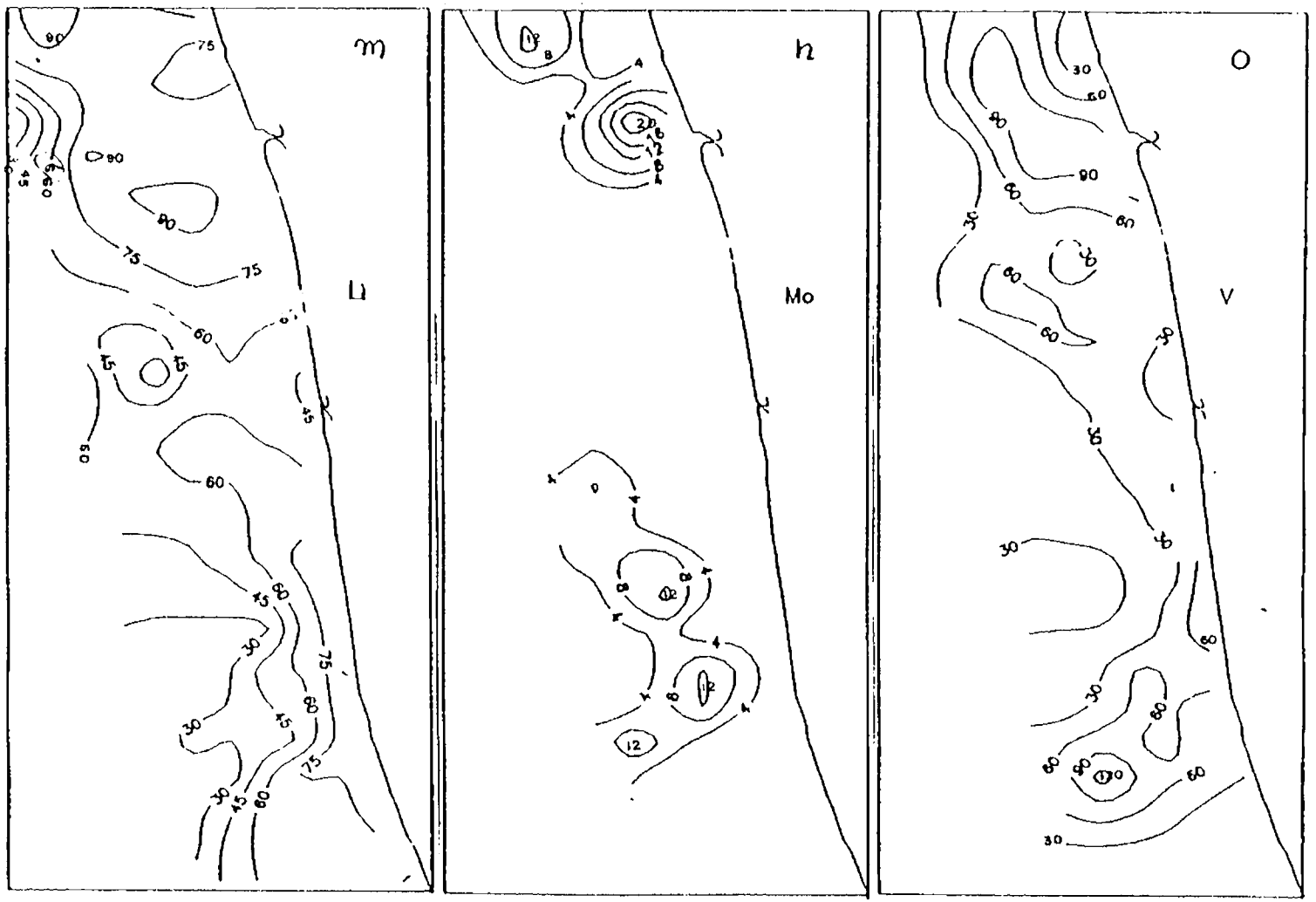

Fig. 4.5 Contd...

shows an increased adherence to the sediments in the nearshore portion of north of Cochin. Li variation is similar to Cu with high values off Cochin.

Cd shows a distribution pattern without any systematic spatial variation, recording low values near Cochin inlet and Alleppey nearshore. Pb also reflects a complexity in distribution with sporadic patches of highs and lows. Ba gives high values near Cochin, seaward part off Manakkodam and nearshore portions north of Alleppey. Only a zone of very high Sr (1134 ppm in location G4) is observed off Manakkodam. Be records high values north and south of Cochin inlet. Mo values show a high concentration around Cochin inlet and in portions bordering the sand-rich zone in the southwestern part. The general tendency of V distribution is a reduction towards the offshore direction. Around Cochin inlet and offshore locations of Alleppey it yields a higher value.

4.4 DISCUSSION

4.4.1 Organic matter

In the shelf sediments, the input of organic matter is essentially controlled by the rate of supply of terrestrial material through run-off, rate of deposition of organic to inorganic constituents, organic productivity in the shelf, rate of decomposition of organic matter and the texture of the sediments. Slow rate of sedimentation allow enhanced decomposition of organic matter by microbiological sulphate reduction prior to burial. Rapid rates reduces decomposition since the exposure time and loss of organic matter due to re-mineralisation are reduced (Muller and Suess, 1979). Because of its preferential preservation or decomposition, the fraction of organic matter that

becomes buried is an extensively modified version of the organic matter supplied and does not necessarily have the same original characteristics (Tegellar, *et al.*, 1989 and Middelburg, 1991). Organic matter plays an important role in modifying the ability of the sediment to fix trace metals and controlling the Eh - pH related stabilities of sedimentary minerals (Garrels and Christ, 1965; Cline *et al.*, 1973).

Previous work on the distribution of organic matter along this innershelf sector is meagre. The distribution pattern shows (Fig. 4.2), an enrichment of organic matter around the Cochin inlet is mainly influenced by input from the Vembanad Lake, where the content of organic matter and amount supplied from terrestrial source was found to be high (Purandara, 1990). The percentage of land-derived organic matter (through estuary) is more significant in the study area than the autochthonously derived organic matter. This is inferred from its distribution pattern characterised by depletion of organic matter in the offshore directions, more specifically away from Cochin inlet. Further, enrichment of organic matter around the estuarine mouth can also result from the deposition of adsorbed organic matter in the suspended particles transported through the estuary by flocculation as it encounters the higher salinity sea water.

Qasim (1977) gave a detailed account of primary productivity along western continental margin of India based on an average annual picture of column productivity. The region off the southwest coast of India (from Calicut to southern tip of India) is identified as a region of high productivity (0.75 to 1.00 $gC/m^2/day$). This is mainly attributed to the well established upwelling phenomena during the southwest monsoon season along this coast. Compared with the world average of organic matter of continental shelf sediments (0.5 %,

given by Emery, 1960), the study area recorded still higher average values (3.73 %) which attests both rich contribution from land and high productivity of shelf waters.

Sympathetic relation of organic matter with clay and silt indicates its size-dependant scavenging. It has been experimentally demonstrated that various clay minerals adsorb a substantial amount of dissolved organic matter formed from the decomposition of phytoplankton (Muller and Suess, 1979). Apart from this, co-sedimentation of organic matter with fine particles due to the similarity in settling velocity is one of the major causes of sympathetic relation of organic matter content to percentage of fine particles. Increase in organic carbon with decrease in grain size is also attributed to the increase in surface area of fine particles (Suess and Muller, 1980).

4.4.2 Geochemistry of major elements

Major elemental chemistry of bulk sediments depends on the detrital and non-detrital factors of the sediment composition. Hirst (1962) pointed out that, for the most part, the major and minor elements are located within the lattices of detrital minerals. The range of chemical composition are influenced by different proportions of major minerals in the sediments, such as, quartz, feldspar, montmorillonite, kaolinite and illite and in those of the minor amounts of heavy minerals. Exceptions are found for some of the elements which are abundant in the non-detrital phases.

The concentration of a given element in a sediment is governed by its concentration in, and the relative proportions of, the various components of detrital, authigenic and biogenous origin. Many elements show tendencies to

be partitioned between two or more mineral components in the sediments and the distribution of an element can not be described in terms of mineralogy alone. There is also a very important elemental partitioning effect brought about by a textural control on the mineralogy of sediments. This factor is of critical importance for nearshore sediments in view of their extreme textural variability (Calvert, 1976). Further, the 'law of grain-size control' on the geochemical variation of sediments is found to be an important factor (Zhao Yiang *et al.*, 1981).

SiO_2 and Al_2O_3: Detrital quartz, alumino-silicates and siliceous skeletons invariably contains SiO_2. Table 4.6 gives a good correlation between textural grades and SiO_2. A high positive correlation with sand and negative loadings with silt and clay are very striking. This is significant in the light of the distribution of Al_2O_3 in the sediments. In marine sediments, Al_2O_3, which is derived principally from the alumino-silicate minerals, is detrital in origin, though some of them could also be derived from authigenic processes (Cronan, 1980). Unlike SiO_2, Al_2O_3 shows (Table 4.6) an antipathetic relation with sand and positive values of correlation with silt and clay. Relative behaviour of the elements in terms of their oxide ratios often reveal significant differences between sediments containing various proportions of sedimentary components. Heath and Dymond (1977) suggested Al for normalization of other elements associated in the sediments, because, Al is usually assigned to the clay hydrolysate fraction. SiO_2/Al_2O_3 ratio ranges from 1.35 to 49.24 with an average value of 3.80 (Table 4.7). The ratio shows a gradual decrease from the sand-rich samples (SiO_2/Al_2O_3 = 49.24 containing 93.83 % sand) to clay-rich sediments (SiO_2/Al_2O_3 = 1.35 with sand content of 1.48 %). This indicates a larger proportion of free quartz in the coarser fractions. Especially, the sand-rich zone in the southwestern part of the study area yields a very high

value of SiO_2/Al_2O_3 indicating insignificant contribution of feldspar and a near total presence of detrital quartz. Clay-rich portions are nearly devoid of or are with subtle presence of quartz. This is in consistency with the petrographic identification.

Fe_2O_3: It probably represents the metalliferous fraction of the sediments. Iron is predominantly present in the clay mineral lattices, iron bearing heavy minerals and also in adsorbed state on the surfaces of other minerals. Iron oxide is transported in the form of ferric oxide hydrosol stabilised by organic colloids. It is generally found that, percentage of iron is comparatively higher in marine sediments. Castano and Garrels (1950) pointed out the flocculation of iron increases with increasing salinity of water. Even though, correlation of Fe_2O_3 with size grades is similar to that of Al_2O_3 (Table 4.6), the negative and positive loadings are much higher than that of Al_2O_3 . This reflects a near total physical partitioning of iron oxide phase with finer sediments. Fe_2O_3/Al_2O_3 ratio ranges from 0.36 to 0.79 with an average value of 0.63. In majority of clay-rich samples, the exceedence of the ratio (> 0.52) suggest that, iron is not only held in structural positions within the alumino-silicates, but also present in authigenic minerals (Calvert, 1976). Petrographic identification has confirmed presence of micro-crystalline framboidal concretions of pyrite within the microfossil cavities. Nominal increase in the Fe_2O_3/Al_2O_3 ratio in the sand rich zone is in consonance with the observed amount of Fe-bearing heavy minerals such as ilmenite (identified as opaques).

CaO: Chemical analysis is performed on bulk sediment samples without removing the shell debris. So the CaO content in the sediments becomes imminent to be a function of both non-carbonate CaO held in alumino-silicates and CaO concentration of carbonate shells. Central part of the study area

(Fig. 4.3d) registers a maximum concentration of CaO (up to 11.48 %) which coincides with the zone of high shell debris consisting mostly of molluscan shells. Lack of a persistent textural control over the concentration of CaO is indicated by a low level of positive values with silt and clay and negative value with sand (Table 4.6). CaO/Al_2O_3 ratio shows a wide variation from 0.06 to 1.14 with an average value of 0.39. Irrespective of the textural patterns, the central portion is characterised by a high ratio. This can be attributed to the 'excess CaO' in the shell components. The low value of CaO/Al_2O_3 of clay-rich sediments in the northern part can be assigned to the effect of excessive input of the estuarine sediments through the Cochin inlet, wherein turbulence caused by the tidal flows, hamper the growth of molluscs. Consistency of the ratio in the sand-rich sediments imply non-carbonate CaO held in the lattices of alumino-silicate minerals.

MgO: Concentration of magnesium in marine environment could be by fixation in clay minerals due to rich concentration of Mg^{++} ions in the overlying water column, especially in montmorillonites. High MgO content can also signify the presence of high magnesium calcite or dolomite in shell debris. Good correlation is established between MgO and size (Table 4.6). Sand yields a negative value whereas, silt and clay show a positive affinity. MgO/Al_2O_3 ratio shows an average value of 0.31. Sand-rich sediments register very small ratio (0.10). The ratio increases with increase in absolute concentration of CaO content (up to 0.87) in the sediment. The increase is suggestive of an excess amount of Mg incorporated into the shell materials as high Mg-calcite (supported by X-ray diffraction studies). In the central part, carbonate rich sediments signifies a higher CaO/MgO ratio. In the case of clay-rich sediments with low carbonate content, CaO/MgO ratio is much smaller. The positive correlation of MgO over silt and clay could be due to the fixation of

Mg in clay minerals. Preferential fixation of Mg for Ca and K by cation exchange in clay minerals was also pointed by Weaver (1967).

Na_2O and K_2O: These alkali elements are present in clay minerals, feldspar and also in some authigenic minerals. In clay fractions, sodium and potassium are tied-up in clay minerals either by adsorption or by cation exchange. The general pattern of distribution of Na_2O tallies with that of K_2O (Fig. 4.3f&g). Na_2O and K_2O show negative loading with sand and positive loading with silt and clay (Table 4.6). However, the value of correlation between K_2O and clay fraction ($r = 0.474$) is not as significant as Na_2O ($r = 0.607$). The low concentration of Na_2O in the sand-rich samples denotes meager amount of feldspars in the sand fraction. Enrichment of Na_2O over K_2O is an indication to the clay mineralogical assemblage as the sediments are abundant in montmorillonite and poor in illite. Na_2O/Al_2O_3 and K_2O/Al_2O_3 ratios keep fluctuating from sample to sample and their average values are 0.23 and 0.07 respectively (Table 4.7). The ratios are very low in sand-rich samples (as low as 0.07 for Na_2O/Al_2O_3 and 0.04 for K_2O/Al_2O_3). This confirms the contention that the sand-rich sediments are poor in feldspar content. Clay-rich sediments yield higher ratios (as high as 0.68 for Na_2O/Al_2O_3 and 0.23 for K_2O/Al_2O_3) marking the abundance of clay minerals. Relative abundance of K_2O and Na_2O from their ratio values (Table 4.7) indicate a near constant value around the average (0.32), with a little variation from 0.25 to 0.55. Though there is no significant difference in the ratio among sand dominant versus clay dominant samples, the spatial variation shows a depletion of the ratio around the Cochin inlet. This could be either due to the absence of authigenic K-bearing minerals (such as glauconite) in this turbulent zone or due to the preferential adsorption of Na^+ from sea water at the estuarine/sea water interface with a loss of exchangeable Ca^{++} leading to relative enrichment

of Na_2O in the sediments. Away from this zone, the ratio improves, but again shows a reduction in the sand-rich southwestern portion. This could be due to the abundance of sodic feldspar over the potash feldspar, though the total feldspar content in sands are in traces.

P_2O_5: Considerable work has been done on the phosphorus distribution of nearshore sediments of Calicut by Seshappa (1953) and Seshappa and Jayaraman (1956). Murty *et al.* (1968) carried out studies on phosphate distribution for the continental margin between Alleppey and Bombay and Rao *et al.* (1987) further extended the investigation up to Indus Canyon in the north.

Distribution of phosphorus in the unconsolidated marine sediments are related to (i) the phosphorus content in the minerals, (ii) concentration and state of dispersion of Mn and Fe compounds in the sediment surface, (iii) distribution of biogenous matter and (iv) chemical precipitation/replacement of existing solid phases. The concentration pattern of P_2O_5 ranges between 0.02 to 0.55 %, which is in agreement with the values reported by Rao *et al.* (1987). As evidenced from the low value of correlation coefficients with size fractions (Table 4.6), the pattern of distribution does not reflect specific adherence to any of the textural grades, though clay fraction exhibits a slight positive loading of 0.272. The lower P_2O_5/Al_2O_3 ratio (average 0.013) could imply the low content of P_2O_5 in the terrigenous fraction of the innershelf sediments. Presence of P_2O_5 in subtle amount around the Cochin inlet is an additional clue to this inference. Sand-rich zones as well as carbonate-rich portions exhibits sub-minimum concentration of P_2O_5. Petrographic identification did not confirm the presence of apatite in sand fraction. Average values of P_2O_5 are higher in the clay-rich sediments. This is found to be in general

agreement with the observation of Rao *et al.* (1987) who noticed that between Mangalore and Cochin, phosphorus has significant loadings on fine-grained alumino-silicates. This sympathetic behaviour obviously indicate the presence of phosphate in fine-grained sediments as ferri-phosphate, adsorbed phosphate and phosphate associated with organic matter. High productivity of this part of the innershelf favours P_2O_5 enrichment in the finer fractions. Apart from this, availability of inorganic phosphate in the shelf waters (of the order of 0.4 to 3.0 μMdm^{-3} reported by Reddy and Sankaranarayanan, 1968) can also result in the precipitation or replacement of existing solid phases of phosphates.

TiO_2: In crustal rocks, Ti exists in insoluble heavy minerals such as ilmenite, rutile, anatase and sphene (Goldschmidt, 1954). Disaggregation during weathering and subsequent transport by river water leads to hydrodynamic sorting of crustal matter. Higher the energy of the suspended load, larger will be the fraction of Ti-bearing minerals compared to Al-rich clay minerals. So the absolute and relative enrichment of TiO_2 is an indication to the terrigenous input as well as the hydrodynamics of sedimentation. The negative values of correlation coefficient between TiO_2 and sand percentage and positive values with silt and clay percentages denote an interesting aspect of physical fractionation of TiO_2 (Table 4.6). Silt shows a better positive affinity and this can be attributed to the selective partitioning of TiO_2 into the silt fraction that are abundant in Ti-bearing heavy minerals. A similar fractionation for TiO_2 was reported from Barent Sea sediments (Calvert, 1976). It is found that 99 % of the TiO_2 fixation is lattice-held and hence this is one element which can be taken as an attribute of terrestrial input. The low energy conditions of the innershelf could be one reason for the low concentration of TiO_2 in the finer fractions as the minerals containing the

TABLE 4.7

Range and average of major element ratio

	Minimum	Maximum	Average
SiO2/Al2O3	1.35	49.24	3.80
Fe2O3/Al2O3	0.36	0.79	0.63
CaO/Al2O3	0.06	1.14	0.39
MgO/Al2O3	0.04	0.87	0.31
Na2O/Al2O3	0.07	0.68	0.23
K2O/Al2O3	0.04	0.23	0.07
K2O/Na2O	0.25	0.55	0.32
TiO2/Al2O3	0.04	0.37	0.06
P2O5/Al2O3	0.005	0.04	0.013

TABLE 4.8

Matrix of correlation coefficient of major elements

	SiO2	Al2O3	Fe2O3	CaO	MgO	Na2O	K2O	P2O5	TiO2
SiO2	1.000								
Al2O3	-.896	1.000							
Fe2O3	-.938	.896	1.000						
CaO	-.358	.062	.202	1.000					
MgO	-.731	.580	.663	.433	1.000				
Na2O	-.875	.798	.792	.327	.666	1.000			
K2O	-.735	.694	.679	.292	.473	.839	1.000		
P2O5	-.259	.227	.311	.095	.311	.046	-.033	1.000	
TiO2	-.377	.496	.337	-.049	.132	.368	.296	-.230	1.000

Significant level of r values: >0.22 (0.1 level), >0.26 (0.05 level)
>0.34 (0.01 levle), >0.42 (0.001 level)

element are denser. Another reason could be the dilution factor of Ti-bearing minerals in the innershelf sand fraction, effected by the concentration and deposition of heavy mineral sands on the beaches along this coast owing to selective panning process and transport by incident waves and currents.

TiO_2/Al_2O_3 ratio shows considerable variation from 0.04 to 0.37 with an average value of 0.06. The ratio not only gives the relative enrichment, but also can be used to estimate the energy of a depositional environment (Bhatt, 1974; Schmitz, 1987). Absolute distribution of TiO_2 values show an enrichment near the Cochin inlet (Fig. 4.3i). Despite the negative correlation of TiO_2 with sand fraction, TiO_2/Al_2O_3 ratio gives an higher value for the sand-rich sediments. This could be mainly due to the low percentage of Al_2O_3 in the sand-rich sediments rather than due to the concentration of TiO_2. However, petrographic identification of heavy sand fraction confirmed the presence of Ti-bearing minerals like, ilmenite (which forms most part of the opaques) and rutile, though present in smaller proportions. Barring this sand pocket, the clay-rich zone in general depicts a distinct pattern of TiO_2/Al_2O_3 ratio which decreases with increasing distance from the Cochin inlet.

Inter-element correlation of major elements: Inter-element correlation coefficients are given in Table 4.8. The mode and nature of elemental incorporation in the sediments are discussed above. This section intends to derive the pattern of elemental associations and their significance in the light of overall textural and mineralogical composition of the sediments. Many of the elements yield highly significant values of negative and positive correlations. SiO_2 invariably gives negative loadings on all other major elements. Though many of the values are significant, Al_2O_3, Fe_2O_3, MgO, Na_2O and K_2O exhibit very high level of negative correlation with SiO_2 ($r > 0.7$).

This distinct relationship is shown in Fig. 4.6. The plot of SiO_2 versus MgO, Na_2O and K_2O displays considerable scattering from the linear best-fit line. This deviation in the pattern from that of SiO_2 versus Al_2O_3 and Fe_2O_3 is a reflection of their relation with textural grades as well. Sand-rich samples which are abundant in quartz are poor in alumino-silicates. The uniform increase of Al_2O_3 and Fe_2O_3 with decrease in silica, is a manifestation of decreasing size. But the relation of SiO_2 with MgO, Na_2O and K_2O is not so consistent, which is due to the inhomogeneous distribution of these elements in sediment components. Depending on the distribution pattern of the differing proportions of clay minerals (mainly montmorillonite, kaolinite and illite), Na_2O and K_2O register relative variation in enrichment. This is found to be true in the case of samples containing moderate amount of Na_2O and K_2O, as they show inconsistent relation as evident from the plot Na_2O versus K_2O (Fig. 4.6). Contrary to river clays, half of the exchange sites of clays in sea water are occupied by Na contributing to the relative enrichment of Na_2O (Sayles and Mangelsdorf, 1977). Na_2O/K_2O proportion can also be controlled by selective adsorption of Na for K from the sea water (Weaver, 1967).

In the case of MgO, the 'deviation factor' can be discerned based on its positive affinity with CaO, though the plot of CaO versus MgO illustrates large scale spread of sample points (Fig. 4.6). The scattering is due to the compositional differences of shells and mineral fractions in accommodating CaO and MgO in them. The positive affinity of MgO and CaO with Na_2O and K_2O can be attributed to their association with alumino-silicates. P_2O_5 does not yield significant correlation with other elements, though Fe_2O_3, MgO and Al_2O_3 record a low level of similarity with it. This is supported by the slight positive loading of phosphate with clay fraction.

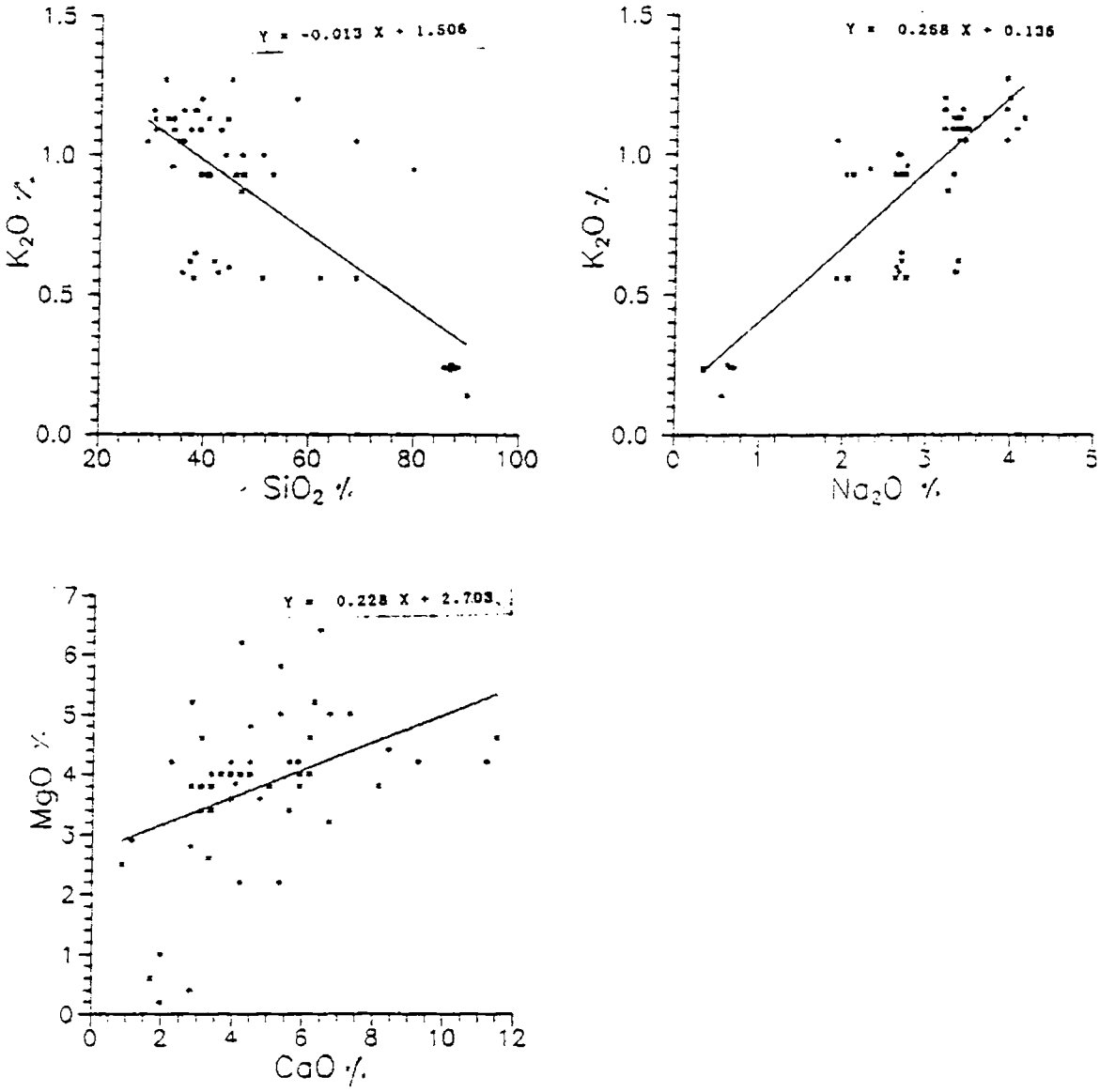

Fig. 4.6 Inter-relationship between various major elements

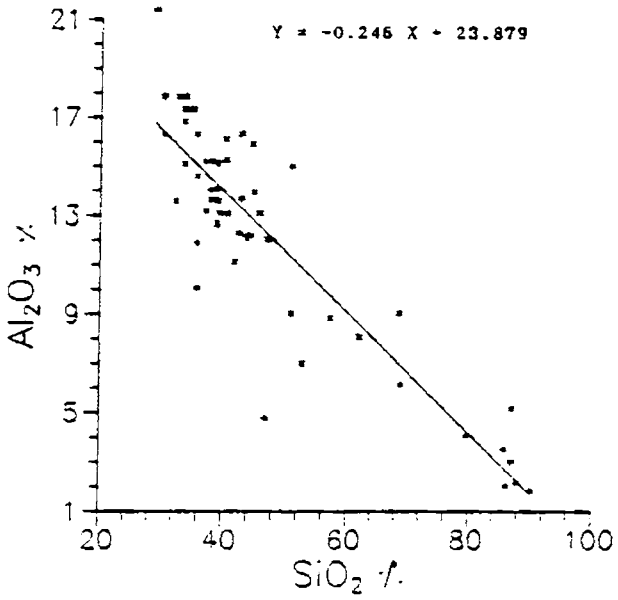
Y = -0.246 X + 23.879
Al_2O_3 %
SiO_2 %
21
17
13
9
5
1
20
40
60
80
100

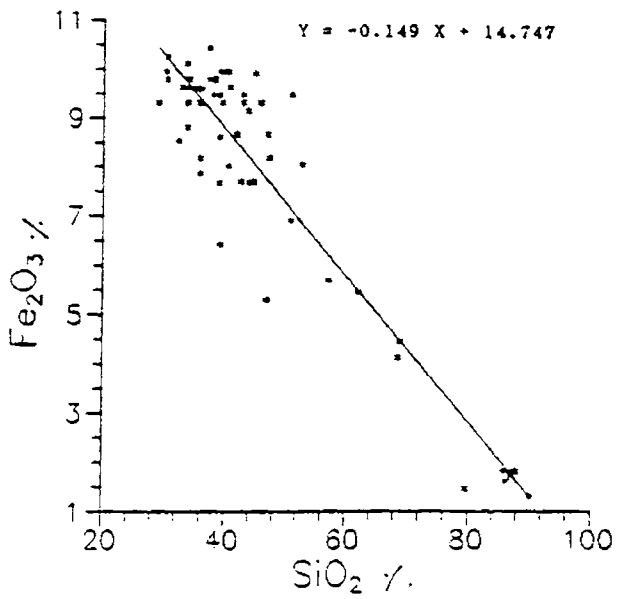
Y = -0.149 X + 14.747
Fe_2O_3 %
SiO_2 %
11
9
7
5
3
1
20
40
60
80
100

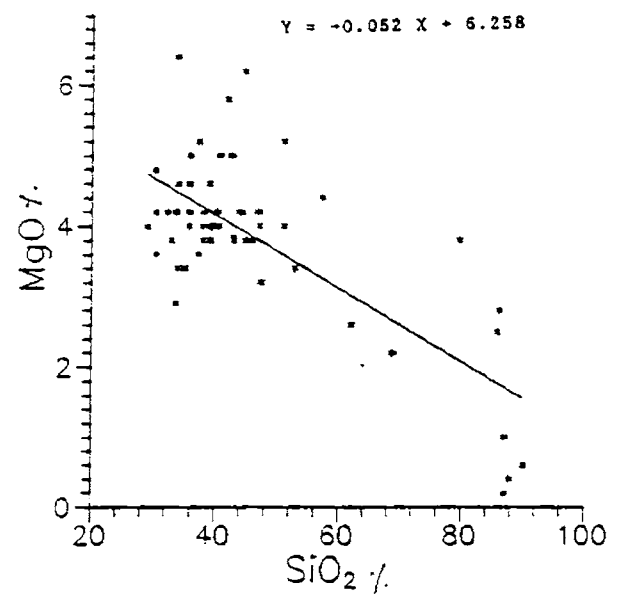
Y = -0.052 X + 6.258
MgO %
SiO_2 %
6
4
2
0
20
40
60
80
100

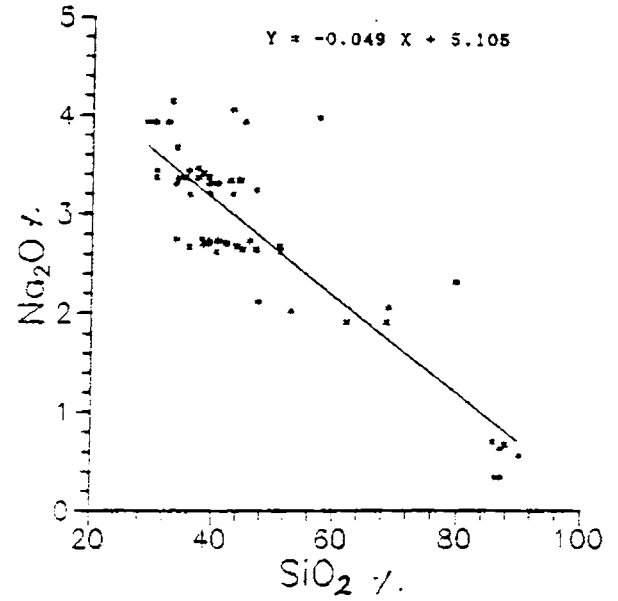
Y = -0.049 X + 5.105
Na_2O %
SiO_2 %
5
4
3
2
1
0
20
40
60
80
100

Fig. 4.6 Contd...

Sympathetic relation between TiO_2 versus Al_2O_3, Na_2O, Fe_2O_3 and K_2O enumerate the absolute 'lattice-held' nature of TiO_2 in association with these elements. Low energy regime of the innershelf is evident from the physical partitioning of TiO_2 in the finer fractions. It is presumed that, except for Fe_2O_3 to a lesser extent, TiO_2 owes its covariance with other elements not for their partitioning in sand fractions but only to the coexistence of them in the minerals present in fine particles.

Cluster analysis: Inter-elemental groupings of major elements are depicted in the dendrogram (Fig. 4.7). Organic matter is also included in the cluster analysis to enumerate its association with major elements. Except for SiO_2, that forms a lone element group, all other elements are closely inter-related. It is slightly a complex picture, with each element related to the other, thereby forming the combined correlation axis longer and longer (indicating decreasing similarities) making it difficult to classify them into distinct groups. However, with an overview of the above discussions, it is possible to consider a comprehensive pattern of clustering of one major group containing Fe_2O_3, Al_2O_3, Na_2O, K_2O and MgO. This is controlled by the alumino-silicate (clay mineral) factor in the fine grained sediments. SiO_2 which forms an independent group obviously represents partitioning specifically with quartz in the sand fraction of the sediments. Though not so significant, CaO and MgO also form a group (part of MgO goes with the other group described above) which is influenced by both alumino-silicate factor and the shell content of the sediments. The elements P_2O_5 and TiO_2 form different entities controlled by a combination of factors such as spatial control of texture and their coexistence in the mineral associations. For P_2O_5, precipitation/ adsorption on to clay particles as ferri-phosphate is presumed to be the chief

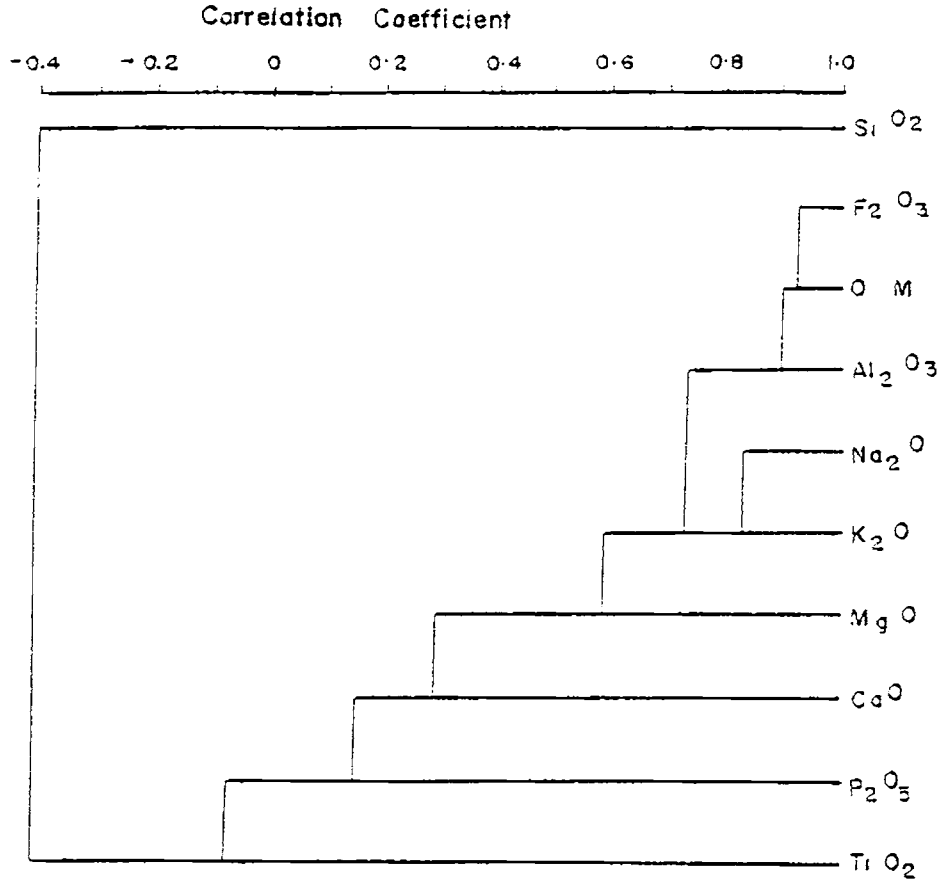

Fig. 4.7 Dendrogram of major elements

controlling factor. The presence of Ti-bearing ilmenite and rutile admixtured in the fine grained sediments are found responsible for TiO_2 variation.

4.4.3 Geochemistry of minor and trace elements

Trace metal concentrations of the sediments are potentially good indicators of the state of an environment (Forstner and Wittmann, 1983). Geochemistry of the distribution of trace elements in marine sediments were concerned chiefly with establishing the overall distribution of the elements (Landergen, 1964). However, recently, attention has been directed towards identifying phases of trace element distribution among the various components of marine sediments (Chester, 1990). Generally, the amount of trace elements in modern sediments are controlled by the elemental solubility in the waters, feeding capacity of the drainage basin and by the prevailing environmental conditions. Trace elements in marine sediments are associated with clay minerals which are formed during weathering, residual minerals resistant to weathering, biogenetic constituents and minerals formed after sedimentation (Koczy, 1951). Authigenic materials which are produced in the marine environment include, hydrogenous, biogenous and adsorbed components. Hence, the partitioning of trace elements in the sediments is a function of relative enrichment of the different components. Classification of such components and elemental associations are essential for a better understanding of the processes of incorporation of these elements, thereby to assess the quality of the environment.

Reasons for the variability of minor and trace elements: Reasonable interpretation of the variability factor of minor and trace elements is possible with

information on the inter-relation of elements and texture, elemental ratios, data on physical and chemical partition.

Textural dependance of elements: Though a major part of the elements come from terrestrial origin, considerable amount of these elements are incorporated into the system by adsorption, and other process such as, sulphide precipitation and organic reactions in the nearshore sediments (Krauskopf, 1956). Total concentration and reactivity of metals in the sediments is a function of organic matter, mineralogy and textural-related qualities of the sediments (Willey and Fitzgerald, 1980). The importance of texture on the authigenic precipitation of elements has been well understood (Rea and Pigula, 1977). This together with size segregation of different minerals during transport and deposition induce a control of texture on the geochemical partitioning. Larger surface area of fine particles facilitates precipitation of metals on to it.

Table 4.9 gives the correlation coefficients of minor and trace elements versus sand, silt and clay fractions. Mn, Cu, Cr, Ni, Rb and Li display similarity in correlation with granulometric components. These elements yield negative loadings on sand and positive values with silt and clays. Co shows covariance with silt fraction ($r = 0.274$). In accordance with this finding Cosma *et al.* (1979) earlier reported that a direct proportionality exists between Cr, Cu, Ni and Mn and the finer fraction.

It has been discussed in the preceding section that many of the major elements and especially the organic matter show very significant level of positive correlation with silt and clay. But with sand they show very strong antipathetic relation. Apart from a surface-area related enrichment of the

TABLE 4.9

Correlation coefficient of minor & trace elements Vs size

	Sand	Silt	Clay
Mn	-.719	.721	.563
Cu	-.742	.640	.668
Co	-.430	.503	.274
Cr	-.724	.458	.794
Ni	-.814	.684	.750
Cd	-.026	.121	-.061
Pb	-.381	.280	.384
Zn	-.670	.545	.633
Ba	.279	-.192	-.293
Sr	-.405	.462	.269
Rb	-.699	.606	.628
Be	-.473	.536	.321
Li	-.883	.697	.852
Mo	.063	.143	-.020
V	-.181	.169	.152

Significant level of r values:

>0.22 (0.1 level), >0.26 (0.05 level)
>0.34 (0.01 levle), >0.42 (0.001 level)

metals, cation exchange capacity (CEC) of sediments and affinity of metal ions for different types of clay surfaces also contribute to the metal-fine fraction proportionality of sediments. Hunt (1981) established that, CEC of sediments improve considerably with increasing organic content and fining size. Association of trace-metals with organic carbon and the correlation of organic carbon with grain size distribution are often make it unclear whether metal distributions results from the influence of grain size or organic matter content. But, Sholkovin (1976) found significant metal association with organic matter. Further, Hunt (1981) pointed out that, in coastal sediments, correlations between metal concentrations, CEC and organic matter could imply that, trace element distributions are dictated by organic carbon, possibly through exchange reactions.

Ability of clays to adsorb or release heavy metal ions have been a subject of intense research (Farrah *et al.* 1980). Electrostatic attraction between negative sites on the clays and the metal ions is certainly a major component of sorption process. The affinity of a cation for a clay surface is a function of so many variables (Eh, pH, nature of sites available, steric effects attributable to structure, nature of counter ions, etc.). Depending on these parameters, the CEC values of metal ion bonding vary with the type of clay. In general, for a set condition, Farrah *et al.* (1980) found that the affinity sequence of clay types is in the order of montmorillonite > illite > kaolinite. At the same time, affinity sequence of different metals were found to vary with clay type. Increase in pH values increases the sorption of metals (World and Pickering, 1981). So in marine environment sorption of metal ions by clay minerals assumes a significant importance.

The different process of incorporation of textural-related metals are described above and the section on the sequential extraction results may throw more light on partition pattern of metals among size fractions.

Metal concentrations and ratios: Absolute concentration of metals are described in the result section and inferences on their variability are drawn here. To facilitate interpretation, the metal ratios are used, which represents the relative behaviour of elements and serve as a basis for comparison to determine the homogeneity and metal association. This has advantages when the comparison of absolute concentrations do not give any meaningful inferences. Elemental or oxide ratios often reveal real differences between sediments having different proportions of sedimentary components (Bischoff *et al.*, 1979). Normalisation of elements with Al_2O_3 is usually assigned to clay-hydrolysate fraction (Landergen, 1964 and Heath and Dymond, 1977). Krishnaswamy (1976), suggested a normalisation procedure with Mn to discern the metal relations with hydrogenous fraction. Selected elemental ratios are given in Table 4.10. Mn/Al_2O_3 ratio shows that it ranges from 5.66 to 21.95 with an average value of 14.35. It does not suggest spatial and textural differentiation except a few deviations without much significance. But the affinity of Mn to fine fractions and its spatial concentration around Cochin inlet and certain other nearshore portions are important indications to its speciation. Mn is transported from the continents in a particulate form both in association with weathered minerals (e.g. the clay minerals, feldspars etc.) and as discrete particles of hydrous manganese oxides. Removal of hydrous manganese or ferro-manganese oxide from solution and their precipitation was discussed by Turekian (1977). Concentration of Mn (average 177.11 ppm) in this study is very much less than the average for nearshore mud (Table 4.11,

TABLE 4.10

Range and average of minor and trace element ratio (*)

	Minimum	Maximum	Average
Mn/Al2O3	5.66	21.95	14.35
Cu/Mn	-	0.48	0.24
Co/Mn	0.15	1.62	0.36
Ni/Mn	0.28	6.17	0.83
Pb/Mn	0.01	0.53	0.28
Zn/Mn	0.21	1.22	0.40
Ba/Al2O3	-	85.60	40.28
Sr/CaO	25.51	621.43	56.43
Be/Al2O3	-	0.48	0.24
Mo/Mn	-	0.11	

(*) calculated based on percentages of oxides and ppm values of elements.

850 ppm). But the Mn values are well within the values reported by Murty et al. (1973) for Cochin and Ambalapuzha shelf sediments (100 - 360 ppm). Depleted concentration of Mn can be chiefly attributed to the source rock and their corresponding differences in the mineralogical concentration. Average values for Vembanad lake (469.80 ppm) reported by Mallik and Suchindan (1984) is higher, and the low value in innershelf is mainly attributed to the dilution factor of Mn-poor sand-rich zone in the southwest part, which are included in the averaging procedure. Geochemistry of Mn in sediment is very important as the sorption process of many other mono- and divalent cations are controlled by manganese oxide phases.

Cu/Mn ratio which ranges up to 0.48 with an average of 0.14 does not reflect any significant pattern, though Cu is also a fine-grained bound element. The ratio also depicts Cu affinity with organic matter. Stumm and Brauner (1975) have shown that copper exists in natural water as various organic complexes. Observations of Plavsic *et al.* (1980) attribute a strong bonding of copper on different hydroxide surfaces and the removal of Cu from sea water is facilitated by the adsorption of labile ionic Cu-complex on to solid particles. Numerous studies have indicated copper-organic complexes and the related adsorption- desorption behaviour (Davis and Leckie, 1978; and Mills and Quinn, 1981). Affinity sequence of clay minerals shows a higher capacity to adsorb Cu by kaolinite followed by montmorillonite and illite. However, in the innershelf, the clay minerals play a dominant factor in deciding the distribution of Cu. Cu concentration in the innershelf sediments is much lower (0 - 43 ppm) than the nearshore mud average (Table 4.11). The Cu values reported by Rao *et al.* (1974) is on the higher side with respect to the Cochin shelf sediment values, but the values reported for the Ambalapuzha

TABLE 4.11

Elemental composition of marine sediments and some continental materials (ppm) :

Element	Continental crust (a)	Continental soil (a)	River particulate matter(a)	Nearshore mud (b)	(c)	Deep-sea clay (a)
Mn	720	1000	1050	850	850	6000
Cu	32	30	100	56	48	200
Co	13	8	20	13	13	55
Cr	71	70	100	60	100	100
Ni	49	50	90	35	55	200
Cd	0.2	0.35	1	--	--	0.23
Pb	16	35	100	22	20	200
Zn	127	90	250	92	95	120
Ba	445	500	600	--	--	1500
Sr	278	250	150	160	--	250
Rb	112	150	100	---	--	110
Li	42	25	25	79	--	45
Mo	1.7	1.2	3	1	--	8
V	97	90	170	145	130	150

a - From Martin & Whitfield (1983)
b - From Wedepohl (1960)
c - From Chester & Aston(1976)

shelf sediments are comparable if the dilution factor caused due to the sand-rich zone in the innershelf sediments are considered.

Co/Mn ratio ranges from 0.15 to 1.62 with an average of 0.36 (Table 4.10) which indicates enrichment of Co than Cu in the sediments. Unlike Cu and Mn, size dependence of Co is very insignificant, though silt fraction yields a significant positive affinity. This is evident from an increase in the Co/Mn ratio in the silt-rich sediments. Relationship of Co with organic matter is also incoherent and is indicative of a difference in partition pattern from that of Mn and Cu. Low level positive correlation with clay fraction could be the result of insignificant contribution of Co into the clay hydrolysate by precipitation. The semblance of Co with silt fraction indicates the availability of Co in the fine-sized heavy fraction containing garnet, hornblende and biotite (Carr and Turekian, 1961). Compared to the average value of Co (13 ppm) reported for the nearshore mud (Table 4.11), enrichment of Co in the innershelf sediments could be a function of source rock, though, the values of the present investigation is slightly more than that of Murty *et al.* (1973) for Cochin shelf (9 - 59 ppm) and Ambalapuzha (8 - 64 ppm).

Concentration of Cr varies widely in the sediments and also indicates a strong sympathetic relation with the fine fraction. Significant covariation of Cr is found with organic matter. Because Cr^{3+} closely resembles Al^{3+} and Fe^{3+} in its chemical properties and ionic size, Cr behaves similarly to these ions (Al and Fe) during weathering processes and are finally concentrated in clays. The enrichment of Cr around the Cochin inlet may be due to the increased sorption of Cr in enhanced pH condition at the estuarine/seawater interface. Cr composition in crust and nearshore mud are 71 and 100 ppm

respectively (Table 4.11) and are comparable with the data obtained from the present investigation.

Ni shows a strong antipathetic relation with sand and positive affinity with silt and clay. High enrichment of Ni is noticed in the present study (average 146.57 ppm). The southern portion of the Cochin inlet shows high values of Ni, indicating an interface deposition from mixing zone. Nickel is easily mobilized during weathering. It is co-precipitated with iron and manganese oxides. Pyroxenes, garnet, hornblende and biotite contains Ni. Potter *et al.* (1963) have shown that marine sediments contain more Ni than fresh water sediments. Ni/Mn illustrates wide variation from 0.28 to 6.17 indicating dissimilarity in the metal association spatially. Ni represents a stronger association with clay than Mn. Perhac (1972) data on partitioning of trace elements in the size fraction of suspensates gives five fold enrichment for Ni in < 0.15 µ fractions compared to > 0.15 µ fractions. Considerable enhancement of Ni in clay could be due to sorption of Ni that are transported from fresh water to saline water. Metals like Ni and V are enriched in crude oils due to their complexation by porphyrins (Hunt, 1979). Transferring of oil from large containers to small ones create oil slicks in the adjacent offshore portions off Cochin, which may facilitate such a porphyrin-complexation with Ni and probably the Ni enrichment in this part. Amount of Ni in the innershelf sediment is three-fold enhanced, than the crustal abundance and in the nearshore mud (Table 4.11). This does not rule out minor local pollution effects, especially around the Cochin mouth.

Cd has long been recognised as a serious environmental contaminant (Forstner and Wittmann, 1983). During weathering, Cd goes into solution containing sulphates and chlorides. As evidenced from correlation coefficients

(Table 4.9), Cd is fairly evenly distributed in the innershelf sediments (average 27.36 ppm) in all the size fractions. Unlike Cu, Cd generally reacts slowly with organics. This is evident from its low level of correlation with organic matter. Distribution pattern of Cd does not show an enrichment pattern in the immediate vicinity of Cochin channel. Danielson (1980) has indicated that a significant portion of Cd is in association with the soft parts of organisms. Earlier, Eaton (1976) reported that samples having low carbonates contain lowest percentage of Cd and also opined that a significant portion of Cd was tightly bound in clays. So the sum total of Cd distribution is a function of riverine input, biological activity and also from anthropogenic input. Ouseph (1987) has reported Cd contribution from effluent discharge of industries along this part. Further, enrichment of Cd in municipal waste water has been reported by Helz (1976).

Pb derived from the weathering of magmatic and metamorphic rocks is expected to be mainly accumulated in detrital sediments in potassium bearing minerals (mica and feldspars). Some amount of Pb can also be transported into the environment as adsorbed on clays, ferric oxides etc. Pb concentration in the innershelf is very significant (average 50.29 ppm) in the light of its low level of correlation with size fractions (Table 4.9). Pb/Mn ratio, which shows wide variation yields higher ratios with sandy samples, indicating the association of Pb in the potassium-rich mineral fractions such as feldspars and micas. Pb primarily occurs in the structure of potassium feldspars and micas of magmatic and metamorphic origin. From the weathering process, some mobilised Pb is adsorbed on clay minerals like kaolinite. This is evident from the slight positive loading of Pb on clay fraction. Chester and Hughes (1969) confirmed that the hydrogenous fraction of Pb can be incorporated by adsorption reactions and also by other processes such as

sulphide precipitation and organic reactions. Framboidal pyrites identified in the sediments suggests partly anoxic nature of the innershelf sediments.

Zn shows its tendency to be predominantly incorporated in certain structural positions of silicates and oxides. Oxide minerals such as spinel, and silicate minerals such as garnet, staurolite, pyroxenes, amphiboles and micas contain considerable amount of Zn. Concentration of Zn in the innershelf sediments is 79.69 ppm (average). Size partitioning is significant with strong antipathetic relation with sand and sympathetic variation with silt and clay fractions. Zn, which occurs primarily in the structures of silicates and oxides, goes into solution during chemical weathering. Subsequently, Zn get concentrated in the fine-grained phases of the sediments during the course of transport by adsorption in clay minerals, iron oxides and organic substances. Hydroxide precipitates of Zn in clay system and its adsorption by montmorillonite suspensions in seawater are the other possible mechanisms of Zn concentration in marine sediments (Chester, 1990). Incorporation of Zn is expected to occur with colloidal iron oxide and iron oxide coatings on other minerals. Affinity of Zn for organic matter is evident from the correlation coefficient.

Ba is generally distributed in mineral structures of feldspars, micas, apatite, calcite etc. Ba with wide compositional variation (0 - 1052 ppm) does not yield any significant correlation with the textural grades (Table 4.9). Nevertheless, slight positive correlation with clay fraction rules out a preferential enrichment of Ba in clays, which is contrary to the reports of Ba adsorption by clays, hydroxides and organic matter. Metal association discerned from the Ba/Al_2O_3 ratio, depicts enrichment of Ba in sand-rich sediments. CaO is also unrelated to Ba, which is an obvious indication of its

non-biogenous association. Again, these observations are contrary to that of Arrhenius (1966) and Turekian (1968). The reasons for this discrepancy is explained in the partition geochemistry section. But, it is possible that Ba is dominantly controlled by feldspars and micas in the sediments with a decreasing proportion from coarse to fine sediments.

In the Earth's crust, bulk of Sr occurs as trace elements in rock-forming and accessory minerals. Distribution of Sr in minerals is controlled by its diodochy with calcium and potassium. Sr concentration in the innershelf sediments shows high variability with an average of 272.57 ppm. Correlation coefficients with size fractions exhibit a negative correlation with sand and positive loadings on silt and clays, though 'r' value on clay is not so significant (0.269). Sr/CaO ratio also registers a large variance with average value of 56.43. Depletion in the absolute value of Sr in sand-rich sediments is supplemented by Sr/CaO ratio which documents very low values indicating the poor availability of Sr in the sand fractions. Whereas, CaO rich (shell abundant) sediments are fairly high in Sr/CaO ratio delineating the incorporation of excess Sr in shells, though only certain variety of molluscs contains good amount of Sr apart from both planktonic and benthic foraminifera (Moore and Bostrom, 1978). Even though silts are poorer in CaO, Sr/CaO ratio depicts an above average value for silt-rich sediments indicating the availability of Sr in feldspars. The distribution pattern of Sr (Fig. 4.5j) illustrates a similarity with that of CaO showing semblance in depleted concentration around Cochin mouth. Small amount of Sr could be incorporated into the different phases of clay fraction by adsorption and exchange reactions and usually they are held more tightly on clay minerals.

With an average value of 25.54 ppm, the distribution of Rb depicts an increased concentration near the Cochin inlet. Size dependence is very significant with sand yielding a negative loading and both silt and clays positive values. Many sand-rich sediments are either completely devoid of or with traces of Rb. Due to the similarity of K and Rb ions, Rb is always associated with K-minerals such as mica and K-feldspar. In a weathering profile, Rb is closely linked with K, but in the later stages of weathering, adsorption may play an important role in the concentration of Rb relative to K. The positive affinity of Rb with fine fractions can be attributed to this. Goldschmidt (1954) found that Rb is held in adsorption positions more firmly than K. A major part of Rb can still be bound in the feldspars and micas of the silt-sized materials in the sediments. In most part, Rb also follows the accumulation pattern of many of the fine-grained partitioned elements.

Some Be-bearing minerals such as beryl and chrysoberyl are highly insoluble in solutions formed during weathering. Plagioclase of granitic rocks also contains considerable amount of Be. Barring a few (5 out of 56 samples), Be is present, though in low concentration, in all samples. Concentration ranges up to 8.6 ppm with an average value of 3.01 ppm. Its relation is antipathetic with sand and sympathetic with silt and clay. Strikingly, silt shows a better positive affinity than clay. Due to its small ionic size and high ionic potential, Be is easily fixed in finely dispersed particles. According to Hirst (1962), Be is generally accumulated in sediments of nearshore area. Clay sediments generally are characterised by higher Be contents than sandy ones (Hirst, 1962). Be/Al_2O_3 ratio averaging 0.24, in general displays a lower value for sand-rich zone, illustrating the poor availability of Be-bearing feldspars. Poor affinity with clay is an indication to the low level of

adsorption in the finely dispersed phases. Significant correlation of silt and Be discerns accumulation of the element in the terrigenous fractions of silts.

Li differs markedly from the other alkali metals in such a way that it is concentrated in femic silicate minerals, where it may replace Mg^{2+}. Soils derived from granitic gneisses and quartz silicate minerals, contain appreciable amount of Li (Mitchell, 1964). Lithium concentration in the innershelf sediments exhibits a strong affinity with silt and clay and inverse relation with sand. During weathering, Li released from the primary minerals is then incorporated into the clay minerals. Silts and clays contain larger amounts of Li than parent material. In poorly drained soil, clay contains 5-10 times of Li than sand fraction. Possibility of Li existing as exchangeable ions on organic matter can not be ignored (Toth, 1970), but the exchange capacity of Li is much lower than that of Rb, K and Na with clays. Resemblance of Li concentration with fine sediments was also reported by Hirst (1962) from the study of Gulf of Paria sediments. Nicholls and Loring (1962) observed that, much of the Li was incorporated in illite clays before deposition. The strong affinity of Li with clay than with silt strongly supports the above contentions of adsorption of Li on clays and organic matter. Whereas the affinity of silt with Li chiefly indicates the mineralogical concentration of Li especially in micas.

Molybdenum occurs naturally in oxidation states ranging from Mo^{3+} to Mo^{6+}, with the later the most stable under oxidising conditions. It is preferentially enriched in minerals containing Ti^{4+} and Fe^{3+}, such as sphene, ilmenite, titanomagnetite and biotite. In the innershelf sediments, only 7 out of 56 samples contain Mo concentration in the lowest detectable level of 10 ppm. Hence, average values does not hold good in evaluating the metal

concentration. Though the correlation coefficients with size does not give any indication about its textural association, it is invariably found to be concentrated in the fine-grained sediments. Mo enrichment in sediments is by uptake on iron, manganese or aluminum oxides. Adsorption, or co-precipitation of Mo has been documented with Fe-Mn oxides and Al-oxides. Co-precipitation of Mo on ferric hydroxides achieves a maximum effectiveness at low pH (Seralathan and Hartmann, 1986). Lower concentrations of V than Mo in sea water is attributed to the much greater co-precipitation of V by iron oxides at pH ranges typical for sea water(7.8 - 8.3).

More than one third of the innershelf samples did not yield any V concentration. Though a direct proportionality of V with size grades are lacking, it is mostly concentrated in fine sediments. Information on the behaviour of V during weathering indicate that, vanadium remains in the residual rock-forming and iron bearing minerals and/or enters minerals in the silt or clay fraction. In the clay fraction, V can be adsorbed and incorporated in clay mineral structures or in iron oxide coatings. V can be removed from a sulphide-rich environment by co-precipitation. The importance of freshly precipitated ferric oxide in adsorbing the metal than manganese oxide, montmorillonite or organic substances was demonstrated by Krauskopf (1956). V accumulation in organic matter is not only due to adsorption but also due to the reducing nature of organic-rich sediments. The chief source of V in the finer sediments could be from the soils derived from laterites which are generally rich in V.

Partitioning of the minor and trace elements: In order to have a direct comparison of metal concentrations in the various chemical extracts of sediments, chemical fractionation method described by Filipek and Owen (1979)

is adopted. This method deals with a sequential extraction scheme which chemically separates the carbonate and amorphous Mn oxides, oxidizable (organic-sulphide), moderately reducible (Fe-oxides and hydroxides) and lithogenous fractions of the sediments. Though the method envisages two complementary steps for physical (grain-size) and chemical partitioning, in the present study, only the chemical partitioning is attempted. Less than 63 μ fraction (mud) of four sediment samples were subjected to minor and trace element analysis using AAS. The sequential leaching was carried out with acetic acid, acidified H_2O_2, NH_2OH-HCl in acetic acid and HNO_3-HF-$HClO_4$ for separating the four respective fractions. Each step was followed by centrifugation to separate the residue to be used in the next step for digestion. The details of the technique were described by Gupta and Chen (1975), Filipek and Owen (1978) and Filipek and Owen (1979). The results of the analysis are presented in Table 4.12.

Non-lithogenous fraction (NLF): The NLF contribution of the elements are the sum total of the first three phases, namely, (i) carbonate and exchangeable metals, (ii) organics, sulphides and Mn-oxides and (iii) moderately reducible Fe-oxides and hydroxides. Metals exhibit a wide range of proportions of NLF and lithogenous fraction (LF). The maximum concentration of NLF contribution is for Cu (84.17 %) and minimum for Ba (6.98 %). The variation is Cu > Sr > Zn > Pb > Mn > Cr > Li > Cd > Be > Ni > Rb > Co > V > Ba in the order of decreasing average abundance of NLF.

Metals in carbonate fraction may be either authigenic or detrital (Stumm and Morgan, 1970). But, metals in exchangeable positions are generally authigenic. However, heavy metals in both these phases are relatively mobile and readily available for biological uptake. Among the metals considered here,

TABLE 4.12

Percentage contribution of elements in each fraction of mud (<63 microns) s

	I	II	III	IV
Mn	12.00	28.65	5.86	53.73
Cu	12.95	63.74	7.49	15.83
Co	2.01	10.01	2.12	85.86
Cr	11.78	19.40	4.36	64.46
Ni	4.99	16.06	2.70	76.27
Cd	8.55	13.83	4.36	73.26
Pb	8.43	41.38	7.51	42.68
Zn	19.38	53.20	6.68	20.73
Ba	0.70	4.50	1.68	93.11
Sr	51.66	23.50	6.26	18.59
Rb	0.68	16.85	0.46	82.00
Be	2.50	17.90	4.45	75.14
Li	1.84	26.22	3.48	68.46
V	2.14	8.08	3.17	86.61

s Average of 4 analyses.

I Crabonates and exchangeable metals
II Organics, sufides and Mn-oxides
III Fe-oxides and hydroxides
IV Lattice-held metals in crystalline mineral grains

carbonate-exchangeable metal phase accounts for a range from 51.66 % of total Sr to 0.68 % of Rb. Zn, Cu, Mn and Cr show significant enrichment in this phase. It was mentioned above that in the case of CaO-rich sediments, the Sr/CaO ratio is higher than other zones, implying the segregation of Sr with carbonates, as it is controlled by diodochy with Ca. The other elements could be in the exchangeable metal phase as they show semblance with fine sediment concentration in the area.

Cu has the highest relative amounts in the organic sulphide fraction. Like Cu, Zn followed by Pb are heavily concentrated in this fraction, which accounts for an average of 53.2 % and 41.38 % of total Zn and Pb respectively. Except Ba and V, all other elements show considerable concentration in this phase. The average organic matter content of the 4 bulk sediment samples, which were subjected to the partition analysis, is 4.68 %. The absolute value of organic matter could be at least two-fold, in the < 63 μ, as it shows size-semblance with finer fractions of the sediments. Fig. 4.8 depicts the relationship of organic matter with various trace elements. Ability of certain heavy metals to form organic complexes, especially in the case of Cu and Zn has been reported (Mills and Quinn, 1981). These metals are characterised by a dispersal pattern decreasing away from the Cochin inlet, which can be attributed to the anthropogenic input flushed out through the Vembanad Lake (Ouseph, 1987). The availability of framboidal pyrite imply slightly reducing conditions at certain parts of the innershelf. Hence, the considerable concentration of Pb in the organic-sulphide phase can be inferred as formed from reactions involving both sulphides and organics. A scrutiny of the data set (Table 4.12) enumerates the importance of this phase and it regulates concentration of many trace elements in the innershelf. But, the enrichment of certain metals in this phase need not necessarily be from authigenic

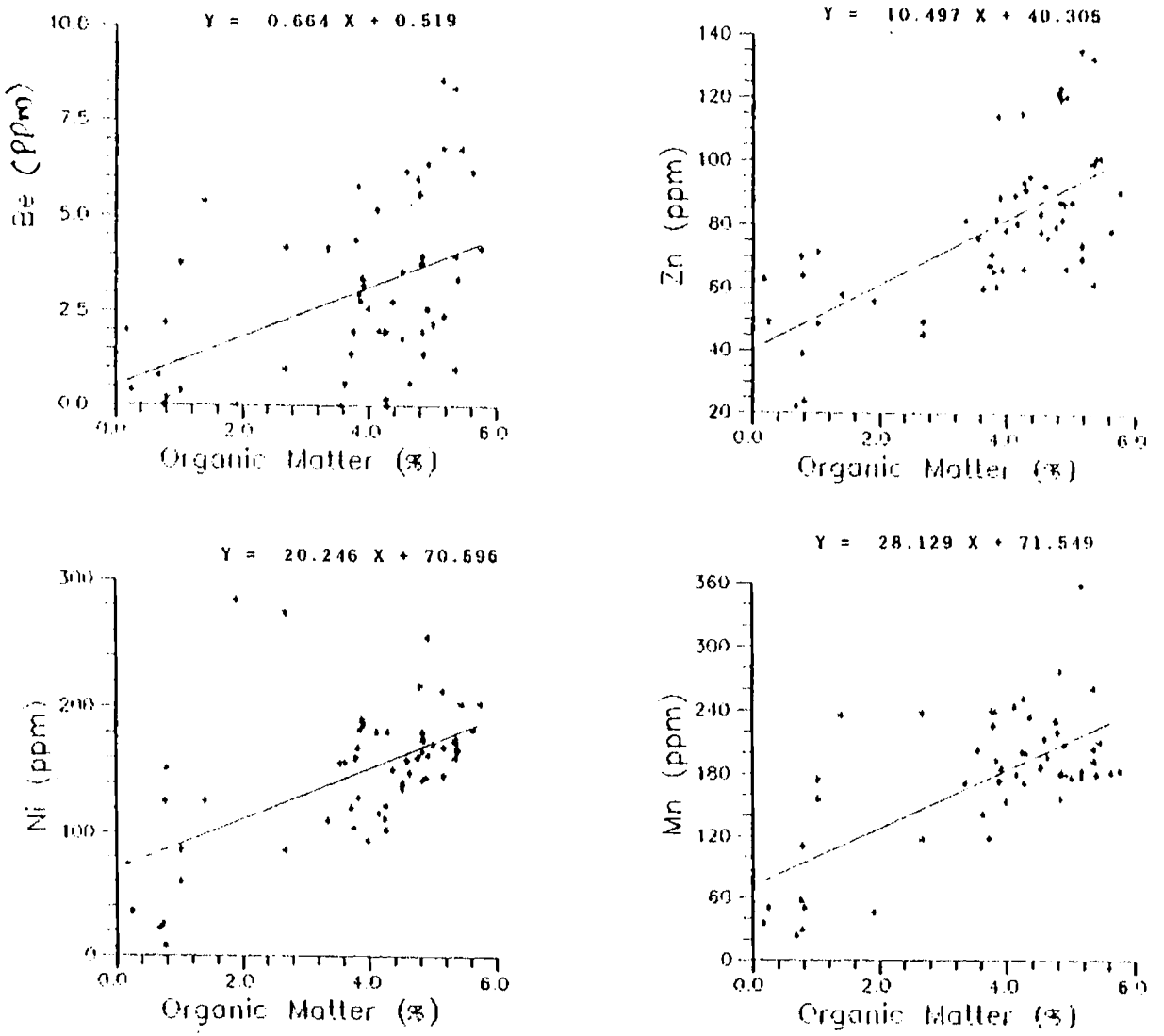

Fig. 4.8 Relationship of organic matter with major and trace elements

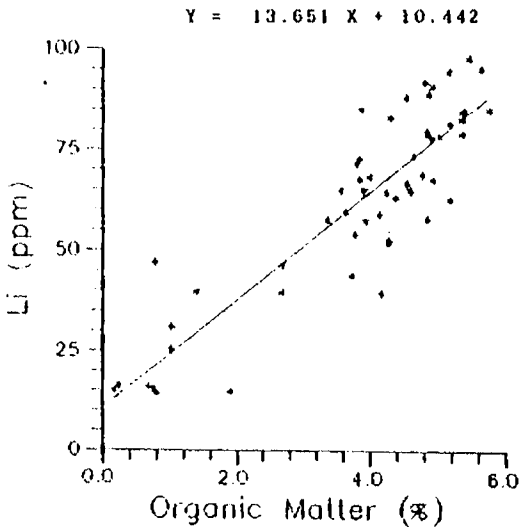
Y = 13.651 X + 10.442
Li (ppm)
Organic Matter (%)

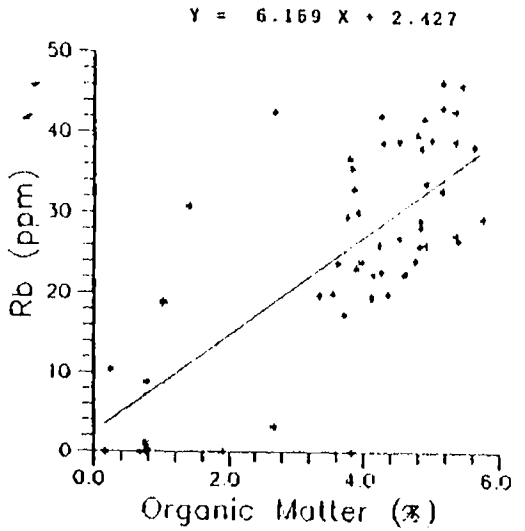
Y = 6.159 X + 2.427
Rb (ppm)
Organic Matter (%)

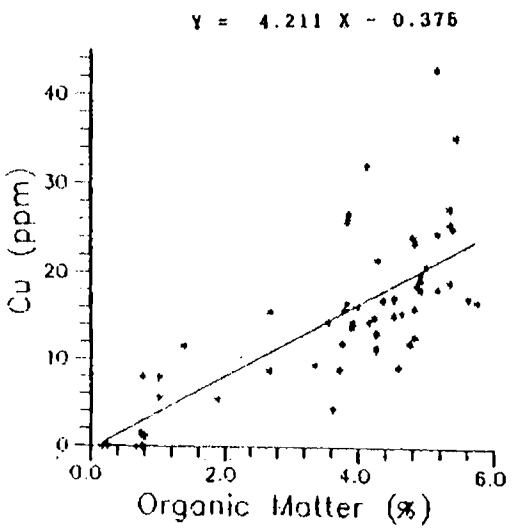
Y = 4.211 X - 0.375
Cu (ppm)
Organic Matter (%)

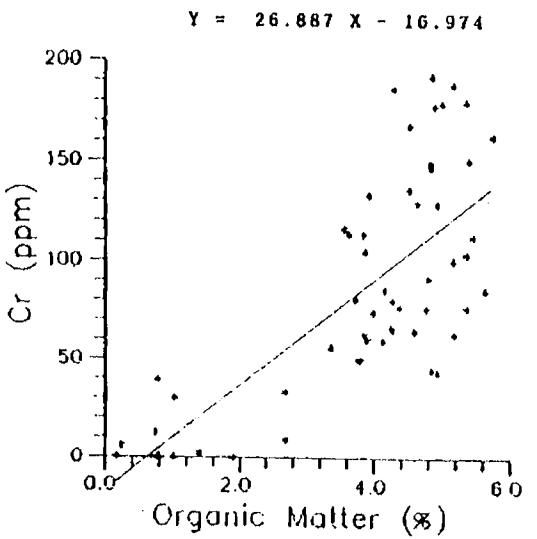
Y = 26.887 X - 16.974
Cr (ppm)
Organic Matter (%)

Fig. 4.8 Contd...

process as the isopleth bulk concentration diagrams of the elements show higher values near the estuarine mouth which gradually depletes towards offshore.

The Fe-oxide-hydroxide phases of the sediments show certain metal concentrations with a maximum enrichment for Pb (7.51 %). Unlike the organic-sulphide phase, adherence of metals to this fraction do not seem to have an important bearing on the sediment chemistry, except for a few elements. Slight enrichment of Cu, Zn and Mn is also noticed here. However, the mechanism of incorporation of metals with hydrous Fe-oxides can be either by co-precipitation or by sorption onto pre-existing oxide coatings. Thus, the amount of metals so incorporated can vary considerably as the process of precipitation/sorption is highly sensitive to redox potential.

Lithogenous fraction (LF): Concentration of heavy metals in lithogenous fraction of the innershelf sediments are dominantly controlled by the mineralogy of the land-derived detrital fragments. Since, the analysis is carried out in < 63 μ fraction, it would consists of clay minerals and other oxide and silicate minerals with minor quantities of heavies in the silt fraction. The order of metal abundance in the LF of the samples is the inverse series given in the NLF section. Ba is almost entirely concentrated in the lithogenous fraction (93.11 %). This can be attributed to the presence of feldspars and micas and is supplemented by the chemical composition of the dominant rock types of this area (Ba ranges from 518 - 2055 ppm : Ravindra Kumar *et al.* 1990). Cu partitioning in the LF is the least among the metals (15.83 %), evidently due to the dearth of minerals containing Cu in structural positions. LF-Sr is also very low as it is redundant that Sr is mostly controlled by biogenic co-precipitation due to its resemblance in chemistry

with Ca. Low concentration of Zn in the structural positions of oxide and silicate minerals is indicated by its negative correlation with sand and depletion in the lithogenous fraction. V, Co, Rb and Be are partitioned dominantly with LF (> 75 %). The reason could be, (i) V is mainly controlled by minerals derived from laterites, (ii) Co availability in the silt-sized heavy minerals such as garnet, hornblende and biotite, (iii) Rb (covaries with K) by feldspar, micas and illites, and (iv) Be is attributed mainly to the feldspars in the fine fractions. Pb, which is enriched in the organic-sulphide fraction show < 50 %, LF. All other elements such as Cd, Li, Cr and Mn illustrates a contribution of 50-75 % in LF.

Correlation matrix of minor and trace elements: Correlation matrix (Table 4.13) and Fig. 4.9 show considerable covariation among various trace metals. Mn is significantly positively correlated ($r > 0.5$) with Rb, Li, Zn and Cu. These elements together depicts considerable size dependence with fine fraction (< 63 μ) and/or enriched in the organics, sulphides and Mn-oxides that are leachable with acidified H_2O_2. Ba, Sr, Cd, Mo and V are not correlated with Mn, evidently because Ba is neither size dependant, nor enriched in the NLF fraction of the sediments; Sr though slightly concentrated in clay fraction is mainly a function of carbonate fraction than organic-suphides, Cd is unrelated with size with slight segregation in organic phase; Mo and V are segregated in lithogenous fraction with a no loading on any size grades. Pb shows weak correlation with Mn, as its granulometric semblance is at a lower level and unlike Mn, it is concentrated in the suphide phase than in the organic-Mn-oxide fraction. Be, Cr, Ni and Co also show considerable sympathetic variation with Mn ($r = 0.35$ to 0.50), as they depict certain amount of chemical enrichment and size segregation similar to Mn.

TABLE 4.13

Matrix of correlation coefficients of minor and trace elements

	Mn	Cu	Co	Cr	Ni	Cd	Pb	Zn	Ba	Sr	Rb	Be	Li	Mo	V
Mn	1.000														
Cu	.506	1.000													
Co	.366	.506	1.000												
Cr	.439	.561	.116	1.000											
Ni	.436	.606	.407	.373	1.000										
Cd	.137	.135	.204	-.460	.035	1.000									
Pb	.236	.395	.183	.255	.299	.170	1.000								
Zn	.510	.662	.126	.546	.436	.157	.328	1.000							
Ba	-.276	-.201	.297	-.232	-.260	.109	-.074	-.250	1.000						
Sr	.037	-.091	.093	-.153	.379	-.121	.048	-.128	-.167	1.000					
Rb	.689	.698	.487	.582	.528	-.091	.202	.460	-.252	-.043	1.000				
Be	.475	.604	.595	.006	.412	.522	.196	.303	-.187	-.042	.477	1.000			
Li	.634	.819	.442	.776	.584	.048	.391	.700	-.217	-.163	.751	.490	1.000		
Mo	.152	.093	-.034	.277	-.017	-.256	.152	.147	.019	-.077	.049	-.246	.096	1.000	
V	.181	.191	-.033	.421	.071	-.342	.013	.256	-.146	-.183	.246	-.153	.273	.367	1.000

Significant level of r values: >0.22 (0.1 level), >0.26 (0.05 level)
>0.34 (0.01 levie); >0.42 (0.001 level).

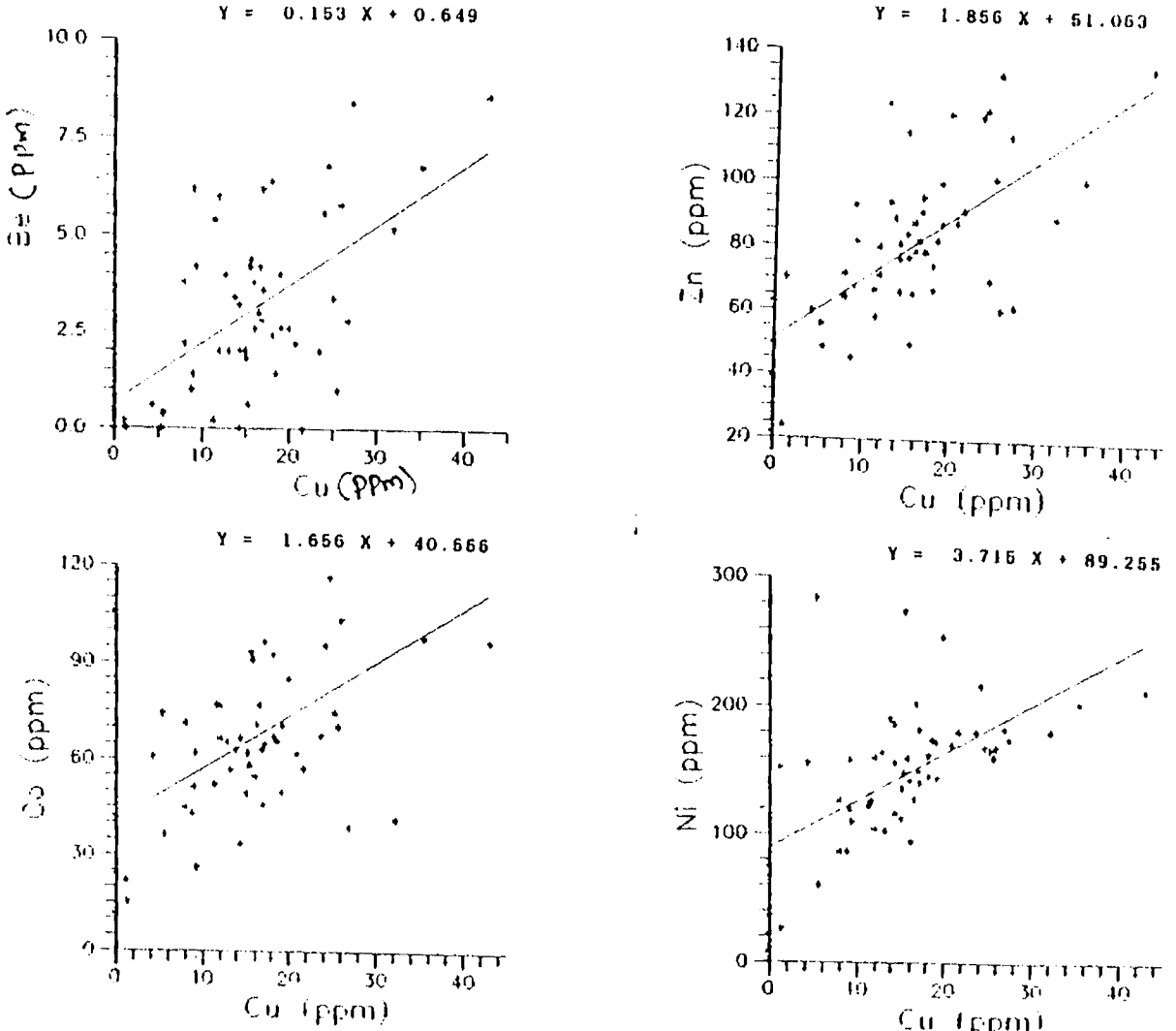

Fig. 4.9 Inter-relationship among minor and trace elements

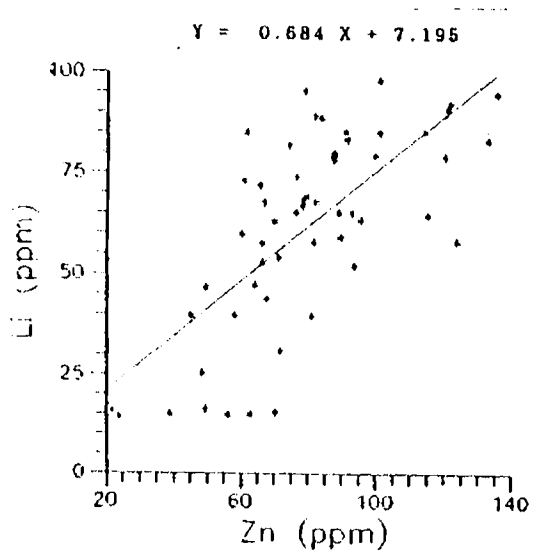
Y = 0.684 X + 7.195
Li (ppm)
Zn (ppm)
100
75
50
25
0
20
60
100
140

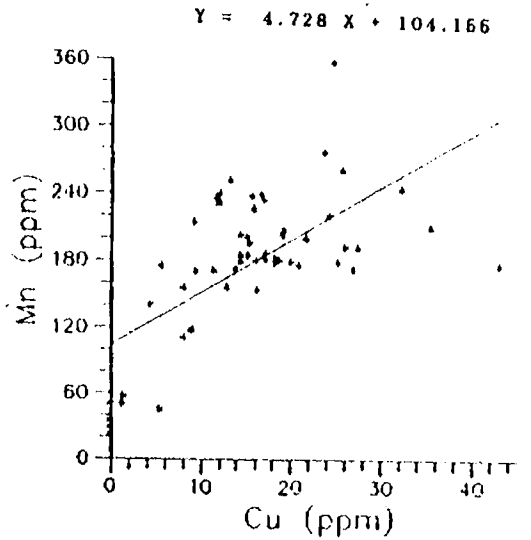
Y = 4.728 X + 104.166
Mn (ppm)
Cu (ppm)
360
300
240
180
120
60
0
0
10
20
30
40

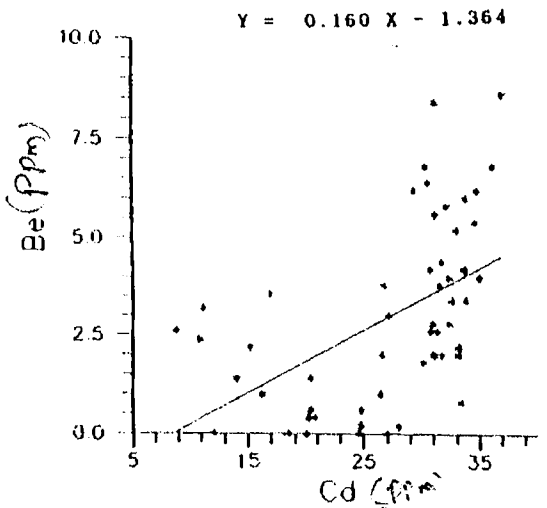
Y = 0.160 X - 1.364
Be (ppm)
Cd (ppm)
10.0
7.5
5.0
2.5
0.0
5
15
25
35

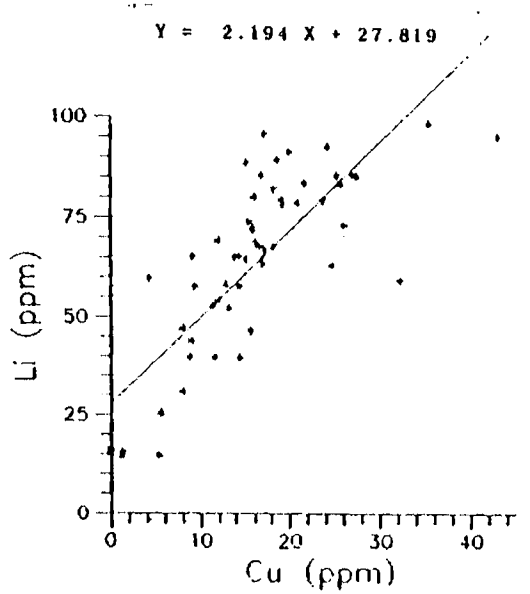
Y = 2.194 X + 27.819
Li (ppm)
Cu (ppm)
100
75
50
25
0
0
10
20
30
40

Fig. 4.9 Contd...

Resemblance in the chemical and physical partitioning of Cu with Li, Rb, Zn, Ni, Be, Cr and Co are indicated from the higher coefficient of correlation ($r > 0.5$). Be and Co enumerates a similarity in distribution, as the control of texture on their partitioning pattern is not so significant owing to the lower NLF speciation. However, their NLF contribution is mainly restricted to the organic-sulphide phase. Similar to the strong association of Cu with Li, elements such as Cr, Rb, Zn and Ni also show conspicuous correlation with Li, marking their identical fractionation. Ba is strikingly unrelated to other elements with an exception of a little positive affinity for Co ($r = 0.297$) as they are dominantly controlled by lithogenous fraction. Sr shows slight positive loading on Ni, which is found to be difficult to explain in terms of physico-chemical fractionation. But there could be a spatial synchronisation in distribution. Despite a lower r value (0.367), the correlation between V and Mo is considered as significant, because Mo is found to be available only in a few samples and the correlation is worked out for the entire set of 56 samples. Their variation is mainly controlled by terrigenous material than NLF.

Cluster analysis of minor and trace elements: Many elemental groupings are depicted by the dendrogram (Fig. 4.10). The major group consists of Zn, Cr, Mn, Cu, Li, Rb, Ni and Pb. These elements are mainly associated with the fine-grained fraction of the sediments. They are significantly fractionated in the organic-sulphide-Mn oxide phases. Be, Co and Cd are grouped together and do not show significant high correlation with any specific size grades. Their NLF abundance is limited. Co and Be are mainly associated with the minerals in the fine fractions, whereas Cd is incorporated in lattices of certain mineral constituents, materials from biogenic activity and anthropogenic input. Mo and V forms another group, indicating their selective partitioning with

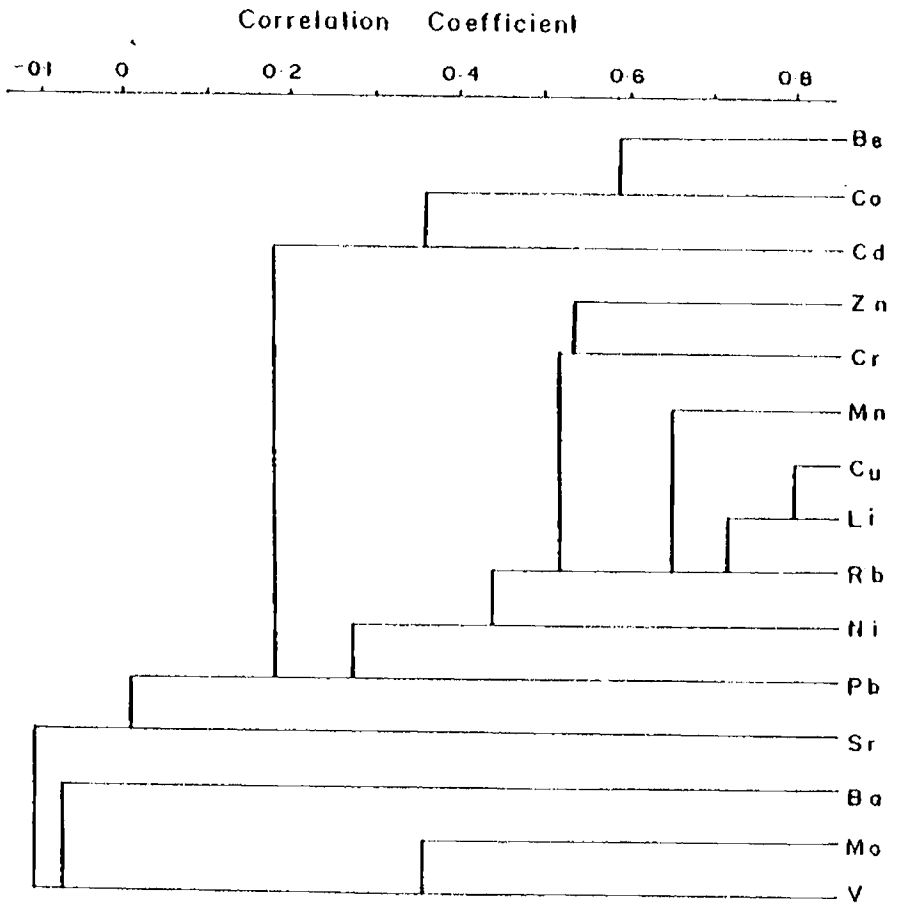

Fig. 4.10 Dendrogram of minor and trace elements

terrigenous fraction. Sr and Ba are separated from other elements, as the former is controlled by the nature and amount of skeletal components, and the later chiefly with lithogenous fraction.

Combined cluster analysis of major, minor and trace elements: The sum total of the organic matter (OM), major, minor and trace element variations and associations are depicted in the cluster diagram (Fig. 4.11). The elemental groupings with their respective controlling factors are as follows:

(1) The central part of the dendrogram shows a strong bonded group of elements consisting of Zn, Cr, Ni, Mn, Cu, Li, Fe_2O_3, OM, Al_2O_3, Rb, Na_2O, K_2O, MgO and Pb. It suggests their strong association with fine-grained sediments, especially with clay minerals and organic matter. Within the clay minerals, these are present in the crystal lattice either as essential constituent or incorporated by cation exchange or adsorbed onto clay platelets. Organic matter plays a significant role in scavenging many of the trace elements, as the NLF contribution of many of the elements are within the organic-sulphide-Mn oxide phases.

(2) The association of Be, Co, TiO_2 and Cd decipher a low level of textural control, but do show some positive affinity especially with silt which indicate their incorporation mainly in the lithogenous components (mostly lattice-held state) of heavy mineral fraction. Cd variation suggests a bearing on the biogenic and anthropogenic incorporation, though to a limited extent, Be and Co also show some association with carbonate and organic phases.

Fig. 4.11 Combined dendrogram of organic matter, major, minor and trace elements.

However, TiO_2 is dominantly lithogenous and its distribution is controlled by the energy regime of the innershelf as evidenced from the physical partitioning with fine-grained sediments.

(3) Good positive correlation between Sr and CaO suggests their presence in the skeletal components, though some amount of CaO is also incorporated in the lattices of clay and other detrital minerals. However, their variation is mainly a function of biogenous contribution as many of the sand-rich sediments contain subminimum concentration of these elements.

(4) Mo and V, along with P_2O_5, form a significant group. While Mo and V are of lithogenous origin, P_2O_5 is chiefly controlled by fine-grained sediments containing ferri-phosphate, adsorbed phosphate and phosphate associated with organic matter. However, the clustering of these elements could be due to the lack of significant textural control over their speciation and association with the lithogenous fraction.

(5) SiO_2 is grouped with Ba. A clear physical association of SiO_2 with sand fraction and their decrease in concentration with increasing clay content is a function of mineralogy. Unlike many of the elements, Ba shows maximum enrichment in the lithogenous fraction. Ba also depicts slight positive affinity with sand content. Hence, the association of SiO_2 and Ba is assigned to the coarser clastics of terrigenous origin.

From the overall pattern of distribution and partitioning, it can be concluded that, the variations of organic matter, major, minor and trace elements are to a greater extent controlled by texture of the innershelf sediments with some exceptions in the cases of elements which are beyond the spectrum of size-related physico-chemical partitioning.

CHAPTER 5

SEDIMENTOLOGY OF MUD BANKS

5.1 INTRODUCTION

Calm patches of turbid water, with a heavy load of suspended matter occurring along certain stretches of Kerala coast during the southwest monsoon season are known as 'mud banks'. Mud bank is locally known as *Chakara, Santhakara, Kettavellam,* and also other less popular names with regional variations. The significance of the mud bank is that, even when the highest monsoonal waves attack the coasts, the mud bank regions appear as very calm. Calmness of this area facilitates easy operation of country boats for fishing as it provides rich resources of fishes. Hence, mud banks are considered as a boon to the fishermen community. Despite the antiquity of reports, a few scientific study of mud banks has been attempted. There are some valuable scientific information available in literature about this phenomenon. But still, a coherent multi-disciplinary attempt to document the mode of formation, stages of development and cessation of this phenomenon is a major lacunae. This chapter provides a brief evaluation of the previous investigations, information on sedimentological aspect of the Alleppey mud bank and comparison of Alleppey mud bank with Quilandy mud bank.

5.1.1 Nature of mud banks

Mud banks are found to occur close to the shore and are more or less semicircular in appearance, with their seaward extend falling within 10 m depth contour. This spreads to a distance of about 3 to 5 km from the shore with an alongshore stretch of about 3 to 6 km. Mud bank areas are striking, with the absence of waves during southwest monsoon, when the other areas are under severe impact of waves. Another important feature is its high

turbidity which imparts a muddy appearance to the water column. Depending on its nature, Gopinathan and Qasim (1974) classified mud banks as active, passive and persistent. Active mud bank areas are those, where the waves are dampened at the periphery by the special property of the mud bank, during the southwest monsoon. Passive mud banks are those areas without any noticeable change in the wave characteristic from the other areas. Persistent mud banks are those which become active practically every year during the southwest monsoon or whenever there is a strong wave action.

5.1.2 Locations of mud bank formation

Mud banks have been reported from time to time at more than 28 locations. They are the following and are shown in Fig. 5.1:

Ullal, Uppala, Kumbala, Kasaragod, Cannanore, Mahe, Kollam (Quilandy), Calicut, Beypore, Veliyangode, Chetwai, Nattika, Vadanappally, Kodungallur (north and south of Kodungallur river mouth), Narakkal, Vypin, Mannasseri, Chellanam, Shertalai, Alleppey, Punnapra, Nirkunnam, Kakkazham, Ambalapuzha, Purakkad, Thottappally, Thrikunnapuzha and Kayamkulam.

Of the above, the most persistent are the mud bank that occur north of the estuarine mouth at Cochin (Narakkal), the one south of Alleppey (Purakkad) and the mud bank near Quilandy.

5.1.3 Previous work

For the last three centuries, occurrence of mud banks has been a regular phenomenon along the Kerala coast. Though several records on mud bank formation exist since 1678, no detailed investigation was done till

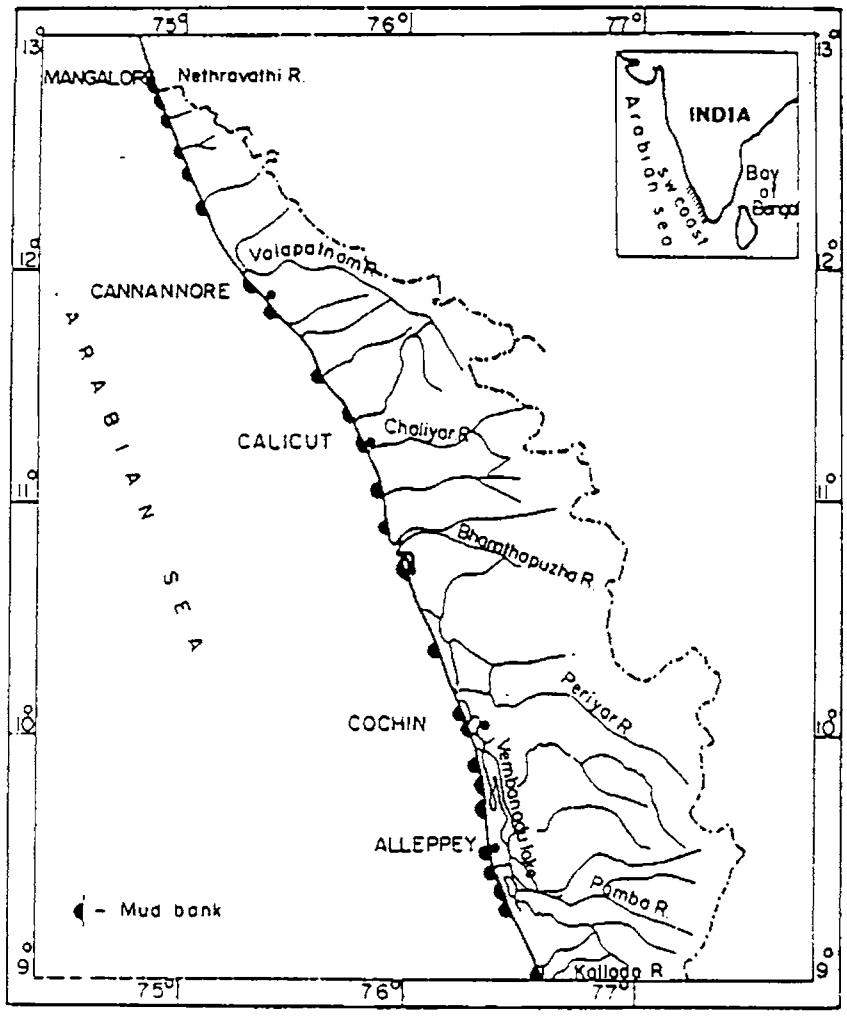

Fig. 5.1 Locations of occurrence of mud banks along southwest coast of India

recently. But in 1938, an organised effort was made by the Cochin Port authorities to study the nature and formation of mud bank. Bristow, the then Port Engineer published two volumes (History of Mud Banks, 1938) on mud banks, summing up the information available till then. Further, he proposed some hypotheses pertaining to its origin, movement and other features. Bristow (1938) made an elaborate treatment of the various hypotheses proposed by Rhode, Dr.Lake and Coggin Brown. Apart from this, Du Cane *et al.* (1938) brought out a report on the movement of mud banks. These studies have encouraged subsequent workers to examine various aspects of mud bank development in nearshore waters.

Attempts to investigate the physical, biological and chemical characteristics of the mud banks include those of Seshappa (1953), Seshappa and Jayaraman (1956), Damodaran and Hridayanathan (1966), Nair and Murty (1968), Dora *et al.* (1968), Hiranandini and Gole (1969), Varma and Kurup (1969), Moni (1971), Iyer and Moni (1971), Kurup (1972), Damodaran (1973), Gopinathan and Qasim (1974), Jacob and Qasim (1974), Kurup and Varadachari (1975), Nair (1976), Kurup (1977), Silas (1984), Ramachandran and Mallik (1985), Shenoi and Murty (1986), Mallik *et al.* (1988), Ramachandran (1989), Mathew and Baba (1991), and Ramachandran and Samsuddin (1991). A report detailing much of the known information on the mud banks was brought out by Mallik and Ramachandran (1984).

5.1.4 Hypotheses on mud bank formation

Rhode's (1886, In: Bristow, 1938) hypothesis states that, mud banks are formed by the mud flow from the backwaters by hydraulic pressure through some subterranean channel in the narrow strip of land that separates the

backwater from the sea. This flow was considered to be maintained by the hydrostatic pressure head created in the backwater developed due to their higher water level during monsoon. But the validity of this theory has been questioned by various researchers. . A pressure of 2 lb/inch^2 generated by a 5 ft level of rise in backwater during the monsoon period is considered to be insufficient to cause an underground mud discharge of such a dimension (Kurup, 1977). Another point raised against this theory is the compositional difference of mud in backwaters from that of mud bank (Du Cane *et al.*, 1938).

Du Cane *et al.* (1938) suggested that the high waves of the monsoon season churn up the bottom mud enabling transportation of suspensates to the mud bank. They pointed out the parameters like reduction of salinity by surface run off and supply of suspended matter through river discharge, tend to keep the sediments in suspension for a long period. Though mud is distributed all along the coast, this theory does not explain the localisation of mud banks.

Ramasastry and Myriand (1959) postulated that upwelling and divergence near the bottom between 20 - 30 m as the possible driving force for the suspension and deposition of mud, to the locations of mud bank. But, it is a matter of debate on the scientific rationale of attributing the drastic deposition of mud to such a slow process of upwelling.

Varma and Kurup (1969) observed that none of the above hypotheses explain the mechanism of triggering of mud bank at definite localities along the coast. They found a zone of converging littoral currents for higher period waves, which result in the generation of rip flows. These rip flows carry finer sediments offshore and prevent the onshore transport of sediment

by waves. Salinity dilution due to rip flow of nearshore water towards offshore facilitates deflocculation of sediments. This helps the sediments to be in suspension for a longer time, which accounts for continued existence of mud banks.

5.1.5 Wave energy dissipation in mud banks

The most striking feature of the mud bank is the lack of waves. These calm zone is a boon to the local fishermen for easy operation of their country craft during the rough monsoon. Mud banks also act as natural breakwaters, protecting the beach behind it from erosion.

Even though King (1884) attributed the calmness of mud banks to the oil in the mud, no such oily matter was reported from the mud at Alleppey (Keen and Russel, In: Du Cane *et al.*, 1938). Based on experiments and principles of hydrodynamics, they emphasized that, the calming effect is due to the kinematic viscosity and thixotropic properties of the muddy suspensions produced by monsoon due to the impact of stresses associated with the crest and trough of the waves. Many researchers (Kurup, 1977; Murty *et al.*, 1984; Shenoi and Murty, 1986) pointed out that the viscosity of the water column is the main reason for the wave attenuation. Based on Gade's (1958) model McPherson and Kurup (1981) proposed that, soft bottom mud is responsible for the energy dissipation in the mud bank areas. But Murty *et al.* (1984) contested the applicability of the model and argued that, the physical conditions assumed in that mathematical model are not identical with conditions prevalent in mud banks. Shenoi and Murty (1986) assumed the wave profile over mud banks as solitary like and computed the wave amplitude dissipation owing to viscous shear beneath the solitary wave over a smooth horizontal

surface. They concluded that, the wave energy dissipation in mud banks are due to the high kinematic viscosity of the water layer rather than the effect of soft muddy bottom. Baba *et al.* (1990) did not favour the above view due to the consideration that the wave profile over the mud bank as solitary-like, and also for not taking into consideration the effects of bottom into account in the studies of Shenoi and Murty (1986). From the field study off Alleppey Kurian and Baba (1987) observed that dissipation of wave energy up to 50 % occurs due to bottom friction as the waves propagate in nearshore waters. However, Baba *et al.* (1990) considered that the movement of mud layer and the energy absorption are more significant factors than bottom friction in the case of mud banks.

5.2 METHODOLOGY

5.2.1 Alleppey area

Survey of an area of 60 km^2 was carried out during July 1983 in the offshore area between Alleppey Pier and Mararikulam using a mechanised fishing boat. Perpendicular to the 12 km long coast, 8 profiles approximately at 1.5 km spacing were selected (Fig. 5.2a). Along each profile 4 sampling stations were fixed using Mini Ranger III. Thirty one surface sediment samples using Pettersson grab and 57 water samples from the surface and 1 m above the bottom using Van Dorn water sampler were collected. Water depth was measured at each sampling stations using a lead line. Water samples were analysed for suspended matter using vacuum pump and Buckner funnel filtration method. Textural analysis of sediment samples were carried out as per the methodology described in Chapter 2. Bulk sediment samples were subjected to chemical studies (methodology described in Chapter 4).

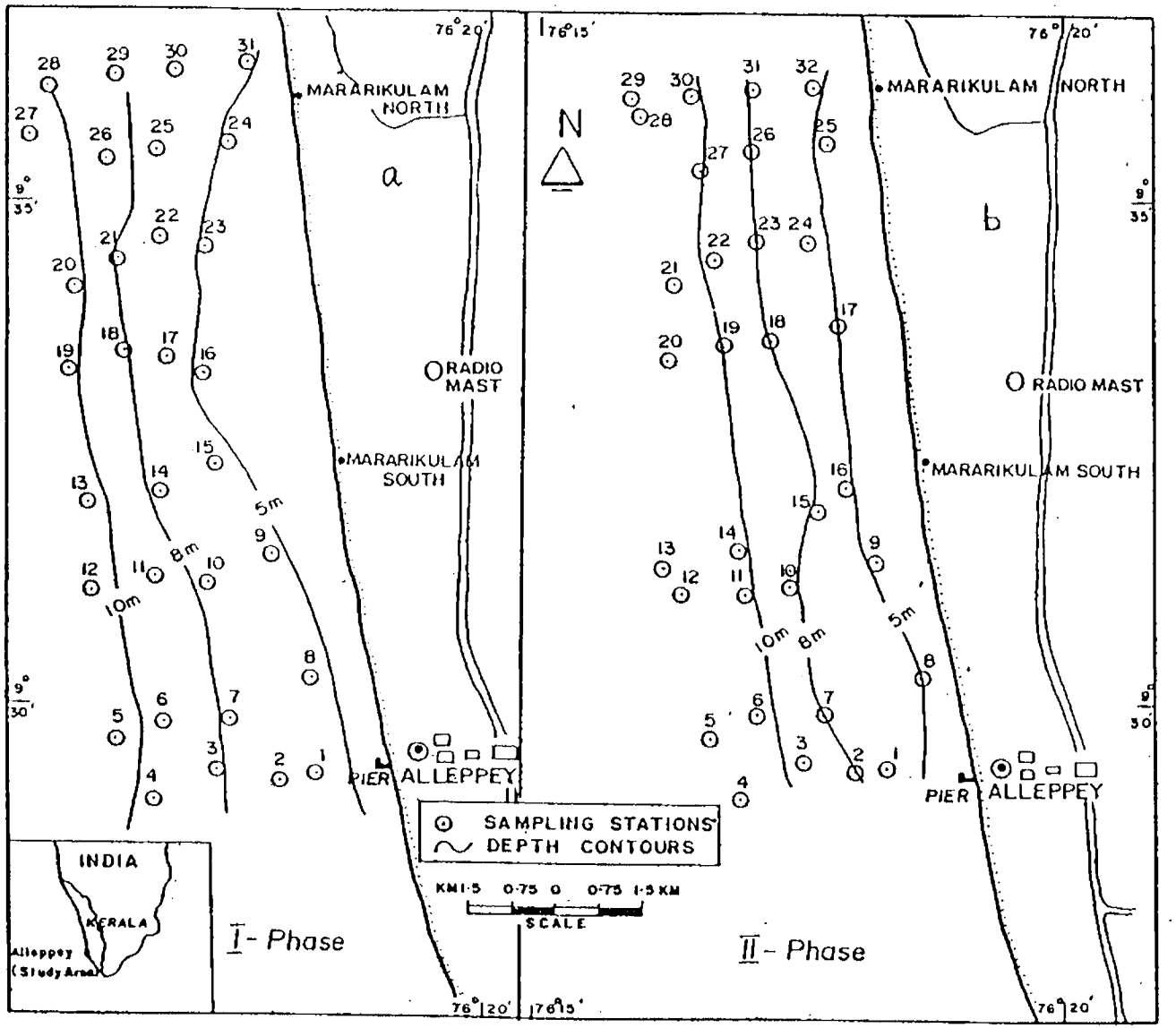

Fig. 5.2 Sampling stations and bathymetry of Alleppey mud bank during (a) July 1983 (b) December 1983

The same area was sampled and surveyed during December, 1983 (Fig. 5.2b). Grab samples (32 nos.) and water samples from surface and 1 m above bottom (30 each) were also collected. The analyses were repeated to determine the textural characteristics and suspended matter concentration.

5.2.2 Quilandy area

The study area (11°22' - 11°28'N and 75°30' - 75°43'E) is covered by the Naval Hydrographic Chart No. 219 and the Survey of India toposheet No. 49 H/11 (Fig. 5.3). A total of 32 grab and 12 core samples were collected from 38 stations in water depths ranging from 1 to 9 m using a fishing trawler during 1984. Each sampling site was located at the intersection of theodolite sightings of the boat undertaken by two shore based surveyors. A Pettersson grab and a gravity corer were used for sediment sampling PVC tubes threaded at both ends were used as the lower barrel which was replaced after each sampling. Textural analysis were carried out as described in the previous section. Smear slides of sediments from different core intervals and surface locations were examined with a petrologic microscope.

5.3 RESULTS AND DISCUSSION

5.3.1 Alleppey mud bank

In the following discussion the samples collected in the Alleppey nearshore during July and December 1983 will be referred as Phase I and Phase II respectively.

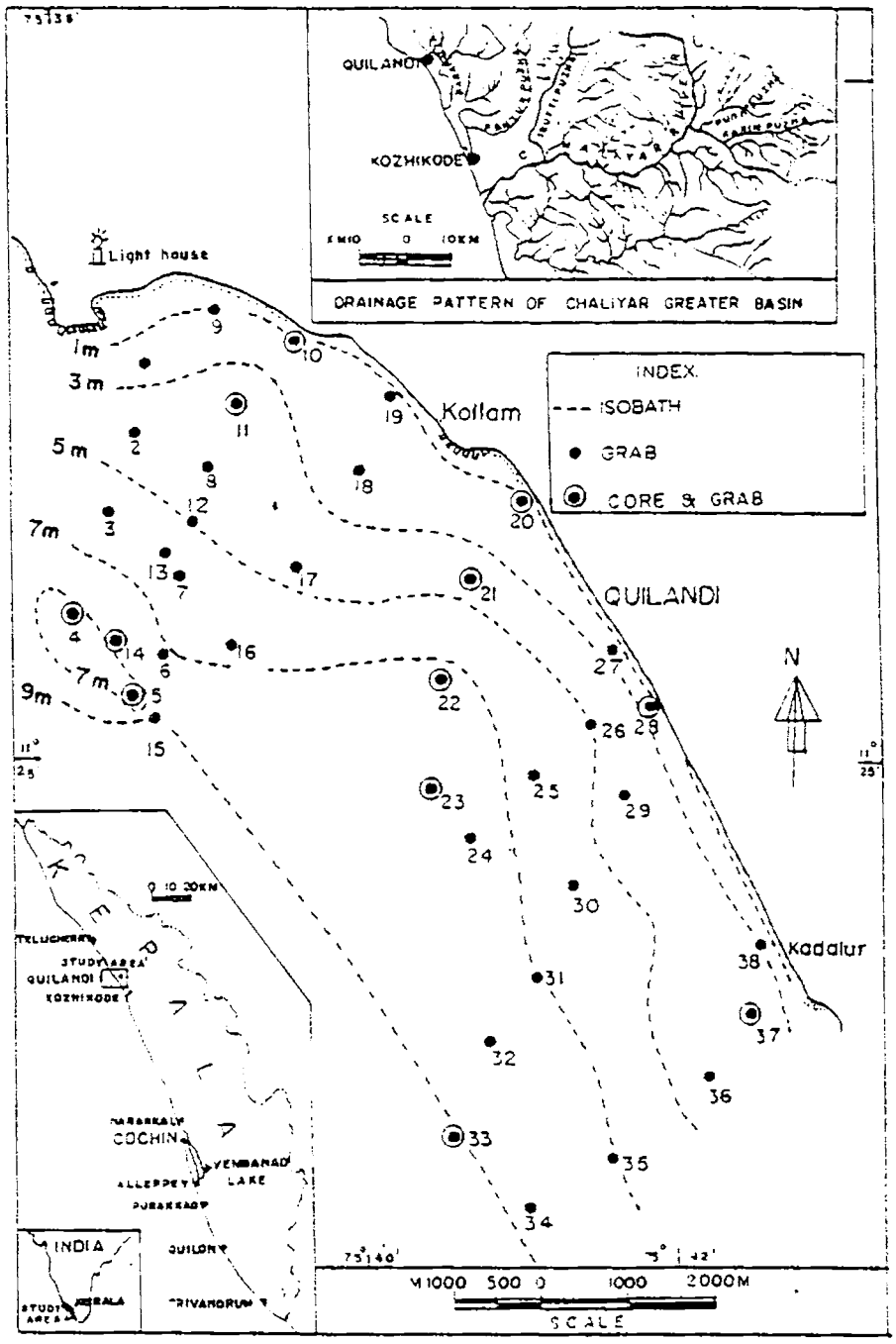

Fig. 5.3 Sampling locations and bathymetry of Quilandy mud bank

Bathymetry: The lead line sounding data for the Phase I survey show that, the depth varies from 3.5 to 11.5 m. At shallower depths samples were not collected due to the difficulty in operating the boat. Based on the lead line data, bathymetric contours are drawn for 5, 8 and 10 m depths in the nearshore. The Fig. 5.2a clearly illustrates an offshore bend in the 5 m contour at the middle portion of the study area, thus making the nearshore very shallow. In the middle portion, the 5 m contour is encountered only at a distance of ≈2.5 km from the shore, though at the north and south, 5 m contour is only at a distance of < 1 km. The 8 and 10 m contours do not show much deviation, which are almost parallel to the coast. The 10 m contour is approximately 5 km from the shore, reflecting a very low slope of approximately 1:500 for the nearshore, though the < 5 m zone is comparatively steeper than the > 5 m part.

The phase II data represents the post mud bank period. There are notable differences in the nearshore bathymetry compared to that of Phase I profiles (Fig. 5.2b). Three contours have marked shifting towards the coast, thus making the nearshore steeper than the monsoonal contours. Contrary to the irregularity noticed especially in the case of 5 m contour in the Phase I profiles, the Phase II bathymetric contours are almost parallel to the coast.

The mud bank formation as reported earlier (Damodaran and Hridayanathan, 1966; Kurup, 1977) is restricted to the nearshore area falling within the seaward limit of the 10 m isobath. The bend in the 5 m isobath and the seaward shift of the other isobaths in the Phase I is indicative of deposition of mud in the central part of the mud bank location. Most researchers generally agree that the mud is deposited in such locations during southwest monsoon, though there are different views regarding the source of mud. But

subsequent history of the mud, following its cessation, has not been dealt with by previous workers. Despite the limitation of the lead line sounding method, an uniform increase in gradient in Phase II compared to Phase I suggests the removal of mud during the post-mud bank season.

Suspended matter distribution: Suspended matter concentration (SMC) in the Phase I water samples ranges between 21 and 212.5 mg/l at the surface, whereas, SMC 1 m above the bottom ranges from 31.8 to 439.3 mg/l (Table 5.1). The distribution pattern of SMC at both the levels are shown in Fig. 5.4. SMC is maximum in central portion both at surface as well as at 1 m above bottom. Suspension is very low at the northern portion, at both the levels. Concentration profiles depicts a gradual depletion in SMC towards offshore as well as towards the southern side. But the decrease is very sharp towards north. The concentration difference between surface and 1 m above bottom ranges from 10.8 to 243 mg/l.

SMC shows a considerably lower concentration during Phase II survey (Table 5.2). Surface samples record a concentration range of 18.5 to 57.3 mg/l, while the range for 1 m above bottom is 52.9 to 101.2 mg/l. The minimum value obtained for the phase II SMC of 1 m above bottom is strikingly higher than that of the Phase I survey. A general increase in the concentration of suspension towards the coast is inferred from the distribution pattern of SMC at both the levels (Fig 5.5). Unlike the Phase I data, the figure does not give a high concentration zone in the central part of the study area. The difference between the SMC values at the surface and bottom layers range between 13.1 and 48.5 mg/l.

TABLE 5.1

Suspended Matter Distribution in Alleppey First Phase Samples

Sample	Surface mg/l	Bottom mg/l
1	159.0	186.8
2	165.5	183.8
3	156.5	175.5
4	203.5	248.0
5	147.3	204.8
6	183.3	187.5
7	176.3	203.8
8	169.0	259.5
9	172.3	285.0
10	180.8	201.0
11	203.5	248.0
13	188.0	206.3
16	203.0	288.3
17	212.5	290.3
18	206.8	439.3
19	41.5	192.5
20	39.3	292.3
21	32.0	48.0
22	21.0	31.8
23	32.5	257.3
24	42.0	-
25	65.0	267.0
26	37.5	40.5
27	37.8	87.5
28	44.5	61.8
29	33.3	50.0
30	25.8	49.8
31	42.0	115.0

TABLE 5.2

Suspended Matter Distribution in Alleppey Second Phase Samples.

Sample	Surface mg/l	Bottom mg/l
1	55.6	93.4
2	51.1	76.8
3	51.2	72.1
4	46.7	81.3
5	49.3	66.8
6	46.2	69.3
7	47.5	76.3
8	45.3	86.5
9	46.9	101.2
10	42.7	81.2
11	45.8	58.6
12	57.3	65.6
13	47.1	84.3
14	49.9	78.3
15	46.7	75.3
16	51.0	69.7
17	46.6	71.2
18	39.2	66.3
19	41.0	84.3
20	18.5	52.9
22	24.8	64.3
23	29.5	59.6
25	34.2	82.7
26	32.9	75.1
27	30.4	62.8
28	31.8	72.4
29	38.5	70.5
30	41.2	69.9
31	40.6	62.3
32	34.7	71.8

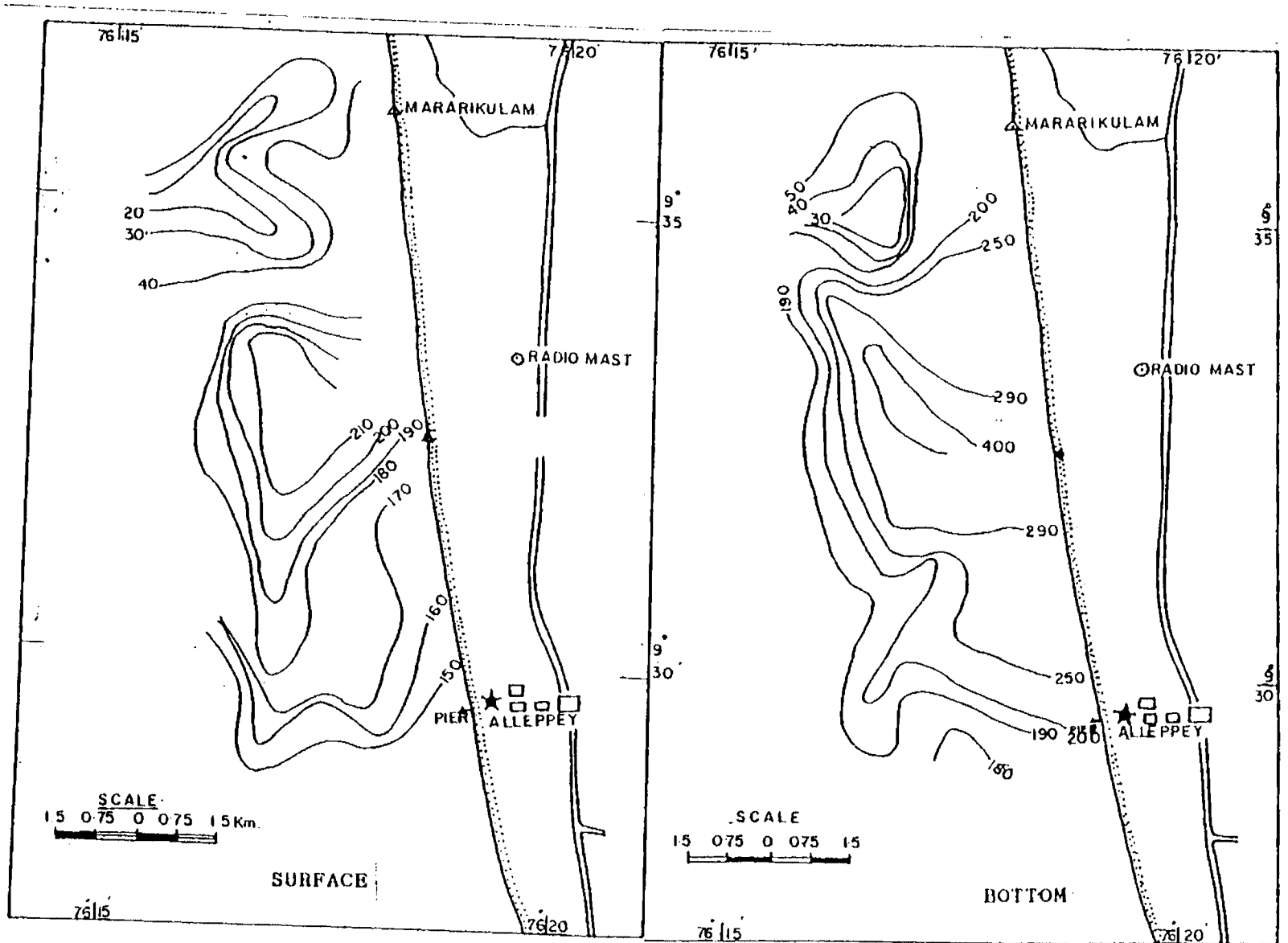

Fig. 5.4 Suspended matter distribution in Alleppey mud bank at surface and 1 m above bottom (During Phase I)

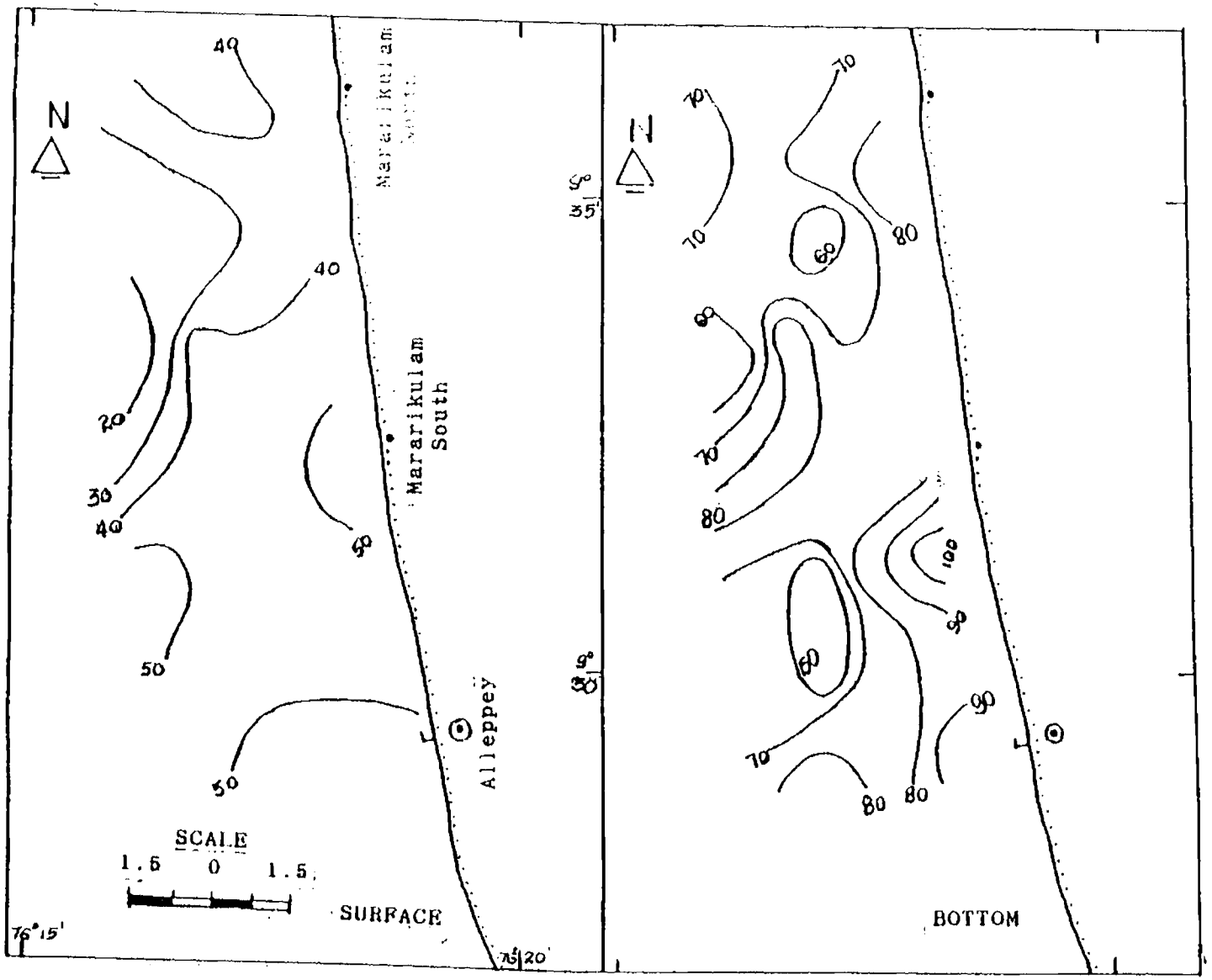

Fig. 5.5 Suspended matter distribution in Alleppey mud bank at surface and 1 m above bottom (During Phase II)

Suspended matter data of the Phase I samples clearly indicate an enriched suspension in the central zone which gradually transcends into low concentration in the north, south and seaward portions. Kurup (1977) observed suspended sediment content of > 1500 mg/l 1 m above the bottom. However, the present investigation shows a low SMC. Earlier observers opined that, when the waves approach shallow water, the finer materials at the bottom are brought into suspension (Damodaran and Hridayanathan, 1966). This is evidenced by the increase in SMC in the nearshore region within 10 m isobath, during the triggering period of mud bank. Subsequently, the waves are dampened due to interface oscillations generated in the top mud layer by the surface waves (McPherson and Kurup, 1981). This period marks the partial settling of the suspended sediments, due to flocculation. Probably this is the reason for a low concentration of suspensates observed during the Phase I period, compared to the observation of Kurup (1977).

The post mud bank period (Phase II) is clearly distinguishable from the mud bank period, by a low SMC. However, the localised concentration of suspension at 1 m above bottom near the Pier could be due to the interplay of wave energy around the pier. But in any case, except for one station, the SMC is observed to be below 100 mg/l at 1 m above bottom.

Sediment distribution: Textural data for Phase I are given in Table 5.3. Majority of the samples show a low percentage of sand, fluctuating between 1.27 and 55.67 %. Silt shows a monotonous distribution pattern without wider variation (ranging between 55.29 and 19.14 %). Clay, which is the most dominant textural fraction in the study area, ranges from 7.74 to 66.14 %. Percent frequency distribution of the textural grades among the samples are

TABLE 5.3

Sand-silt-clay percentages in the surface sediments of Alleppey First Phase Samples

Sample	Sand (%)	Silt (%)	Clay (%)	Texture Description
1	2.44	33.35	64.21	Silty Clay
2	7.41	34.51	58.08	Silty Clay
3	51.65	33.84	14.51	Silty Sand
4	25.85	46.05	28.11	Sand-silt-clay
5	55.67	36.59	7.74	Silty Sand
6	24.99	31.44	43.57	Sand-silt-clay
7	10.28	41.09	48.63	Silty Clay
8	8.93	52.17	38.90	Clayey Silt
9	2.20	46.36	51.44	Silty Clay
10	14.52	39.79	45.69	Silty Clay
11	27.00	44.33	28.67	Clayey Silt
12	14.38	55.29	30.33	Clayey Silt
13	3.25	32.70	64.05	Silty Clay
14	29.52	32.17	38.31	Sand-silt-clay
15	8.28	31.67	60.05	Silty Clay
16	3.10	34.93	61.97	Silty Clay
17	1.27	53.14	45.59	Clayey Silt
18	34.46	30.98	34.56	Sand-silt-clay
19	33.69	35.90	30.41	Sand-silt-clay
20	2.64	31.22	66.14	Silty Clay
21	2.32	43.65	54.03	Silty Clay
22	10.03	31.30	58.64	Silty Clay
23	4.23	36.61	59.16	Silty Caly
24	10.32	23.69	65.99	Silty Clay
25	44.13	19.14	36.73	Clayey Sand
26	44.67	19.87	35.46	Clayey Sand
27	2.01	41.70	56.29	Silty Clay
28	1.96	44.05	53.99	Silty Clay
29	11.81	43.94	44.26	Silty Clay
30	1.77	42.41	55.82	Silty Clay
31	2.17	42.90	54.93	Silty Clay

TABLE 5.4

Sand-silt-clay percentages in the surface sediments of Alleppey Second Phase Samples

Sample	Sand (%)	Silt (%)	Clay (%)	Texture Description
1	0.39	45.91	53.70	Silty Clay
2	3.24	50.96	45.80	Clayey Silt
3	54.70	31.33	13.97	Silty Sand
4	11.54	45.27	45.19	Clayey Silt
5	18.08	56.88	25.04	Clayey Silt
6	1.76	50.47	47.77	Clayey Silt
7	1.41	51.24	47.35	Clayey Silt
8	0.51	30.90	68.59	Silty Clay
9	9.21	41.98	48.81	Silty Clay
10	2.84	36.37	60.79	Silty Clay
11	10.90	39.94	49.16	Silty Clay
12	5.62	22.83	71.55	Silty Clay
13	7.50	57.77	34.73	Silty Clay
14	20.87	43.46	35.67	Sand-silt-clay
15	9.96	41.40	48.64	Silty Clay
16	0.18	38.06	61.76	Silty Clay
17	2.02	29.63	68.35	Silty Clay
18	1.45	21.74	76.81	Clay
19	7.84	38.65	53.51	Silty Clay
20	22.32	33.93	43.75	Silty Clay
21	4.26	31.79	63.95	Silty Clay
22	11.53	34.92	53.55	Silty Clay
23	1.32	30.43	68.25	Silty Clay
24	31.37	43.88	24.75	Sand-silt-clay
25	1.02	30.00	68.98	Silty Clay
26	42.22	25.78	32.00	Sand-silt-clay
27	34.31	36.58	29.11	Sand-silt-clay
28	5.07	41.36	53.57	Silty Clay
29	1.18	42.44	56.38	Silty Clay
30	1.06	39.47	59.47	Silty Clay
31	12.02	35.34	52.64	Silty Clay
32	0.08	27.32	72.60	Silty Clay

shown in Fig. 5.6. The most frequent sand class is 0 - 10 % and that for silt is 30 - 40 %. But clay shows two modes, one in the 30 - 40 % range and the most dominant mode in the 50 - 60 % range. Sediment texture ternary diagram (Shepard, 1954) depicts that the most dominant textural class is silty clay with a good amount of sand-silt-clay and minor amounts of clayey silt, clayey sand and silty sand (Fig 5.7).

Spatial variation of the sediment types are shown in Fig. 5.8. Even though the silty clay fraction covers a major portion of the study area, there is no appreciable textural gradation in the sediment facies. The northern part has a localised distribution of semicircular patch of clayey sand bordered by sand-silt-clay. A zone of sand-silt-clay extends from central portion towards south which broadens near the pier. A patch of silty sand enclosed within this band forms a tongue shaped distribution. The southwest corner of the study area is covered with clayey silt.

Textural data of the phase II samples are given in Table 5.4. Sand content ranges between 0.08 and 54.7 %. Sand frequency histogram shows that more than 65 % of the samples are with < 10 % sand (Fig 5.6). Silt in the sediments also shows considerable fluctuation from 21.74 to 57.77 %. A modal frequency of > 40 % is obtained for the 30 - 40 % class in the histogram (Fig 5.6). The percent variance of clay fraction is from a minimum of 13.97 to a maximum of 76.81. As per the ternary classification of the textural grades, silty clay sediments are the dominate ones (Fig 5.7) followed by sand-silt-clay, clayey silt and clayey sand, in their order of abundance. Only a single sample falls within the clay band and another lone sample in silty sand domain. The abundance of silty clay sediments are attested by their aerial dominance of the sediment type in Fig. 5.8. Patches of sand-silt-clay sediments are

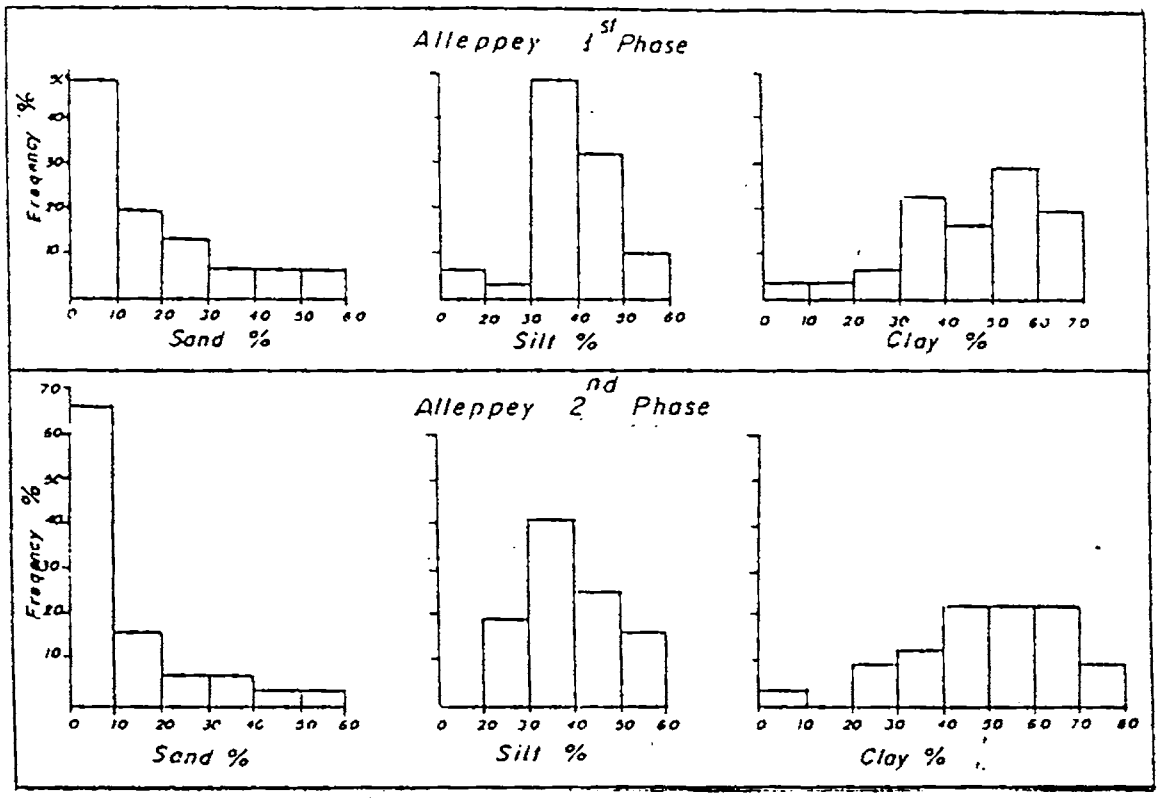

Fig. 5.6 Frequency distribution of sand, silt and clay in Alleppey mud bank area.

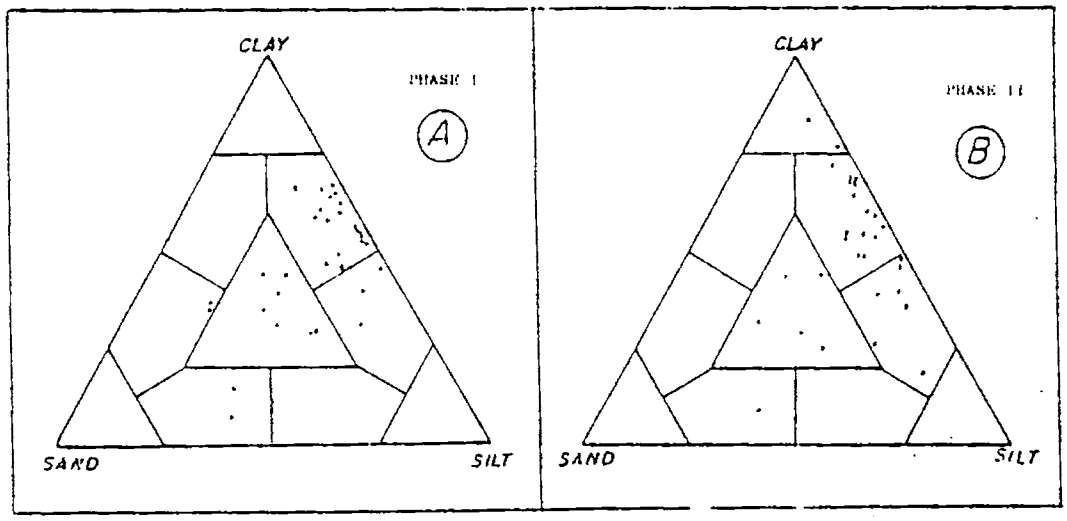

Fig. 5.7 Ternary diagram of sand, silt and clay in Alleppey mud bank area

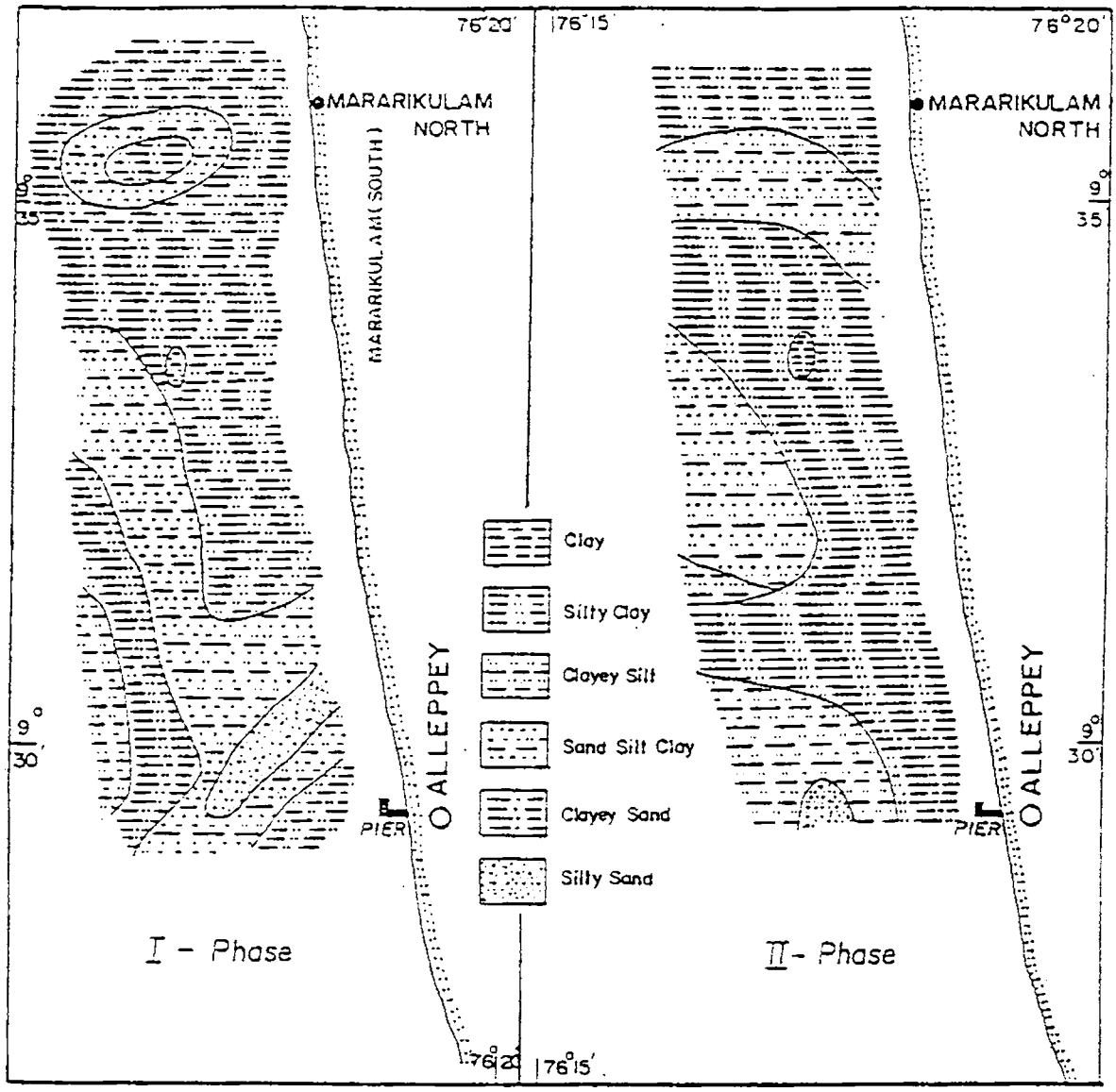

Fig. 5.8 Distribution of sediment types in Alleppey mud bank area

observed bordering the silty clay zones. Clayey silt sediment distribution is restricted only to two patches.

Geochemistry of the mud bank sediments: There are only a few reports existing on the geochemical aspects of mud bank sediments. The earliest one is by Coggin Brown (In: Du Cane *et al.*, 1938), who pointed out that the chemical composition of mud in the mud bank and of laterites are similar with proportions of SiO_2:Al_2O_3:Fe_2O_3 in laterite 3.28:1:0.44 and that of mud of the mud bank 3.91:1:0.45. Seshappa (1953) and Seshappa and Jayaraman (1956) studied the phosphate content in the mud bank sediments. Rao *et al.* (1984) made a comparative study of certain chemical elements of mud bank and Vembanad Lake sediments and concluded that they are of the same nature.

Sediments collected during the Phase I is subjected to chemical analysis to determine major elemental composition. The elements analysed are Fe_2O_3, CaO, MgO, Na_2O, K_2O, TiO_2 and P_2O_5. Table 5.5 presents the chemical data. Range and average statistics of the elemental abundance is given in Table 5.6. The chemical data is comparable with the geochemical data obtained for the innershelf described in the Chapter 4, for the set of samples which falls in the textural types described here. The average variation of the elements show a maximum composition for Fe_2O_3 (8.27 %) and minimum for P_2O_5 (0.51 %). The order of abundance of the elements based on their mean values are Fe_2O_3 > CaO > Na_2O > MgO > TiO_2 > K_2O > P_2O_5. The difference in the pattern of average abundance of the elements with that of the innershelf sediments is mainly due to the wide spectrum of grain size of the innershelf sediments. But, for the sediments with comparable textural characteristics, the chemistry of both mud bank and innershelf sediments is found to be similar.

TABLE 5.5

Major Element Composition of Alleppey (First Phase) Sediments

Sample	Fe2O3	CaO	MgO	Na2O	K2O	TiO2	P2O5
1	10.060	3.920	1.200	2.690	.800	.670	.500
2	10.060	5.040	1.000	2.290	.860	.830	.460
3	6.070	7.000	2.000	1.040	.360	.580	.410
4	7.820	9.800	1.800	1.480	.480	.670	.460
5	6.550	4.760	3.800	.900	.330	.670	.460
6	8.920	4.300	2.400	1.770	.630	.830	.460
7	8.620	4.760	2.600	1.980	.780	.830	.460
8	8.460	6.720	.400	1.770	.710	.670	.460
9	10.700	3.360	.200	2.270	.870	.830	.570
10	8.120	4.200	1.200	2.020	.760	.670	.500
11	8.300	3.920	2.400	1.680	.610	.830	.530
12	9.100	3.920	2.000	1.180	.550	.920	.500
13	11.500	3.460	1.000	2.370	.800	.830	.570
14	7.980	3.760	.800	1.540	.550	1.170	.460
15	11.500	4.200	1.400	2.350	.890	1.080	.500
16	8.780	3.920	1.600	2.210	.860	.830	.500
17	10.850	3.080	1.800	2.690	.830	.830	.460
18	7.350	3.920	2.000	1.220	.430	.830	.460
19	8.460	4.200	2.000	1.560	.460	.990	.460
20	9.260	4.200	.800	2.570	.860	.670	.460
21	7.980	2.800	2.000	2.300	.890	.830	.570
22	7.190	3.640	1.200	2.510	.870	.830	.570
23	7.350	3.360	1.200	2.450	.860	.750	.570
24	7.190	2.800	1.200	2.480	.900	.830	.570
25	6.070	2.800	2.800	1.820	.660	.830	.570
26	4.790	5.360	2.400	1.230	.480	.990	.460
27	7.980	3.920	1.200	2.210	.940	.830	.570
28	7.350	3.640	.800	2.240	.830	.990	.570
29	6.860	3.080	1.600	2.140	.830	.830	.570
30	7.660	3.360	.800	2.270	.870	.830	.530
31	7.500	3.640	1.200	2.270	.900	.830	.530

Though the elements show fluctuation in composition from sample to sample, the standard deviation indicate a lower scattering of values (Table 5.6). Except in the case of the MgO concentration, the percent variance of the elements are much below 50. MgO gives a percent deviation around 50 (Mean = 1.57 and S.D. = 0.77). Among the other elements, P_2O_5 shows least deviation around mean (percent variance is < 10) as indicated by the range from 0.41 to 0.57. Percent variance is 10 - 20 for Fe_2O_3 and TiO_2 around the mean, and CaO, Na_2O and K_2O yield > 40 % variance.

Grain size versus elemental concentration: Strong tendency of chemical elements to partition with various granulometric components of the sediments have been reported earlier (Zhao Yiang *et al.*, 1981). To understand the significance of such a partitioning in the mud bank sediments, correlation coefficients are computed between various elements and corresponding percentage of sand, silt and clay (Table 5.7). High positive loading of sand fraction with MgO and less significant positive correlation with CaO indicate the presence of shell fragments in the sand-rich sediments. The higher level of correlation of MgO with sand can be attributed to its abundance in the detrital sand fraction. Except TiO_2, all other elements yield significant negative correlation with sand fraction. With an exception of Fe_2O_3 ($r = 0.32$), silt does not yield any significant correlation with the elements. CaO and MgO yields negative relation with clay. All other elements, except TiO_2, give significant positive loadings. TiO_2 for instance, does not indicate any size partitioning and this could be due to the presence of TiO_2 bearing minerals in all the size fractions.

It is clear from the correlation matrix of size versus elements (Table 5.7) that, texture plays a pivotal role in segregating the elements. If

TABLE 5.6

Range and Mean Statistics of Alleppey Sediments

Element	Range		Mean	Std. Dev.
	Minimum	Maximum		
Fe2O3	4.79	11.50	8.27	1.59
CaO	2.80	9.80	4.22	1.42
MgO	0.20	3.80	1.57	0.77
Na2O	0.90	2.69	1.98	0.51
K2O	0.33	0.94	0.72	0.18
TiO2	0.58	1.17	0.83	0.13
P2O5	0.41	0.57	0.51	0.05

TABLE 5.7

Correlation Coefficients of Element Vs Size fractions in Alleppey Mud Bank Sediments

Element	Sand	Silt	Clay
Fe2O3	-0.584	0.320	0.457
CaO	0.358	0.137	-0.483
MgO	0.701	0.211	-0.628
Na2O	-0.857	0.043	0.911
K2O	-0.900	0.131	0.907
TiO2	-0.039	-0.148	0.133
P2O5	-0.477	0.013	0.532

positive affinity of elements with textural grades are considered as controlling factors, Na_2O and K_2O are almost entirely controlled by clay-sized materials as their loadings are very high (0.911 and 0.907 respectively). To a major extent, P_2O_5 is also controlled by the clay fraction. High positive loading of Fe_2O_3 on clay and silt are indicative of the adherence of Fe_2O_3 to the mineralogical assemblages in both clay and silt materials.

Inter-relationship of elements: Inter-elemental association is worked out using correlation matrix and cluster analysis. Table 5.8 shows the correlation matrix of the elements. Fe_2O_3 gives significant positive loadings on Na_2O and K_2O (r = 0.496 and 0.413 respectively) and negative loading on MgO (r = -0.394). Though CaO does not show significant positive affinity with any of the elements, it is negatively correlated with P_2O_5, K_2O, Na_2O and TiO_2. The antipathetic relation of MgO with Fe_2O_3, K_2O and Na_2O is also significant. Strong co-existence of Na_2O with K_2O and in turn with P_2O_5 can be clearly recognised from the high positive affinity among them as shown in Table 5.8.

Dendrograms based on the correlation matrix is given in Fig. 5.9. It clearly illustrates the clustering pattern of different elements, with the major cluster consisting of the elements Na_2O, K_2O and P_2O_5, which in turn are correlated, though at a lower level with Fe_2O_3. This clearly indicate that, the variation of these elements are mainly controlled by fine fraction of the sediments. Na_2O and K_2O are segregated in the clay minerals such as montmorillonite, kaolinite and illite, which are found to be enriched in this area in the $< 4\ \mu$ fraction. Enrichment of P_2O_5 in the clay fraction can be attributed to the sorption process on to clay surfaces, as reported earlier by Mallik *et al.* (1988). Fe_2O_3 in the sediments can either occur as discrete phases of iron-oxides on the clay particles or incorporated into the clay itself. But the

TABLE 5.8

Correlation Matrix of Major Elements in Alleppey Phase I Sediments

	Fe_2O_3	CaO	MgO	Na_2O	K_2O	TiO_2	P_2O_5
Fe_2O_3	1.000	-.144	-.394	.496	.413	.104	-.006
CaO	-.144	1.000	.099	-.484	-.506	-.378	-.611
MgO	-.394	.099	1.000	-.587	-.603	-.078	-.291
Na_2O	.496	-.484	-.587	1.000	.928	-.002	.533
K_2O	.413	-.506	-.603	.928	1.000	.068	.629
TiO_2	.104	-.378	-.078	-.002	.068	1.000	.146
P_2O_5	-.006	-.611	-.291	.533	.629	.146	1.000

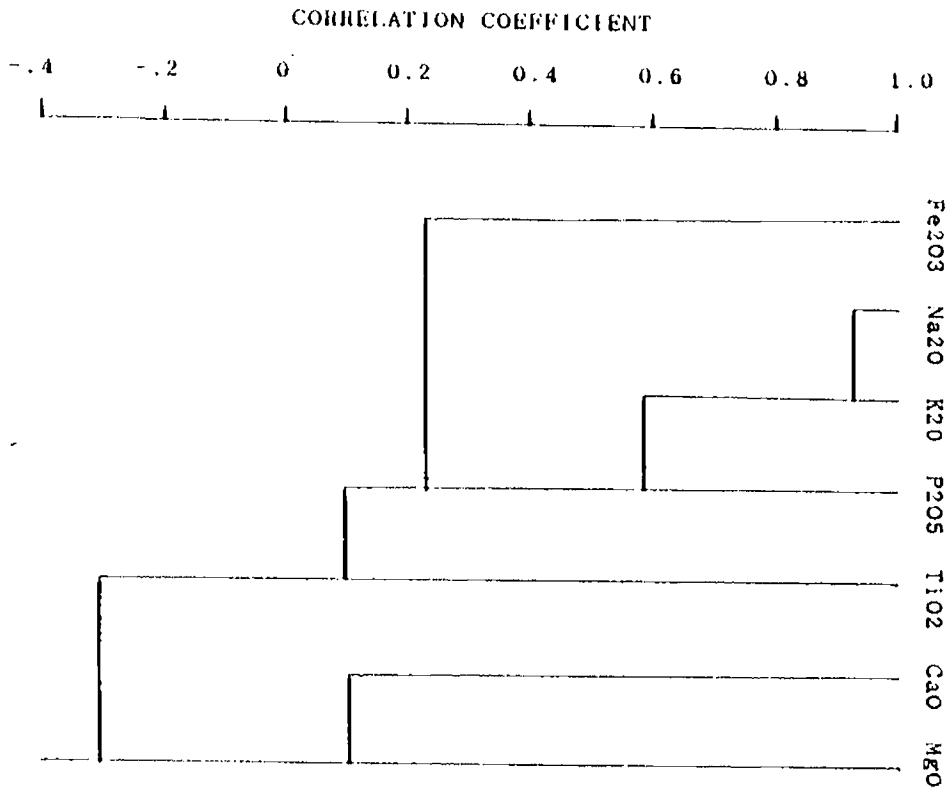

Fig. 5.9 Dendrogram of chemical composition of mud bank sediments

occurrence of Fe_2O_3 in the silt fraction owes its origin to the terrigenous minerals such as ilmenite, pyroxenes and amphiboles.

Sediment suspension in mud bank: Different views have been expressed regarding cause and maintenance of mud bank suspension. Du Cane *et al.*, (1938) attributed the suspension to the wave turbulence during monsoon. But during the active phase of mud bank, wave activity is considerably low due to wave energy dissipation; hence incapable of churning the sea bed. Varma and Kurup (1969) stressed the need of a continuous supply of suspended sediment to the mud bank region. Kurup (1977) opined that, the suspension in mud bank is nothing but "plume formations of a larger scale associated with convergence of littoral currents and the resulting offshore (rip) flows". Though, Reddy and Varadachari (1973) reported convergence of littoral currents at several points along the Kerala coast from wave refraction pattern, strong offshore currents were not observed in mud banks (Mathew, 1992). In this context, other possibilities need to be verified.

When clay particles (micelles) are in suspension, they do not settle individually but flocculate into agglomerates in response to a combination of chemistry and clay mineralogy of the sediments, and salinity of the media (Van Olphen, 1977). During monsoon, the salinity decreases considerably due to heavy precipitation (Kurup, 1977). This in turn stimulates the process of dispersion and the continued suspension of clay particles. Ramachandran (1989) argued that, the initial triggering that brings the suspension can only be explained in terms of physical action during the onset of southwest monsoon, but the sustenance of suspension could be through a chemical mechanism.

Source of mud for the mud bank: The investigation at Alleppey enumerates that, the nearshore area experiences mud deposition. But, pertaining to the probable source of mud for contemplating a drastic deposition in mud bank, researchers stipulated various hypotheses. It was postulated that the mud banks are formed by the flow of mud from the backwaters by hydraulic pressure through some subterranean channel in a narrow strip of land that separate the backwater from the sea (Bristow, 1938). Such a possibility was discredited by many in the later years. Du Cane *et al.* (1938) pointed out that the sediments from the backwater is quite different from that of mud bank area, the former contains high percentage of carbon and is full of vegetable debris. Coggin Brown (In: Du Cane *et al.*, 1938) attributed the source of mud in mud bank to the laterites based on the observed similarity in the chemical composition of laterites and the mud. But the argument can not supplement a drastic supply of sediments just at the onset of monsoon to the localities of mud bank formation. Further, it can not justify the localised formation of mud bank, and especially off the backwater backed zones of Cochin and Purakkad stretch.

There is no direct influx of fluvial sediments into the sea along the 85 km long coastal stretch extending from Cochin to Thottappally as all the rivers in this part discharges into the Vembanad Lake. Hence, the sedimentation pattern is mainly controlled by the innershelf hydraulic regime. Shideler (1978) proposed that pattern of dispersal of fine-grained sediments can be derived from a isopleth map of silt/clay ratio of the sediments. The silt/clay ratio map (Fig. 5.10) shows a decreasing tendency towards the central part, suggesting the direction of dispersal of finer materials. Dearth of direct influx of river sediments in this area, necessitates a sediment dispersal pattern essentially to be maintained by onshore-offshore transportation of mud

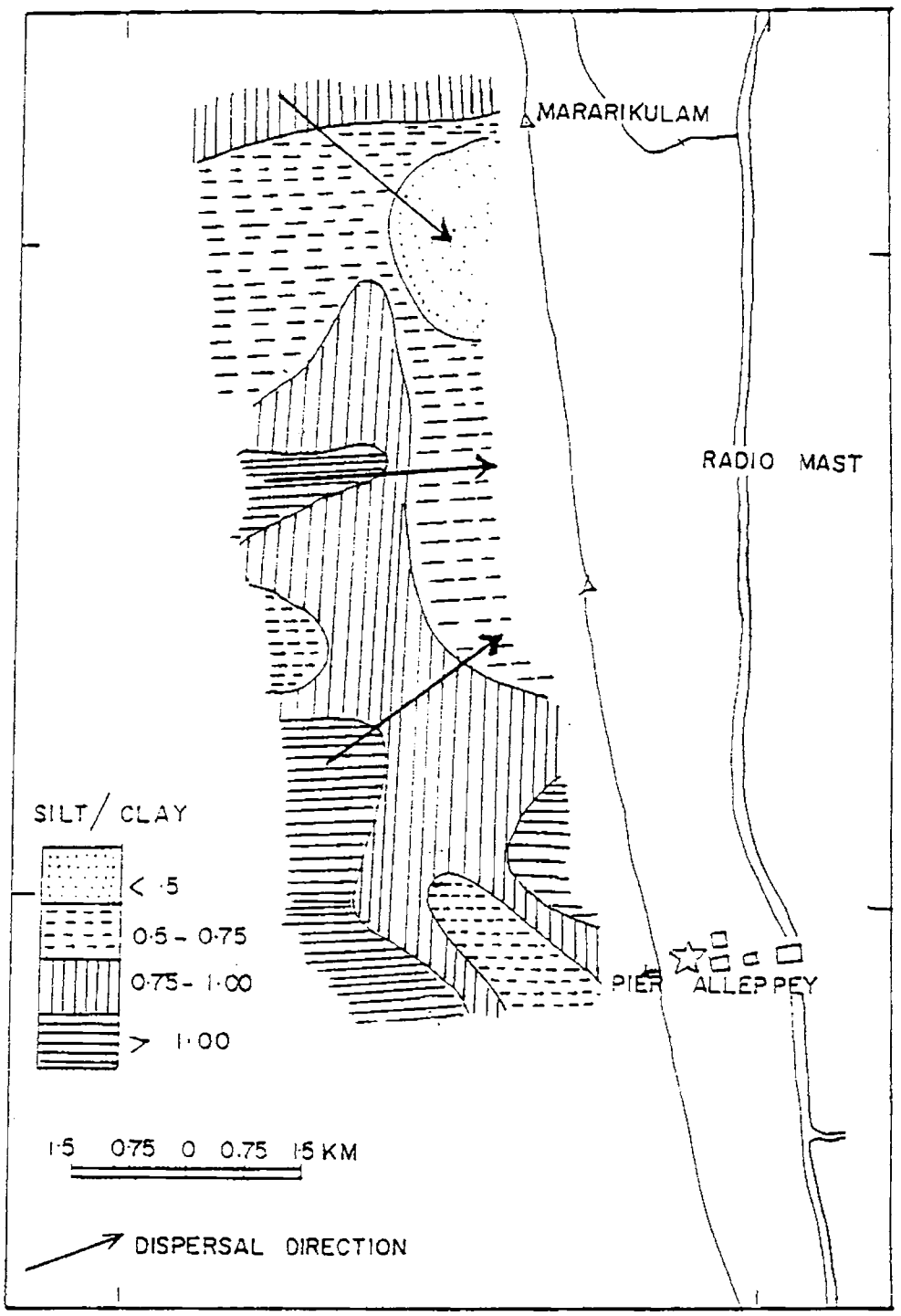

Fig. 5.10 Dispersal pattern based on silt/clay ratio

from the shelf by waves and currents. Prabhakar Rao (1968) has reported that mud flats off Varkala extend further north in the offshore. This may act as the probable source of mud for the mud bank region (Ramachandran and Mallik, 1985). The sediment distribution map in the innershelf extending from Narakkal to Purakkad also suggests that, clay-rich sediments are abundant in the innershelf (Fig. 2.6), barring an elongated sand-rich zone in the southwestern portion. Similarity observed in the proportions of the chemical constituents of mud bank and innershelf sediments also supports that the source of mud in mud banks are of innershelf origin.

The wave climate on the shelf waters off the west coast of India indicates strong seasonality and consists of a combination of long period swells and sea waves during the monsoon. Especially during the onset of monsoon, wave height was found to be higher. Mathew (1992) is of the view that, such a wave pattern can exert shear stress at the bottom, which can overcome the binding force of the individual particles in the cohesive bottom sediments. This wave-mud interaction accelerates the bed erosion process at the offshore, which can happen either by particle-by-particle suspension or by bed fluidisation. Nair and Hashimi (1987) opined that though the period of the monsoon is considerably shorter (three months) than the total fair weather period of nine months, the total energy (in qualitative forms) expended on the sea floor and the resulting sediment distribution will be greater during the monsoon months than that expended during the fair weather months. The energy thus expended transforms the physical characteristics of the bed. The sediment samples analysed from the mud bank region yielded a high water content (70 - 85 %), which is an indication to the fluidisation of the cohesive bed. The fluidised sediment then get transported to the nearshore region *en masse*. A combination of wind-drift (current

associated with the strong onshore winds during the southwest monsoon) and wave-drift currents can transport the sediment once set into motion (Nair and Hashimi, 1987).

Orbital velocity associated with waves at different depths for the most possible periods and wave height during monsoon along this coast are computed using the formula given by Dyer (1986) and is given in Table 5.9. The computation is restricted up to 30 m contour, mainly because, the sediment distribution pattern described in the second chapter depicts a linear patch of sand extending beyond 30 m depth parallel to the coast. Waves of 3 m height with period of 12 s gives an orbital velocity of 61.4 cm/s even at a depth of 30 m. The speed required to initiate the movement of sediments consisting mainly of silts and clays with varying proportion of sand ranges from 20 to 100 cm/s (Nair and Hashimi, 1987). Hence there is a possibility of initiating movement of sediments at the bed right from the 30 m depth. Sediment transport along the direction of wave propagation could be possible even with a lower shear velocity as bulk density of the fluidised bed is considerably less. Apart from the onshore component generated by waves, coastal currents which intensify during the monsoon, also contribute to the transportation of sediment to mud bank locations. The sediment transport model explained in the second chapter discerns a low energy southward movement of sediments in the nearshore waters of < 15 m depth. Though the sand-rich zone starts from 20 m isobath in the innershelf region off Alleppey (Fig. 2.6), piling up of mud at the mud bank location can be facilitated by removal of mud from the immediate offshore and longshore transport by currents. This proposition is supported by the dispersal pattern surmised from the silt/clay map (Fig. 5.10).

TABLE 5.9

Orbital velocity for different depths, periods and wave heights

Depth	5m	10m	15m	20m	25m	30m
			T = 6 seconds			
H	1.00	1.00	1.00	1.00	1.00	1.00
L	38.07	48.37	53.03	55.00	55.74	56.02
U	56.80	30.90	18.20	10.80	6.30	3.60
H	2.00	2.00	2.00	2.00	2.00	2.00
L	38.07	48.37	53.03	55.00	55.74	56.02
U	113.60	61.70	36.50	21.50	12.65	7.20
H	3.00	3.00	3.00	3.00	3.00	3.00
L	38.07	48.37	53.03	55.00	55.74	56.02
U	170.30	92.60	54.70	32.30	18.95	10.90
			T = 9 seconds			
H	1.00	1.00	1.00	1.00	1.00	1.00
L	60.38	81.68	95.51	105.14	111.90	116.72
U	64.20	41.20	30.20	23.30	18.30	14.50
H	2.00	2.00	2.00	2.00	2.00	2.00
L	60.38	81.68	95.51	105.14	111.90	116.72
U	128.30	82.40	60.40	46.50	36.60	28.90
H	3.00	3.00	3.00	3.00	3.00	3.00
L	60.38	81.68	95.51	105.14	111.90	116.72
U	192.50	123.60	90.70	69.80	54.90	43.40
			T = 12 seconds			
H	1.00	1.00	1.00	1.00	1.00	1.00
L	82.00	113.20	135.30	152.30	165.85	176.90
U	66.70	44.80	34.70	28.40	23.90	20.50
H	2.00	2.00	2.00	2.00	2.00	2.00
L	82.00	113.20	135.30	152.30	165.85	176.90
U	133.40	89.70	69.40	56.80	47.80	40.90
H	3.00	3.00	3.00	3.00	3.00	3.00
L	82.00	113.20	135.30	152.30	165.85	176.90
U	200.10	134.50	104.10	85.20	71.80	61.40

H = Wave hieght in meters; L = Wave length in meters;
U = Orbital velocity in cm/s; T = Wave period

The source and dispersal pattern of the mud bank sediments discussed above explain the localised distribution of mud bank, which many other theories have failed to contain. The locations of mud banks are decided essentially by the locations where the mud get piled up during the southwest monsoon. This is mainly due to the effect of the wave energy distribution and transport pattern, which facilitate deposition of the mud eroded and transported from the offshore and alongshore. This view has been corroborated by wave refraction studies carried out by Mathew (1992).

Removal of mud from mud bank locations during post monsoon: Most of the researchers agree that the mud is deposited in mud bank locations during southwest monsoon, though opinion differs on the source and mode of deposition. If the mud get accumulated in such locations year after year during monsoon, then the accretion in the nearshore should result into a shoal. But such a disposition in the nearshore is not observed. At the same time, the subsequent history of the mud, following the cessation of mud bank has not been dealt by earlier observers. Here an attempt is made to investigate the nature of sedimentation in the Alleppey mud bank area during the post-monsoon season in comparison with the monsoon data.

The bathymetric details of Phase I and Phase II survey in the Alleppey mud bank location illustrates that, post-mud bank profiles depict removal of mud from the location. Detailed textural attributes of the sediments of Phase II are utilized to enumerate the processes of sediment removal, due to dearth of current data.

Though the textural distribution pattern (Fig. 5.8) shows notable differences, no systematic change is evident in the grain size characteristics

of the surficial sediments during both the phases. Hence, hydrodynamics of the transport and deposition are evaluated based on the results obtained from the detailed textural analysis of the post-mud bank (Phase II) sediments.

Mean size varies between 5.6 ϕ and 9.87 ϕ with an average value of 8.27 ϕ (Table 5.10). The sediments are dominantly clay with sporadic patches of high percentage of sand and silt. Abrupt changes in the spatial variation of mean size are noticed from Table 5.10. Such distribution probably reflect various levels of mixing of clastic particles from multiple sources deposited under processes of diverse intensities. The histogram of mean size indicates that the major part of the sediments is clustered between 8 and 9 ϕ (Fig. 5.11a). The sediments are poorly sorted as the sorting values vary between 2.14 and 3.16. Sorting shows clustering of values around 2.75 to 3.75 (Fig. 5.11b). This values are considered as characteristic of neritic silts and clays (Folk, 1974). In general, the sediments are negatively to very positively skewed (Fig. 5.11c). The southern area shows an abundance of coarser materials when compared to the northern sector. Spread of size frequency over large size classes is indicated by platy/very platykurtic nature of the samples (Fig. 5.11d). This implies a poorer sorting presumably resulted from sediments deposited under diverse physical processes. The size frequency distribution curves show multi-peakedness around various phi classes (Fig. 5.12). This amply supports the view that, lack of systematic fractionation imparts a mixed nature to the sediments. Such a pattern of distribution hints transportation of sediments in flocculated form rather as individual particles due to cohesion.

Further, CM, LM and AM diagrams are constructed to decipher the processes involved in resulting the textural heterogeneity of the sediment

TABLE 5.10

Grain Size Parameters of Alleppey Phase II Samples

Sample	Mean	Std.Dev.	Skewness	Kurtosis
1	9.00	2.93	0.21	0.80
2	8.35	3.11	0.26	0.70
3	5.60	2.14	0.56	1.99
4	7.97	3.52	0.25	0.72
5	6.95	3.40	0.37	1.06
6	8.67	2.82	0.30	0.87
7	8.72	2.92	0.35	0.77
8	9.42	2.61	0.17	0.65
9	7.95	3.55	0.32	0.59
10	8.93	3.10	0.02	0.67
11	8.10	3.42	0.15	0.72
12	9.35	3.39	-0.30	0.76
13	7.42	3.23	0.43	0.70
14	6.90	3.43	0.58	0.68
15	8.17	3.49	0.11	0.63
16	8.67	3.19	-0.11	0.68
17	9.38	2.89	-0.06	0.75
18	9.83	2.44	0.06	0.96
19	8.67	3.35	-0.14	0.68
20	7.37	3.53	0.36	0.65
21	9.52	2.96	-0.10	0.70
22	8.48	3.65	-0.11	0.87
23	9.50	3.05	-0.17	0.87
24	6.00	3.08	0.69	0.96
25	9.87	2.86	-0.21	0.82
26	6.53	3.55	0.59	0.67
27	6.25	3.45	0.63	0.76
28	8.67	3.39	-0.03	0.67
29	8.85	3.37	-0.12	0.57
30	8.88	3.25	-0.06	0.69
31	8.33	3.49	0.01	0.84
32	9.62	2.99	-0.17	0.77

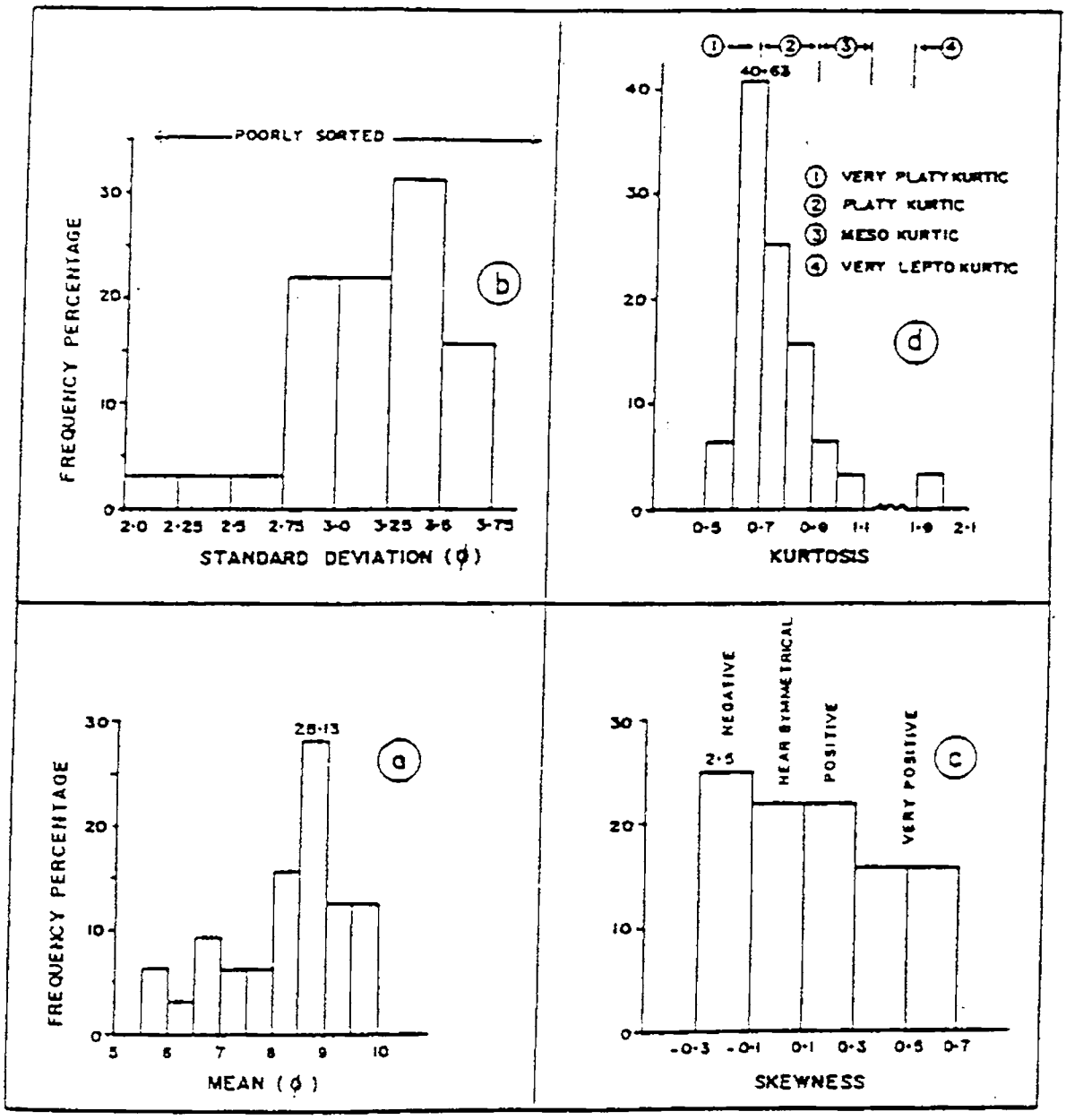

Fig. 5.11 Frequency distribution of size parameters in the Phase II samples of Alleppey mud bank area

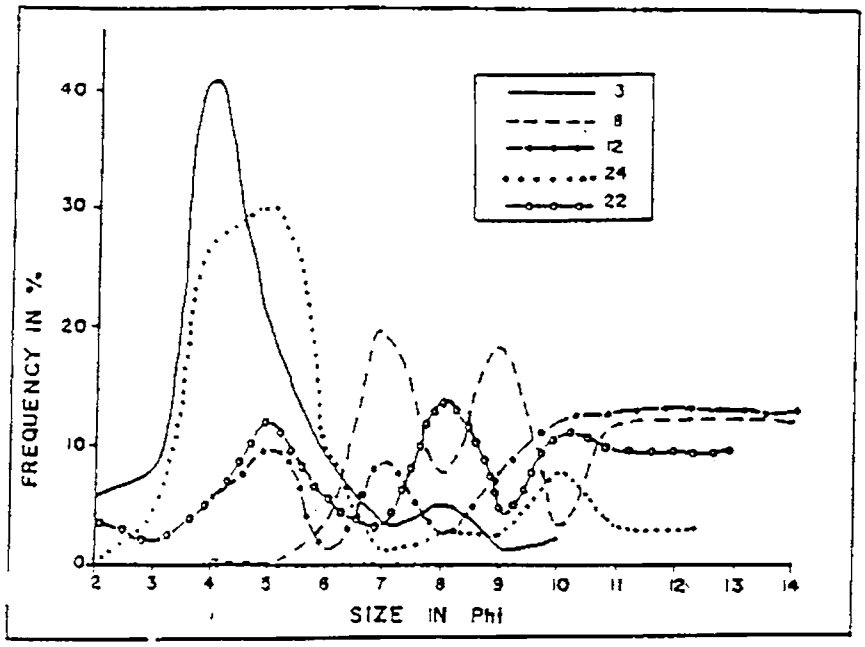

Fig. 5.12 Size frequency distribution of some samples in the Phase II of Alleppey area

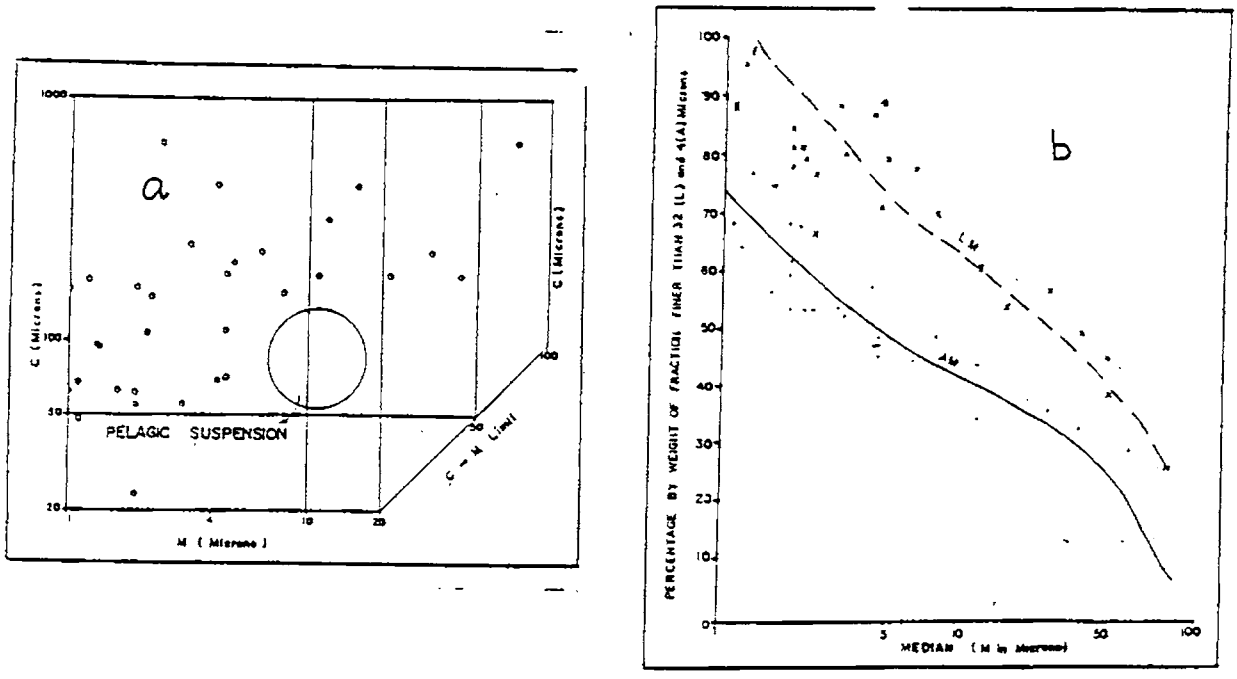

Fig. 5.13 (a) CM pattern, (b) LM and AM diagram of Phase II samples

composition. Majority of the samples points are located surrounding the pelagic suspension zone (Fig. 5.13a). A few sample points also fall in the uniform suspension zone. From this, it can be inferred that, the main process of transportation of the sediments is in a pelagic suspension state and to a lesser degree uniform suspension. While, CM diagrams typically represents the coarser half of the textural population, the LM and AM diagrams represent the finer part of population of a deposit. Plots of percentage of fractions finer than 32 μ and 4 μ in the sediments (L and A) and M, the median in a semi-logarithmic graph are considered as an effective tool to identify the mode of deposition of a wide variety of environments (Passega and Byramjee, 1969). Like CM pattern, the LM and AM diagrams also show considerable degree of scattering (Fig. 5.13b). Especially in the case of the samples with fine median size, both LM and AM plots show maximum scattering. This indicates that, with a finer median, lutite percentage indicates a poorer sorting for silt-sized materials. This could be due to (i) panning of sand-sized materials by waves and (ii) resuspension and transportation of finer particles offshore and alongshore probably in flocculated form, thus leaving behind silt-sized materials.

A model suggested by McLaren and Bowles (1985) is used here to understand the transportation mechanisms of the sediments. Details of the model were discussed in the second chapter. The progressive changes in the textural characteristics were drawn with a basic assumption that, compared to heavier grains, lighter grains are easily lifted, transported and deposited in the down drift side. Sediment pathways are derived from the downdrift variation of the moment statistics (Table 5.11), viz., mean (first moment), sorting (second moment) and skewness (third moment), as moment measures are more realistic than graphic measures in accounting for the sediment pathways

TABLE 5.11

Moment Measure Size Parameters of Alleppey Phase II Samples

Sample	Mean	Std.Dev	Skewness
1	9.05	3.08	-0.21
2	8.70	3.06	0.10
3	4.56	2.17	1.39
4	8.27	3.53	0.01
5	6.68	3.36	0.47
6	8.62	2.83	0.24
7	8.78	2.92	0.16
8	9.57	2.55	0.05
9	8.26	3.65	0.09
10	8.88	3.03	-0.03
11	8.05	3.30	0.14
12	9.50	3.09	-0.18
13	7.34	3.26	0.55
14	6.98	3.21	0.49
15	8.20	3.46	0.07
16	8.65	2.88	-0.09
17	9.48	2.68	-0.27
18	9.70	2.32	-0.25
19	8.17	3.24	0.12
20	7.36	3.56	0.32
21	9.34	2.84	-0.24
22	8.40	3.45	-0.25
23	9.47	2.82	-0.39
24	5.91	3.06	1.14
25	9.67	2.79	-0.35
26	6.49	3.67	0.65
27	6.27	3.42	0.75
28	8.72	3.30	-0.03
29	8.77	3.31	-0.07
30	9.05	3.06	-0.20
31	8.40	3.27	-0.10
32	9.62	2.84	-0.45

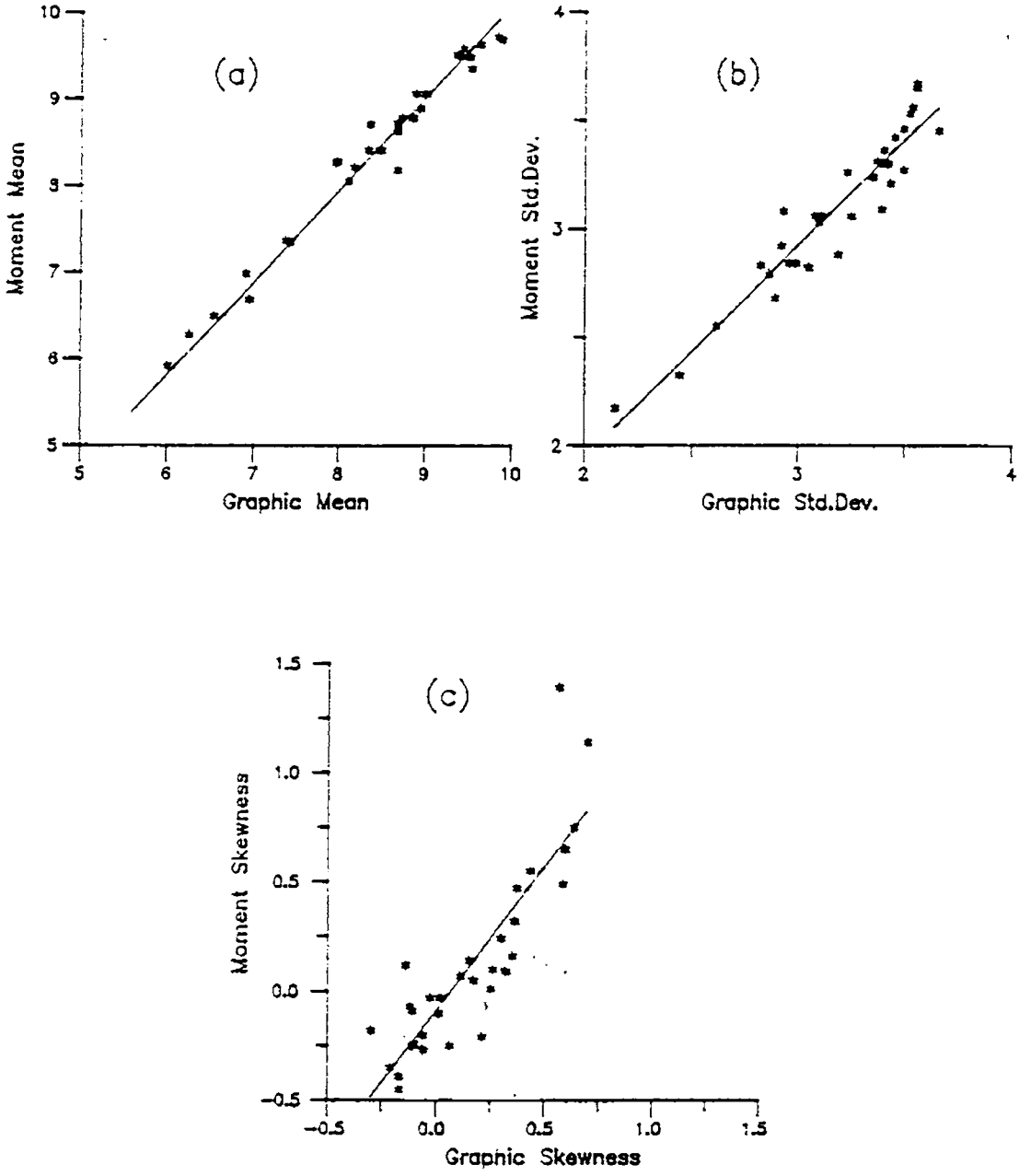

Fig. 5.14 Relationship between graphic and moment measures

(McLaren, 1981). A comparison is attempted to correlate the moment measures with graphic measures, the graphic plots of which are given in Fig. 5.14. The plots are comparable with Fig. 2.19 obtained for the innershelf sediments. Mean and standard deviation give a one-to-one correlation devoid of larger dispersion from the fit-line. But skewness shows smaller dispersion, unlike the innershelf plot, probably because the range of skewness values in the case of later is wider than the former. This implies that, if the parameters are within a smaller range, even the graphic measures will suffice for elucidating the transport model.

By considering better sorting as the criterion, when the mean size, sorting and skewness are compared for two samples of adjacent locations, out of the eight possible trends, two possible cases are selected as is the case described in Chapter 2. They are, towards the direction of flow, the sediment becomes (i) finer, better sorted and more negatively skewed (Case B) and (ii) coarser, better sorted and more positively skewed (Case C).

Sediment pathways were worked out along the 5, 8, 10 and > 10 m bathymetric contours where the sediments are highly mobile. The contours were identified by taking into consideration the control of bathymetry over erosion/deposition. Table 5.12 summarizes the pairs producing transport trends along the isobath. Fig. 5.15 demonstrates significant variations in directions of transport at 5, 8, 10 and > 10 m isobaths. The 5 m contour, which shows a very significant northward Case B trend, denotes decreasing energy conditions towards the flow direction, whereas the Case B trend in both south and north directions also suggests the occurrence of low-energy transport regime at 8 m isobath. A Case C southerly trend which is significant at 0.01 level is observed at 10 m indicating a difference in the

TABLE 5.12

Summary of number of pairs producing transport trends

	5 m line		8 m line	
	North trend	South trend	North trend	South trend
Case B	N = 28 X = 12 Z = 4.86"	N = 28 X = 6 Z = 1.43	N = 28 X = 11 Z = 4.29 "	N = 28 X = 9 Z = 3.14"
Case C	N = 28 X = 3 Z = -0.29	N = 28 X = 4 Z = 0.29	N = 28 X = 1 Z = -1.43	N = 28 X = 1 Z = -1.43
	10 m line		> 10 m line	
	North trend	South trend	North trend	South trend
Case B	N = 28 X = 5 Z = 0.88	N = 28 X = 5 Z = 0.88	N = 28 X = 12 Z = 4.86"	N = 28 X = 7 Z = 2.00'
Case C	N = 28 X = 2 Z = -0.86	N = 28 X = 12 Z = 4.86"	N = 28 X = 2 Z = -0.86	N = 28 X = 4 Z = -0.29

' Significant at 0.05 level, " Significant at 0.01 level

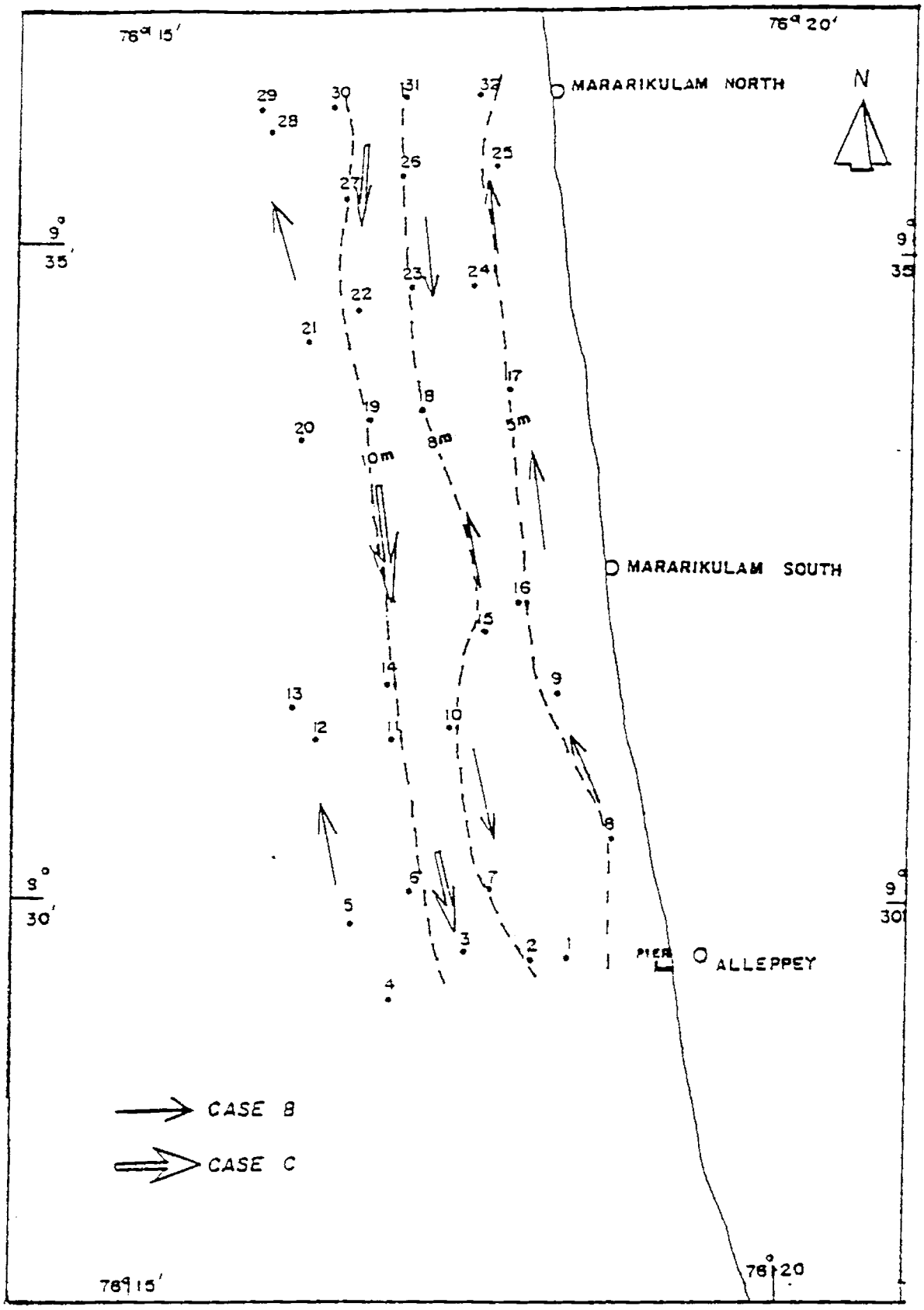

Fig. 5.15 Sediment transport directions for 5, 8, 10 and >10 m depth contours.

energy level. A northerly reversal of current with a less significant southerly component which is observed at >10 m, indicates a further change in the energy conditions (Case B) of the area. From the foregoing discussion on the sediment pathways in the innershelf, it is clear that the net transport direction is southerly within the 15 m isobath. The overall picture of sediment dispersal for the Alleppey nearshore is found to be northerly, which seems to contradict the previous observation. But the data on the innershelf is collected during October 1984 against the Alleppey nearshore, which is collected in December 1983. Previous studies indicate intensification of northerly current during December. So it is presumed that, the transport direction in the Alleppey nearshore is the manifestation of localised seasonal transport phenomena. Monsoon transport being the strongest one, the net southerly transport pattern described for the innershelf is fully justifiable.

In general 5 and > 10 m isobaths show a northward low-energy transport direction. Similarly, Samsuddin and Suchindan (1987) reported the occurrence of northerly longshore currents during the post-monsoon season along the Kerala coast. Since there are no rivers directly debauching into the sea along this coast, it is presumed that the sediment budget in this nearshore area is mainly influenced by the onshore-offshore-longshore transport regimes. The region, which has a wide surf zone with persistent breaking of incident surface waves, provides sufficient momentum for the generation of alongshore currents and foreshore circulation cells. Ramachandran and Mallik (1985) reported an offshore sediment source and rapid sedimentation in the mud bank region during the monsoon season. Cessation of monsoon results in the reversal of longshore currents and marked variations in the energy distribution along the coast (Samsuddin and Suchindan, 1987). Shoaling waves which induce shoreward bottom currents,

not only tend to keep the sands nearer the shore, but also act on the nearshore bottom, thus keeping the fine materials in suspension. The shoreface movement of the sand is compensated by a seaward counter current, initiating seaward transportation of the suspended materials. Rip currents also contribute to the offshore transport of the sediments. The low-energy northerly flow direction derived from the sediment pathways coincides with the northerly longshore current of post-monsoon season observed by Samsuddin and Suchindan (1987) and Baba (1988). The change in the overall circulation pattern of the coastal circulation in the Indian Ocean towards north by late October reaffirms the above view (Rao *et al.*, 1983).

The Alleppey nearshore sediments which are highly cohesive in nature are unlikely to get eroded, unless the bed shear stresses are drastically increased due to storm-induced currents. However, sudden storm surges are a rarity along the west coast of India. Hence the question of storm surge in augmenting the resuspension of the materials is ruled out. It is inferred that due to the decrease in the interstitial water contents, the bulk density of the sediments (which is normally around 1.25 g/cc), is found to increase during the post-monsoon season. Thus the increase in the bulk density of the sediments helps in the resuspension of the particles, which are transported seaward and alongshore by the prevailing longshore/offshore currents. This is evidenced by the smoothening of nearshore sea bed marked by shift in the bathymetric contours (Fig. 5.2).

5.3.2 Quilandy mud bank

Geomorphological set up of Quilandy area is widely different from that of Alleppey. While Alleppey area is part of a backwater/barrier beach system,

without direct influx of any river, Quilandy is characterised by fluviatile influence. But Quilandy area is also known for persistent occurrence of mud banks. Following sightings of a mud bank at Quilandy by the local fishermen and the Port Officer of Kozhikode (Rajan, personal communication., 1984), the present study was taken up. This is to have a brief understanding of the sedimentological aspects of the mud bank phenomenon and also to make a comparative evaluation of Alleppey and Quilandy mud banks. This is especially meant to identify the parameters that essentially contribute to the formation of mud banks. Moreover, there are not much work done in this direction and the mud banks investigated in the northern Kerala coast is sparse.

Fig. 5.3 shows the sampling locations, bathymetry and also the drainage pattern of the study area. 9 m contour is more or less parallel to the coast. But all other contours show considerable irregularity. At the seaward portion of the norther part, a shoal formation at 7 m contour is observed. The coast-line itself is not straight, with rocky stacks at the norther tip, where the light house is situated. Rocky exposures are seen along the coastline at Kadalur and Kollam.

The Chaliyar river is the main river in the study area (Fig. 5.3). The drainage areas of the Korapuzha, the Kallai, the Chaliyar and the Kadalundi rivers comprise the Greater Chaliyar basin, having a total area of 4765 km^2 (Public Works Department, 1974). The annual sediment discharge through the streams and backwater outlets is considered to be high and a major part of the sediment input into the coastal water takes place during the monsoon.

Sediment texture: Table 5.13 gives the result of granulometric studies of sediment samples. In general, predominant constituent of the sediment is clay

TABLE 5.13

Sand-silt-clay percentages in the surface sediments of Quilandy Samples

Sl.	Sample	Sand (%)	Silt (%)	Clay (%)	Texture Description
1	C1	56.58	32.75	10.67	Silty Sand
2	C2	41.91	37.51	20.58	Sand-silt-clay
3	C3	63.84	29.29	6.87	Silty Sand
4	C4	30.09	41.51	28.40	Sand-silt-clay
5	C5	12.54	46.51	40.95	Clayey Silt
6	C6	12.24	18.00	69.77	Silty Clay
7	C7	40.25	39.89	19.86	Silty Sand
8	C8	44.97	35.47	19.56	Silty Sand
9	C9	5.35	8.20	86.45	Clay
10	C11	58.46	18.97	22.57	Clayey Sand
11	C12	24.55	34.25	41.20	Sand-silt-clay
12	C13	38.72	40.77	20.57	Sand-silt-clay
13	C14	5.09	44.20	50.71	Silty Clay
14	C15	25.59	43.91	30.50	Sand-silt-clay
15	C16	5.83	42.18	51.99	Silty Clay
16	C17	32.76	25.32	41.92	Sand-silt-clay
17	C18	0.86	12.53	86.61	Clay
18	C19	3.22	7.35	89.43	Clay
19	C20	0.95	6.47	92.58	Clay
20	C21	0.64	7.23	92.14	Clay
21	C24	0.21	17.71	82.04	Clay
22	C25	1.69	23.28	75.03	Clay
23	C26	2.84	6.25	90.91	Clay
24	C27	1.64	44.73	53.63	Silty Clay
25	C28	1.67	26.12	72.21	Silty Clay
26	C29	3.27	21.06	75.67	Clay
27	C30	4.48	20.06	75.46	Clay
28	C31	2.21	12.80	84.99	Clay
29	C32	21.34	33.35	45.31	Sand-silt-clay
30	C34	47.77	15.40	36.83	Clayey Sand
31	C35	51.00	27.81	21.19	Sand-silt-clay
32	C36	12.83	20.31	66.86	Silty Clay
33	C38	1.39	30.38	67.23	Silty Clay

followed by silt and sand. Based on the percentages of clay, silt and sand, individual distribution maps have been prepared (Fig. 5.16a-c). These size distribution maps help in delineating different sediment facies. Percentage of clay varies between 6.87 and 92.58 with more than half of the area containing > 60 % clay. Maximum clay concentration is at central part and decreases towards the northern and southern ends. Silt percentage varies from 6.25 to 46.51. Silt-sized particles are of high concentration in the northwestern and southeastern portions compared to the central part. More than half of the area is covered with sediment types containing < 20 % of silt. Sand content in the sediment ranges from 0.21 to 63.84 %. In contrast to clay distribution, sand is found to be more concentrated in the northern and southern flanks. About half of the study area consists of sediments with < 10 % sand. Frequency distribution of sand, silt and clay and also ternary plot of the textural composition following Shepard's (1954) scheme are presented in Fig. 5.17. The disposition of the sample points enumerates that, clay is the most dominant sediment type, followed by silty clay and sand-silt-clay. Silty sand and clayey sand textures are also observed with lone sample falling in the clayey silt category.

Sediment distribution: Aerial variation in texture of the sea bed is shown in Fig. 5.18. Clay occurs in the central area and covers the major part of the study area, nearly extending to Kadalur point in the north. The central clay belt passes into the silty clay zone which narrows to the north, and widens to the south. Narrow, irregular areas of sand-silt-clay occur west and southwest of Kollam and Kadalur respectively. Small patches of clayey sand appear south of Kadalur point and southwest of Kadalur. A restricted occurrence of a small silty sand zone can be observed south of Kadalur Point.

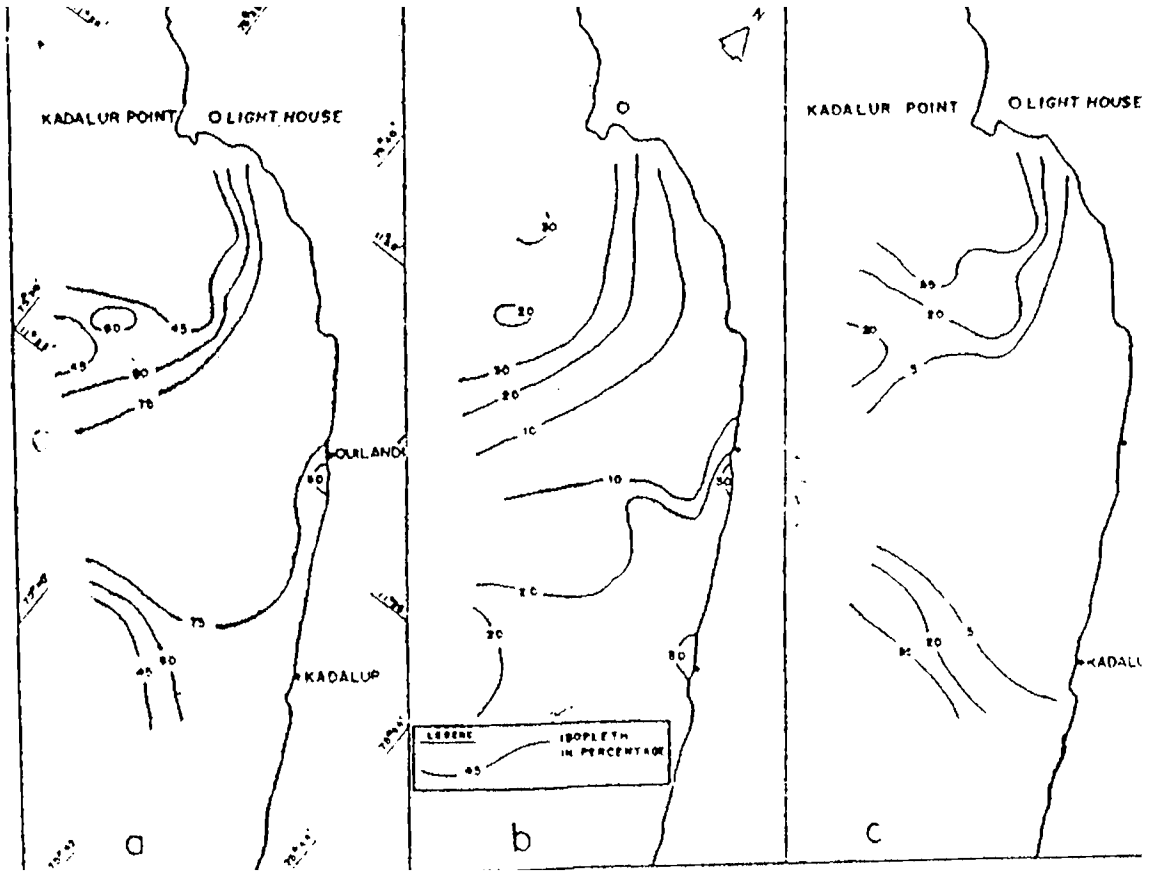
KADALUR POINT
LIGHT HOUSE
KADALUP
a
LEGEND
ISOPLETH IN PERCENTAGE
b
KADALUR POINT
LIGHT HOUSE
c

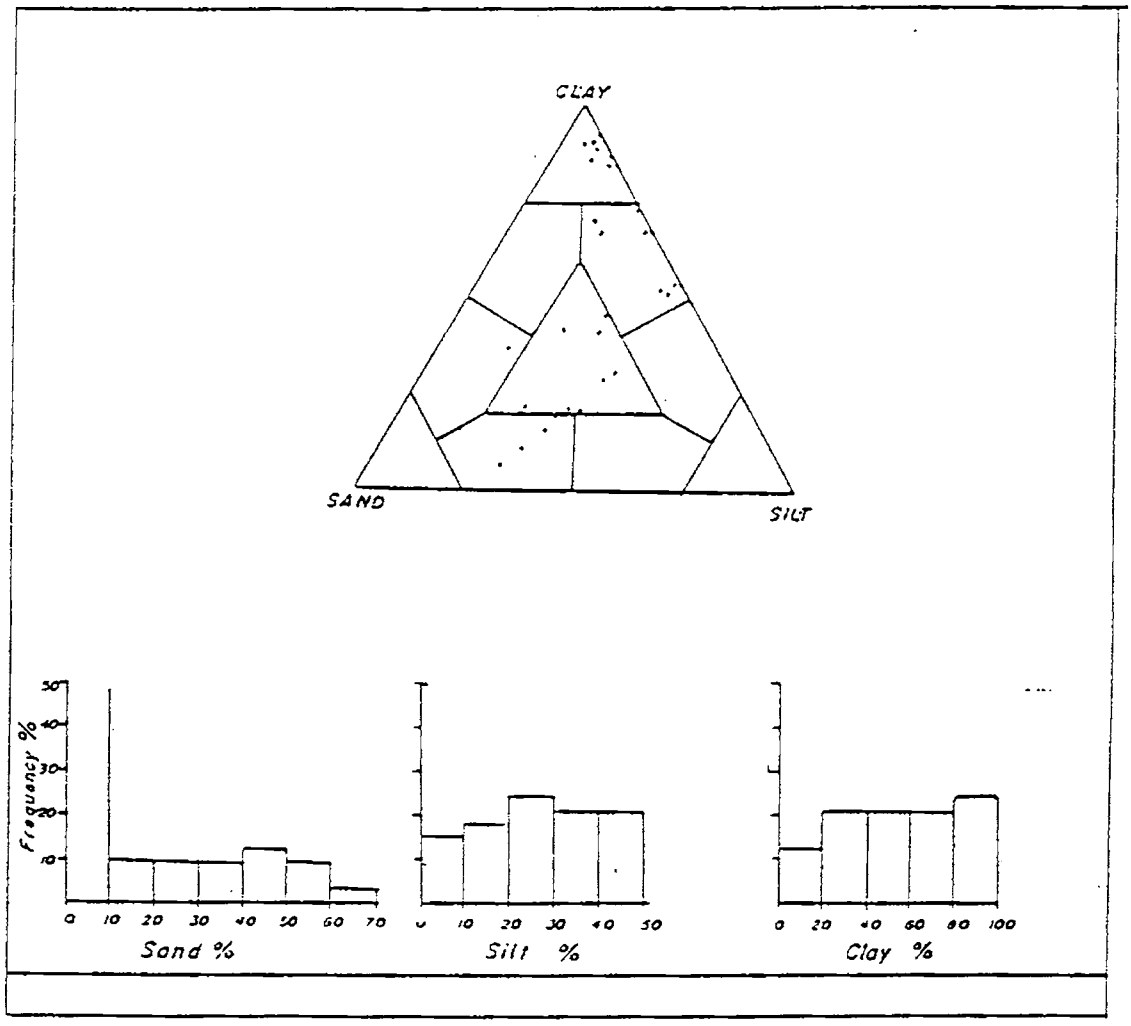

Fig. 5.17 Ternary plot and freqency distribution of sand, silt and clay in Quilandy mud bank area.

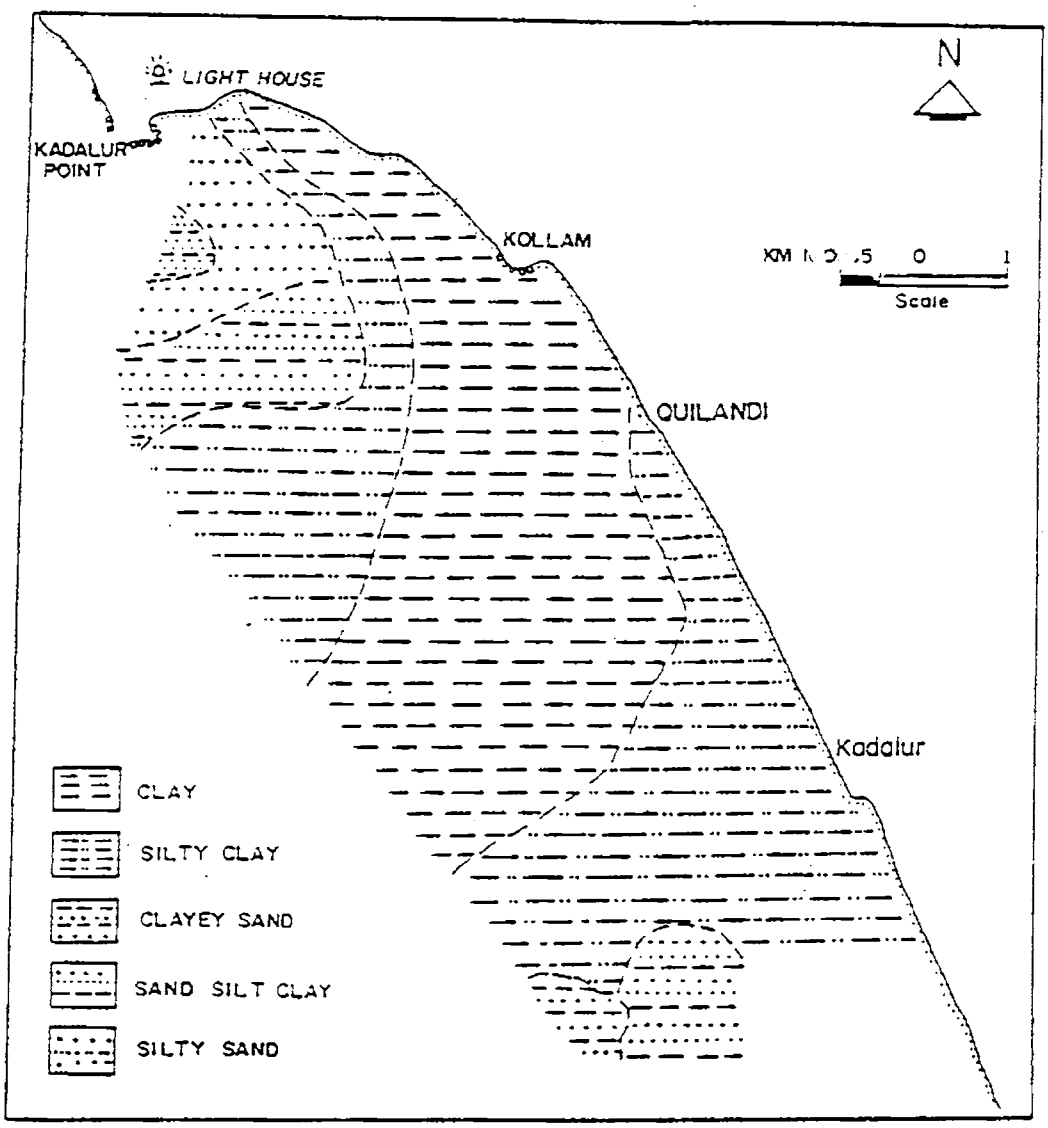

Fig. 5.18 Distribution of sediment types in Quilandy mud bank area

Sediment composition: Examination of sediment smear slides indicated iron oxides, phosphate, glauconite, framboidal pyrite, quartz and clay minerals as common constituents in all samples. Skeletal grains and other biogenic matter formed a minor portion (Maximum, 10 %) of the total composition. Foraminifera, diatoms, molluscs and brown plant matter are the chief organic component. The clay and silt are grey olive green (5GY3/2) and a weak pelleted texture in the clay can be recognised in some samples.

Sediment cores: Sediment cores up to a maximum length of 73 cm were collected and based on the overall visible macroscopic features of the texture, three distinct sediment units can be recognised in the cores (Fig. 5.19). The topmost unit is grayish olive green in colour, sticky, fairly uniform in thickness (20 - 25 cm) and with weak lamination. This unit is found throughout the entire region. The basal unit is a fine sand showing a planar and very sharp contact with the overlying clay. Core recovery from the sandy unit was poor and coring did not penetrate the entire sediment thickness. The upper most grayish clay forms a distinct wedge-shaped body with significant thickening adjacent to the shore, thinning towards the 9 m isobath. The middle clay unit is uniform in thickness and overlies the basal sand.

Regarding the composition, the sand unit contains, 50 - 55 % skeletal grains (foraminifera, molluscan fragments and other remains) as well as brown plant matter (10 - 15 %). Quartz comprises 10 - 20 % of the silicate mineral fraction, the remainder being silts and clays. Except for minor apatite in the heavy fraction, phosphate minerals are absent in the sand. All cores show a downward decrease in iron oxide and plant (cellular) materials, and the skeletal fraction remains nearly uniform (10 %) at all depths. The light sand fractions contain quartz (35 %), varying amounts of carbonate (15 - 18 %),

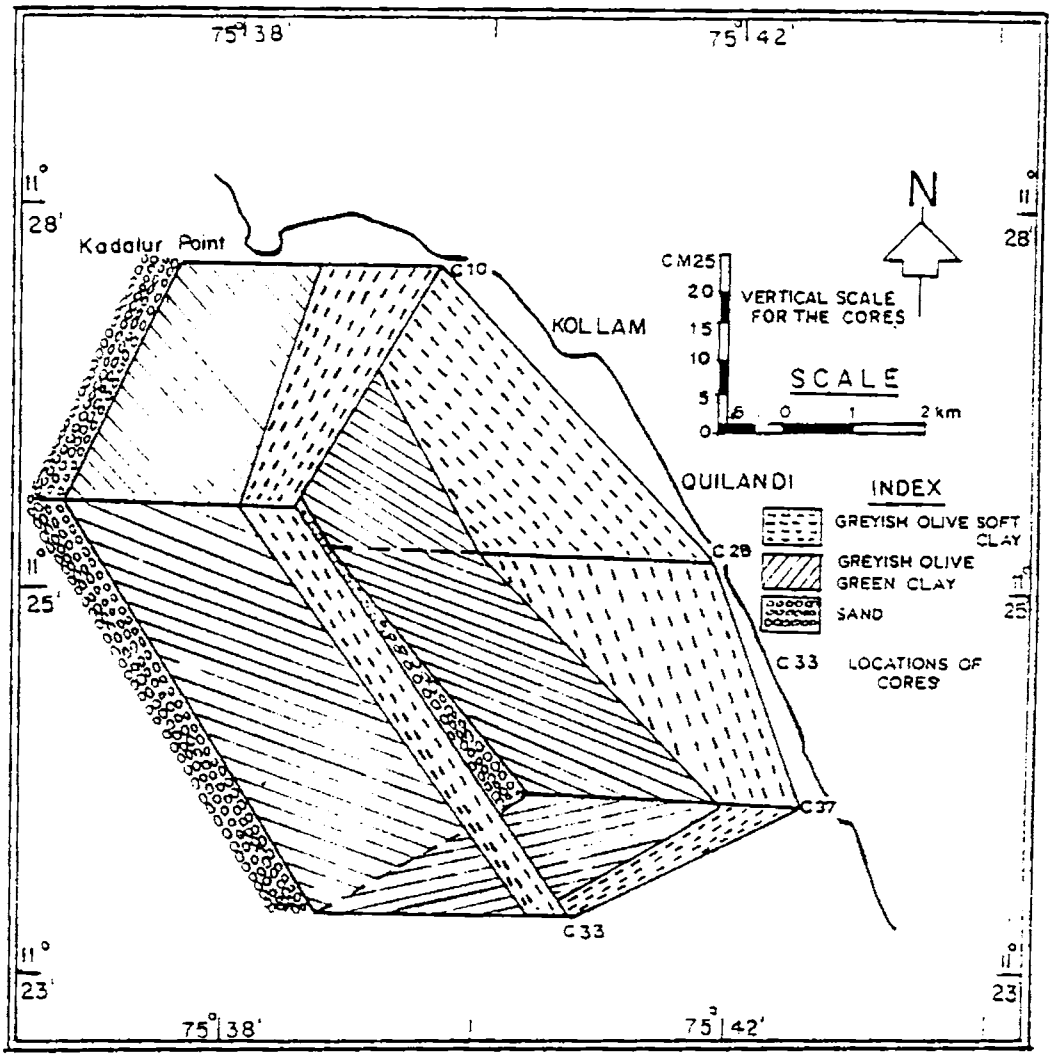

Fig. 5.19 Fence diagram of core lithology in Quilandy mud bank

brown organic (plant) matter ranging from 21 to 31 % and feldspar in minor quantities. Polychaete burrows are present in all cores located 1 km or more from the shore and except for the watery clay zone, burrow structures can be observed in all sedimentary units.

SEM analysis carried out to study the fabric of the core litho-logs were described by Mallik *et al.* (1988). Samples from the upper watery fluid clay unit were highly porous and exhibited numerous randomly disposed, small clay aggregate domains with edge-to-edge and edge-to-face contacts between the platelets. The domains appeared variable in size and in some cases individual clay grains were linked face-to-face in an offset en echelon fashion to form simple grain aggregates. Small simple plates and linked chains of clay minerals were the most visible grain aggregate morphologies. Occasional nano-plankton and diatoms appeared to be enclosed in the clay aggregates with the latter tangentially attached to the skeletal grain surfaces. In the middle clay horizon, there was a strong alignment of the clay mineral aggregates with a large number of flat, thickened plates with predominant face-to-face grain contacts. Occasional large, isolated pores between the clay aggregate were not uncommon. In contrast to the samples from the upper clay unit, the en echelon chains increased in number and size. These en echelon units cross linked with other chains form wide, platy aggregates; these aggregates in turn held in edge-to-face contact, yield a stable (cohesive) supportive framework in the sediment.

The information on the characteristics and distribution of the sediment confirms that a dominantly clay sea bed with minor amounts of silt and sand, and a water column with high suspended sediment load forms a major feature of the fluid mud areas. Based on silt and clay fractions in the surface

samples, a sediment dispersal map has been prepared following Shideler's (1978) scheme (Fig. 5.20). The silt/clay ratio ranges between 0.07 and 4.26 and the ratio gradient shows a persistent decline towards the central part of the nearshore. Reduction in silt/clay ratio in the central part appears to be due to a net transport towards this area from all sides. Also, it should be noted that the surface zone of very high turbidity develops directly over the underlying central clay zone. The sediment build up from the clay litho-logs also supports the thickening of the central part with fluidised mud attaining a maximum thickness of 40 cm, indicating a fresh deposition.

Observations suggest that fluid mud development starts from the offshore and extends landward in a nearly circular or elongate elliptical fashion to a distance of about 5 km offshore, beyond the 9 m isobath, and runs for more than 10 km along the coast. The wedge shaped geometry of the upper watery fluid clay in the fence diagram (Fig. 5.19) also suggests localised piling of mud by marine processes. The active agent may be persistent high monsoon swell. Wells *et al.* (1978) observed that normal waves change into solitary-like waves on reaching shallow water (1 - 5 m) over the clayey sea bed. Except for occasional spilling, the transformation into solitary waves cause continuous attenuation of open sea swell and a general mass transport of clay towards the shore. This mode of fine sediment transport adequately explains the shoreward thickening of water-rich mud on the sea bed as revealed in the sediment cores. The alongshore decrease in the silt/clay ratio towards the central segment of the sea bed from both the northern and southern areas suggests a net transport of fine clay to the principal site of mud suspension in the central portion, in a manner analogous to that described by Shideler (1978) on the Texas shelf.

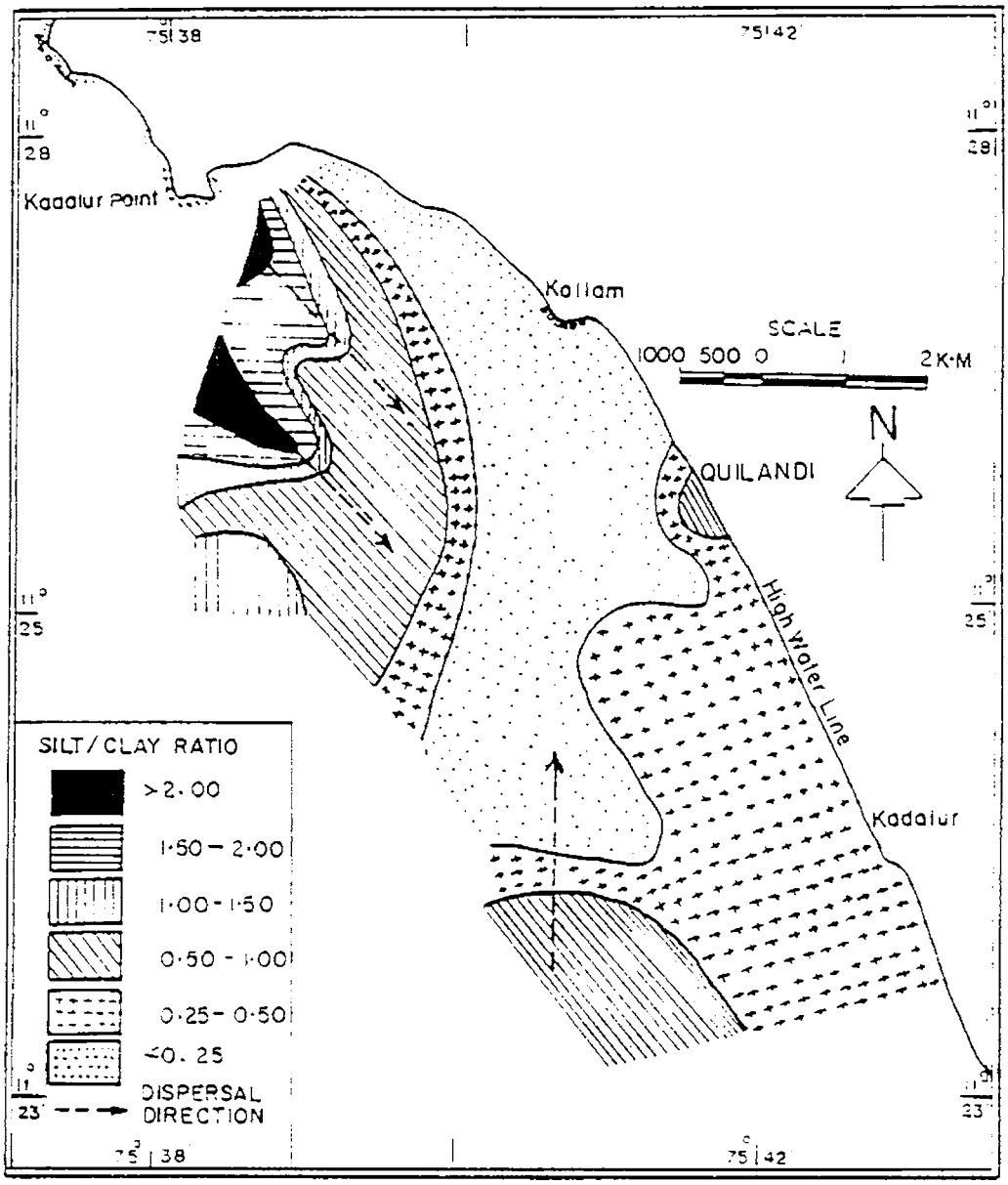

Fig. 5.20 Dispersal pattern of sediments in Quilandy mud bank based on silt/clay ratio

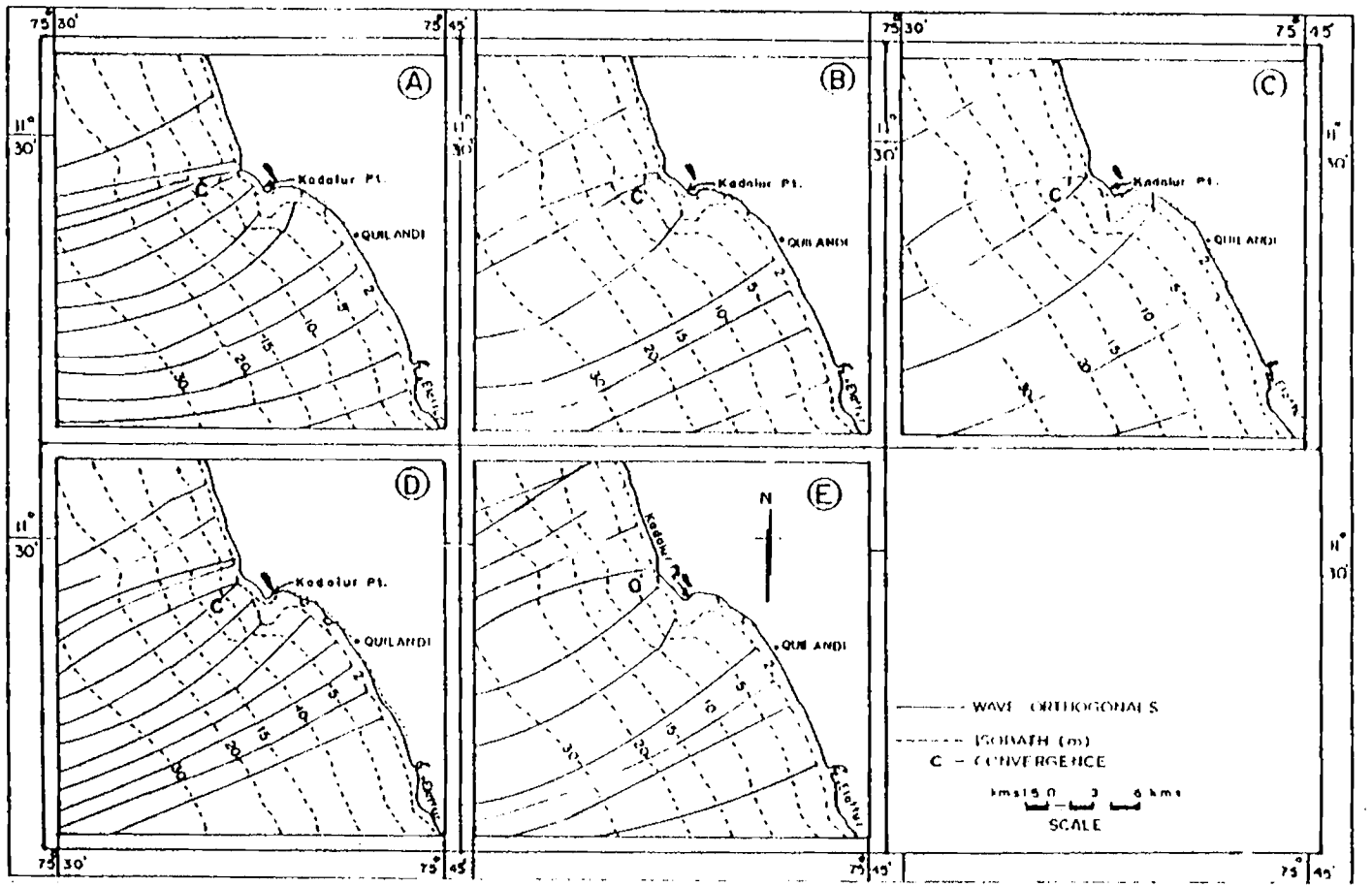

Fig. 5.21 Wave refraction off Quilandy. (A) Wave Direction (D)=west, Period (P)=7s; (B) D=west, P=9s; (C) D=west, P=11s; (D) D=west-southwest, P=7s; (E) D=west-southwest, P=9s.

Shrivastava *et al.* (1968) reported the approach of strong swells towards the Kerala coast from west-northwest to west-southwest during the monsoon period. Wave refraction diagrams have been constructed in order to understand the nature of the energy concentrations along the coastal tract. Adopting the method of Arthur *et al.* (1952) and using Naval Hydrographic Chart No. 219, wave orthogonals were drawn for waves of periods 7, 9 and 11 s approaching the coast from the west and the west-southwest (Fig. 5.21A-E). The figures show the zones of convergence along the 2 m isobath for lower period waves. The distance between the wave rays in deep and shallow water suggests zones of convergence near Kadalur Point and weaker divergence further south of Quilandy. Low wave heights were observed in the suspended mud area and are inferred to result from the dissipation of wave energy. The divergent zone south of the Kadalur Point thus facilitates deposition of fine sediments.

Geochemistry of Quilandy mud bank sediments: Percentage ranges of major elements (SiO_2, Al_2O_3, Fe_2O_3, CaO, MgO, TiO_2, Na_2O and K_2O) in 19 surficial sediment samples are given in Table 5.14 along with the range and mean statistics (Table 5.15). In terms of mean element abundances $SiO_2 > Al_2O_3 > Fe_2O_3 > CaO > Na_2O > MgO > K_2O > TiO_2$ reflecting the mineralogical characteristics of the sediments. MgO and TiO_2 show a percent variance of more than 50, where as K_2O gives 40 - 50 % variance. All other elements yield < 30 % variance around the mean.

Aerial distribution of elements are depicted in Fig. 5.22. SiO_2 and CaO are found to be comparatively more concentrated in the northern and southern flanks, than in the central portion of the study area. Contrary to the distribution of SiO_2 and CaO, Al_2O_3 and Fe_2O_3 show a selective adherence to

TABLE 5.14

Major Element Concentration in Quilandy Mud Bank Sediments (in %)

		SiO2	Fe2O3	Al2O3	CaO	MgO	TiO2	Na2O	K2O
1	C1	64.450	7.180	9.560	5.320	2.200	.160	2.200	.500
2	C3	51.590	13.160	12.260	5.320	1.600	.140	2.190	.490
3	C4	49.760	10.170	13.760	5.880	2.000	.140	2.460	.580
4	C7	61.410	7.660	11.670	4.480	.800	.100	2.020	.440
5	C8	51.710	9.310	11.690	5.880	2.200	.110	2.490	.560
6	C15	51.800	11.210	13.210	4.480	1.000	.330	2.560	.450
7	C16	36.410	14.230	15.290	3.920	.800	.140	3.440	.580
8	C17	47.600	11.710	13.250	5.040	2.800	.100	3.000	.550
9	C19	34.250	15.210	17.810	3.080	.200	.110	3.700	.590
10	C20	33.980	15.040	16.310	3.640	1.000	.140	3.870	.610
11	C24	33.320	14.440	19.880	2.240	.800	.140	3.530	.440
12	C25	34.650	15.670	18.960	2.800	.600	.140	3.530	.460
13	C27	33.100	14.680	17.330	2.800	2.200	.130	3.870	.480
14	C29	34.260	16.200	18.330	2.520	2.400	.250	3.500	.500
15	C31	33.100	14.000	17.330	2.800	2.000	.170	3.870	.510
16	C34	65.840	9.250	10.160	3.640	1.200	.330	2.560	.440
17	C35	63.760	8.110	10.160	3.640	3.200	.120	2.430	.480
18	C36	39.850	13.920	14.070	3.640	3.400	.830	3.300	.420
19	C38	33.240	15.580	15.530	4.760	2.600	.170	3.440	.400

TABLE 5.15

Range and Mean Statistics of Quilandy Major Elements

Element	Range		Mean	Std. Dev.
	Minimum	Maximum		
SiO2	33.10	65.84	44.95	12.28
Al2O3	9.56	19.88	14.55	3.18
Fe2O3	7.18	19.07	12.46	3.01
CaO	0.28	5.88	3.99	1.15
MgO	0.20	3.40	1.74	0.93
TiO2	0.10	0.83	0.20	0.17
Na2O	2.02	4.95	3.05	0.65
K2O	0.40	0.61	0.55	0.25

TABLE 5.16

Matrix of correlation of elements in Quilandy sediments

	SiO2	Al2O3	Fe2O3	CaO	MgO	TiO2	Na2O	K2O
SiO2	1							
Al2O3	-0.93	1						
Fe2O3	-0.92	0.86	1					
CaO	0.19	-0.23	-0.22	1				
MgO	0.07	0.02	0.18	0.06	1			
TiO2	-0.01	-0.09	0.09	0.25	0.24	1		
Na2O	-0.86	0.80	0.86	-0.26	0.30	-0.02	1	
K2O	0.04	-0.03	-0.53	0.13	0.05	-0.39	-0.03	1

the sediments in the central portion. The abundance of TiO_2 seems to be least among the elements considered here. However, isolated patches of higher TiO_2 concentration is noticed in the northern and southern ends. Distribution of MgO concentration is generally insignificant. Central and southern portions show relatively higher concentration of MgO. Na_2O concentration appears to be decreasing towards south and northwest portions. Generally, the sediments have lesser percentage of K_2O. Though the variation of K_2O content is subtle, it generally follows the distribution pattern of Na_2O.

Textural dependance of elements: The distribution pattern of individual elements (Fig. 5.22) are compared with the aerial distribution of different sediment size-grades (Fig. 5.16). There is a striking similarity between the distribution finer sediments (< 62 μ) and of Al_2O_3, Fe_2O_3, Na_2O and K_2O. An interesting aspect of sediment textural dispersal pattern is the increase in finer material content towards the central portion of the study area. The processes involved in the deposition of finer materials were discussed by Mallik *et al.* (1988). Presence of a layer of sediment-laden soupy water was conspicuous in the sediment water interface over the finer sediment zone. Moreover, flocculation and deposition of finer sediment in the form of a kaolinite veneer is indicated by the increase in Al_2O_3 and K_2O content in this region. Higher percentage of kaolinite among the clay minerals was indicated by previous studies (Nair and Murty, 1968). Surplus value of Fe_2O_3/Al_2O_3 ratio (> 0.52) indicates the presence of authigenic Fe-bearing minerals (Calvert, 1976). Occurrence of framboidal pyrite supports the above view.

SiO_2 distribution patterns show a significant dependence on the amount of sand-sized fractions. Distribution of SiO_2/Al_2O_3 ratio follows the sand distribution. This indicates the availability of larger proportions of free

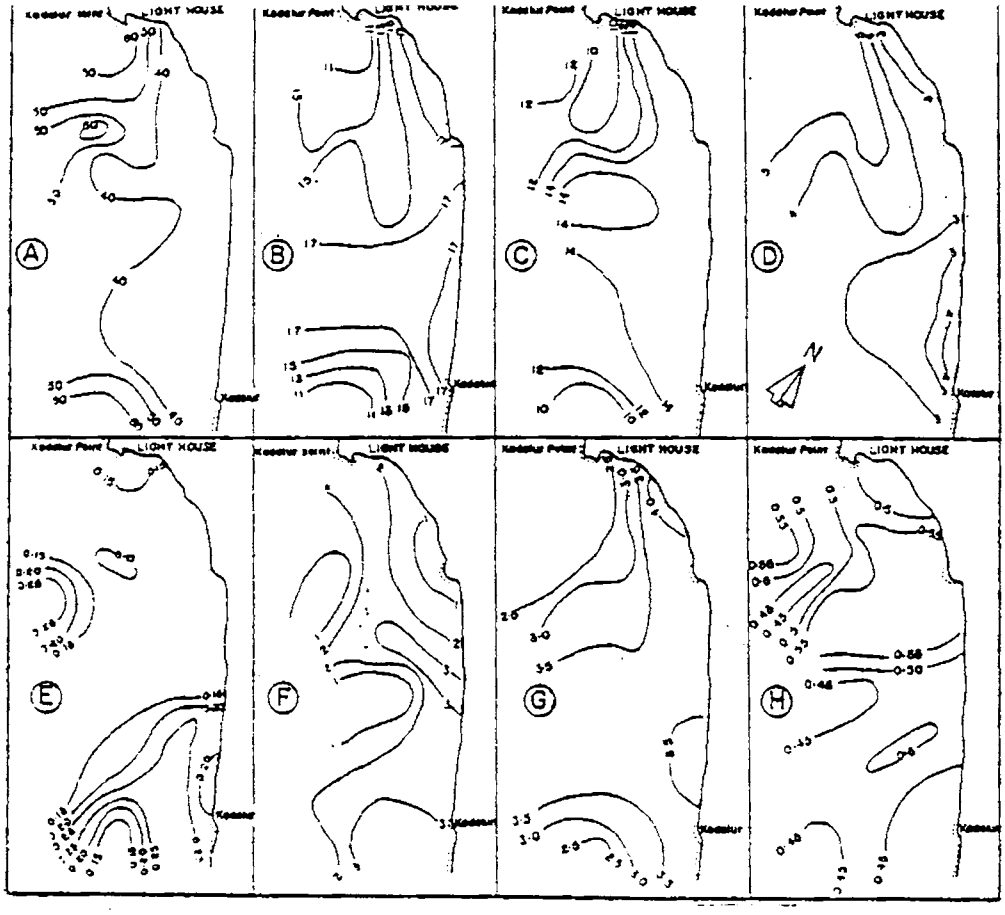

Fig. 5.22 Isopleth concentration map (%): (A) SiO2 (B) Al2O3 (C) Fe2O3 (D) CaO (E) TiO2 (F) MgO (G) Na2O (H) K2O

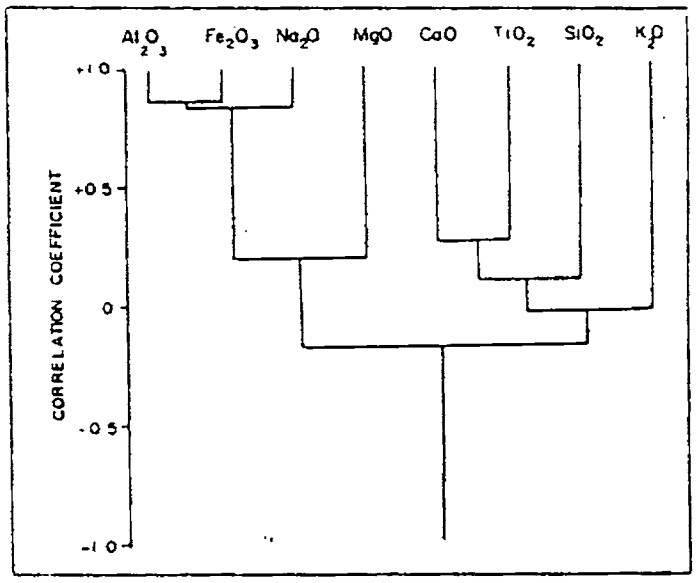

Fig. 5.23 Cluster diagram of chemical compositions of Quilan mud bank sediments

quartz in the sediments. A positive correlation between TiO_2 and percentage distribution of silt is observed. Microscopic examination of light minerals reveled that the sand fraction contains 35 % quartz, 14 - 18 % carbonates and 25 to 31 % brown organic matter. Hence, the variation of CaO, which is not size-dependent, is a function of both elemental concentration in the minerals present and the amount of skeletal remains, since the samples were analysed without removing skeletal matter. The distribution pattern of MgO also does not coincide with the isopleths of any size grade.

'The law of grain-size control' on the geochemical variation of sediments is reported by several workers (Hirst, 1962; Zhao Yiang *et al.*, 1981). Investigation on the geochemical variation of sea-bed sediments of the Taiwan Bank showed that the average content of Fe, Mn, Ti and P increased gradually with decrease in grain size. Similar observations are reported for the Gulf of Paria (Hirst, 1962). Thus, textural variation imparts a major control over the chemical composition of sediments.

Cluster analysis: Cluster analysis is carried out to substantiate the interpretation of the geochemical data. This has helped in understanding the interrelations among the elements. Table 5.16 gives the correlation coefficients among the different elements. Based on the correlation coefficients, dendrogram (Fig. 5.23) was constructed by arithmetic averaging method (Davis, 1973). The correlation between the cophenetic correlation and original correlation was significant ($r = 0.76$).

Al_2O_3 and Fe_2O_3 show a significantly high value of correlation which, in turn, is correlated at a higher level with Na_2O, whereas all other elements are showing a low level of correlation. The cluster analysis suggests that

three main interrelated groups of elements are responsible for the geochemical variability in the nearshore sediments. They can be readily identified with the following controlling factors:

1. The group containing Al_2O_3, Fe_2O_3, Na_2O and MgO probably controlled by hydrous alumino-silicate factor in the finer sediments.
2. TiO_2, CaO and SiO_2 group controlled by coarser fractions and CaO especially by carbonate shell fragments.
3. The third group containing lone element K_2O mainly depends on alumino- silicates and feldspars.

Geochemistry in relation to mud bank formation: Mud bank regions are characterised by high suspended matter concentration. Control of suspension was attributed to physical causes. The Quilandy nearshore sediment are abundant mostly with clay sized materials. Dora *et al.* (1968) reported that Narakkal mud bank sediments contained 55 % of particles < 1 μ in size. The results suggest that finer materials contain more Al_2O_3 and Fe_2O_3. Spencer and Sachs (1970) reported that mineralogy of the suspended matter is essentially the same as that of the fine-grained part of the sediments. Apart form the physical causes of suspension, chemistry of the bottom sediments are also significant in maintaining the suspension (Ramachandran, 1989).

Condensation and dispersion are the two general ways in which suspensions are formed. Condensation process requires formation of super-saturated solution in which individual molecules or ions combine to form particles of colloidal dimensions (Yariv and Cross, 1979). During monsoon season salinity reduction from 33.5 to 8 due to precipitation was reported for

the Purakkad mud bank area (Kurup and Varadachari, 1975). Damodaran and Hridayanathan (1966) have also reported a similar decrease in salinity for Narakkal mud bank area. Hence, condensation process can not be attributed to mud bank suspension. Present study suggest 'dispersion' as a possible mechanism of suspension in mud bank regions. Detachment of particles from the upper layer of sediment and peptization are the important stages involved in the process of dispersion. Kurup (1977) explained detachment of particles from the surficial sediments in terms of physical mechanisms. But 'peptization' is a chemical phenomena and Yariv and Cross (1979) used the term to describe the process of conversion of unconsolidated particulate rock-material into colloid solutions and suspension. Further, they stressed the necessity for an optimum concentration of electrolyte for increased suspension. Probably this can be applied to the mud bank region. Earlier work pointed out the dependence of suspension on salinity (Kurup, 1977). It was observed that alumina and ferric oxide were especially having this remarkable property called 'thixotropy'. Nair (1976) suggested that, sustained suspension in mud bank regions could be due to the process of thixotropy, though no details were provided. Quilandy sediment are abundant in Al_2O_3 and Fe_2O_3. Abundance of Al, Fe in suspension reported by Spencer and Sachs (1970) from the Maine Bay lends credence to the presumption that a similar mechanism can also work in the mud bank area.

Phosphate concentration in the Quilandy mud bank sediment ranges from 1118 to 6140 ppm (average 2967 ppm; Mallik *et al.*, 1988). Distribution pattern showed an increase in concentration towards the central clay zone. High phosphate content of mud bank sediment along Malabar coast has also been reported (Seshappa, 1953). Presence of phosphate in sediments act as a natural peptizer. They are sorbed onto the edges of the layers of clay

minerals changing their charges from positive to negative and hence preventing aggregation (Szanto, 1962; Glasstone, 1974).

The above results suggests that surficial sediments in the mud bank region is enriched in clay-sized particles. Partitioning pattern of the major elements suggests a selective adherence of Al_2O_3 and Fe_2O_3 in the clay-rich sediments. Enrichment of phosphate in the sediments followed by upwelling along the southwest coast of India has been noticed. Monsoonal waves and coastal currents trigger initial physical suspension in mud banks. Subsequently, reduction of salinity in the overlying water column due to monsoonal precipitation creates an ideal condition for chemical suspension. Peptization due to the enrichment of phosphate accelerates the process of deflocculation and suspension of alumina and ferric oxide-rich fine surficial sediments.

5.3.3 Comparison of Alleppey and Quilandy mud banks

A comparison is attempted from the results and discussion presented above on Alleppey and Quilandy mud banks. The geomorphological set up and the coastal setting of the two regions are of diverse nature. But the observations point to the fact that, mud banks that forms at these locations remain visually the same. The basic characteristics of Kerala mud banks, turbidity and calmness, are manifested in both the locations. Even with such diverse physical settings, if the two locations favour the occurrence of mud banks of similar nature, then, it is presumed that, a comparison of the bed characteristics can give some new insight into the formation of mud banks.

Granulometric composition of the sediments from the two locations show that, they are abundant in fine clastics. Distribution pattern of the sediment texture of sea bed at Alleppey as well as at Quilandy, illustrates a clay-rich surficial sediment blanket with soupy fluidised nature in the central part of the mud bank location. This zone invariably coincides with the zone of highly turbid water column. Even the dispersal pattern of sediments at these locations depicts striking similarity, with silt/clay ratio isopleth maps registering declining ratio towards the central part of the study locations. This is an indication to the resemblance in the process of mud deposition in such locations. It is inferred that the sort of sediment build up observed at Quilandy may find its analogy at Alleppey also though core lithological studies were not undertaken. At Quilandy, the curvature of the coast with rocky stacks at its northern side, results in divergence of wave energy at the mud bank location, thereby facilitating deposition of fine clastics. But the coastal setting at Alleppey does not favour such divergence and this is overcome by the bottom topography, which induces refraction of waves to create a zone of divergence.

Previous workers gave different sources of mud for different locations of mud bank formation. According to some of the observations, the source of mud for the backwater backed Alleppey region was presumed to be from the Vembanad Lake, and Quilandy from the adjoining rivers. In the preceding part of the discussion, it was mentioned that mud deposition precedes the formation of mud bank and this happens just at the onset of southwest monsoon. Precipitation and subsequent run-off through rivers can not account for such a drastic deposition of mud at specific location, though there is little doubt that the sediments discharged through rivers get deposited in the shelf. But, these sediments get reworked and redistributed due to waves

and currents. Thus, such a sedimentation pattern adds up to the sediment cover on the shelf. But the drastic nature of deposition happening in the mud bank location could be, as mentioned in the preceding sections, from the immediate offshore and alongshore by fluidisation and mass erosion due to the high waves reported along this coast marking the onset of monsoon. Nurturing of the shelf, definitely to a major extend, is by the terrestrially derived sediments, but source of the mud for the mud bank location is most likely to be a reappropriation process of the innershelf mud zone. Cessation of mud bank marks the removal sediments and its redistribution over the shelf, thus keeping cyclicity in the deposition-removal episodes. The comparison of the textural pattern of the sediments in both the areas attests drastic deposition of fine sediments as a prerequisite for mud bank location. The study also enumerates a similarity in the process-related source and depositional aspects. Even it could be presumed that, the shoreward thickening of the soupy mud layer should attain a critical geometry to create an active phase of mud bank, though the results of the present study does not dealt it in detail.

Similarity in the textural composition of the sediments need not necessarily give a correspondence in the mineralogical and chemical composition of the sediments from the two locations, as it depends on the source. Scanning of the results on the geochemical characteristics of the sediments from both the areas display differences in the elemental association and partitioning pattern. Comparison of mean concentration of elements show that Fe_2O_3 is enriched in the sediments of Quilandy than Alleppey (12.46 and 8.27 % respectively) and this is so even in the case of minimum value of Fe_2O_3, the minimum at Quilandy is 7.18 and Alleppey 4.79 %. Na_2O shows relatively much higher value than K_2O in the Quilandy sediments. Since these elements are found to be basically controlled by the clay proportions in the sediments, the

differences can be attributed to the compositional diversity of clay mineral assemblages. TiO_2 percentage is very low in Quilandy than at Alleppey, reiterating the dissimilarity in the mineralogical assemblages of the sediments. This is indicative of the differences in the provenance of the sediments in the two areas. But the semblance in the case of grain size control over the speciation of elements is remarkable, with a minor deviation in the case of K_2O, which is enriched both in the clay mineral factor and the feldspar content of the sediments in Quilandy area, but mainly in the former in the case of Alleppey sediments. The minor variations observed in the chemical composition does not influence to alter the physical characteristics of the sediments to a greater extent. Hence, the process of removal and deposition of sediments which are mostly dependant on the physical properties of the sediments remains to be similar. Apart from this, the hypothetical considerations made on the chemical means of suspension also can be applied to both areas, as the phosphate which act as a natural peptizer is stored in the clay rich sediments as evidenced from the relationship between clay and phosphate in both the areas. Hence it is concluded that, the mud banks of Alleppey and Quilandy are similar in nature, the formation of which are resulted from a similar set of process with some minor differences in the sediment constituents and physical aspects owing to the coastal settings and provenance of sediments.

5.3.4 Mud bank or Fluid mud?

While working in the nearshore areas off Quilandy and Alleppey and other well known areas of mud bank formation in Kerala, it is found that the term 'mud bank' is not really applicable to the phenomenon that has been observed (Mallik *et al.*, 1988). According to Bates and Jackson (1980) a 'mud bank' is defined as a "submerged or partly submerged ridge or relatively flat

topped elevation on the sea floor at shallow depth which may remain unexposed at low tide". A large part of the current confusion on 'mud bank' genesis results from the misuse of the descriptive terminology and it is important to note that a mud layer on the shallow sea floor is present along the entire inshore region where 'mud banks' occur. The early observations of Cope (In: Silas, 1984) correctly resulted in the description of the formation of muddy coastal waters as a 'mud bay'. Later workers referred to a very calm water mass with a high load of suspended sediments as a 'mud bank' with no reference to the nature of the sediment substrate on the sea floor Jacob and Qasim (1974) described 1 - 2 m elevations on the sea bottom with consolidated mud in the form of a 'mud bank', but no information on the geometry of the mud layer was given. Kurup (1977) stated that 'mud banks' off the Kerala coast were due to sediment resuspension associated with convergence of littoral currents. Such mud suspension result from a heavy load of suspended mud in the shallow nearshore waters along many coastal area where river discharges are high (Eisma and Van der Marel, 1971). The term 'fluid mud' is applied to a fine-grained sediment-water mixture containing more than 10,000 mg/l of sediments (Wells *et al.*, 1979). Usually, the sediment concentration in the Kerala mud suspension area is less and ranges between 100 and 1500 mg/l at 1 m above the sea bed. But the recent observation of Mathew (1992) gives a figure on the soupy mud suspension over the sea bed as 174,000 mg/l. He also suggested mechanisms of fluid mud generation during the onset of the southwest monsoon based on wave-mud interaction process in the nearshore. The term 'fluid mud' was proposed by Mallik *et al.* (1988) to describe the sediment clouding in the nearshore water in mud bank locations. Based on the observations at Alleppey and Quilandy, and also on the recent studies of Mathew (1992), this investigation supports the proposal

of Mallik *et al.* (1988) to describe the phenomenon as 'fluid mud'. Such a terminology can remove many of the confusion pertaining to this phenomenon by the use of the terminology 'mud banks' and also can be comprehended by the international scientific community working on similar problems.

5.3.5 Comparison with other reported occurrence of mud banks

Nearshore regions with very high suspended particle concentrations are reported from other parts of the world. In recent years, the tropical muddy shallow inner shelves of Surinam (Rine and Ginsburg, 1978, 1985; Wells, 1978; Wells and Coleman, 1981a & b) and Louisiana (Wells and Roberts, 1980) have been studied in detail. Mud deposition and very high concentration of suspended sediments in the nearshore of the above locations are same as along Kerala. The Amazon river is considered to be the primary source of the mud for the Guyana coast, which is temporarily deposited as large 'mud banks' (Eisma and Van der Marel, 1979). The mud is very mobile (sling mud) and contain an admixture of calcite, aragonite and chlorite. A comparative analysis of the Surinam-Guyana coast and Kerala was presented by Mallik *et al.* (1988).

The Kerala mud banks do not occur as an annual relief-forming feature as do mud banks described from other known muddy coasts. The transient nature, the extremely unpredictable periodicity and the unpredictable location of their appearance clearly demonstrate the major differences with other similar phenomena reported elsewhere. Although a mud bottom is an essential prerequisite and a thick mud layer is overlaying the innershelf, the mere presence of mud is not sufficient to generate a dense sediment suspension in the overlying water column. A critical sediment concentration, in terms of

texture and quantity and hydrodynamic conditions has to be facilitated in order to form a fluid mud. The muddy nature of the substratum, proximity to the coast and the very high amount of suspended sediments are the features which the Kerala fluid mud events have in common with other muddy coasts of the world.

CHAPTER 6

SUMMARY AND CONCLUSIONS

The continental shelf of southwest coast of India (Kerala) is broader and flatter compared to that of the east coast. The unique characteristic feature of the study area (innershelf between Narakkal and Purakkad) is the intermittent appearance of 'mud banks' at certain locations during southwest monsoon. The strong seasonality manifests significant changes in the wind, waves, currents, rainfall, drainage etc., along this area. Peculiar geomorphological variation with high, mid and lowlands in the narrow strip of the hinterland, the geological formations mainly consisting of rocks of metamorphic origin and the humid tropical weathering conditions play significant role in regulating the shelf sedimentation.

Granulometric composition of the sediments in the innershelf exhibits heterogeneity in the percent constituents of different textural grades. Sand, silt and clay contents of the sediments vary from a minimum percentage of 0.18, 0.16 and 0.00 to maximum of 99.38, 78.27 and 69.00 respectively. Distribution pattern of sand depicts higher concentration in the seaward portions beyond 20 m depth, except off Alleppey region where the enrichment of sand shows considerable shoreward shift. A complementary pattern of distribution is observed for clay that shows an abundance in the nearshore. Silt, to a major extent, depicts semblance with clay distribution. Bathymetric control over the textural distribution pattern is evident from the significant positive correlation of depth with sand and negative correlation with silt and clay. Spatial variation of mean size confirms the above distribution pattern, i.e., the offshore portions, especially the southwestern (sand-dominant) area render a low phi mean (< 3 ϕ). The mean size varies from 1.29 to 9.63 ϕ. In general, the innershelf is dominant with fine grained (cohesive) sediments as

evidenced from the modal range of phi mean size between 7 and 9. These finegrained sediments are poorly sorted, whereas the sand zone depicts well sorted to moderately sorted nature. Poorest sorting is exhibited by sediments containing sub-equal proportions of sand, silt and clay representing the mixed zone of sediment distribution.

Summation of the total asymmetry of grain size distribution are inferred from the variation of skewness and kurtosis. The negatively skewed sediments contain only very small percentages of sand, while the positively skewed sediments show a predominance of coarser fractions. Similarly, fine-grained sediments depict polymodality in lieu of their marked platykurtic nature. The mesokurtic and leptokurtic nature of the sand-dominant samples confirm their better sorted characteristics and corresponding gradual decrease in the higher and lower phi fractions around the mean.

The CM diagram depicts that the fine sediments are mostly formed under the transportation pattern of pelagic suspension and the coarse deposits by rolling and graded suspension under maximum and minimum turbulence. The sand-rich sediments resemble a typical beach regime, whereas the finer sediments are resulted from the present-day shelf processes. The beach regime of the coarser deposits are further confirmed from the probability curves of separated log-normal distributions in comparison with the modern beach sediments from the Alleppey coast. Of the two saltation populations, which is typical of beach sediments, the dominant coarser saltation represents the strong swash process while the finer saltation corresponds to a weak backwash regime of the then (relict) beach environment.

Q-mode factor analysis reveals that the sedimentation process in the innershelf are controlled by three important factors. Each factor is found to be an expression of different energy regimes for which the size spectrum forms equilibrium sub-ranges. Factor I implies a low energy regime where the transportation and deposition phases are controlled mostly by pelagic suspension process as the factor loadings are dominant on finer phi sizes. The second Factor is inferred to be the result of a high energy regime which gives higher loadings on coarser size fractions. The third Factor which might be a transition phase (medium energy regime) representing the resultant flux of coastal circulation of the re-suspension/deposition and an onshore-offshore advection by reworking and co-deposition of relict and modern sediments. The spatial variations of the energy regime based on the three end-member factor model exhibits high energy zone in the seaward portion transcending to a low energy one towards the coast.

As the circulation pattern of the innershelf based on direct measurement of currents are lacking, a transport model based on certain statistical consideration of the textural aspects of sediments are presented. The model assigns a significant southward transport of sediments along the shelf. Further, the shallower area are characterised by low energy regime whereas a high energy regime exists beyond 20 m depth. Since such a strong energy regime beyond 20 m contour can not be a manifestation of the present day shelf processes (even when the adjoining nearshore area itself is classified as a low energy environment) it is concluded that, the sediment path ways beyond this depth are influenced by the relict (coarse sediment) beach deposit. The dispersal pattern of the cohesive sediments in the innershelf is dominantly controlled by strong southward monsoonal currents.

Scanning electron microscopic studies of quartz grains decipher mechanical and chemical processes of transportation/deposition and subsequent diagenetic changes. The better rounded appearance of the quartz grains in the sand-zone indicates pronounced mechanical action due to rolling and abrasion in a high energy regime. Mechanical features like 'V' pits and conchoidal fractures suggest long duration and higher intensity of subaqueous agitations. Further, the abundance of well preserved chatter marks are related to the response of mechanical abrasion of the grains caused by glancing blow across the face of the grain. Superimposition of chemical dissolution features and silica precipitation in the form of sugary coating and silica globules are considered as repositories of periodic evaporation of inter granular water. They represent different stages of diagenetic history. It is emphasized from the above observations that, the innershelf sand being part of the relict beach sediments are product of subaqueous transport under high energy conditions.

From the combined analysis of granulometry and SEM studies, it is concluded that the sandy patches beyond 20 m depth are of relict nature. They are the resultant responses of beach activity during the lower stand of sea level in the Holocene. Re-crystallisation features on the quartz grains indicate that they were exposed to subaerial weathering process subsequent to their deposition. Further they have undergone episodes of transgression, thus resulting in their present depth of occurrence. The mixing process on the shelf is not strong enough due to the insufficient physical energy of waves and currents to obliterate the original textural characteristics of the sediments. However, a part of the relict sands have undergone considerable reworking and redistribution along with the modern fine grained sediments resulting in the mixed sediment facies bordering this sand-zone. The fine-

grained nature of the modern sediments in the nearshore is mainly due to the selective transmission of fines through the backwater system effected by the filtering action of the estuaries.

The textural details of the core lithology depicts uniform vertical distribution of mud with marginal variation giving rise to a thick blanket of mud on the inshore region of the shelf. Thus, it suggests that sedimentation was essentially continued in analogous to that of the present day process for a considerable period. Cores at certain depths bordering the sand-zone enumerates increase in sand content towards bottom indicating process of mixing of modern and relict sediments.

The heavy mineral study reveals that, irrespective of the type of sediments and locations, the total heavies in the coarser fraction is lower than the finer fraction. The concentration difference of heavies between the two fractions in the sand-rich zone is many fold when compared to that of clay-rich zone. The impoverishment of heavies in the coarser fraction of relict sands are considered to be the result of the wave-induced deposition, wherein the fraction of heavies deposited are finer equivalence of the mean size of the sediments owing to the density-based selective sorting process. Distribution pattern of total heavies depicts a general increase towards the sand-rich seaward zone. The dearth of heavies in the nearshore are evidently due to the low-energy regime, that resulted in the deposition of fine-grained sediments.

The average abundance of individual heavy minerals in the finer fraction is in the decreasing order of opaques > sillimanite > hornblende > zircon > orthopyroxene > biotite > framboidal pyrite > garnet > rutile >

monazite > clinopyroxene > kyanite > actinolite/tremolite > tourmaline. Nearly 80 % of the variations are controlled by opaques, sillimanite, hornblende and zircon. A comparative evaluation of heavy minerals in the coarser with that of finer fraction shows that opaques and hornblende are enriched in the finer, whereas sillimanite shows an abundance in coarser fraction. Higher proportion of biotite association with the coarser fraction is indicative of density-shape based sorting action. Overall variation of the heavy minerals in the two fractions remains almost the same including that of the minerals available in traces.

Analogous distribution pattern of opaques, sillimanite, zircon, rutile and monazite are conspicuous with a seaward increase from the nearshore, which is in agreement with the variations in texture and total heavies. Hornblende, orthopyroxene and clinopyroxene are concentrated more towards the shore, thus elucidating a converse pattern from the above said minerals. This sort of polarity in the heavy mineral assemblage of sand-rich sediments (abundant in opaques, sillimanite, zircon, rutile and monazite) and clay-rich (abundant in other minerals) sediments manifests hydraulic-based sorting process. This is supported by the significant positive loadings obtained among opaques, sillimanite, zircon, monazite and rutile and strong antipathetic relation of opaques with hornblende, orthopyroxene, clinopyroxene, biotite and framboidal pyrite.

Total variation of heavy minerals based on cluster analysis depicts two distinctive groups. The first group of minerals (consisting of opaques, rutile, sillimanite, zircon and monazite) are characteristic mineral species in the relict sand zone. This supports the above contention that relict sediments were repositioned at the present depth of occurrence by transgression. The mineralogy of the relict beach (like texture) is not obliterated much due to the

prevailing hydraulic conditions (low-energy) of the innershelf. The second group consists of two inter-related subgroups of minerals (subgroup 1: hornblende, orthopyroxene, clinopyroxene and tourmaline; subgroup 2: biotite and framboidal pyrite) are enriched in the finer sediments of the nearshore. Dispersal pattern of the first subgroup (associated with hornblende) depicts a direct derivation from the terrestrial source. Framboidal pyrite, which is part of the second sub-group, is of authigenic origin formed under reducing condition and less turbulence. The unbroken nature of the micro-organisms containing pyrite infillings indicate that they are not transported ones. Association of biotite with the framboidal pyrite exemplifies the relatively turbulent-free depositional set-up. Apart from a source characterisation, hydraulic control over the sorting of the minerals is also evident from the clustering pattern. Reworking of the relict sand zone minerals (mainly denser heavies) is elucidated by the depletion of the minerals shoreward. Contrary to the above, the other group contains lighter heavies, which portray a depletion towards offshore due to the incompetency of offshore transport.

Collation of information on the mineralogical abundance on the major rock types of the hinterland area, and heavy mineral assemblages of river, beach and innershelf indicates that, the heavy minerals are chiefly derived from charnockite-khondalite suite of rocks. This study also shows that, the denser heavies are either settled along course of the rivers or filtered in the lake (estuary) with a selective flushing of the lighter heavies along with some denser heavies onto the shelf. The poor maturity of the innershelf sediments indicated from the concentration of ferro-magnesium minerals, is attributed to the higher yield of the surface run off restricted to a small period of heavy monsoonal precipitation and the high gradient geomorphological set up.

A comparison of the average mineral composition of the innershelf (including sand-rich) sediments with that of relict sand (outer-innershelf) sediments apparently denotes a reduction in opaques, pyroxenes and amphiboles in the former compensated by a relative enrichment of sillimanite, zircon and monazite in the later. The depletion of unstable minerals resulted in the relative enrichment of sillimanite, zircon, monazite and rutile in the sand-rich sediments. Subaerial exposure for a considerable period is the main reason for the selective dissolution of ferro-magnesium minerals by intrastratal solution in the relict sands. Thus, the heavy mineral study of this area confirms that, the innershelf mud zone is of recent origin whereas the sands in the outer-innershelf are relict beach sediments.

Semiquantification of X-ray diffraction pattern shows that the clay minerals present in the innershelf sediments are montmorillonite, kaolinite, illite and gibbsite in the decreasing order of their abundance. Spatial distribution of clay minerals depicts considerable depth dependance. In general, montmorillonite content increases towards offshore. Kaolinite distribution is converse to that of the above as it displays shoreward enrichment. Illite depicts similarity with montmorillonite distribution. Gibbsite is present only in subtle amounts with sporadic distribution pattern.

Crystallinity index (V/P) of montmorillonite indicates that the mineral is mostly Al-rich. The increase in amount of this mineral from terrestrial to marine environment through lacustrine system is a function of its preferential settling owing to the finer size, differential flocculation in saline conditions and to a limited extent the transformation process (inverse weathering). The events of suspension in mud banks coinciding with high monsoonal waves keep montmorillonites in suspension thus facilitating its removal further offshore.

A reverse pattern of decreasing concentration from terrestrial to marine environment is observed for kaolinite. Seaward decrease of kaolinite discerns that (i) they are of terrestrial origin (mainly from kaolin deposits, weathering of rocks and laterites) and (ii) preferential settling due to its larger size and flocculation at a lower salinity.

Illite behaviour is similar in nature with montmorillonite marking a small but steady increase from land to sea as the size and flocculation behaviour of it is intermediate to the other two dominant clay minerals. However, this region is characterised by a poor illitic input of terrestrial materials. Presence of gibbsite indicates humid tropical conditions of weathering. The extensive stretches of laterite in the hinterland contributes substantial amount of this mineral.

Thus, the clay mineral assemblages indicate that the fine fraction of the sediments essentially contain the products of intense chemical weathering. They get segregated and altered during river transportation and further modified in the Vembanad Lake before entering the marine environment by differential transportation coupled with chemical transformation depending on the physico-chemical characteristics of the transporting medium.

Chemical analysis of the sediments show considerable spatial variation. The clay-rich modern sediments of the nearshore and the sand-rich relict beach sediments of the outer innershelf give distinguishable compositional difference of elements. In general, organic matter content decreases towards offshore. Concentration of major elements show SiO_2 > Al_2O_3 > Fe_2O_3 > CaO > MgO > Na_2O > K_2O > TiO_2 > P_2O_5 series. Significant enrichment in the nearshore and seaward decrease in concentration is noticed in the cases of

Al_2O_3, Fe_2O_3, Na_2O and K_2O. SiO_2 depicts a converse trend and CaO concentration is restricted to certain pockets. P_2O_5 enrichment is observed in some nearshore locations and TiO_2 shows relative abundance in the northern half.

Size dependant scavenging of organic matter is evident from its sympathetic relation with silt and clay. The higher values of organic matter attest contribution from land and high productivity of shelf waters. Co-sedimentation with fine particles also plays a significant role in organic matter accumulation.

Many of the major elements depict textural control over their variation. Except SiO_2 all other minerals show positive affinity with silt and clay. Fe_2O_3, Al_2O_3, Na_2O, K_2O and MgO discern highly significant positive loadings on silt and clay and negative loadings on sand indicating their selective semblance with finer fractions. TiO_2 also shows certain amount of affinity with fines, especially so with silt. CaO does not show significant association with any size fraction. Enrichment of P_2O_5 with clay is also noticed.

SiO_2 variation in the sediments is mainly controlled by the amount of quartz-rich sand fraction. Especially the sand-rich sediments (relict beach) in the seaward portions yield higher percentage of SiO_2. The clay-rich zones are nearly devoid of quartz and the low value of SiO_2 in these sediments are mainly a function of the silica content in the hydrous alumino-silicates (clay minerals). Al_2O_3 variation is mainly attributed to the clay minerals and the contribution from feldspar is very limited in both sandy as well as in the clayey sediments. Apart from the lattice-held portion of Fe_2O_3 in the clay minerals and other detrital (heavy) minerals, it is present in the adsorbed state in fine fractions as well as in authigenic precipitates such as framboidal

pyrite. The 'excess CaO' content is mainly held in skeletal fragments, while CaO present in small quantity in finer sediments are present in the clay minerals. Likewise, some amount of MgO is also contributed by the shell fragments (high Mg-calcite), whereas major part of MgO is partitioned with clay minerals (especially montmorillonites). Since, the amount of feldspar and other detrital minerals containing Na and K are present in traces in the sediments, the presence of Na_2O and K_2O in the samples are then primarily governed by the proportions of clay minerals. The enrichment of Na_2O over K_2O is a clear indication of abundance of montmorillonite than other clay minerals, though exchange reaction favouring substitution of Na for other elements also contribute to its enhanced level in the marine environment. Adherence of P_2O_5 with clay fraction is mainly due to its presence as ferri-phosphate, adsorbed phosphate and phosphate associated with organic matter. Lithogenous partitioning of phosphate is negligible. TiO_2 speciation is mainly brought about by selective partitioning among the heavy minerals (ilmenite, rutile and other Ti-bearing detritals) which are especially present in the finer fractions. Their distribution is a manifestation of the hydrodynamics of the innershelf.

Clustering pattern of major elements is characterised by a close inter-relation of all the elements except SiO_2. Close association among Al_2O_3, Fe_2O_3, Na_2O, K_2O and MgO clearly depicts their selective partitioning with the clay minerals, either in the lattice-held or in the adsorbed state. But, P_2O_5 and TiO_2 form slightly a different pattern as they are controlled by combination of factors such as spatial control of texture and their existence in the mineral fractions.

Minor and trace elements in the sediments show an order of relative abundance of Ba > Sr > Mn > Ni > Cr > Zn > Co > Li > Pb > V > Cd > Rb > Cu > Be > Mo. Considerable fluctuations are observed in their concentration. Similarity in the pattern of distribution is observed for the elements Mn, Cu, Co, Cr, Ni, Zn, Rb and Li, with an enrichment in the nearshore and a seaward decrease. But the other elements do not show a systematic pattern of variation. Mn, Cu, Cr, Ni, Rb and Li show selective adherence to fine particles. The partitioning of these minor and trace elements is not only due to the physical criteria of size, but also to the cation exchange capacity of the metal ions for different types of clay surfaces with fining size. The enrichment of organic matter in the fine sediments also considerably enhances the CEC of metals.

The Mn incorporation is mainly in the particulate form both in association with weathered minerals and as discrete particles of hydrous manganese oxides. The depleted concentration of Mn, compared to the reported values from elsewhere is chiefly attributed to the mineralogical association of source rocks which are depleted in Mn-minerals. Adsorption capacity of clay minerals and formation of various organic complexes control the variation of Cu. Co exhibits incoherent relationship with clays and organic matter. Its positive affinity with silt is an indication to its partitioning with the fine-sized heavy minerals. Cr and Ni depict sorption onto clay minerals and organic matter in an enhanced pH condition. In addition to this, Cr and Ni show some enrichment in the mafic minerals of the sediments. Cd is fairly evenly distributed in all the fractions of the sediments. Apart from the tightly bound Cr in clays, some amount of Cr is also contributed by the biogenic materials. Pb is more often incorporated in clay minerals by adsorption process than it being controlled by the

terrigenous input. Partly anoxic nature of some of the innershelf locations favour sulphide precipitation and organic incorporation of Pb. Zn is dominantly controlled by sorption process along with the structural incorporation in silicates and oxides. But, Ba shows a selective partitioning with terrigenous materials.

Sr concentration is mainly a function of its diodochy with Ca, as it shows a semblance with the distribution of CaO. Sand fraction invariably gives a low value of Sr indicating the poor abundance in mineral fractions. Rb is closely linked with K-minerals manifesting an increased concentration among the clay fraction. Finely dispersed particles of the sediments are enriched in Be, as it depicts a strong association with fine sediments. Concentration of Li is a function of its incorporation in the clay minerals and organic matter. Preferential enrichment of Mo with certain minerals, such as ilmenite and biotite is evident from their sporadic and subtle presence in the sediments. Similarly, V is also partitioned among the mineral components of terrigenous origin, especially in the soils derived from laterites.

Cu contributes the maximum percentage (84.17) of non-lithogenous fraction (NLF) and Ba the minimum (6.98 %). The order of variation of minor and trace elements in the NLF is Cu > Sr > Zn > Pb > Mn > Cr > Li > Cd > Be > Mn > Rb > Co > V > Ba. Among the NLF portion of metals, the carbonate exchangeable metal phase accounts for a range from 0.68 % (for Rb) to 51.66 % (for Sr). Zn, Cu, Mn and Cr show significant enrichment in this phase. The organic-sulphide-Mn-oxide phases of the sediments have considerable bearing in regulating the concentration of many trace metals in the study area. Amongst which, Cu followed by Zn and Pb are heavily concentrated in this fraction. The former two are enriched especially in the organic phase and the

later in the sulphide phase. However, the enrichment of certain metals in the organic phase is not wholly contributed by authigenic process as the spatial variations signify supply of them from the estuary (Vembanad Lake). Though not a significant one, the Fe-oxide-hydroxide phases of NLF contribution decipher some enrichment of Cu, Zn and Mn. The elements, which are abundantly of lithogenous origin are Ba, V, Co and Rb. The order of enrichment of LF among the metals are the reverse order of NLF enrichment.

Cluster analysis of minor and trace elements show distinct grouping, of which Zn, Cr, Mn, Cu, Li, Rb, Ni and Pb are the most significant group. Many of the elements are partitioned in the fine-grained fraction, either due to their structural incorporation in the minerals (especially in the case of Rb) or scavenged by organic-sulphide phases and CEC related sorption process. The group containing Be, Co and Cd do not show appreciable size-dependency, as more specifically their partitioning is controlled by more of lithogenous detritus. However, Cd contribution from biogenic and anthropogenic activities can not be ruled out. Control of terrigenous input over metal incorporation in sediments is clearly depicted by Mo and V. Sr and Ba are distinctly separated from other elemental associations, as they are controlled by nature and amount of skeletal components (for Sr) and the lithogenous abundance (for Ba).

From the cluster diagram (Fig. 4.11) the cardinal factors regulating the sum total of the diversities and similarities in the elemental partitioning are as follows:

(1) Strong association among Zn, Cr, Ni, Mn, Cu, Li, Fe_2O_3, Al_2O_3, Rb, Na_2O, K_2O, MgO and Pb indicates that the elements are controlled

by (i) clay minerals, (ii) organic matter and (iii) exchange process resulting in the co-precipitation with Fe-Mn hydrolysates.

(2) Be, Co, TiO_2 and Cd decipher low level of textural control and dominant contribution from lithogenous fraction, especially in the lattices of heavy minerals in the silt fraction. But an apparent contribution from biogenic and anthropogenic sources for Cd is a likely possibility.

(3) Skeletal components are responsible for the incoherent relation of CaO and Sr with the textural grades.

(4) Though Mo and V are associated with P_2O_5, a marked difference is observed in their speciation. However, an analogous property exhibited by these elements is probably related to the significant absence of textural control over their variation.

(5) A clear physical association of SiO_2 and Ba with sand fractions is indicative of their terrigenous origin, supplemented by the dominantly lithogenous nature of Ba.

Bathymetric studies of the Alleppey mud bank region show considerable amount of mud deposition in the central portion during the occurrence of mud banks. Removal of mud is noticed during the post-mud bank period. Suspended matter concentration (SMC) is characterised by an increase in the central part of the mud bank location, which coincides with the area of mud accumulation during the active phase of mud bank (Phase I). SMC registers sharp decrease following the cessation of mud bank (Phase II). The distribution pattern of sediment facies shows abundance of fine particles with dominance of silty clays. However, no noticeable variation in the textural characteristics is observed during the post-mud bank period. Chemical constituents show considerable textural dependance. Geochemistry of mud

bank and innershelf sediments is similar for sediments with comparable textural characteristics.

Sediment dispersal pattern is characterised by mud transportation from offshore and alongshore to the location of mud bank. Fluidisation of cohesive bed in the offshore by waves during the rough monsoon period and its subsequent shoreward transport facilitates piling up of mud at the mud bank location. Thus, localised distribution of mud bank is mainly a function of wave energy distribution. The build up mud in the mud bank location is removed during the post-monsoon period. Re-suspension process by waves and its transportation by the prevailing offshore and coastal currents are mainly responsible for mud removal. This marks the cessation of mud banks. The recycling of mud by transporting fluidised mud layer from innershelf to the mud bank location during monsoon, and its removal and re-deposition back to the innershelf (during post-monsoon) augments the importance of innershelf sediment dynamics in modulating the episodes of mud bank formation.

Quilandy mud bank location is characterised by direct fluviatile influence unlike the Alleppey location (which is part of the backwater-barrier beach coastal set up). Sediment accumulation in Quilandy nearshore shows enrichment of clay especially in the central part. The subsurface geometry of the sediment build up depicts an uppermost soft, soupy, grey clay unit. This unit shows distinct wedge shape with significant thickening adjacent to the shore and thinning seawards. Fabric study confirms highly fluidised nature of the top mud layer. The dispersal pattern of the sediments document a net transport of mud from all sides indicating localised piling up of fresh mud by marine processes. Weaker divergence of waves south of Kadalur Point facilitate such a pattern of mud deposition.

Geochemical studies depict selective semblance of certain major elements with texture, mineralogy and organic matter related incorporation/sorption processes. Three main inter-related elemental groups with corresponding controlling factors such as, hydrous alumino-silicates in the finer sediments, shell fragments and other detrital minerals are identified. The heavy load of suspension in the initial stage of mud bank formation is essentially triggered by physical processes. But the sustenance of suspension for a longer period is attributed to chemical mechanisms. Presence of phosphate (a natural peptizer) facilitates peptization of the fine bottom sediments containing enhanced levels of Al_2O_3 and Fe_2O_3. Particles from the peptized bed that come into suspension remain in water for a longer period presumably due to the optimum salinity concentration of overlying water column.

Alleppey and Quilandy mud banks show striking similarities in sediment texture and dispersal patterns. Though Quilandy area receives direct influx of riverine sediments, high rate of sedimentation required to build up the uppermost fluidised mud layer can not be explained fluviatile contribution alone. To a major extent in both the locations wave energy distribution controls deposition of fluid mud. The dispersal pattern and the evidences culminated from textural and chemical analyses suggest that the mechanism of deposition in the two locations (Alleppey and Quilandy) are apparently similar. This is due to the transportation of fluidised muddy layer from offshore and alongshore. The minor variations observed in the chemical compositions of the sediments in the two locations do not alter the physical properties of sediments considerably. So, it is concluded that, the mud banks of Alleppey and Quilandy are similar in nature and the formation of which are resulted from a similar set of processes. The minor differences in sediment

constituents and physical aspects of these locations are due to the differences in coastal settings and provenance of sediments.

The term 'fluid mud' appears to be a more precise terminology to describe this phenomenon than the current usage of 'mud banks'. The Kerala mud banks do not occur as an annual relief-forming feature as do mud banks described from other known muddy coasts. The transient nature, the extremely unpredictable periodicity and the inconsistency in localised occurrences clearly demonstrate the major differences with other similar phenomena reported elsewhere. A critical sediment concentration, and hydrodynamic condition have to be facilitated in order to form a fluid mud in the nearshore. The muddy nature of the substratum, proximity of the coast and the very high amount of suspended sediments are the features which the Kerala fluid mud events have in common with other muddy coasts of the world.

REFERENCES

Ananthakrishnan, R. Parthasarathy, B. and Pathan, J.M., 1979. Meteorology of Kerala. In: Contribution to marine sciences (dedicated to Dr. C.V. Kurian). G.S.Sharma, A.Mohandas and A.Antony (Eds.), pp. 60-125.

Arrhenius, G.O.S., 1966. Sedimentary record of long-term phenomena. In: Advances in Earth Science, P.M. Hurley (Ed.), M.I.T. Press, Cambridge, Mass., pp. 155-174.

Arthur, R.S., Munk, W.H. and Issacs, J.D., 1952. The direct cosntruction of wave rays. EOS Trans. American Geophys. Union, v. 23, pp. 855-865.

Baba, M., 1988. Wave characteristics and beach processes of the south-west coast of India - a summary. In: Ocean waves and beach process, M.Baba and N.P.Kurian (Eds.), CESS, Trivandrum, pp. 225-239.

Baba, M. and Joseph, P.S., 1988. Deepwater wave climate off Cochin and Trivandrum. In: Ocean waves and beach processes, M.Baba and N.P. Kurian (Eds.), CESS, Trivandrum, pp. 129-139.

Baba, M., Kurian, N.P. and Mathew, J., 1990. Wave attenuation in mudbanks of Kerala coast. First Year's Report, CESS, Trivandrum, 50p.

Bates, R.L. and Jackson, J.A., 1980. Glossary of Geology. American Geol. Inst., Falls Church, Va., 751p.

Beiersdorf, H., Kudrass, H.R. and Von Stackelberg, U., 1980. Placer deposits of ilmenite and zircon in the Zambezi shelf. Geol Jahrb., Reihe D., v. 9 (36), pp. 5-85

Berthois, L., 1961. Observation directe des particules sedimentaires fines dan l'eau. Revue. Geogr. Phys. Geol. Dyn., v. 4, pp. 39-42.

Bhatt, J.J., 1974. Ti/Al ratio as chemical index of paleoenvironment - a note. Chem. Geol., v. 13, pp. 75-78.

Biscaye, P.E., 1965. Mineralogy and sedimentation of recent deep sea clays in the Atlantic Ocean seas and oceans. Geol. Soc. America Bull., v. 76, pp. 803-832.

Bischoff, J.L., Heath, G.R. and Leinen, M., 1979. Geochemistry of deep-sea sediments from the Pacific Manganese Nodules Province: DOMES Sites A,B and C. In: J.L. Bischoff and D.Z. Piper (Eds.), Marine Geology and Oceanography of the Pacific Manganese Nodules Province, Plenum Press, New York, pp. 397-426.

Boles, J.R. and Franks, S.G., 1979. Clay diagenesis in Wilcox sandstones of southwest Texas. Jour. Sed. Petrol., v. 49, pp. 55-70.

Booth, J.S. 1973. Textural changes as an indicator of sediment dispersion in the northern channel island passages, California. Jour. Sed. Petrol., v. 43, pp. 238-250.

Bristow, R.C., 1938. History of Mud Banks. Vol I & II, Cochin Govt. Press.

Bruland, K.W., Bertine, K., Koide, M. and Goldberg, E.D., 1974. History of metal pollution in Southern California coastal zone. Environ. Sci. Technol., v. 5, pp. 425-432.

Bull, P.A., 1977. Glacial deposits identified by chattermark trails in detrital garnets - Comment. Geology, v. 5, pp. 248-249.

Bull, P.A., 1978. Quantitative approach to SEM analysis of cave sediments. In: Scannin electron microscopy in the study of the sediments, W.B. Whalley (Ed.), pp. 201-226.

Bull, P.A., Culver, S.J. and Gardner, P., 1980. Chatter mark trails as palaeo-environmental indicators. Geology, v. 8, pp. 318-322.

Burns, V.M., 1979. Marine placer minerals. Mineral. Soc. Amer. Short course Notes., v.6, pp. 347-380.

Calvert, S.E., 1976. The mineralogy and geochemistry of nearshore sediments. In: Chemical oceanography, J.P Riley and R.Chester (Eds.), Academic Press, v.6, pp. 187-280.

Carmody, D.J., Pearce, J.B. and Yasso, W.E., 1973. Trace metals in sediments of the New York Bight. Mar. Poliut. Bull., v. 4, pp. 132-135.

Carver, R.E., 1971. Procedures in sedimentary petrology. John Wiley and Sons. 653p.

Casteno, J.R. and Garrels, R.M., 1950. Experiments on the deposition of iron with special reference to the Clinton iron ore deposits. Econ. Geol., v. 45, pp. 755-770.

Chacko, T., Ravindra Kumar, G.R., Meena, J.K. and Rogers, J.J.W., 1988. Geochemistry of granulite facies supracurstals of Kerala khondalite belt, south India. (in press: Precambrian Res.).

Chester, R., 1990. Marine Geochemisty. Unwin Hyman, London, 698p.

Chester, R. and Hughes, M.J., 1969. The trace element geochemistry of a North Pacific pelagic clay core. Deep Sea Res., v. 16, pp. 639-654.

Chester, R. and Aston, S.R., 1976. The geochemistry of deep-sea sediments. In: Chemical Oceanography, J.P. Riley and R. Chester (Eds.), Academic Press, London, v. 6, pp. 281-390.

Churchman, G.J., 1980. Clay minerals formed from micas and chlorite in some New Zealand soils. Clays and Clay Min., v. 15, pp. 59-76.

Clemens, K.E., 1987. Along-coast variations of Oregon beach-sand compositions produced by the mixing of sediments from multiple sources under a transgressing sea (unpublished master's thesis): Corvallis, Oregon State University, 75 p.

Clemens, K.E, and Komar, P.D., 1988. Oregon Beach-sand composition produced by the mixing of sediments under a transgessing sea. Jour. Sed. Petrol, v. 58 pp. 519-529.

Cline, J.T., Hillson, J.B. and Upchruch, S.B., 1973. Mercury mobilization as an organic complex. Proc. 16th Conf. Great Lakes Research., Int. Assoc. Great Lakes Res., pp. 23-242.

Connah, T.H., 1961. Beach sand heavy mineral deposits of Queensland. Geol. Surv. Queensland, Publ. v.302, pp. 1-31.

Cosma, B., Drago, M., Picazzo, M., Scarponi, G. and Tucci, S., 1979. Heavy metals in Lingurian Sea sediments: distribution of Cr, Cu, Ni and Mn in superficial sediments. Mar. Chem., v. 8, pp. 125-142.

Cronan, D.S., 1972. Skewness and kurtosis in polymodal sediments from the Irish sea. Jour. Sed. Petrol., v. 42, pp. 102-106.

Cronan, D.S., 1980. Underwater Minerals. Academic Press, London, 362p.

Damodaran, R., 1973. Studies on the mud banks of the Kerala coast. Bull. Dept. Mar. Biol. Oceanogr. Univ. Kerala, v. 6, pp. 1-126.

Damodaran, R. and Hridayanathan, C., 1966. Studies on the mudbanks of the Kerala coast. Bull. Dept. Mar. Biol. Oceanogr. Univ. Kerala, v. 2, pp. 61-68.

Danielson, L.G, 1980. Cadmium, cobalt, copper, iron, lead, nickel and zinc in Indian Ocean water. Mar. Chem., v. 8, pp. 199-215.

Davis, J.C., 1973. Statistics and data analysis in geology. John Wiley & Sons, Inc., 550p.

Davis, J.A. and Leckie, J.O., 1978. Effect of adsorbed complexing ligands on trace metal uptake by hydrous oxides. Env. Sci. Technol., v. 12, pp. 1309-1315.

Degens, E.T. and Mopper, K., 1976. Factors controlling the distribution of early diagenesis of organic material in marine sediments. In: Chemical Oceanography, J.P. Riley and R.Chester (Eds.), Academic Press, v. 6, pp. 59-113.

Dora, Y.L., Damodaran, R. and Jos-Anto, V., 1968. Texture of the Narakkal mud bank sediments. Bull. Dept. Mar. Biol. Oceanogr. Univ. Kerala, v. 4, pp. 1-10.

Du Cane, C.G., Bristow, R.C., Coggin Brown, C., Keen, B.A. and Russel, E.W., 1938. Report of the special committee on the movement of mud banks. Cochin Govt. Press, 57p.

Dyer, K.R., 1986. Coastal and estuarine sediment dynamics. John Wiley & Sons, New York, 432p.

Eaton, A.D., 1976. Marine geochemistry of cadmium. Mar. Chem., v. 4, pp. 146-154.

Eisma, D. and Van Der Marel, H.W., 1971. Maarine muds along the Guyana coast and their origin from the Amazon basin. Contrib. Mineral. Petrol., v. 31, pp. 321-334.

El Wakeel, S.K. and Riley, J.P., 1957. The determination of organic carbon in marine sediments. Jour. Cons. Per. Int. Expl. Mer., v. 22, pp. 180-183.

Emery, K.O., 1960. The sea off southern California: a modern habitat of petroleum. John Wiley Sons, New York, 366p.

Erlenkeuser, H., Suess, E. and Willkomm, H., 1974. Industrialisation affects heavy metal and carbon isotope concentrations in recent Baltic Sea sediments. Geochim. Cosmochim. Acta, v. 38, pp. 823-842.

Farrah, H., Hattom, D and Pickering, W.F., 1980. The affinity of metal ions for clay surfaces. Chem. Geol., v. 28, pp. 55-68.

Filpek, L.H. and Owen, R.M., 1978. Analysis of heavy metal distributions among different mineralogical states in sediments. Can. Jour. Spectrosc., v. 23, pp. 31-34.

Filipek, L.H. and Owen, R.M., 1979. Geochemical associations and grain-size partitioning of heavy metals in lacustrine sediments. Chem. Geol., v. 26, pp. 105-117.

Folk, R.L., 1974. Petrology of sedimentary rocks. Hemphill, Austin, 121p.

Folk, R.L., 1975. Glacial deposits identified by chattermarks in detrital garnets. Geology, v. 8, pp. 473-475.

Folk, R.L. and Ward, W.C., 1957. Brazos river bar, a study in the significance of grain-size parameters. Jour. Sed. Petrol., v. 27, pp. 3.27.

Forstner, U. and Wittmann, G.T.W., 1983. Metal pollution in aquatic environment. Springer-Verlag, N.Y., 486p.

Franzier, D.E., 1974. Depositional episodes, their relationship to the Quarternary stratigraphic framework in the northwestern portion of the Gulf Basin. Univ. Texas, Austin, Bureau of Econ. Geol., Geol. circular, v. 74, 28p.

Friedman, G.M., 1961. Distribution between dune, beach and river sands from their textural characteristics. Jour. Sed. Petrol., v. 31, pp. 514-529.

Friedman, G.M., 1962. On sorting, sorting coefficients and the log-normality of the grain-size distribution of clastic sandstones. Jour. Geol., v. 70, pp. 737-753.

Friedman, G.M., 1967. Dynamic processes and statistical parameters compared for size frequency distribution of beach and river sands. Jour. Sed. Petrol., v. 37, pp. 327-354.

Gade, H.G., 1958. Effects of non-rigid, impermeable bottom on plane surface waves in shallow water. Jour. Mar. Res., v. 16, pp. 61-82.

Garrels, R.M., 1984. Montmorillonite/illite stability diagrams. Clays and Clay Min., v. 32 pp. 161-166.

Garrels, R.M. and Christ, C.L., 1965. Solutions, minerals and equilibria. Harper and Row, New York, N.Y., 450p.

Georgiev, V.M. and Stoffers, P., 1980. Surface textures of quartz grains from late Pliestocene to Holocene sediments of the Persian Gulf, Gulf of Oman: an application of scanning electron microscopy. Mar. Geol., v. 36, pp. 85-96.

Gibbs, R.J., 1977. Transport phases of transition metals in the Amazon and Yukon Rivers. Geol. Soc. Am. Bull., v. 88, pp. 829-843.

Glasstone, S., 1974. Textbook of physical chemistry. The MacMillan Company of India Ltd., 2nd Edition, 1320p.

Goldberg, E.D, and Griffin, J.J., 1970. The sediments of northern Indian Ocean. Deep sea Res., v. 17, pp. 513-537.

Goldschmidt, V.M., 1954. Geochemistry. Clarendon Press, Oxford, 438p.

Gopinathan, C.K. and Qasim, S.Z., 1974. Mud banks of Kerala: their formation and characteristics. Indian Jour. Mar. Sci., v. 3, pp. 105-114.

Gravenor, C.P., 1982. Chattermarked garnets in Pleistocene glacial sediments. Bull. Geol. Soc. America, v. 93, pp. 751-758.

Gravenor, C.P., 1985. Chattermarked garnets found on soil profiles and beach environment. Sedimentology, v. 32, pp. 295-306.

Gravenor, C.P, and Levitt, R.K., 1981. Experimental formation and significance of etch patterns on detrital garnets. Jour. Earth Sci., v. 18, pp. 765-775.

Gravenor, C.P., McLelwain, T.A. and Stupavsky, M., 1977. Chattermark trails on heavy minerals in glacial sediments. Geology, v. 6, pp. 61-63.

Griffiths, J.C., 1951. Size versus sorting in some Carribbean sediments. Jour. Sed. Petrol., v. 59, pp. 211-243.

Griffin, G.M., 1962. Regional clay mineral facies-products of weathering intensity and current distribution in the northeastern Gulf of Mexico. Bull. Geol. Soc. America, v. 73, pp. 737-768.

Griffin, J.J., Windon, H. and Goldberg, E.D., 1968. The distribution of clay minerals in the world oceans. Deep Sea Res., v. 15. pp. 433-459.

Grim, R.E., 1968. Clay mineralogy, 2nd ed., McGraw-Hill Book Co., 596 pp..

Gupta, M.V.S., 1973. Planktonic forminifera from the shelf sediments off Cochin. Indian Jour. Mar. Sci., v. 2, pp. 147-148.

Gupta, S.K. and Chen, K.Y., 1975. Partitioning of trace metals in selective chemical fractions of nearshore sediments. Environ. Lett., v. 10, pp. 129-158.

Hameed, T.S.S., 1988. Wave climatology and littoral processes at Alleppey. In: Ocean waves and beach processes, M.Baba and N.P.Kurian (Eds.), CESS, Trivandrum. pp 67-90.

Hashimi, N.H. and Nair, R.R., 1981. Surficial sediments of the continental shelf off Karnataka. Jour. Geol. Soc. India., v. 22, pp 226-273.

Hashimi, N.H. and Nair, R.R., 1986. Climatic aridity over India 11,000 years ago; evidence from feldspar distribution in shelf sediments. Palaeogeography, palaeoclimatology, palaeoecology, v. 53, pp 309-320.

Hashimi, N.H., Nair, R.R. and Kidway, R.M., 1977. Sediments of the Gulf of Kutch - A high energy tide dominated environment. Indian Jour. Mar. Sci., v. 7, pp. 1-7.

Hashimi, N.H., Kidway, R.M. and Nair, R.R., 1978. Grain size and coarse fraction studies of the sediments between Vengurla and Mangalore on the western continental shelf of India. Indian Jour. Mar. Sci., v. 7, pp. 231-238.

Hashimi, N.H., Kidway, R.M. and Nair, R.R., 1981. Comparative study of the topography and sediments of the western and eastern continental shelves around Cape Comorin. Indian Jour. Mar. Sci., v. 10, pp. 45-50.

Heath, G.R. and Dymond, J., 1977. Genesis and transformation of metalliferous sediments from the East Pacific Rise, Bauer Deep and Central Basin, Northwest Nazca Plate. Bull. Geol. Soc. America, v. 88, pp. 723-733.

Helz, G.R., 1976. Trace element inventory for the northern Chesapeake Bay with emphasis on the influence on man. Geochim. Cosmochim. Acta., v. 40, pp. 573-580.

Helz, G.R., Huggett, R.J. and Hill, J.M., 1975. Behavior of Mn, Fe, Cu, Zn, Cd and Pb discharged from a waste water treatment plant into an estuarine environment. Water Res., v. 9, pp. 631-636.

Hey, R.W., Krinsley, D.H. and Hyde, P.J.W., 1971. Surface texture of sand grain from Herfordshire pebble gravels. Geol. Mag., v. 108, pp. 377-382.

Hill, P.R. and Nadeau, O.C., 1989. Storm-dominated sedimentation on the inner shelf of the Canadian Beaufort sea. Jour. Sed. Petrol., v. 59, pp. 455-468.

Hiranandani, M.G. and Gole, C.V., 1969. Formation and movement of mud banks and their effect on south westerly coast of India (Abstract). Int. Oceanogr. Cong. American Assoc. Adv. Sci., Washington, pp. 623-624.

Hirst, D.M., 1962. The geochemistry of modern sediments from the Gulf of Paria- I : The relation between the mineralogy and the distribution of major elements. Geochim. Cosmochim Acta, v. 26, pp. 309-334.

Holmes, C.W., 1982. Geochemical indices of fine sediment transport, northwest Gulf of Mexico. Jour. Sed. Petrol., v. 52, pp. 307-321.

Hope, K., 1968. Methods of multivariate analysis. Unibooks, Univ. London Press, 165p.

Hunt, J.M., 1979. Petroleum Geochemistry and Geology. W.H. Freeman, San Francisco, CA, 617p.

Hunt, C.D., 1981. Regulation of sedimentary cation exchange capacity by organic matter. Chem. Geol., v. 34, pp. 131-149.

Imbrie, J., 1963. Factor and factor analysis programmes for analysing geologic data. Office Naval Res., Geogr. Branch Tech. Rep., v. 6, 83p.

Imbrie, J. and Purdy, E., 1962. Classification of modern Bahamian carbonate sediments. In: Cassification of carbonate rocks. Mem. American Assoc. Petrol. Geol., v. 7, pp. 253-272.

Imbrie, J. and Van Andel, Tj.H., 1964. Vector analysis of heavy mineral data. Geol. Soc. America Bull., v. 75, pp. 1131-1156.

Ingle, J.C., 1966. The movement of beach sand. In: Developments in sedimentology. Elsevier, New York, 221p.

Inman, D.L., 1949. Sorting of the sediments in the light of fluid mechanics. Jour. Sed. Petrol., v. 19, pp. 51-70.

Inman, D.L., 1952. Measures for describing the size distribution of sediments. Jour. Sed. Petrol., v. 22, pp. 125-145.

Iyer, V.L. and Moni, N.S., 1972. Effect of mud banks on the south-west coast of India. Paper presented at the 42nd annual research section of CBIP., pp. 89-98.

Jacob, K., 1956. Ilmenite and garnet sands of the Chowghat (west coast), Tinnevelly, Ramnad and Tanjore coasts (east coast). Rec. Geol. Surv. India, v. 82 (4), pp. 567-602.

Jacob, P.G., and Qasim, S.Z., 1974. Mud of the mudbank in Kerala, southwest coast of India. Indian Jour. Mar. Sci., v. 3, pp. 115-119.

Karpovich, R.P., 1971. Surface features of quartz sand grains from the north east gulf of Mexico. Trans. Gulf coast Assoc. Geol. Soc., v. 21, pp. 451-461.

Keller, W.D., 1970. Environmental aspects of clay minerals. Jour. Sed. Petrol. v. 40, pp. 788-814.

King, W., 1884. Mudbanks of Narakkal and Alleppey on the Travancore coast. Rec. Geol. Surv. India, 17p.

Klovan, J.E., 1966. The use of factor analysis in determining depositional environments from grain size distributions. Jour. Sed. Petrol., v. 36; pp. 115-125.

Koczy, F.F., 1951. Factors determining the element concentration in sediments. Geochim. Cosmochim. Acta., v. 1, pp. 73-85.

Kolla, V. and Biscaye, P.E., 1973. Deep-sea zeolites; variations in space and time in the sediments of the Indian Ocean. Mar. Geol., v. 15, pp. 11-17.

Kolla, V., Henderson, L. and Biscaye, P.E., 1976. Clay mineralogy and sedimentation in the western Indian Ocean. Deep Sea Res., v. 23, pp. 949-961.

Kolla, V., Kostecki, J.A., Robinson, F., Biscaye, P.E. and Ray, P.K., 1981. Distribution and origin of clay minerals and quartz in surface sediments of the Arabian Sea. Jour. Sed. Petrol., v. 51, pp. 563-569.

Komar, P.D., 1976. Beach processes and sedimentation. Prentice Hall Inc., New Jersey, 429p.

Komar, P.D. and Wang, C., 1984. Processes of selective grain transport and the formation of placers on beaches. Jour. Geol., v. 92, pp. 637-655.

Komar, P.D., Clemens, K.E., Li, Z. and Shih, S., 1989. The effects of selective sorting on factor analyses of heavy-mineral assemblages. Jour. Sed. Petrol., v.59, pp. 590-596.

Krank, K., 1975. Sediment deposition from flocculated suspension. Sedimentology, v. 22, pp. 111-123.

Kraus, N.C., 1987. Application of portable traps for obtaining point measurements of sediment transport rates in the surf zone. Jour. Coastal Res., v. 3, pp. 139-152.

Krauskopf, K.B., 1956. Factors controlling the concentration of thirteen rare metals in sea-water. Geochim. Cosmochim. Acta., v. 9, pp. 1-32B.

Krinsley, D.H. and Donahue, J., 1968. Environmental interpretation of sand grain surface textures by electron microscopy. Bull. Geol. Soc. America., v. 79, pp. 743-748.

Krinsley, D.H. and Margolis, S.V., 1971. Grain surface textures. In: Procedures in sedimentary petrology, Wiley Interscience, New York, pp. 151-180.

Krinsley, D.H. and Doornkamp, J., 1973. Atlas of quartz surface textures. Cambridge University Press, 91p.

Krishnan, M.S., 1960. Geology of India and Burma. Higginbothams, Madras, 555p.

Krishsnaswami,S.1976.Authigenic transition elements in Pacific pelagic clays, Geochim.Cosmochim.Acta v. 40, pp. 425-434.

Krumbein, W.C., 1934. Size frequency distribution of sediments. Jour. Sed. Petrol., v. 4, pp. 65-77.

Krumbein, W.C., 1937. Sediments and exponential curves. Jour. Geol., v. 45, pp. 577-601.

Krumbein, W.C., 1938. Size frequency distribution of sediments and the normal phi curve. Jour. Sed. Petrol., v. 8, pp. 84-90.

Krumbein, W.D., and Rasmussen, W.C., 1941. The probable error of sampling beach sand for heavy mineral analysis. Jour. Sediment. Petrol., v. 11, pp. 10-20.

Kuehl, S.A., Nittrouer, C.A. and DeMaster, D.J., 1988. Microfabric study of fine-grained sediments: Observations from the Amazon subaqueous delta. Jour. Sed. Petrol., v. 58, pp. 12-23.

Kulm, L.D., Scheidegger, K.F., Byrne, J.V. and Spigal, J.J., 1968. A prelimary investigation of the heavy mineral suites of the Coast rivers and beaches of Oregon and Northern California: The Ore Bin, v. 30, pp. 165-180.

Kurian, C.V., 1969. Studies on the benthos of the southwest coast of India. Bull. Natl. Inst. Sci. India, v. 38, pp. 649-656.

Kurian, N.P. and Baba, M., 1987. Wave attenuation due to bottom friction across the southwest Indian continental shelf. Jour. Coastal Res., v. 3, pp. 485-490.

Kurup, P.G., 1972. Littoral currents in relation to the mud bank formations along the coast of Kerala. Mahasagar-Bull. Natn. Inst. Oceanogr., v. 2, pp. 158-162.

Kurup, P.G., 1977. Studies on physical aspects of the mud banks along the Kerala coast with special reference to the Purakkad mud bank. Bull. Dept. Mar. Sci. Univ. Cochin, v. 8, pp. 1-72.

Kurup, P.G. and Varadachari, V.V.R., 1975. Hydrography of Purakkad mud bank region. Indian Jour. Mar. Sci., v.4, pp. 18-20.

Landergen, S., 1964. On the geochemistry of deep-sea sediments. Reports of the Swedish dep-sea expedition, v. 10, Spec. Invest. no. 5, pp. 61-148.

Lewis, D.W., 1984. Practical sedimentology. Stroudsburg, Pennsylvania, Hutchinson Ross, 229p.

Machado, X.T. and Baba, M., 1984. Movement of beach sand in Vizhinjam Bay, west coast of India. Indian Jour. Mar. Sci., v. 13, pp. 144-146.

Mackenzie, F.T. and Garrels, R.M., 1966. Chemical mass balance between rivers and oceans. American Jour. Sci., v. 26, pp. 507-525.

Mac Pherson, H. and Kurup, P.G., 1981. Wave damping at the Kerala mudbanks. Indian Jour. Mar. Sci., v. 10, 154-160.

Mahadevan, C. and Rao, B.N., 1950. Black sand concentrates of Visakhapatnam coast. Curr. Sci., v. 19, pp. 48-49.

Mallik, T.K., 1974. Heavy mineral placers in the beaches and offshore aras-their nature, origin, economic potential and exploration. Indian Miner., v. 28, pp. 39-46.

Mallik, T.K., 1986a. An inexpensive hand-operated device for cutting core liners. Mar. Geol., v. 70, pp. 307-311.

Mallik, T.K., 1986b. Micromorphology of some placer mineals from Kerala beach, India. Mar. Geol., v.71, pp. 371-381.

Mallik, T.K. and Ramachandran, K.K., 1984. Mud banks of Kerala coast - a state of the art report. Rep. State Comm. Sci. Techn. Govt. Kerala., 21p.

Mallik, T.K. and Suchindan, G.K., 1984. Some sedimentological aspects of Vembanad lake, Kerala, West coast of India. Indian Jour. Mar. Sci., v.13, pp. 159-163.

Mallik, T.K., Vasudevan, V., Verghese, P.A. and Machado, T., 1987. The Black sand placer deposits of Kerala beach, South west India. Mar. Geol., v.77, pp. 129-150.

Mallik, T.K., Mukherji, K.K. and Ramachandran, K.K., 1988. Sedimentology of the Kerala mud banks (fluid mud?). Mar. Geol., v. 80, pp. 99-118.

Martin, J.-M., and Whitfield, M., 1983. The significance of the river input of chemical elements to the ocean. In: Trace metals in sea water, C.S. Wong, E.A. Boyle, K.W. Bruland, J.D. Burton and E.D. Goldberg (Eds.), Plenum, New York, pp. 265-296.

Marson, B., 1951. Pricipies of Geochemistry. John Wiley and Sons, N.Y., 310p.

Mathew, J., 1992. Wave-mud interaction in mudbanks. Ph.D. thesis submitted to the Cochin Univ. Sci. Technol., Cochin, (Unpublished).

Mathew, J. and Baba, M., 1991. On generation of mudbanks. Proc. Third Int. Conf. Coastal and Port Engng. Developing Countries, Kenya, pp. 918-924.

Mazzullo, J. and Crisp, J., 1985. Sources and dispersal of coarse silt on the Texas continental shelf. Mar. Geol., v. 69, pp. 131-148.

McCammon, R.B., 1962. Efficiencies of percentile measures for describing the mean size and sorting of sedimentary particles. Jour. Geol., v. 70, pp. 453-465.

McKinney, T.F. and Friedman, G.M., 1970. Continental shelf sediments of Long Island, New York. Jour. Sed. Petrol., v. 40, pp. 213-248.

McLaren, P., 1981. An interpretation of trends in grain size measures. Jour. Sed. Petrol., v. 51, pp. 611-624.

McLaren, P. and Bowles, D., 1985. The effects of sediment transport on grain size distributions. Jour. Sed. Petrol., v. 55, pp. 457-470.

Meyer, K., 1983. Titanium and zircon placer prospect of Palmoddi. Sri Lanka Mar. Min., v. 4, pp. 139-166.

Mezzadri, G, and Saccani, E., 1989. Heavy mineral distribution in late quaternary sediments of the southern Aegean Sea: Implications for provenance and sediment dispersal in sedimentary basins at active margins. Jour. Sed. Petrol., v. 59, pp. 412-422.

Middelburg, J.J., 1991. Organic carbon, sulphur, and iron in recent semi-euxinic sediments of Kau Bay, Indonesia. Geochim. Cosmochim. Acta, v. 55, pp. 815-828.

Middleton, G.V., 1976. Hydraulic interpretation of sand distribution. Jour. Geol., v. 84, pp. 405-426.

Milliman, J.D., Butenko, J., Barbot, J.P. and Hedberg, J., 1982. Depositional patterns of modern Orinoco/Amazon mud on the northern Venezuelan shelf. Jour. Mar. Res., v. 40, pp. 643-657.

Mills, G.L. and Quinn, J.G., 1981. Isolation of dissolved organic matter and copper organic complexes from estuarine waters.

Mitchell, R.L., 1964. Trace elements in soils. In: Chemistry of the soil. 2nd Edn., F.E.Bear and Reinold (Eds.), New York, pp. 320-368.

Mohana Rao, K., Rajamanickam, G.V. and Rao, T.C.S., 1989. Holocene marine transgression as interpreted from bathymetry and sand grain-size parameters off Gopalpur. Proc. Indian Acad. Sci., v. 98, pp. 173-181.

Moni, N.S., 1971. Study of the mud banks along the south-west coast of India. Proc. Symp. Coastal Erosion and Protection, KERI, Peechi, Kerala, F.8, 1-F. 8.8.

Moore, C. and Bostrom, K., 1978. The elemental composition of lower marine organisms. Chem. Geol., v. 23, pp. 1-9.

Morton, A.C., 1984. Stability of detrital heavy minerals in Tertiary sandstone from the North Sea basin. Clay minerals, v. 19, pp. 287-308.

Morton, A.C., 1985. New approach to provenance studies - Electron microprobe analysis of detrital garnets from Middle Jurassic sandstones of the northern South sea. Sedimentology, v. 32, pp. 553-566.

Muller, P.J. and Suess, E., 1979. Productivity, sedimentation rate and sedimentary organic matter in the oceans I. - Organic carbon preservation. Deep-sea Res., v. 26, pp. 1347-1362.

Murty, A.V.S., Rao, D.S., Raghunathan, A., Gopinathan, C.P. and Mathew, K.J., 1984. Hypothesis on mud banks. Bull. Cent. Mar. Fish. Res. Inst. Cochin, v. 51, pp. 8-18.

Murty, P.S.N., Rao, Ch. M. and Reddy, C.V.G., 1973. Partition pattern of iron, manganese, nickel and cobalt in the shelf sediments of west coast of India. Indian Jour. Mar. Sci., v. 2, pp. 6-12.

Murty, P.S.N., Rao, Ch.M. and Paropkari, A.L., 1980. Distribution patterns of aluminium, manganese, nickel, cobalt and copper in the non-lithogenous fraction of sediments of the northern half of the western continental shelf of India. Indian Jour. Mar. Sci., v. 9, pp. 56-61.

Murty, P.S.N., Reddy, C.V.G. and Varadachari, V.V.R., 1968. Distribution of Total phosphorus in the shelf sediments off the west coast of India. Proc. Natn. Inst. Sci. India, v. 34, pp. 134-141.

Naidu, A.S., Mowatt, F. T.C., Somayajulu, B.K.K, and Sreeramachandra Rao, K., 1985 Characteristics of clay minerals in the bed loads of major rivers of India. Mitt. Geol. Palaeontol. nInst. Univ. Hamburg, SCOPE/UNEP Sonderb., v.58, pp. 559-568.

Nair, R.R., 1971. The continental shelf, souvenir, seminar on scientific, technological and legal aspects of the Indian continental shelf. Jour. Indian Geophys. Union., v

Nair, R.R., 1972. Outer shelf carbonate pinnacles and troughs on the western continental shelf of India. Jour. Indian Geophys. Union, v. 10, pp. 135-140.

Nair, R.R., 1974. Holocene sea levels on the western continental shelf of India. Proc. India Acad. Sci., v. 79, pp. 197-203.

Nair, R.R., 1975. Nature and origin of small scale topographic prominence on the western continental shelf of India. Indian Jour. Mar. Sci., v. 4, pp. 25-29.

Nair, R.R., 1976. Unique mud banks, Kerala, southwest India. Bull. American Assoc. Petrol. Geol., v. 60, pp. 616-621.

Nair, R.R. and Murthy, P.S.N., 1968. Clay mineralogy of mud banks of Cochin. Curr. Sci., v. 37, pp. 589-590.

Nair, R.R. and Pylee, A., 1968. Size distribution and carbonate content of the western shelf of India. Bull. Natn. Inst. Sci., v. 38, pp. 411-520.

Nair, R.R. and Hashimi, N.H., 1980. Holocene climate inferences from the sediments of the western Indian continental shelf. Proc. Indian Acad. Sci., v. 89, pp. 299-315.

Nair, R.R. and Hashimi, N.H., 1981. Mineralogy of the carbonate sediments - western continental shelf of India. Mar. Geol., v. 41, pp. 309-319.

Nair, R.R. and Hashimi, N.H, 1987. On the origin of the cohesive and non-cohesive sediment boundary on the western shelf of India. Contributions in Mar. Sci., Natn. Inst. Oceanogr., Goa, pp. 413-425.

Nair, R.R., Hashimi, N.H. and Guptha, M.V.S., 1979. Holocene sea levels on the western continental shelf of India. Jour. Geol. Soc. India, v. 20, pp. 17-23.

Nair, R.R., Hashimi, N.H. and Rao, P.V., 1982. Distribution and dispersal of clay minerals on the western continental shelf of India. Mar. Geol., v. 50, pp. M1-M9.

Nair, R.R., Murty, P.S.N. and Varadachari, V.V.R., 1966. Physical and chemical aspects of mud deposit of Vypeen beach, Int. Indian Ocean Exp. Newsletter, Symp., v. 4, pp. 1-10.

Nair, R.R., Hashimi, N.H., Kidway, R.M., Guptha, M.V.S., Paropkari, A.L., Ambre, N.V., Muralinath, A.S., Mascarenhas, A. and D.Costa, G.P., 1978. Topography and sediments of the western continental shelf of India-Venguria to Mangalore. Indian Jour. Mar. Sci., v. 7, pp. 77-86.

Narayanaswamy and Ghosh, S.K., 1987. Laterisation of gabbro-grnophyre rock units of the Ezhimala complex of north Kerala, India. Chemical Geol., v. 60, pp. 251-257.

Nelson, B.W., 1960. Clay mineralogy of the bottom sediments, Rappahannock River, Virginia. Clays and Clay Min., 7th Conf., Pergamon Press, New York, pp. 135-147.

Nicholls, G.D. and Loring, D.H., 1962. The geochemistry of some British Craboniferous sediments. Geochim. Cosmochim. Acta., v. 26, pp. 181-223.

Nigam, R. and Thiede, J., 1984. Recant foraminifera from the innershelf of the central west coast- A reappraisal using factor analysis. Proc. Indian Acad. Sci., v. 92, pp. 121-128.

Nigam, R., Setty, M.G.A.P. and Ambre, N.V., 1979. A check list of benthic foraminiferids from the innershelf of Dabhol-Vengurla region, Arabian sea. Jour. Geol. Soc. India, v. 20, pp. 244-247.

Nittrouer, C.A. and DeMaster, D.J., 1986. Sedimentary processes on the Amazon continental shelf: past, present and future research. Cont. Shelf Res., v. 6, pp. 5-30.

Ouseph, P.P.,1987. Heavy metal pollution in the sediments of Cochin esturies system. Proc. Natn. Seminar on Estuarine Management, Trivandrum, pp. 123-127.

Park, Y.A., Kim, S.C. and Choi, J.H., 1986. The distribution and transportation of fine-grained sediments on the inner continental shelf off the Keum river estuary, Korea. Cont. Shelf Res., v. 5, pp. 499-519.

Paropkari, A.L., 1990. Geochemistry of sediments from the Mangalore-Cochin shelf and upper slope off southwest India: Geological and environmental factors controlling dispersal of elements. Chemical Geol., v. 81, pp. 99-119.

Passega, R., 1957. Texture as characteristic of clastic deposition. Bull. American Assoc. Petrol. Geol., v. 41, pp. 1952-1984.

Passega, R. 1964. Grain size representation by CM patterns as a geological tool. Jour. Sed. Petrol., v. 34, pp. 830-847.

Passega, R. and Byramjee, R., 1969. Grain size image of clastic deposits. Sedimentology, v. 13, pp. 233-252.

Passega, R., Rizzini, A. and Borgheth, G., 1967. Transport of sediments by waves, Adriatic coastal shelf, Italy. Bull. American Assoc. Petrol. Geol., v. 51, pp. 1304-1319.

Passega, R., 1977. Significance of CM diagrams of sediments deposited by suspensions. Sedimentology, v. 24, pp. 723-733.

Perhac, R.M., 1972. Distribution of Cd, Co, Cu, Fe, Mn, Ni, Pb, and Zn in dissolved and particulate solids from two streams in Tennessee. Jour. Hydrol., v. 15, pp. 177-186.

Peterson, C., Komar, P.D. and Scheideggar , K.F., 1985. Distribution, geometry and origin of heavy mineral placer deposits on Oregon beaches. Jour. Sed. Petrol., v.56, pp. 67-77.

Peterson, C., Komar, P.D. and Scheideggar , K.F., 1986. Distribution, geometry and origin of heavy mineral placer deposits on Oregon beaches. Jour. Sed. Petrol., v.34, 830-847.

Pettijohn, F.J. , 1941. Persistence of heavy minerals and geological age. Jour. Geol., V. 49, pp. 610-625.

Pettijohn, F.J., 1975. Sedimentary Rocks (second edition), Harper Brothers, New York. 718 p.

Piper, D.,1974. Rare-earths in ferromangenese nodules and other marine phases. Geochim. Cosmochim. Acta, v. 38, pp. 1007-1022.

Plavsic, M., Koza, S., Krznaric, D., Bilinski, H.,and Branica, M., 1980. The influence of organics on the adsorption of Copper(II) on α-Al_2O_3 in sea water, Model studies with EDTA. Mar. Chem., v. 9, pp. 175-182.

Potter, P.E., Shimp, N.F. and Witters, J., 1963. Trace elements in marine and fresh water argillaceous sediments. Geochim. Cosmochim. Acta., v. 27, pp. 669-694.

Prabhakar Rao, G., 1962. Some aspects of the placer deposition of India. D.Sc. Thesis, Andhra University, Waltair,(unpublished).

Prabhakar Rao, G., 1968. Sediments of the nearshore region off Neendakara coast and the Ashtamudi and Vatta estuaries, Kerala, India. Bull. Natl. Inst. Sci., v. 30, pp. 513-551.

Preston, J., 1977. An usual occurrence of quartz and amorphous silica at Carmean, Moneymore. Geol. Mag., v. 5, pp. 389-392.

Prithviraj, M. and Prakash, T.N., 1989. Sediment distribution and transport studies of the innershelf zone off the Central Coast of Kerala, India. Jour. Coastal Res., v. 5, pp. 275-280.

Prithviraj, M. and Prakash, T.N., 1991. Surface microtextural study of detrital quartz grains of inner shelf sediments off Central Kerala coast, India. Indian Jour. Mar. Sci., v. 20, pp. 13-16.

Public Works Department, 1974. Water resources of Kerala. Govt. Kerala, 110p.

Purandara, B.K., 1990. Provenance, sedimentation and geochemistry of the modern sediments of the mud banks off the central Kerala coast, India. Ph.D. thesis, Cochin University of Science & Technology, Cochin.

Qasim, S.Z., 1977. Biological productivity of the Indian Ocean. Indian Jour. Mar. Sci., v. 6, pp. 122-137.

Radhakrishna, T., Thampi, P.K., Mitchell, J.G. and Balaram, V., 1989. Cretaceous Tertiary mafic dyke intrusions in Kottayam region, south western India: Geochemical implications for continental magmatism and lithospheric processes. Continental magmatism. Abs. IAVCEI New Mexico bureau of mines and mineral resources bulletin, v. 131, 220p.

Ramachandran, K.K. and Mallik, T.K., 1985. Sedimentological aspects of Alleppey Mud bank. west coast of India. Indian Jour. Mar. Sci., v. 14, pp. 133-135.

Ramachandran, K.K., 1989. Geochemical characteristics of mudbank environment - a case study from Quilandy, west coast of India. Jour. Geol. Soc. India, v. 33, pp. 55-63.

Ramachandran, K.K. and Samsuddin, M., 1991. Sediment removal from Alleppey nearshore during post-mud bank formation. Proc. Indian Acad. Sci., v. 100, pp. 195-203.

Rama Raju, V.S., 1973. Indian continental shelf in relation to the hundred fathom line. Jour. Indian Geophys. Union, v. 10, pp. 75-92.

Ramasastry, A.A. and Myrland, P., 1959. Distribution of temperature, salinity and density in the Arabian sea along the south Malabar coast (S.India) during the post monsoon. Indian Jour. Fish., v. 6, pp. 223-255.

Rao, Ch. M., Murty, P.S.N. and Reddy, C.V.G., 1972. Distribution of titanium in the shelf sediments along the west coast of India. Proc. Indian natn. Sci. Acad., v. 38A., pp. 114-119.

Rao, Ch. M., Murty, P.S.N. and Reddy, C.V.G., 1974. Partition pattern of copper in the sediments of the western continental shelf of India. Indian Jour. Mar. Sci., v. 3, pp. 12-15.

Rao, Ch.M., Paropkari, A.L., Mascarenhas, A. and Murty, P.S.N., 1987. Distribution of phosphorus and phosphatisation along the western continental margin of India. Jour. Geol. Soc. India, v. 30, pp. 423-438.

Rao, D.S., Raghunathan, A., Mathew, K.J., Gopinathan, C.P. and Murty, A.V.S., 1984. Mud of the mud bank: its distribution and physical and chemical characteristics. Bull. Cent. Mar. Fish. Res. Inst., Cochin, v. 31, pp. 21-25.

Rao, K.K., 1972. Planktonic foraminifera in sediment samples from the Eastern Arabian sea. Indian Jour. Mar. Sci., v. 1, pp. 1-7.

Rao, K.K., 1973. Quantitative distribution of planktonic foraminifera in the SW coast of India. Indian Jour. Mar. Sc., v. 2, pp. 54-61.

Rao, R.R. and Molinari, R.L., 1991. Surface meteorological and near surface oceanographical atlas of the tropical Indian Ocean. NOAA, Tech. Mem. ERL AOML-69

Rao, V.P., Nair, R.R. and Hashimi, N.H., 1983. Clay mineral distribution on the Kerala continental shelf and slope. Jour. Geol. Soc. India, v. 24, pp. 540-546.

Rao, V.P. and Nagendernath, B., 1988. Nature, distribution and origin of clay minerals in grain size fraction of sediments from manganese nodule field, Central Indian Ocean basin. Indian Jour. Mar. Sci., v. 17, pp. 202-207.

Rasmussen, W.C., 1941. Local areal variations of heavy minerals in beach sand. Jour. Sediment. Petrol., v. 11, pp. 98-101.

Rateev, M.A., Gorbunova, Z.N., Listizin, A.P., 1969. The distribution of clay minerals in the ocean. Sedimentology, v. 13, pp. 21-43.

Ravindra Kumar, G.R., Srikantappa, C. and Hansen, E.C., 1985. Charnockite formation at the Ponmudi, southern India. Nature, v. 313, pp. 207-209.

Ravindra Kumar, G.R., Rajendran, C.P. and Prakash, T.N., 1990. Charnockite-Khondalite belt and tertiary-quaternary sequences of southern Kerala. Excursion Guide, Geol. Soc. India, 116p.

Ray, I., Mallik, T.K. and Venkatesh, K.V., 1975. Fluorescent tracer studies in Calicut and Beypore area, Kerala - A preliminary appraisal. Indian Minerals, v. 29, pp. 42-46.

Rea, D. K. and Pigula, J.D., 1977. Sediment distribution and inferred transport processes in Little Traverse Bay, Lake Michigan. 20th Conf. on Great Lakes Res., Ann. Arbor, Mich.

Reddy, C.V.G. and Sankaranarayanan, V.N., 1968. Distribution of nutrients in the shelf waters of the Arabian sea along the west coast of India. Bull. Natn. Inst. Sci. India, v. 38, pp. 206-220.

Reddy, M.P.M. and Varadachari, V.V.R., 1973. Sediment movement in relation to wave refraction along the west coast of India. Jour. Indian Geophys. Union, v. 10, pp. 526-527.

Reddy, N.P.C. and Durga Prasada Rao, N.V.N., 1992. A mid-Holocene strandline deposit on the innershelf of Cochin, West coast of India. Jour. Geol. Soc. India, v. 39, pp. 205-211.

Reiche, P., 1962. A survey of weathering processes and products. The University of New Mexico Press., Alburquerque, 95p.

Ribault, L., 1975. L'exacopie. Method et application. Compagnie Francaise des Petroles, Notes et Memoris. 231p.

Rine, J.M. and Ginsberg, R.N., 1978. A cyclic sedimentary sequence created by migrating mud banks on an open Holocene shelf, Surinam. Section 1. Ann.. Meet. Geol. Assoc. Canada, Toronto, v. 3, 478p.

Rine, J.M. and Ginsberg, R.N., 1985. Depositional facies of a mud surface in Surinam, south America - a mud analogue to sandy shallow marine deposits. Jour. Sed. Petrol., v. 55, pp. 633-652.

Rittenhouse, G., 1943. Transportation and deposition of heavy minerals. Bull. Geol. Soc. America, v. 54, pp. 1725-1780.

Roy, B.C., 1958. Ilmenite sand along Ratnagiri coast, Bombay. Rec. Geol. Surv. India, v. 87, pp. 438-452.

Rubey, W.W., 1933. Settlinhg velocities of gravel, sand and silt particles. American J. Sci., 5th Series, v. 25, pp. 325-338.

Sallenger, A.H.,1979. Inverse grading of hydraulic equivalence in grain flow deposits. Jour. Sed. Petrol., v.49, pp. 553-562.

Samsuddin, M., 1986. Textural differentiation of foreshore and breaker zone sediments on the northern Kerala coast, India. Sed. Geol., v. 46, pp. 135-145.

Samsuddin, M., 1990. Sedimentology and mineralogy of the beach, strand plain and innershelf sediments of the northern Kerala coast. Ph.D. thesis, Cochin Univ. Sci. Technol., Cochin.

Samsuddin, M. and Ramachandran, K.K., 1992. Distribution, selective dissolusion and provenance of heavy minerals from the coastal environments of Kerala, India. (Paper communicated).

Samsuddin, M. and Suchindan, G.K., 1987. Beach erosion and accretion in relation to the seasonal longshore current variation in the northern Kerala coast, India. Jour. Coastal Res., v. 3, pp. 55-62.

Santosh, M., 1987. Cordierte gnesses of south Kerala, India, Petrology, fluid inclusion and implication on uplift history. Contrib. Mineral petrol., v. 97, pp. 343-356.

Santosh, M. and Drury, S.A., 1988. Alkali granites with Pan African affinities from Kerala S. India. Jour. Geol., v. 96, pp. 616-626.

Sayles, F.L. and Mangelsdorf, P.C., 1977. The equilibrium of clay minerals with sea water: exchange reactions. Geochim. Cosmochim. Acta, v. 41, pp. 951-960.

Scheidegger, K.F., Kulm, L.D. and Runge, E.J., 1971. Sediment sources and dispersal patterns of Oregon continental shelf snads. Jour. Sed. Petrol. v. 41, pp. 1112-1120.

Schmitz, B. 1987. The TiO2/Al2O3 ration in the Cenozoic Bengal Abyssal Fan sediments and its use as paleostream energy indicator. Mar. Geol., v. 76, pp. 195-206.

Seralathan, P. and Hartmann, M., 1986. Molybdyenum and vanadium in sediment cores from the NW African continental margin and their relation to the climatic and environmental conditions. Met. Fors. Erg., C. No.40, pp. 1-17.

Seshappa, G., 1953. Phosphate content of the mud banks along the Malabar coast. Nature, v. 171, pp. 526-527.

Seshappa, G. and Jayaraman, R., 1956. Observations on the composition of bottom muds in relation to phosphate. Proc. Indian Acad. Sci., v. 8, pp. 288-301.

Setty, M.G.A.P., 1972. Holocene planktonic foraminifera from the shelf sediments off Kerala coast. Jour. Geol. Soc. India, v. 13, pp. 131-138.

Setty, M.G.A.P., 1974. Holocene benthic forminifera from the shelf sediments off Kerala coast. Bull. Earth Sci., v. 3, pp. 21-28.

Setty, A.G.P and Guptha, M.V.S., 1972. Recent planktonic foraminifera from sediments of Karwar and Mangalore. Proc. Indian Natl. Sci. Acad., v. 38, pp. 148-160.

Setty, M.G.A.P. and Nigam, R., 1980. Microenvironmental and anomalous benthic foraminiferal distribution within the neritic regime of the Dabhol-Vengurla sector of the Arabian sea. Revista Italiana de Paleontologia e Stratigrafia, v. 86, pp. 417-428.

Shenoi, S.S.C. and Murty, C.S., 1986. Viscous damping of solitary waves in the mud banks of Kerala. Indian Jour. Mar. Sci., v. 15, pp. 78-83.

Shepard, F.P., 1954. Nomenclature based on sand-silt -clay ratios. Jour. Sed. Petrol., v. 24, pp. 141-158.

Shideler, G.L., 1973. Textural trend analysis of coastal barrier sediments along the middle Atlantic Bight, north Carolina. Sed. Geol., v. 9, pp. 195-220.

Shideler, G.L., 1978. A sediment dispersal model for the south Texas continental shelf, northwest Gulf of Mexico. Mar. Geol., v. 26, pp. 289-313.

Shideler, G.L., 1979. Regional surface turbidity and hydrographic variability on the South Texas continental shelf. Jour. Sed. Petrol., v. 49, pp. 1195-1208.

Sholkovitz. E.R., 1976. Flocculation of dissolved organic and inorganic matter during the mixing of sea water. Geochim. Cosmochim. Acta, v.40, pp. 831-845.

Shrivastava, P.S., Nair, D.K.R. and Kartha, K.R.R., 1968. Monthly wave characteristics of the Arabian sea. Indian Jour. Meteorol. Geophys., v. 19, pp. 329-330.

Siddiquie, H.N. and Srivastava, P.C., 1970. Study of sediment movement by fluorescent tracers at Haldia anchorage. Curr. Sci., v. 39, pp. 451-454.

Siddiquie, H.N. and Rajamanickam, G.V., 1974. The geomorphology of the western continental margin of India. Initial report and data files, INS Darshak 1973-74, oceanographic expeditions, v. 74, pp. 228-233.

Siddiquie, H.N. and Rajamanickam, G.V., 1979. Surficial mineral deposits of the continental shelf of India. Proc. International Sem. Offshore Resources, France, BRGM documents, v. 7, pp. 91-118.

Siddiquie, H.N., Hashimi, N.H., Vora, K.H. and Pathak, M.C., 1987. Exploration of the continental margins of India. International Hydrographic Review, v. LXIV, pp. 90-110.

Silas, E.G., 1984. Mud banks of Kerala-Karnataka - the need for integrated study. Bull. Cent. Mar. Fish. Res. Inst., v. 31, pp. 2-7.

Solohub, J.T. and Klovan, J.E., 1970. Evaluation of grain size parameters in lacustrine environment. Jour. Sed. Petrol., v. 40, pp. 81-101.

Solomons, W., Hotman, P., Boclens, R. and Mook, W.G., 1975. The oxygen isotopic composition of the fraction less than 2 microns in recent sediments from Western Europe. Mar. Geol., v. 18, pp. M23-M28.

Spencer, D.W. and Sachs, P.L., 1970. Some aspects of the distribution, chemistry and mineralogy of suspended matter in Gulf of Maine. Mar. Geol., v.9, pp. 117-136.

Spiegel, M.R., 1961. Theory and problems of statistics. Schaum's outline series, McGraw-Hill Book Co., New York, 359p.

Srikantappa, C., Raith, M. and Spiering, B., 1985. Progressive charnockitisation of leptynite-khondalite suite in southern Kerala, India - Evidence for fromation of charnockites through decrease in fluid pressure. Jour. Geol. Soc. India, v. 26, pp. 849-872.

Srinivasa Rao, P., Krishna Rao, G., Durgaprasada Rao, N.V.N. and Swamy, A.S.R., 1990. Sedimentation and sea level variations in the Nizampatnam Bay, east coast of India. Indian Jour. Mar. Sci., v. 19, pp. 261-264.

Statteger, 1986. Heavy minerals and provenance of sands - Modelling of lithologic and end members from river sands of northern Australia and from sandstone of the Austro-alpine Gosau formulation (Late Cretaceous). Jour. Sed. Petrol., v. 57, pp. 301-310.

Stumm, W. and Brauner, P.A., 1975. Chemical speciation. In: J.P. Riley and G. Skirrow (Eds.), Chemical Oceanography, Vol. I, Academic Press, London, 2nd edn., pp. 173-239.

Stumm, W. and Morgan, J.J., 1970. Aqutic Chemistry. Wiley-Interscience, New York, N.Y.,583p

Subramainam, K.S., 1978. How old are laterites in the Indian Peninsula: a suggestion. Jour. Geol. Soc. India, v. 19, pp. 269-272.

Suess, E. and Mueller, P.J., 1980. Productivity, sedimentation rate and sedimentary organic matter in the Oceans-II. Elemental fractionation: Colloq. Internat. du C.N.R.S., No.293, Biogeochemie de la Materie Organique a 1'Interface Eausediment Marin, Paris, France, pp. 17-26.

Szanto, F., 1962. On the electrochemical properties and disaggregation of bentonites. Acta Geologica (Budapest), v. 7, pp. 305-314.

Tegellar, E.W., De Leeuw, J.W., Derenne, S. and Largueau, C., 1989. A reappraisal of kerogen formation. Geochim. Cosmochim. Acta., v. 53, pp. 3103-3106.

Thomas, R.L., Kemp, A.L.W. and Lewis, C.F., 1972. Distribution and characteristics of the surficial sediments of Lake Ontario. Jour. Sed. Petrol., v. 42, pp. 66-84.

Tipper, G.H., 1914. The monazite sands of Travancore. Rec. Geol. Surv. India, v. 44, pp. 186-196.

Toth, S.J. and Ott, A.W., 1970. Charactarisation of bottom sediments cation exchange capacity and exchangable cation status. Environ. Sci. Technol. v.4, pp. 935-939.

Trask, P.D., 1930. Mechanical analysis of sediments by centrifuge. Econ. Geol., v. 25, pp. 581-599.

Trask, P.D., 1952. Sources of beach sand at Santa Barbara, California, as indicated by mineral grain studies. Beach Erosion Board Tech. Memo. No. 28, U.S.Army Corps of Cngrs., 24p.

Turekian, K.K., 1968. Deep-sea depositon of barium, cobalt and silver. Geochim. Cosmochim. Acta, v. 32, pp. 603-612.

Turekian, K.K., 1977. The fate of metals in the oceans. Geochim. Cosmochim. Acta., v. 41, pp. 1139-1144.

Udden, J.A., 1914. Mechanical composition of clastic sediments. Bull. Geol. Soc. America., v. 25, pp. 655-744.

Van Andel, Tj.H. and Postma, H., 1954. Recent sediments of the Gulf of Paria. In: Reports of the Orinoco shelf expedition, K. Nedrl, Akad. Wete Sch. Verb., v. 20, pp. 42-56.

Van Andel, Tj.H., 1964. Recent marine sediments of Gulf of California. In: Marine geology of the Gulf of California, Memoir 3, Tj. H. Van Andel and G.G.Shore (Eds.), American, Assoc. Petrol. Geol., pp. 216-310.

Van Olphen, H., 1977. An introduction to clay colloid chemistry. Interscience, 301p.

Varma, P.U. and Kurup, 1969. Formation of the chakara (mud bank) on the Kerala coast. Curr. Sci, v. 38, pp. 559-560.

Velde, B., 1969. The compositional join muscovite-pyrophyllite at moderate pressures and temperatures. Bull. Soc. fr. Miner. Crist., v. 92, pp. 360-368.

Velde, B. and Nicot, E., 1985. Diagenetic clay mineral composition as a function of pressure, temperature and chemical activity. Jour. Sed. Petrol., v. 55, pp. 541-547.

Visher, G.S., 1967. Grain size distributions and depositional processes. Intl. Sed. Cong., Reading and Edinburg, England, 4p.

Visher, G.S., 1969. Grain size distribution and depositional processes. Jour. Sed. Petrol., v. 39, pp. 1074-1106.

Viyard,J.P. and Breyer, J.A., 1979. Description and hydraulic interpretation of grain size cumulative curves from the Platter River system. Sedimentology, v. 26, pp. 427-439.

Vogel, A.I., 1978. A text book of quantitative inorganic analysis. Longman Group Limited, 975p.

Weaver, C.E., 1967. The significance of clay minerals in the sediments. Fundamental aspects of petroleum geochemistry. In: B. Nagy (Ed.), Elsevier, Amsterdam, pp. 37-75.

Wedepohl, K.H., 1960. Spurenanalytishe Untersuchungen an Tiefseetonen aus dem Atlantik. Geochim. Cosmochim. Acta, v. 18, pp. 200-231.

Wentworth, C.K., 1922. A scale of grade and class terms for clastic sediments. Jour. Geol., v. 30, pp. 377-392.

Wells, J.T., 1978. Shallow-water waves and fluid-mud dynamics, coast of Surinam, South America. Coastal Studies Institute, Center for Wetland Resources, Louisiana State Univ., Bator Rouge, Louisiana, TR No. 257.

Wells, J.T. and Roberts, H.H., 1980. Fluid mud dynamics and shoreline stabilisation, Lousiana Chenier plane. Proc. Coastal Eng. Conf., Sydney, v. 2, pp. 1382-1401.

Wells, J.T. and Coleman, J.M., 1981a. Physical processes and fine grained sediment dynamics, coast of Surinam, South America. Jour. Sediment. Petrol., v. 51, pp. 1053-1068.

Wells, J.T. and Coleman, J.M., 1981b. Periodic mud flat progradation, northeastern coast of South America: A hypothesis. Jour. Sediment. Petrol., v. 51, pp. 1069-1075.

Wells, J.T., Coleman, J.M. and Wiseman, W.J., 1979. Suspension and transportation of fluid mud by solitary like waves. Proc. Coastal Eng. Conf., Hamburg, v. 16, pp. 1932-1951.

Willey, J.D. and Fitzgerald, R.A., 1980. Trace metal geochemistry in sediments from the Miramichi estuary, New Brunswick. Can. Jour. Earth Sci., v. 17, pp. 254-265.

Whitehouse, G., Jefferey, L.M. and Debbrecht, J.D., 1960. Differential settling tendencies of clay minerals in saline waters. Clays and Clay Minerals, v. 7, pp. 1-79.

Wickremaratne, W.S., 1986. Preliminary studies on the offshore occurrence of monazite-bearing heavy-mineral placers, southwestern Sri Lanka. Mar. Geol., v. 72, pp. 1-9.

World, J. and Pickering, W.F., 1981. Influence of electrolytes on metal ion sorption by clays. Chem. Geol., v. 33, pp. 91-99.

Yariv, S. and Cross, H., 1979. Geochemistry of colloid systems for earth scientists. Springer-Verlag, 450p.

Zhao Yiang, Che Chengui, Yang Hailan and Jia Fengmei, 1981. Geochemistry of Fe, Mn, Ti and P in the sea-bed sediments of Taiwan Bank, China. Acta Geologica Sinica, v. 55, pp. 118-126.